NAS 1.55: 2223/v.1

NASA Conference Publication 2223

Vibrational-Rotational Spectroscopy for Planetary Atmospheres

Volume I

ORIGINAL
COMPLETED

Proceedings of a workshop held at
Annapolis, Maryland
March 17-19, 1980

NASA

NASA Conference Publication 2223

Vibrational-Rotational Spectroscopy for Planetary Atmospheres

Volume I

Edited by
Michael J. Mumma
Goddard Space Flight Center

Kenneth Fox
University of Tennessee

John Hornstein
Computer Sciences Corporation

Proceedings of a workshop held at
Annapolis, Maryland
March 17-19, 1980

National Aeronautics
and Space Administration

Scientific and Technical
Information Branch

1982

I

Blank Page

II

PREFACE

In the last part of the 1970's we experienced a dramatic and exciting explosion of our knowledge about the other planets in our Solar System as NASA's Pioneer, Voyager and Viking spacecraft swept past Jupiter and Saturn, orbited Venus and Mars, and entered the atmospheres of Venus and Mars. For the first time we obtained comprehensive information on the composition and dynamics of these varied atmospheres. New observations resulted in new demands for supporting laboratory studies. Data were needed for a variety of molecular species to better understand the spectra observed from the spacecraft, to interpret atmospheric structure measurements, to aid in greenhouse and cloud physics calculations, and to plan the next generation of experiments which would build upon the findings of this generation of exploration.

It was in this exciting and hopeful atmosphere that some 75 physicists, chemists and planetary astronomers gathered in Annapolis to exchange their current findings and identify their needs as individuals and as a group. The interaction was fruitful. New ideas were spawned and our knowledge of the structure of things large and small, of planets and of molecules, was expanded.

As this volume goes to press, the original purpose is clouded by an uncertain future. The next generation of spacecraft experiments now appears to belong to the next generation. It is our hope that it will not be so for long. But if it is, then here is a piece of our wisdom...for the next generation.

Robert E. Murphy
Discipline Scientist
Planetary Atmospheres

Blank Page

Volume I

CONTENTS

Page

PREFACE iii

INTRODUCTION 1

EXECUTIVE SUMMARY 3

PARTICIPANTS 7

A ROUND TABLE DISCUSSION ON PROSPECTS FOR OBSERVATIONS IN THE NEXT DECADE (1980-1990) 13

- The Space Telescope – John Caldwell 14
- The Future of Ground-Based Near-IR Observations – Uwe Fink 17
- The Next Decade in Space-Based Observations – Rudi Hanel 19
- Next Generation Infrared Spectroscopy of the Planets – Michael Mumma 20
- The 10 μm Region – Alan Tokunaga 23

INTRODUCTION TO PLANETARY SPECTROSCOPY 27

- Molecular Spectroscopy and Planetary Exploration from Space – Rudolph A. Hanel 29
- Radiative Transfer and Remote Sensing – Barney J. Conrath 47
- Rayleigh, Raman and Particulate Scattering – William D. Cochran 63

REVIEW OF THEORETICAL AND EXPERIMENTAL SPECTROSCOPIC METHODS 87

- Prediction of Molecular Infrared Band and Line Intensities – Willis B. Person 89
- New Theoretical and Experimental Methods for Pressure-Broadened Linewidths and Their Interpretation – Jack J. Gelfand 125
- Laboratory Molecular Spectroscopy – Jack Margolis 149
- Microwave Rotational Spectroscopy – H. Pickett 171

SPECTROSCOPIC DATA COMPILATIONS 189

- The JPL Millimeter, Sub-Millimeter, and Microwave Line Catalog – Herbert Pickett 191
- The AFGL Molecular Line Atlases – Laurence Rothman 195

---

*Volume I of II

CONTENTS (Continued)

Page

THE TERRESTRIAL PLANETS – CURRENT KNOWLEDGE 209

Thermal Balance of Venus – Martin Tomasko 211
Neutral Species in the Atmosphere of Venus – Andrew Young 229
Transient Species on Mars and Venus – Yuk L. Yung 243

SPECTROSCOPY PERTINENT TO THE INNER PLANETS 253

Gaseous Infrared Absorption in the Lower Atmosphere of Venus – C. Chackerian, Jr. and R. W. Boese 255
The Spectroscopy of Venus – Reinhard Beer 271
Spectroscopic Measurements of Mars and Venus with Heterodyne Techniques – Albert Betz 277
Infrared Absorption by OH-Containing Compounds – John J. Hillman 295
Infrared Absorption of Sulfur-Bearing Compounds 311

THE OUTER PLANETS – CURRENT KNOWLEDGE 331

Thermal Structure of Jupiter and Saturn – Glen Orton 333
Composition of Jupiter – Ronald Prinn 363
Voyager IRIS Measurements of the Jovian Atmosphere – Virgil G. Kunde 387
Jupiter and Saturn from 2 to 6 μm – Harold P. Larson 407

Volume II

CONTENTS

Page

LABORATORY SPECTROSCOPY PERTINENT TO THE OUTER PLANETS 429

- H_2 and HD Spectroscopic Status – Jack Margolis 431
- Collision-Induced Sharp Features in the Infrared Spectrum of HD – R. M. Herman 439
- Far Infrared Spectra of H_2 and Mixtures of H_2-CH_4 and H_2-He* – George Birnbaum 449
- A Review of Acetylene, Ethylene and Ethane Molecular Spectroscopy for Planetary Applications – W. C. Maguire 473
- Current Studies of CH_4 from 2.5 to 7 μm – Linda Brown 503
- Line Intensities from Band and Diode Laser Measurements: ν_4 of CH_4 – Kenneth Fox 529
- Random Walks with the 6420- and 6825-Å Features of Methane: Lost in the Wilderness – Barry Lutz 549
- Current Band Model Studies of CH_4 at Wavelengths Less than 2.5 Microns – Uwe Fink 559
- Long-Pathlength Absorption Spectroscopy of CH_4 – Peter Silvaggio 585
- Current Studies of CH_3D: Ye Olde Line Drive – Barry Lutz 599
- Spectra of Ammonia – K. Narahari Rao 611
- Current Studies of PH_3 – A. Goldman 635

SPECTROSCOPY OF MINOR BODIES 655

- Gaseous SO_2 on Io – John Pearl 657
- Titan on the Eve of Voyager Encounter – John Caldwell 673
- Organic Chemistry in Titan's Atmosphere – Thomas Scattergood 679
- Spectroscopy of Triton and Pluto: Status and Prospects – Dale Cruikshank 699
- Comments on Pluto's Atmosphere – L. Trafton 709
- Speculations on the Infrared Molecular Spectra of Comets – Michael J. Mumma 717

SUMMARY OF THE WORKING SESSION 745

---

*Volume II of II

Blank Page

INTRODUCTION

This workshop was sponsored by Dr. Robert Murphy, Head of the Planetary Atmospheres Program at NASA Headquarters, who recognized the need for an intensive inter-disciplinary scientific meeting devoted to assessing the current status of, and present and future needs for spectroscopy supporting the study of planetary atmospheres. Initial discussions between Dr. L. Wallace and Dr. M.J. Mumma, co-chairmen, and Dr. Murphy produced a concensus for a workshop of limited size and scope. The size was restricted to forty participants with a goal of providing several experts in each sub-discipline needed to adequately address the topic. The scope was restricted to vibrational-rotational spectroscopy in order to keep the length of the workshop manageable. The important topic of electronic molecular spectroscopy, corresponding roughly to the visual through extreme ultraviolet wavelength range, deserved thorough treatment but was beyond the scope of this workshop. In contrast to ultraviolet spectroscopy, infrared studies of the planets generally probe lower altitudes where the chemistry and compositions are often very different. Furthermore, the infrared spectroscopic and theoretical communities are essentially independent of their counterparts working on electronic-transitions, and adequate representation of both communities would have dictated a much larger group, hence a less favorable environment for in-depth discussion and free exchange of ideas.

The organizing committee (M.J. Mumma, L. Wallace, K. Fox, V. Kunde) chose a three-day format for the workshop, with approximately one-half of the available time allocated to formal talks and one-half to discussion. Because the participants' backgrounds and fields varied greatly, we decided to devote the first session to general reviews of current knowledge and problems in areas directly related to planetary spectroscopy, such as radiative transfer and remote sensing, theoretical molecular spectroscopy, laboratory molecular spectroscopy, and observational capabilities from spacecraft and from the ground. Subsequent sessions were usually keyed to a specific planet and typically began with an invited review on current understanding and problems relating to that atmosphere, followed by more specific papers on detailed topics such as supporting laboratory spectroscopy of particular molecules, planetary observations, or planetary modelling. Highlights included a panel discussion on future space-borne observations of planets ("Prospects for Observations in the Next Decade") and a working session on Recommendations and Conclusions. The papers reproduced in this volume represent the substance of the talks, all of which were invited. Discussions followed each paper and were transcribed from tape recordings. These were reviewed by the editors, who made typographical corrections of grammar, and deleted unintelligible comments. Wherever possible, the name of the discussant has been provided.

The papers presented here represent the state of our knowledge as of March, 1980. Therefore new results obtained by the Voyager flyby of Saturn and its satellites are not reflected in these papers.

Topics for invited talks were chosen by the Organizing Committee to provide foci for discussion and a structural framework for the workshop. The specific topics chosen reflect, unavoidably, some professional preference on our part, but we hope this was minimal.

We wish to acknowledge the excellent support of Dorothy Vanscoy (CSC) of in providing local arrangements and to Kathie Pierce (CSC) and Ellen Kokolakis for (CSC) transcription of the oral proceedings, a singularly difficult and exasperating task. One of us (K. Fox) wishes to acknowledge financial support from the National Aeronautics and Space Administration and the University of Tennessee (Knoxville) during the editorial phase. We particularly wish to acknowledge excellent support from Cheryl Powell (GSFC) in preparing the Conference Proceedings.

The Organizing Committee

Michael Mumma, Chairman
Lloyd Wallace, Co-Chairman
Kenneth Fox
Virgil Kunde

December, 1981

Executive Summary of Recommendations

Certain general themes and many specific problems were identified as needing further study (in some cases, a first study). The participants felt that a vigorous program in theoretical and experimental spectroscopy was essential to enable full interpretation of planetary infrared spectra now in hand or expected to be obtained in the near future. Specific recommendations, listed below, were distilled from the discussions following individual papers from the Working Session on Recommendations and Conclusions, and from written comments solicited from the participants.

Recommendations:

1. Theoretical molecular studies are vital to the interpretation of planetary spectra, and NASA should increase its support of this area.

Three particularly important areas for planetary spectroscopy are: 1) Reduction of fundamental molecular constants from measured laboratory spectra, 2) ab-initio calculations (particularly of band strengths and positions) for those planetary molecules which are particularly difficult to study in the laboratory, mainly free radicals and ions, and 3) theoretical analysis of line shapes and pressure-shifts. For the latter case, a unified theory of pressure broadening is needed and this requires good inter-molecular potential energy curves for planetary constituents.

2. A well-structured program concerning laboratory spectroscopy of planetary molecules is essential, and should be established.

A vigorous program supporting measurements of spectroscopic data under conditions simulating planetary atmospheric conditions, as closely as possible, is critically important. Because the pressure regimes encountered in the interpretation of planetary infrared spectra vary from the very high (many atmospheres) to the very low (micro-bars), it is imperative to support laboratory studies over a wide range of spectral resolutions, from the Doppler-limited low pressure domain to the highly pressure-broadened domain. Laboratory studies at low temperatures (typical of tropopause regions for the outer planets, or $\lesssim$ 100K), and at both long and short path lengths are very important. Particular attention must be given to the temperature dependence of the pressure-broadening coefficients for self-and foreign-gas broadening and to determination of the temperature dependence of line strengths. Theoretical and experimental work must be supported on the shapes and shifts of pressure-broadened molecular lines in cases where they are not well known (most cases). Determination of frequencies, strengths, quantum identifications, and lower state energies for the individual spectral lines comprising a molecular band are critically important, and reduction of these experimentally determined parameters to molecular constants must be supported as discussed in Recommendation 2. Relaxation coefficients are needed for interpretation of vibrational energy transfer in regions of planetary atmospheres where non-equilibrium effects are important. Independent confirmation of spectroscopic data is imperative and is closely connected to a critical evaluation of the data, mandating that depth be established in the number of groups supported.

3. A National repository or central data facility for spectroscopic data relevant to planetary atmospheres should be established.

The purpose is to make existing data more easily accessible to the planetary spectroscopy community. The Repository staff should maintain a continuously updated and critically evaluated data base which is closely coupled to planetary needs and therefore to the planetary community. Support for this Repository must come from NASA, since it is the agency principally responsible for planetary research. A proposal for a National Spectroscopy Center was discussed, but no conclusion was reached regarding the wisdom of establishing it.

4. Coordination and communication among molecular theorists, atmospheric modellers, laboratory spectroscopists, and planetary observers must be

improved.

Current scientific meetings sponsored by professional societies do not provide a sufficiently focussed yet broad forum for this purpose, and do not allow sufficient time during scheduled sessions for in-depth interaction and discussion. For example, the annual meeting of the Division of Planetary Astronomy of the American Astronomical Society attracts many planetary astronomers, some atmospheric modellers, a few laboratory spectroscopists, and virtually no molecular theorists. One acceptable but not exclusive method for providing a programmatically focussed forum would be to establish a bi-annual workshop such as the present one. We recommend that the Planetary Program Office sponsor such an appropriate forum.

5. Many specific spectroscopic problems were identified as needing study to resolve current problems in planetary atmospheres.

The needs are numerous, and are discussed in some detail in the section of this Proceedings labeled "Summary of the Working Session." A few key problems have been abstracted from the Summary and are given here as examples:

- A key to understanding the greenhouse effect on Venus is availability of better data on the opacity of the mixtures CO_2:N_2, CO_2:CO_2, and H_2O:CO_2 at high pressures and temperatures.

- Photochemical models for Mars and Venus need to be verified by spectroscopic detection of OH molecules (H_2O_2, HO_2, e.g.) for Mars and sulfur- and chlorine-bearing species for Venus (SO_2, SO_3, $C\ell_2$, $C\ell O$, e.g.)

- Collision-induced opacity measurements among (H_2, HD, He, CH_4, N_2) are needed for interpreting spectra of the outer planets, as are high resolution data (for H_2, CH_4, NH_3, PH_3, e.g.). High and moderate resolution data are needed for constituents suggested by thermo-chemical or photo-chemical models (CH_2, CH_3, C_3H_8, H_2S, e.g.).

- Doppler-limited spectroscopy is needed for wind measurements and for sounding and abundance determinations. This is important for the major planets and is critical for comets.

- Laboratory measurements are needed on the spectra of condensed phases (i.e., ices, liquids, and snows) for interpretation of aerosols and solid-surface compositions of planetary bodies.

Additional important problems are identified in the "Summary of the Working Session."

Participants in the Workshop on

Vibrational-Rotational Spectroscopy for Planetary Atmospheres

March 17-19, 1980, Annapolis, MD.

Dr. Reinhard Beer (FTS) 792-4748
Space Sciences Division (213) 354-4748
MS 183-301
Jet Propulsion Laboratory
4800 Oak Grove Drive
Pasadena, CA 91103

Dr. Albert L. Betz (FTS) 458-5604
Department of Physics (415) 642-5604
University of California
366 Le Conte Hall
Berkeley, CA 94720

Dr. George Birnbaum (301) 921-3331
National Bureau of Standards
Bldg. 221/B 312
Washington, D.C. 20234

Dr. Robert W. Boese* (FTS) 448-5501
Mail Stop 2915-6
NASA Ames Research Center
Moffett Field, CA 94035

Dr. Linda R. Brown (FTS) 792-2940
Mail Stop 183B-365 (213) 354-2940
Jet Propulsion Laboratory
4800 Oak Grove Drive
Pasadena, CA 91103

Dr. William Brunk, Chief (301)755-3660
Planetary Astronomy
Code SL-4
NASA Headquarters
Washington, DC 20546

Dr. John J. Caldwell (516) 246-7148
Earth and Space Sciences
SUNY at Stony Brook
Stony Brook, NY 11704

Dr. Charles Chackerian (FTS) 448-6300
Mail Stop 245-6 (415) 965-6300
NASA Ames Research Center

Moffett Field, CA 94035

Dr. William D. Cochran (512) 471-4481
University of Texas
Astronomy Department
Austin, TX 78712

Dr. Barney J. Conrath (FTS) 344-6088
Infrared and Radio Astronomy Branch (301) 344-6088
Code 693.2
NASA/Goddard Space Flight Center
Greenbelt, MD 20771

Dr. Dale Cruickshank* (808) 948-7211
Institute for Astronomy
University of Hawaii at Manoa
2680 Woodlawn Drive
Honolulu, HI 96822

Dr. Uwe Fink (602) 626-2736
Lunar & Planetary Laboratory
University of Arizona
Tucson, AZ 85721

Dr. Kenneth Fox (615) 974-4180
Department of Physics & Astronomy
University of Tennessee
503 Physics
Knoxville, TN 37916

Dr. Jack J. Gelfand (906) 452-4745
Dept. of Mechanical and Aerospace Engineering
Princeton University
Princeton, NJ 08544

Dr. Aaron Goldman (303) 753-1964
Physics Department
University of Denver
Denver, CO 80210

Dr. Rudolf A. Hanel (FTS) 344-8283
Laboratory for Extraterrestrial Physics (301) 344-8283
Code 690
NASA/Goddard Space Flight Center
Greenbelt, MD 20771

Dr. Roger Herman (814) 865-6092
Department of Physics
The Pennsylvania State University
University Park, PA 16802

Dr. John J. Hillman, Head (FTS) 344-7974
Molecular Astronomy Section (301) 344-7974
Code 693.1
NASA/Goddard Space Flight Center
Greenbelt, MD 20771

Dr. Donald Jennings (FTS) 344-8707
Code 693.1 (301) 344-8707
Infrared and Radio Astronomy Branch
NASA/Goddard Space Flight Center
Greenbelt, MD 20771

Dr. Theodor Kostiuk (FTS) 344-8431
Code 693.1 (301) 344-8431
Infrared and Radio Astronomy Branch
NASA/Goddard Space Flight
Greenbelt, MD 20771

Mr. Virgil G. Kunde (FTS) 344-5693
Code 693.2 (301) 344-5693
Infrared and Radio Astronomy Branch
NASA/Goddard Space Flight Center
Greenbelt, MD 20771

Dr. Harold P. Larson (602) 626-3574
Lunar & Planetary Laobratory
University of Arizona
Tucson, AZ 85721

Dr. Barry Lutz (602) 774-3358
Lowell Observatory
P.O. Box 1269
Flagstaff, AZ 86002

Dr. William C. Maguire (FTS) 344-5693
Code 693.2 (301) 344-5693
Infrared and Radio Astronomy Branch
NASA/Goddard Space Flight Center
Greenbelt, MD 20771

Mr. Arthur G. Maki (301) 921-2021
Infrared & Micro Spect Sect.,
Natl. Bureau of Standards
Washington, D.C. 20234

Dr. Jack S. Margolis (213) 354-3616
Jet Propulsion Laboratory
4800 Oak Grove Drive
Pasadena, CA 91103

Dr. Michael E. Mickelson Department of Physics Denison University Granville, OH 43023	(614) 587-0810 ext. 467
Dr. Michael J. Mumma, Head Infrared and Radio Astronomy Branch 693.0 NASA/Goddard Space Flight Center Greenbelt, MD 20771	(FTS) 344-6994 (301) 344-6994
Dr. Robert E. Murphy, Chief Planetary Atmospheres Code SL-4 NASA Headquarters Washington, D.C. 20546	(FTS) 755-3660 (202) 755-3660
Dr. W. Bruce Olson National Bureau of Standards Washington, D.C. 20234	(301) 921-2021
Dr. Glenn Orton Mail Stop 183-301 Jet Propulsion Laboratory 4800 Oak Grove Drive Pasadena, CA 91103	(FTS) 792-4748 (213) 354-7430
Dr. John C. Pearl Code 693.2 Infrared and Radio Astronomy Branch NASA/Goddard Space Flight Center Greenbelt, MD 20771	(FTS) 344-5978 (301) 344-5978
Dr. Willis B. Person Department of Chemistry University of Florida Gainesville, FL 32611	(904) 392-0528
Dr. Herbert Pickett Mail Stop 168-327 Jet Propulsion Laboratory 4800 Oak Grove Drive Pasadena, CA 91103	(FTS) 792-6861 (213) 354-6861
Dr. Ronald G. Prinn Department of Meteorology Mass. Inst. of Technology Cambridge, MA 02139	(617) 253-2452
Dr. K. Narahari Rao Department of Physics Ohio State University 144 West 18th Avenue	(614) 422-6505 or 8865

Columbus, OH 43210

Dr. Lawrence Rothman (617) 861-2336
Infrared Physics Branch
Air Force Geophysics Lab.
Hanscom Air Force Base, MA 01731

Dr. Thomas Scattergood (FTS) 448-6163
Extraterrestrial Research Division (415) 965-6163
NASA/Ames Research Center
Moffett Field, CA 94035

Dr. Peter M. Silvaggio (FTS) 532-6545
Lawrence Livermore Laboratory (415) 422-6545
of California
P.O. Box 808
Mail Stop L-11
Livermore, CA 94550

Dr. Darrell F. Strobel (202) 767-3067
Plasma Physics Division
Naval Research Laboratory
Code 6780
Washington, D.C. 20375

Dr. Alan Tokunaga (808) 948-6691
Institute for Astronomy
University of Hawaii
2680 Woodlawn Drive
Honolulu, HI 96822

Dr. Martin Tomasko (602) 626-3655
Lunar and Planetary Laboratory
University of Arizona
Tucson, AZ 85721

Dr. Robert A. Toth (FTS) 354-6860
Mail Stop T1166 (213) 792-6860
Jet Propulsion Laboratory
4800 Oak Grove Drive
Pasadena, CA 91103

Dr. Laurence Trafton (512) 471-4481
Astronomy Department
RLM Rm. 16.342
University of Texas at Austin
Austin, TX 78712

Dr. Prasad Varanasi (516) 246-6007
State SUNY at Stony Brook
Department of Mech.
Stony Brook, NY 11794

Dr. Lloyd V. Wallace (602) 327-5511
Kitt Peak National Observatory
P.O. Box 26732
Tucson, AZ 85726

Dr. Andrew T. Young (713) 693-6993
1200 Holleman Drive
College Station, TX 77840

Prof. Yuk L. Yung (213) 795-6811 ext.2940
Division of Geological & Planetary Sciences
California Institute of Technology
Pasadena, CA 91125

*Indicates two individuals whose papers were read at the Workshop, but who were unable to attend in person.

A ROUND-TABLE DISCUSSION ON PROSPECTS FOR OBSERVATIONS IN THE NEXT DECADE (1980-1990)

Page

The Space Telescope -- John Caldwell 14

The Future of Ground-Based Near-IR Observations – Uwe Fink 17

The Next Decade in Space-Based Observations – Rudi Hanel 19

Next Generation Infrared Spectroscopy of the Planets – Michael Mumma 20

The 10 μm Region – Alan Tokunaga 23

The Space Telescope

John Caldwell

The Space Telescope will be launched in early 1984 into polar orbit. It consists of a 2.4 meter telescope with room on board for five scientific instruments. The f-ratio is dependent upon the secondary objects within the range of the various scientific instruments, but varies from at least 12 to 200. In the first complement there will be two cameras, a high-speed photometer capable of 16 microsecond temporal resolution, and two spectrographs. The mission is planned for a 20-year lifetime but will be refurbishable at about 2-1/2 year intervals, at which times the scientific instruments can be replaced.

The first of the two spectrographs in the initial complement of instruments is called the faint-object spectrograph. The emphasis here is on faint. The idea is to get spectra of cosmologically distant objects, but it's also of interest to planetary workers. Its maximum spectral resolving power is about 10^3 and its spectral range is from Lyman-alpha to 7,000 Å. The second spectrograph is the high-resolution spectrograph and here the emphasis is on high. Its spectral resolving power is up to 10^5. Its range may be disappointing to many of you; from Lyman-alpha to only 3,000 . The reason is that the people who built it were very worried about leaping into long wavelength parts of the spectrum, and they didn't feel they could shield their instrument adequately. That's controversial, but that's the way it will fly.

In terms of infrared capabilities, I do like to stress that real opportunity exists. If somebody fancies himself to be an instrument builder, there will be occasions for new instruments and any proposal would be welcomed, although competition will be keen. If you like to do that kind of thing, let me give you typical instrument parameters. The current generation instruments typically weigh about 600 pounds, consume about 150 watts of power when they're working, and are allocated about 50 watts in the hold mode. The latter seems to be necessary to keep them in mechanical alignment, and to keep the electronics alive, etc. Their physical shape can best be described by saying that those who build them refer to them affectionately as "the coffins."

I can't give you any specific results here, but let me point out one favorite hobby horse of mine. Reinhard alluded to it. That is, that the spectrum indeed does not stop at 1 micron but extends to the ultraviolet. One can detect molecules there. As an example, Warren Moos and his colleagues at Johns Hopkins have observed spectra of Saturn with the International Ultraviolet Explorer. They found that absorption peaks in the lab spectra of acetylene coincide with minima in the reflection spectra of Saturn. To the best of my knowledge, people who do ultraviolet spectroscopy don't worry very much about things like pressure broadening and so on, but I can think of no reason why we shouldn't be concerned about it if we are trying to do qualitative work there. This spectrum contains every bit as much information as the ν_5 fundamental at 13.7 microns, and is an independent way of measuring a remote planetary atmosphere. I think it's good to pursue it. The planetary community would be remiss in not pushing the laboratory types to remember that there are electronic transitions and that they do contain very important quantitative information.

Question: How close to the Sun can the telescope point?

Answer: That is somewhat a function of how hard you want to work at it. The telescope can get to Venus but it has to do it during part of an orbit; you slew during the nighttime. Yet it turns out that the question has a political side, too. If one takes as a given that you want to point as far away from the Sun as possible to minimize the zodiacal light and thereby enhance the cosmological capabilities, then it becomes prohibitively difficult to slew down to Venus in the daytime and get a quick spectrum. I've had some discussions with the project on this and maybe the planetary people will have to get together and make our collective weight felt. The cosmologists pay the penalty of very long exposure times, and we may pay other penalties but planetary studies may require a comparable investment of time.

Question (George Birnbaum): You put in a request for pressure-broadening information in the hard UV where Doppler widths may be quite significant. You have to go to high pressures to see the pressure-broadening effects. Can you estimate whether, for the type of spectra you are looking at, pressure-broadening is important at these frequencies?

Response: If you can convince me that it's not, I'd be grateful. I speak not as an expert on how pressure affects the molecules, but I know that in the past people have been very cavalier.

The Future of Ground-Based Near-IR Observations

Uwe Fink

I decided to break the subject down into wavelength areas, the first one being from about 1 to 2 1/2 microns, where we are still detector-noise limited in Fourier spectroscopy. We are not background-noise limited. and that means that the full multiplex advantage of Fourier spectroscopy holds, and therefore considerably better signal-to-noise ratios can be achieved if we can make improvements in detectors. So in this particular region the major emphasis should be on detector improvement, so that we can get the best possible spectra.

Consider first the terrestrial planets - Mercury, Venus, Mars. There doesn't seem to be much sense in looking at Mercury since it doesn't have an atmosphere. Very high resolution spectra of Venus have been obtained by Connes, but some argue that more observations on Venus are necessary. I don't know whether I would agree with this too strongly since I feel that the Connes data themselves (the latest Connes data from the 200-inch) have never been really totally analyzed or carefully looked at.

Comment (Andrew Young): This neglects the problem of temporal variations. For example, we see variations from day to day in CO_2 absorptions. There are big variations in both spatial and temporal water absorption, and also for minor constituents like $HC\ell$ and HF. We need to understand how they interact in the dynamics and photochemistry of the cloud, and this requires spatial and temporal resolution as well as spectral resolution.

Answer: That's true. The spatial resolution is going to be somewhat hard to get, especially for Venus, since you have to observe in the daytime when the seeing is usually bad. But you can certainly get temporal resolution. My own personal bias is that sometimes you can spend an awful lot of time and very great effort for very small scientific return. Alternatively, one can be surprised and discover some very unusual phenomena. I would certainly think that some effort and time should be devoted to that type of research.

On Mars I feel there is even less to do than on Venus since we have the Viking lander there which analyzed the atmosphere in situ. The atmosphere is thin. I don't believe it has any more unknown constituents, at least not in major proportions, and therefore it really wouldn't make much sense to do an extensive Fourier spectroscopy program on Mars.

Now for the major planets. They are dominated by methane atmospheres, and I will discuss this further in my talk on laboratory spectroscopy. For those bands, we certainly could get better spectra at high resolution. However, even now we are stuck with interpreting what we have, and the hang-up here is really laboratory spectroscopy; we really have to unsort the whole spectrum of methane (CH_4 and CH_3D) from 1 to 3 microns before we can make any progress.

There is also a third area: If we can make sufficient improvements in our detectors (that's certainly feasible; basically it's just a question of money) we can get Fourier transform spectra of some of the fainter satellites in the Solar System, and also spectra of Pluto and Triton. Those two would be the final objects from 1 to 2.5 microns. We are, as we said, not background-noise limited.

Now a few comments about the region from 3 to 5.5 microns (I understand that Alan Tokunaga will talk about longer wavelengths). Jupiter has a very prominent 5 micron window in which many interesting molecules have been discovered. The resolution limit in this particular window has not yet been reached, but this has to be tackled from the C-141. Our group is working on this and I think high resolution spectra of Jupiter can be obtained in this window. Saturn has two sufficiently interesting windows. It has a very nice window at 4 microns in addition to the 5-micron window; both windows look very interesting, and I think should be explored more. The 4-micron window can be partially explored from the ground, but again the C-141 is better suited to it. Five-micron data fromthe C-141 become somewhat difficult because Saturn's flux is way down and it becomes difficult to cancel the thermal background from the sky, especially in the moving airplane where the telescope is not as steady as on the ground. For the 5-micron window on Saturn we have a spectrum from the ground, and I think with the opening of the Hawaii Infrared Facility much better data should be possible in the 5-micron region of Saturn. The ground-based spectra, particularly on days when the atmospheric water content is very low - may produce some interesting results in that area.

The Next Decade in Space-Based Observations

Rudi Hanel

The most significant step forward will be the shuttle-based infrared telescope, a Coude telescope, which will allow the use of cooled detectors and cooled interferometers. As far as free flyers are concerned, progress will hinge on the technology, and again on the cooling technology. Will it be feasible to have a cool device which can last long enough to get you to Jupiter, Saturn, or Neptune, and still provide you with a cool detector? That would allow a quantum step over the spectra I showed you this morning, which are admittedly from a "Model-T" instrument. The next advance will come when spaceborne instruments become background limited; you then have to go to something like a post-dispersion system where the output of the interferometer is dispersed across a detector array so that each individual detector may still be limited by its own noise level rather than by the background, and you retain the benefit of the multiplex advantage. Technologies like that, and the cooling, will play a major role over the next decade.

Next Generation Infrared Spectroscopy of the Planets

Michael J. Mumma

We've been asked to address advances in space in planetary spectroscopy in the next ten years. Considering that there will be no high-resolution infrared spectrometer on Galileo (there is one with low resolution for studying surfaces of the satellites), none on VOIR, and that the instrument weight budgeted for a possible fast-flyby of P/Halley precludes an infrared spectrometer on that mission as well; there appears to be very little prospect for infrared spectroscopy from planetary spacecraft in the next decade. This is extremely unfortunate, because it's clear not only from Rudi Hanel's presentation this morning, but also from some of the work that Al Betz described, that there are significant data which cannot be obtained in any other way.

We therefore need to look to earth-orbiting facilities to provide high-resolution spectroscopy in the next decade. Fortunately, SIRTF does become viable in this time frame with the possibility of having a high resolution spectrometer on board, capable of good planetary and stellar astronomy.

The one point that has not yet been adequately stressed in the workshop is that a truly different class of information is obtained when lines are observed to their true limit in spectral resolution (as opposed to the instrumentation limit). For this reason, an instrument such as a Fourier transform spectrometer operating from 1 to 20 microns with both post-dispersed detector array and cryogenic temperatures, coupled with a very high resolution instrument such as an infrared heterodyne spectrometer, would together give an extremely complementary and complete picture of the physics occurring in planetary atmospheres.

Our current knowledge of the better known atmospheres may be summarized (simplistically) as follows: We understand Mars in a gross sense (in terms of the temperature structure and major atmospheric constituents), the same is true for Venus, may be true for Saturn, and is certainly true for Jupiter. A major thrust for the next decade should be an investigation of the minor constituents, i.e., trace species that occur let's say in the stratosphere or even in the troposphere, and in many cases control the local chemistry. Even on Mars, which we all agree has probably one of the best understood atmospheres, we have not yet detected most of the minor constituents, so we don't know to what degree current chemical models are correct (e.g. Yuk Yung's paper). Only by studying the trace species can we understand fully the photochemistry of extra-terrestrial atmospheres and be able to relate them to our own.

Another more-or-less neglected area of planetary spectroscopy (because the focus has rightly been on determining the temperature fields, major constituents, and related first order parameters) is that of the detailed physics occurring in various regions in the atmosphere and its effect on different states of the molecules in question. A good example of this is provided by the ν_3-$2\nu_2$ (10μm) band of CO_2 on Mars. The Einstein-A coefficient for the ν_3 band is about 420 sec^{-1}, and the collisional relaxation rate is unusually small ($K \sim 3 \times 10^{-15}$ cm^3 sec^{-1} at 200K) suggesting that on Mars the ν_3 level should go out of LTE at about 2 millibars pressure ($\sim$ 5 Km altitude). By contrast, ν_2 of CO_2 should go out of LTE at about 50 km altitude. Recent analysis of fully resolved shapes of ν_3-$2\nu_2$ lines by the Goddard group shows that vibrational LTE fails in the first 12 Km above the surface, in agreement with prediction. Furthermore, an unexpected non-thermally pumped emission at line center was discovered by Al Betz and is being studied further by the Goddard group. At even moderately high (say 10^4) spectral resolution these lines would appear in absorption, completely masking the non-LTE phonenoma.

As a final point, I think it's clear from this workshop that substantially more laboratory spectroscopy is needed (relevant to the interpretation of planetary atmospheres) particularly on such parameters as absolute line strengths, line-by-line frequencies, pressure-broadening coefficients and their temperature dependence. Most importantly, it is essential to couple into the effort those first-rank molecular theorists who can perform ab initio calculations of line strengths or integrated band strengths for radicals and ions that are not readily measurable in the laboratory, and for interpretation of observed laboratory spectra.

Question (Andrew Young): Let me say a couple of words about Mars since you raised the issue of trace constituents there. Several people here have said, "Oh, we don't need to worry about Mars because we have Viking." But let's remember that the O_2 and CO limits on Mars are both still based on ground-based infrared spectra. Viking didn't do a thing for those limits. Various aeronomical models exist for these species; they're supposed to vary with time but nobody has ever observed this. Two guys have observed oxygen on Mars, got about the same numbers, and everybody said, "That's it!", and quit.

Response: I think your criticism of incompleteness is valid. That is one reason I asked Yung a question here today on whether he and Don Hunten agreed on the peroxide abundance on Mars. Yuk gave us the impression earlier that the photochemistry of Mars was well understood, that we knew what all the minor constituents were, and that we knew what the important processes were. I spoke with him a little later and he said, "Well, what he really meant to say . . . was that as far as the model can be checked or has been checked, it seems to be consistent." However, no one has ever observed peroxide or HO_2 on Mars. There are data on water vapor, and a few other species on Mars but that's it. We just don't know what most minor constituents are doing. By analogy with the Earth's atmosphere, those are the important constituents in terms of understanding stratospheric chemistry.

The 10 μm Region

Alan Tokunaga

I shall be very brief. The best way to extrapolate is to show what we can do today. So here is a figure (missing from text-Ed.) of some data on Jupiter taken in the 10 micron region; most of the absorption is due to ammonia and there is some emission by ethane at 12 microns. The point is, this spectrum was taken 2 years ago using the 4-meter FTS spectrometer at Kitt Peak; Steven Ridgeway of Kitt Peak deserves the credit for the quality of the spectrum. That was 2 years ago, and just recently (just this month) there was another observing run using the same instrument in which we believe we can do a factor of 2 better on signal-to-noise, and so the advances are continuing. My best guess for the future is that in the next 5 or 10 years, a spectrum of this quality can be obtained on Jupiter with a resolution somewhere in the range of .01 or .02 cm^{-1}.

It's going to be a challenge to interpret spectra of this quality and resolution, given the relative lack of laboratory data at low temperatures. This is, as you know, a low-temperature spectrum, say between 120 and 145K. Very little laboratory work has been done on parameters such as the line width as a function of temperature (the line profile even for ammonia is under some question, I believe). Also in parts of this spectrum, when I did the analysis, there was some question about the line intensities, especially for high-J transitions (e.g., for the Q-branch, for J greater than 10) at low temperatures. I think there are some temperature-dependent effects that are not known or haven't been studied yet. Furthermore, note the emission spectrum of ethane. This is still the best published low-temperature spectrum of that gas, and so clearly more work needs to be done at low temperature: a subject which hasn't been discussed very much today.

Comment (Beer): You should point out the 1950 cm^{-1} ammonia band as it is perhaps more visible.

Response: Yes, there are also 15 ammonia transitions which are very poorly studied, although Prasad Varanasi has been doing some work lately on that gas.

Comment (Mike Mumma): Can you leave the viewgraph (Figure ?) up for a moment? I just wanted to point out that if you look at the peak intensity of the ethane Q-branch and estimate the temperature it comes up to about 145 K even though the instrument does not resolve the structure of the branch. I guarantee that the individual line intensities, if looked at by a sufficiently high resolution spectrometer, would be well in excess of that brightness temperature.

Future Developments

Reinhard Beer

I'll mention a couple of future developments that I think are very interesting. First, there have already been a few beginning stumbling attempts made in the short wavelength (2.5 micron region I think) infrared with a combination of imaging detectors and Fourier spectrometers; a very potent combination. One attempt was made by Mike Belton at Kitt Peak, who used a 200 x 200 silicon CID. The problem one runs into is one that Jack Margolis alluded to this morning, i.e., the terrifying data processing. On a somewhat more modest scale, a 32 x 32 indium antimonide CID array imager, or a combination of that and the Fourier spectrometer offers exceedingly interesting possibilities. One can also use the identical kind of array with grating spectrometers in a background-limited mode, whereby you use one dimension of spatial dispersion and one dimension of energy. I think that's a very promising future development that could in fact be beginning now.

The second development is one that Jack Margolis mentioned in passing, and I think is worth emphasizing, gas correlation spectrometers combined with frequency shifters (apparently active frequency shifters are about to become a reality). You need the frequency shifter because the gas correlation spectrometer works on a lab rest frequency; just because of the Earth's orbital motion, for example, Jupiter has a ± 26-27 km/sec orbital radial velocity charged on frequency shifts at 5 microns. That's almost 0.2 cm^{-1} which, with a correlation spectrometer, would be enough to move you clear out of the range. So frequency shifters have to be part and parcel of it. With that, I think one can start measuring in the near infrared with the kind of precision that the heterodyne people were talking about. For radial velocity, one can think in terms of measuring the velocity down to the order of a few meters per second; and abundances down to almost any number you care to think of, because you're looking at the whole spectrum, the whole time. It really is a multiplexing technique, and I think it's something that deserves a lot more future development.

Comment: That's a limb-scanning method that you're talking about, i.e., using the correlation spectrometer.

Response: I think it can be used on planetary disks if you can get the frequency shifters.

End of Session

INTRODUCTION TO PLANETARY SPECTROSCOPY

Page

Molecular Spectroscopy and Planetary Exploration from Space – Rudolph Hanel 29

Radiative Transfer and Remote Sensing – Barney J. Conrath 47

Rayleigh, Raman and Particulate Scattering – William D. Cochran 63

Blank Page

Molecular Spectroscopy and Planetary Exploration from Space

Rudolf A. Hanel, NASA/GSFC

Molecular spectroscopy and planetary astronomy have been closely connected for many decades. Even before man's adventure into space, astronomers have learned much about the composition of planetary atmospheres by interpreting spectroscopic data recorded at ground based telescopes. Molecular spectroscopy from a spacecraft passing close to a planet, or even better from an orbiter, has a number of advantages over ground based techniques: it is possible to obtain spectra over a wide spectral range (1) without the obscuring effect of Earth's atmosphere, (2) at much higher spatial resolution, and (3) from directions and with phase angles inaccessible from Earth. For example, the polar regions of Mars have been explored at low emission angles by Viking and the dark side of the Galilean satellites have been investigated by Voyager.

Except for data obtained by the atmospheric probes and landers on Venus and Mars, most information on the planets has been obtained by remotely sensing either reflected sunlight or thermal and, in some cases, non-thermal emission. Reflected sunlight and non-thermal emission, particularly in the ultraviolet, yield information on atomic constituents because many atomic resonances fall into this spectral range. More complex molecules have their vibration and rotation spectra at longer wavelength in the infrared and it is for that reason that the exploration of the infrared spectrum of the planets has been so important. Furthermore, in the thermal infrared, the spectral radiance, the quantity which is measured by spectroscopic instruments, is intimately linked with the local temperature through the Planck function which appears in the radiative transfer equation. Therefore, analysis of the thermal emission spectrum yields atmospheric temperatures as well as information on the chemical composition.

In this talk, I will show examples of the role which molecular spectroscopy has played in the interpretation of the thermal emission spectra of Earth, Mars, and Jupiter (Fig. 1). Earth was explored by the Michelson interferometers (IRIS) on Nimbus 3 and 4 launched in 1969 and 1970,

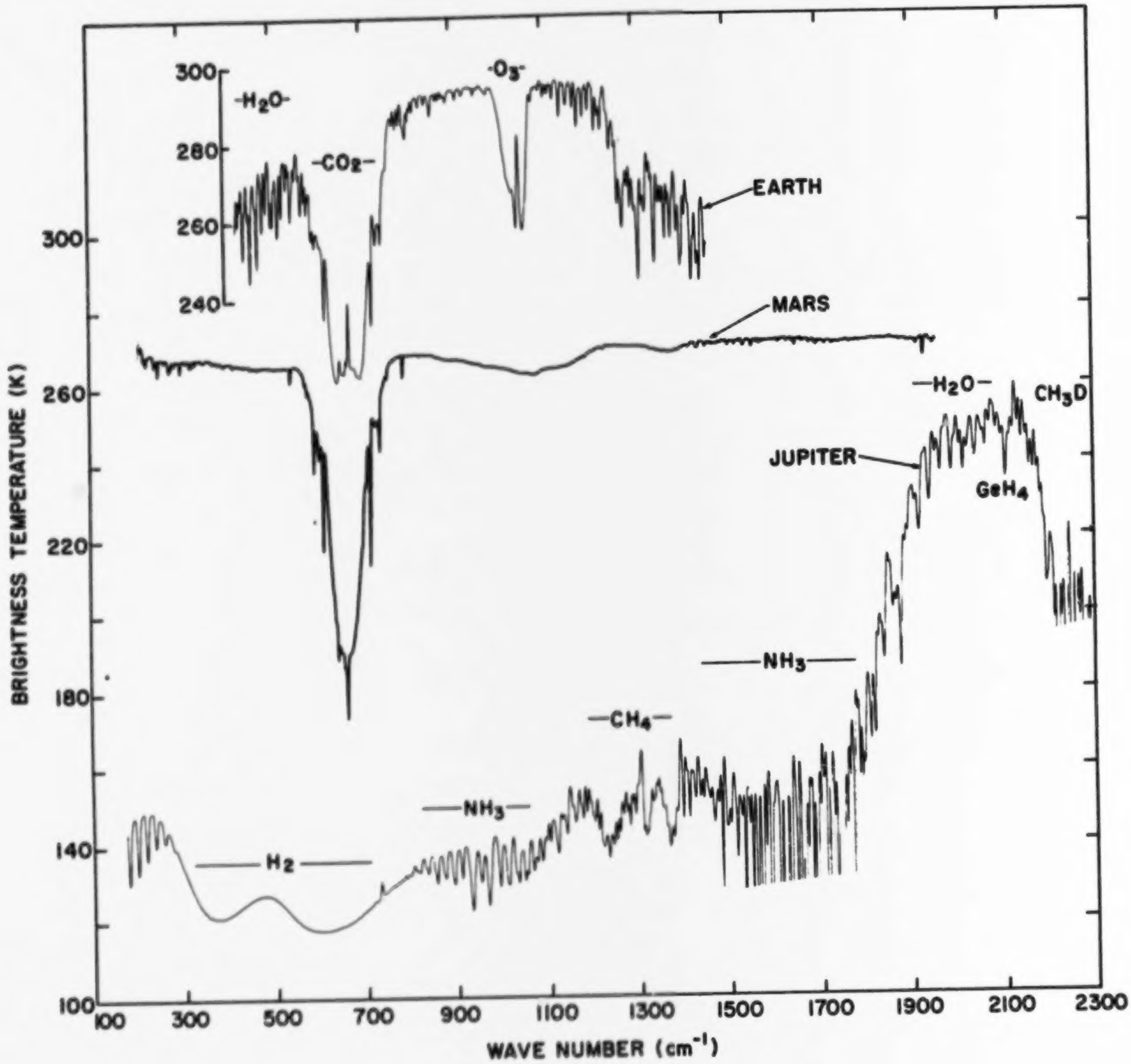

Figure 1. The thermal emission, spectra of Earth, Mars and Jupiter recorded by Nimbus 4, Mariner 9, and Voyager 1, respectively. The spectra are shown in terms of brightness temperatures. Mars and Jupiter are on the same scale. Earth is vertically displaced to avoid overlap with the Martian spectrum. The inserted scale applies to the Earth spectrum.

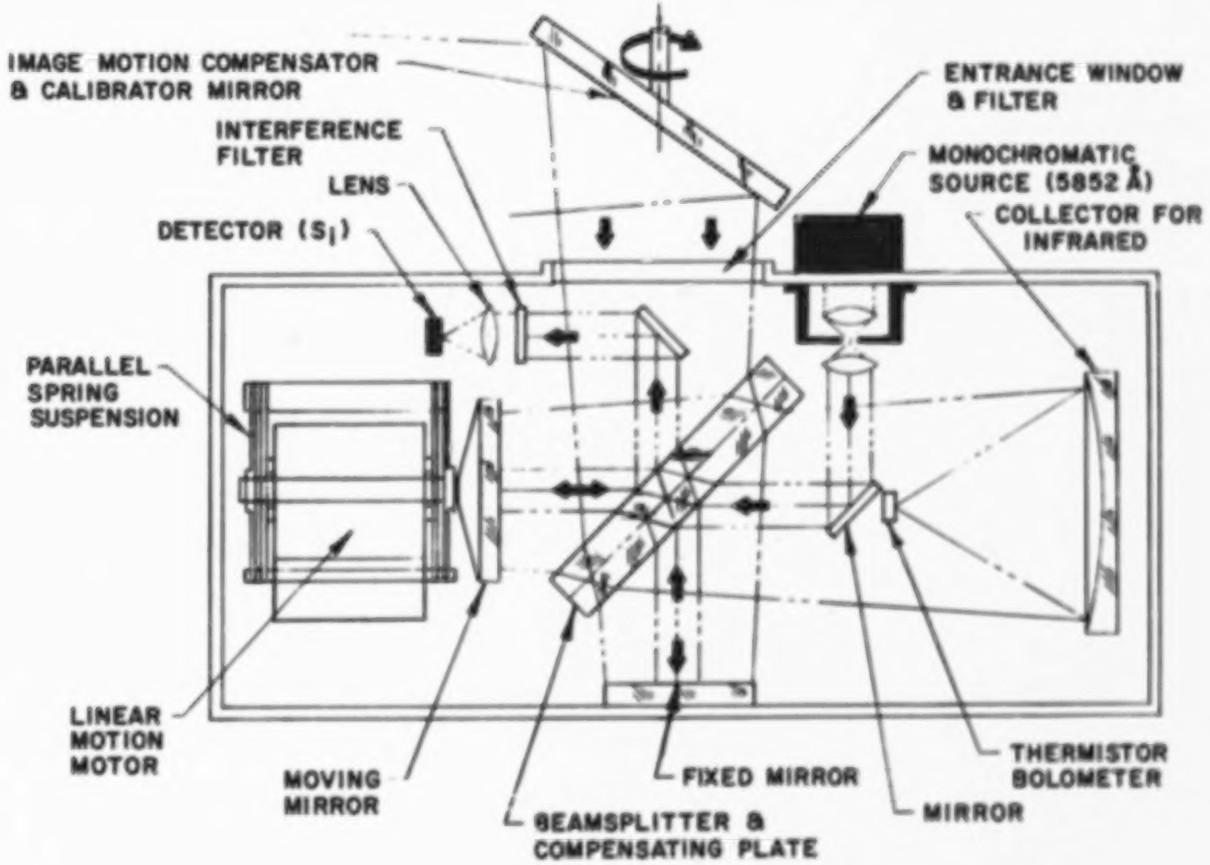
IMAGE MOTION COMPENSATOR & CALIBRATOR MIRROR
ENTRANCE WINDOW & FILTER
INTERFERENCE FILTER
LENS
MONOCHROMATIC SOURCE (5852 Å)
DETECTOR (S$_1$)
COLLECTOR FOR INFRARED
PARALLEL SPRING SUSPENSION
LINEAR MOTION MOTOR
MOVING MIRROR
FIXED MIRROR
BEAMSPLITTER & COMPENSATING PLATE
THERMISTOR BOLOMETER
MIRROR

Figure 2. Conceptual diagram of IRIS. For Nimbus and Mariner the image motion compensation and calibration mirror can be oriented so that IRIS sees the planet, deep space or an onboard blackbody.

respectively (Hanel et al., 1969; Conrath et al., 1970; Hanel et al., 1972a; Kunde et al., 1974; Prabhakara et al., 1976). An advanced version of the Nimbus interferometer was flown on the Mariner 9 orbiter around Mars in 1971/72 (Hanel et al., 1972b; Hanel et al., 1972c; Conrath et al., 1973). In 1977 two Voyager spacecraft were launched on a long journey to Jupiter, Saturn and possibly further on to Uranus. In March and August 1979, the Voyager 1 and 2 spacecraft, respectively, passed through the Jovian system and the infrared instruments have obtained information on the planets and on the Jovian satellites (Hanel et al., 1979a; Pearl et al., 1979; Hanel et al., 1979b). Molecular spectroscopy and the theory of radiative transfer have provided the basis for the interpretation of the data. In many cases it was apparent that our present state of knowledge of molecular parameters is inadequate. A vigorous effort in laboratory spectroscopy and molecular theory are of fundamental importance for space exploration. Before exploring the planetary spectra further, I will briefly discuss the IRIS instrument and summarize the theory of remote sensing in the thermal infrared.

The Infrared Interferometric Spectrometer (IRIS)

The first Nimbus interferometer was patterned after a breadboard which was constructed by L. Chaney from the University of Michigan and our group at the Goddard Space Flight Center. After a successful balloon flight and extensive laboratory testing, the Michigan team pursued further balloon activities and the GSFC team space application. The conceptual layout of the interferometer is indicated in Fig. 2. Texas Instruments, Inc. in Dallas, Texas, built all of the space flight versions of the instrument.

The first launch in 1968 was a disaster due to a malfunction in the guidance system of the rocket; the spacecraft fell into the Pacific Ocean. A year later Nimbus 3 was launched and the interferometer functioned well (Hanel et al., 1970). On Nimbus a conventional grating spectrometer, SIRS, and IRIS obtained vertical temperature profiles of the atmosphere; in addition, IRIS obtained water vapor and ozone distributions (Wark et al., 1969; Hanel et al., 1969). On Nimbus 4 the resolved spectral interval was decreased from 5 to 2.8 cm^{-1} and several other design changes contributed to the generally better performance of this instrument, as compared to its predecessor.

A major design change was implemented in the next generation of IRIS, earmarked to fly on Mariner to Mars. In the Nimbus instrument, the potassium bromide beamsplitter material limited the spectral range to wavenumbers greater than 400 cm^{-1} (Hanel et al., 1971). However, the range between 200 and 400 cm^{-1} contains strong rotational water vapor lines, crucial to the Mars investigation. A change to cesium iodide was therefore made, although CsI is very soft, hard to polish and difficult to maintain flat (Hanel et al., 1972). Again one of the two spacecraft, Mariner 8, was lost, this time in the Atlantic Ocean, but after a 6 month cruise Mariner 9 reached Mars. IRIS as well as the spacecraft performed beyond expectation.

The largest and most ambitious step in the evolution of IRIS came in response to demanding requirements for exploration of the outer planets. Temperatures there are only slightly higher than that of liquid nitrogen; under these circumstances the measurement of the thermal emission spectrum is not an easy task. Moreover, the instruments had to survive for years in space and had to function in the severe high-energy particle environment which exists in the vicinity of Jupiter (Hanel et al., 1980).

The optical layout of the Voyager IRIS is shown in Fig. 3. The whole instrument, including the half-meter telescope, weighs only 18.4 kg and operates with an average power of 14 Watt. The Cassegrain telescope forms an image of the object at the focal plane aperture which limits the field of view to 0.25° full cone angle. A dichroic mirror channels the visible and near infrared portion of the spectrum into a radiometer, and the lower wavenumbers into the Michelson interferometer which analyzes the spectrum between 180 and 2500 cm^{-1} with a 4.3 cm^{-1} apodized resolution. The main interferometer and the reference interferometer (which controls the motor speed and the wavenumber calibration) are shown for convenience in Fig. 3 in the plane of the paper, although they are in reality perpendicular to it. As all previous IRIS, the Voyager instrument is thermostatically controlled by thermally insulating the entire assembly from the spacecraft, and allowing the instrument to cool by radiating to space. The instrument is held at a constant temperature of 200 K by the thermostatic action of small electrical heaters. Voyager IRIS has three independent thermostats, one for the interferometer

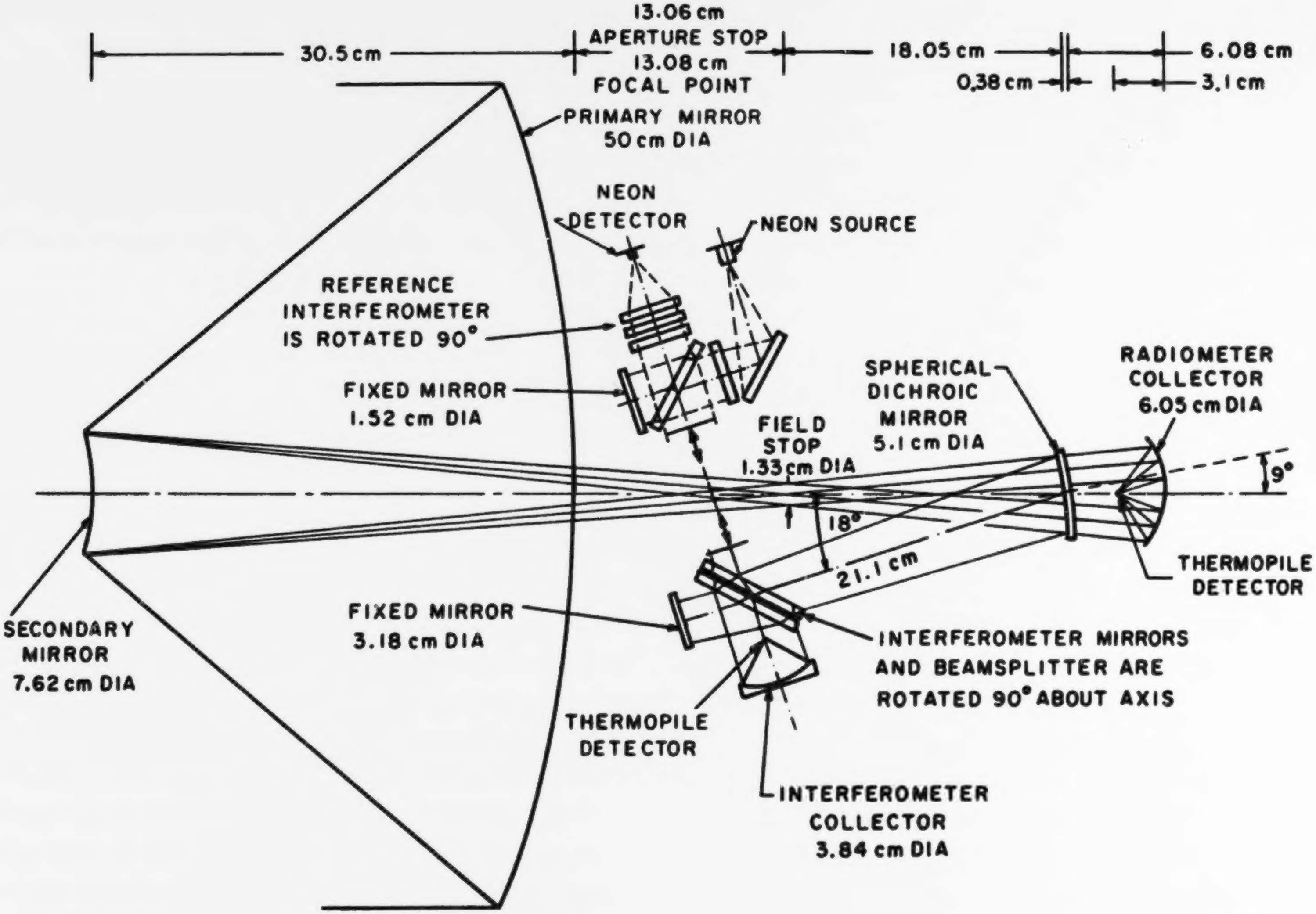
30.5 cm
13.06 cm
APERTURE STOP
13.08 cm
FOCAL POINT
18.05 cm
0.38 cm
6.08 cm
3.1 cm
PRIMARY MIRROR
50 cm DIA
NEON
DETECTOR
NEON SOURCE
REFERENCE
INTERFEROMETER
IS ROTATED 90°
FIXED MIRROR
1.52 cm DIA
FIELD
STOP
1.33 cm DIA
SPHERICAL
DICHROIC
MIRROR
5.1 cm DIA
RADIOMETER
COLLECTOR
6.05 cm DIA
9°
18°
21.1 cm
THERMOPILE
DETECTOR
SECONDARY
MIRROR
7.62 cm DIA
FIXED MIRROR
3.18 cm DIA
INTERFEROMETER MIRRORS
AND BEAMSPLITTER ARE
ROTATED 90° ABOUT AXIS
THERMOPILE
DETECTOR
INTERFEROMETER
COLLECTOR
3.84 cm DIA

Figure 3. Optical layout of the Voyager infrared instrument. Calibration of the interferometer is accomplished by occasionally observing deep space and by precise temperature control of interferometer and telescope. Calibration of the radiometer is accomplished by occasionally viewing a diffusor plate mounted on the spacecraft and illuminated by the Sun.

proper, one for the primary, and one for the secondary telescope mirror. The Voyager interferometers have performed well although a slight optical misalignment, more pronounced on Voyager 2 than on 1, has been noted.

Remote Sensing Concept and Results

The art of remote sensing is to infer physical and chemical conditions from radiance measurements at different wavenumbers and zenith angles. This task must be based on radiative transfer theory. The physical quantity measured by these interferometers is the spectral radiance expressed, for example, in W cm^{-2} sr^{-1} $(cm^{-1})^{-1}$. Sometimes it is more instructive, as in the case of Fig. 1, to plot the spectra in units of brightness temperature, defined as the temperature of a blackbody which emits, at a particular wavenumber, an equal amount of radiation as the object under investigation.

Restricting the case to thermal emission from a plane parallel atmosphere in thermodynamic equilibrium, of optical thickness τ_1, above a lower boundary of emissivity ϵ_G and temperature T_G, the spectral radiance can be expressed by (Hanel et al., 1977)

$$I(o,\mu) = \epsilon_G B(T_G)\, e^{-\frac{\tau_1}{\mu}} + \frac{1}{\mu}\int_o^{\tau_1} B[\tau(T)]e^{-\frac{\tau}{\mu}}\, d\tau. \qquad (1)$$

B is the Planck function and $\cos^{-1}\mu$ the emission angle. All quantities in Eq. 1, except μ and T, depend on the wavenumber, ν. The optical depth τ is defined by

$$\tau(\nu,z) = \int_z^{\infty} \sum_i [k_i(\nu,z',T)\; \rho_i(z',T)]\, dz', \qquad (2)$$

where k_i and ρ_i are the absorption coefficient and density of gas i, and z and z' are altitudes. Eqs. 1 and 2 are valid only for monochromatic radiation; a convolution with the instrument function is required before computed and observed radiances can be compared.

The first term in Eq. 1 represents emission from a solid surface and the second term emission from atmospheric layers. In cases of the Galilean satellites (except the 1350 cm^{-1} range of Io) only the first term needs to be considered. In a deep and opaque atmosphere, such as that of Jupiter, only the second term is important. On Earth and Mars both terms are significant depending on the actual value of the optical depth, τ, at a particular wavenumber. The task of deriving atmospheric temperatures from a measurement of I_ν requires an inversion of the integral equation 1 which, in the early days of remote sensing, was often compared to the task of reconstructing an egg from its scrambled state. However, much has been learned about this process in the last decade so that today the inversion technique is generally not a limiting factor in the interpretation of planetary spectra (see eg. Deepak 1977).

One can always compute a synthesized spectrum by assuming a vertical profile of temperature and a reasonable distribution of atmospheric constituents, comparing the calculated to the observed spectrum, making adjustments to the assumptions, and iterating the process until agreement exists across the spectrum. A careful error analysis must be performed because solutions are not always unique. All inversion procedures assume that the absorption coefficients of all absorbers involved are adequately known as a function of temperature and pressure. Line by line computational methods must be applied which require a precise knowledge of line position, line strength and their dependence on temperature and pressure (Kunde and Maguire 1974). Within a band even weak lines and lines from isotopes must be taken into account. Even for CO_2, which has been studied extensively because of its importance for the retrieval of vertical temperature profiles in the Earth's atmosphere, it was necessary to include many very weak bands and even bands of isotopes, including ^{13}C and ^{17}O into our molecular models before the spectrum of the 667 cm^{-1} Martian CO_2 band, shown in Fig. 4, was fully explained (Maguire 1977).

Furthermore, the theory of line shape needs to be better understood, particularly the contributions of the wings of strong lines far away from the center. Absorption by the far wings affects the continuum transmission of spectral windows such as the 8-12 μm window on Earth and the 5 μm window on Jupiter.

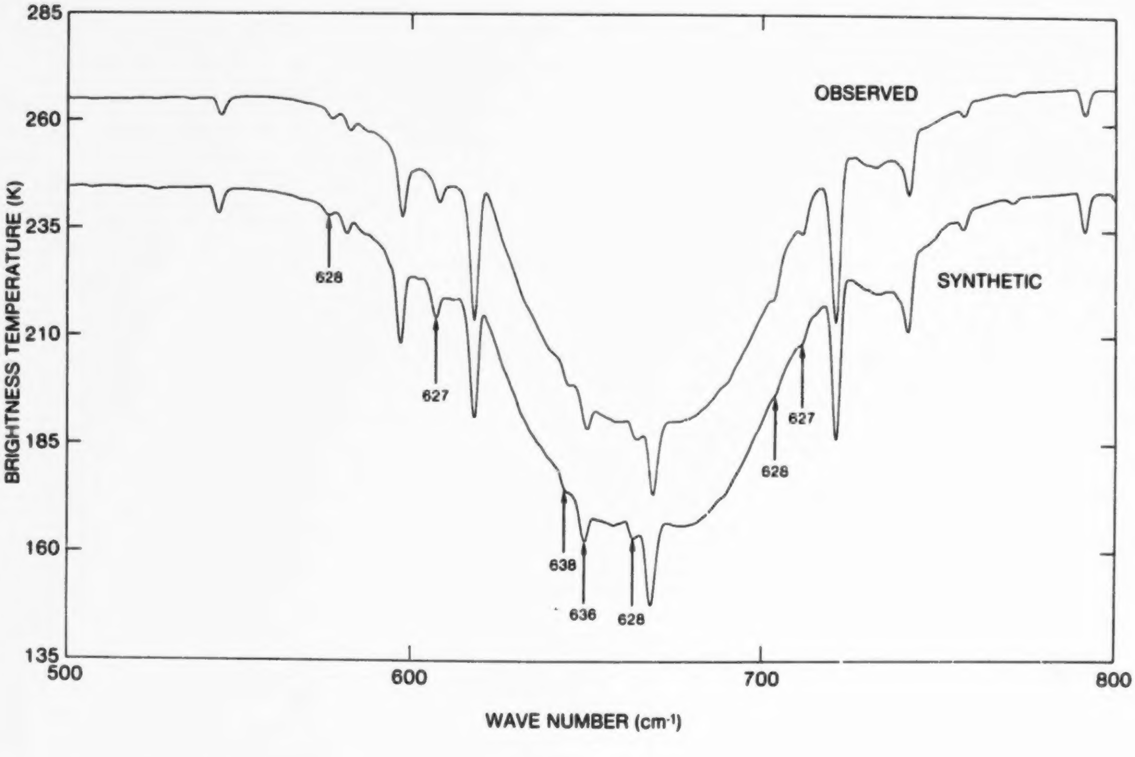

Figure 4. Comparison of measured and synthesized spectra of Mars in the region of the strong 667 cm^{-1} CO_2 band. The main spectral features are labeled with a three-digit number representing the isotope; thus $^{16}O^{13}C^{18}O$ is abbreviated 638. Unlabeled features are due to the main isotope $^{16}O^{12}C^{16}O$. The synthetic spectrum is displaced 20.3 K.

Earth

Emission spectra of the lower Sahara region, of the Mediterranean Sea and an Antarctic spectrum are shown in Fig. 5. The highest spectral radiances occur in the most transparent part of the atmospheric window near 825 cm^{-1} indicating a surface temperature of about 318 K. In contrast the arctic spectrum indicates surface temperatures below 200 K. The CO_2 band centered at 667 cm^{-1} shows also marked differences between the low latitude and the arctic cases. Without going through a formal inversion of Eq. 1, one can say that at low latitudes atmospheric temperatures must fall with height to a temperature minimum and then increase again because the intensities generally fall between 650 and 700 cm^{-1} and the Q branch at 667 cm^{-1} shows an opposing trend. In the arctic all bands of CO_2, H_2O and O_3 appear in emission indicating that atmospheric temperatures throughout the troposphere and stratosphere are higher than the temperature of the surface.

Mars

The most dominant spectral feature in the mid-latitude spectrum of Mars (Fig. 6), the 667 cm^{-1} CO_2 band, shows great similarity in the overall shape to the same band in the Sahara spectrum. However, intensities are much smaller (due to the generally lower Martian temperatures) and the Q branch at 667 cm^{-1} appears in absorption and not in emission as on Earth which indicates the absence of a stratospheric temperature inversion on Mars. The north polar spectrum (it was late fall in the north at the time of measurement) shows again a warmer atmosphere over a very cold surface at about 145 K, very near the condensation point of CO_2 at the Martian surface pressure.

The south polar spectrum is more complicated because a large fraction of the frost deposit has already evaporated exposing the darker underlying surface which heats in the Martian midnight sun to much higher temperatures than the still frost covered fraction within the field of view. The CO_2 band indicates a warm atmospheric layer sandwiched between a colder surface and a colder upper atmosphere. Water vapor lines and features of atmospheric dust are also apparent in the spectrum.

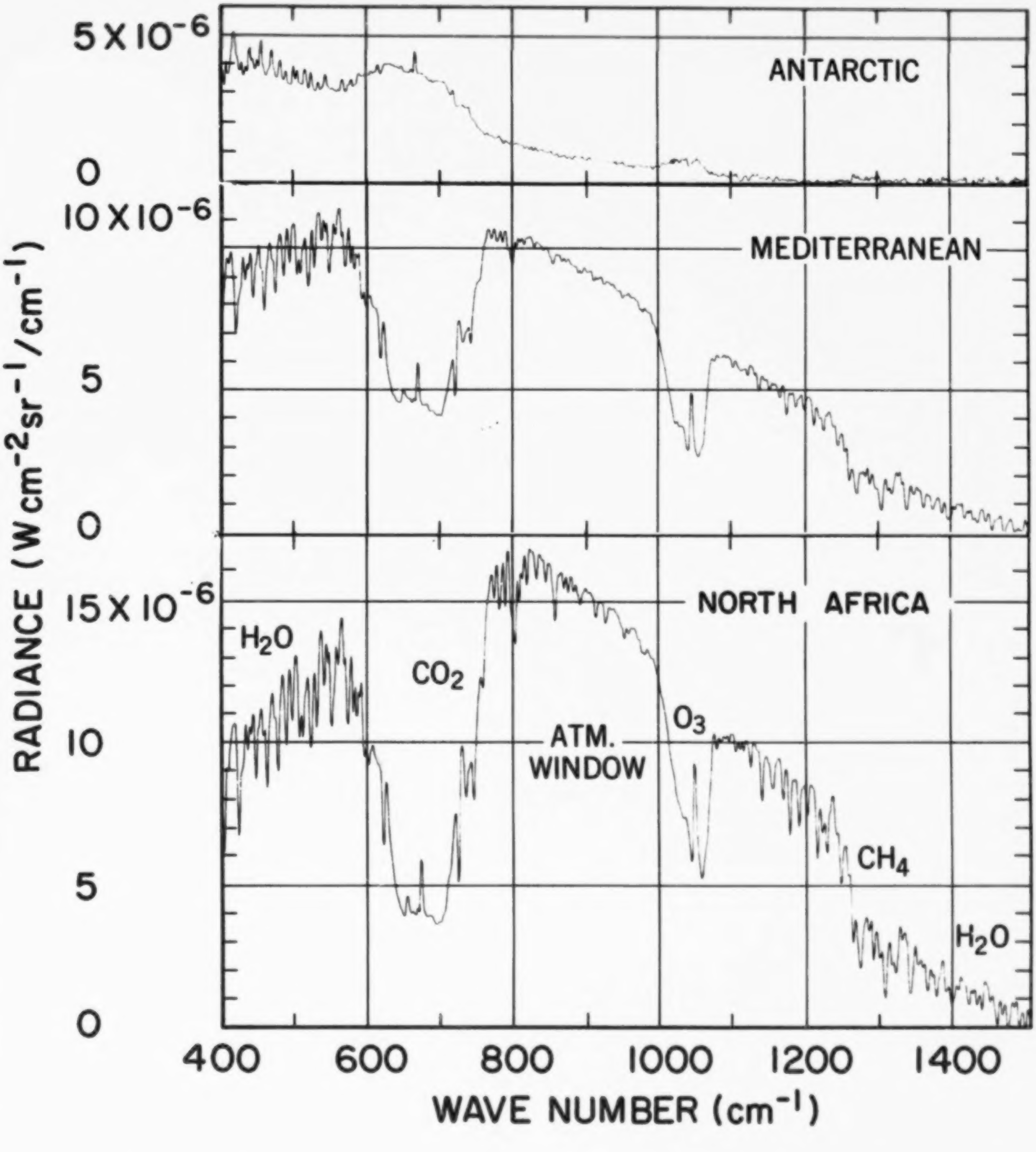

Figure 5. Thermal emission spectra of the Antarctic, the Mediterranean and the Sahara recorded by Nimbus 4 in April 1970.

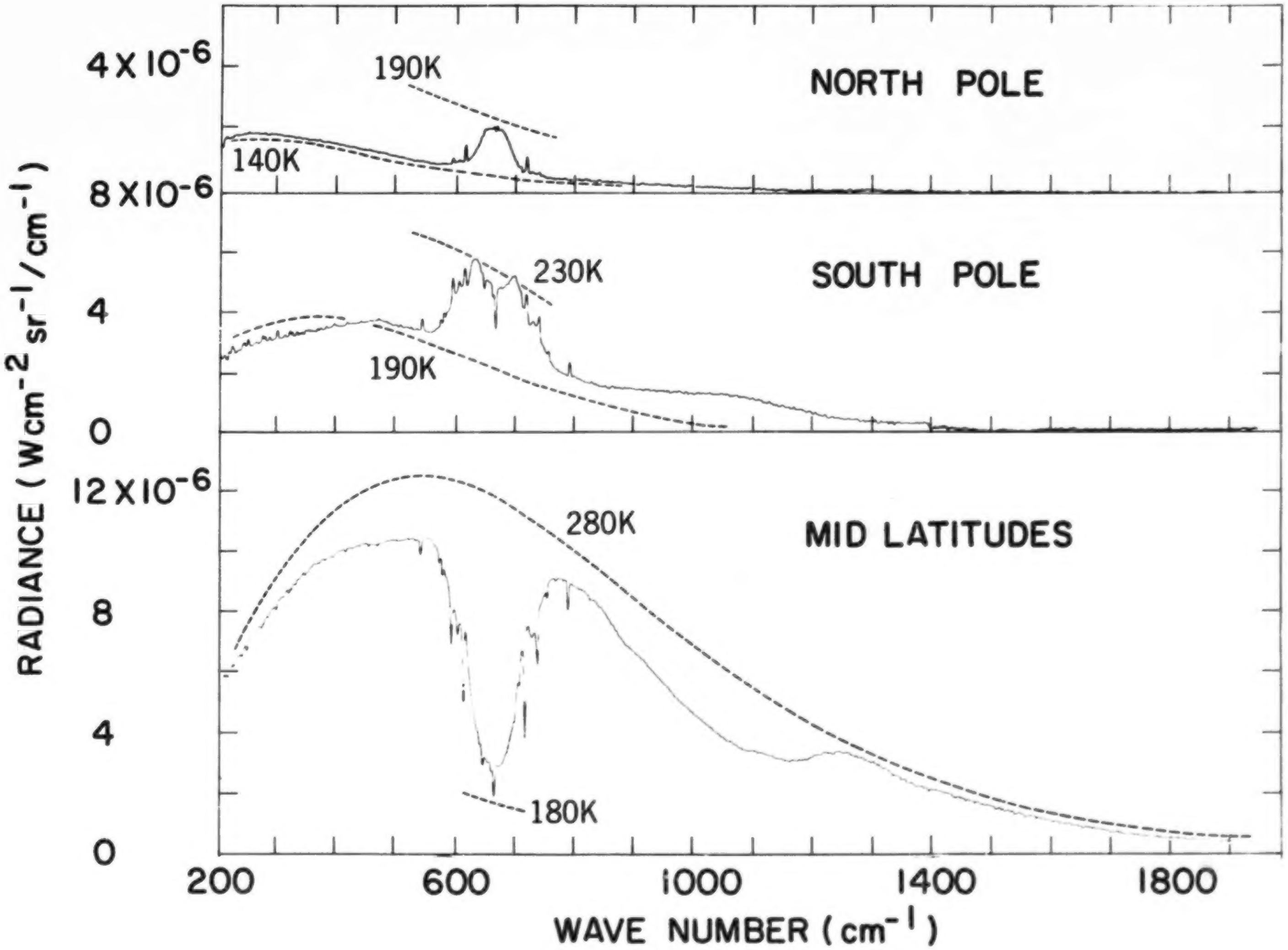

Figure 6. Thermal emission spectra of the north and south polar regions and of mid-latitudes on Mars recorded by Mariner 9 in Dec. 1971 and Jan. 1972.

Jupiter

Examples of a Jovian spectrum are shown in Fig. 7 and 8. Jupiter has a predominantly hydrogen atmosphere with about 20% helium per mass. Small fractions (NH_3, PH_3, CH_4, C_2H_2 and C_2H_6) exist and their signatures are indicated in Fig. 7. The spectral intensities of the broad pressure-induced S(0) and S(1) lines of H_2 at 350 and 600 cm^{-1} have been used to derive atmospheric temperatures and the helium abundance on Jupiter. The major uncertainty in the helium abundance is not in the spacecraft measurement but in the associated coefficients of pressure induced hydrogen and helium absorption, pointing again to the need of better supporting laboratory measurements. Interesting features appear at 354.4 cm^{-1} and 557.1 cm^{-1}, the S(0) and S(1) lines of the free H_2 molecule. The features are small and difficult to see in the figure. Their shape, reminiscent of a dispersion curve, and their true nature have not been fully explained.

A Jovian hot spot spectrum is reproduced in Fig. 8. Brightness temperatures up to 260 K have been observed. The region below 1800 cm^{-1} is obscured by NH_3 and above 2200 cm^{-1} by PH_3 and CH_4. A quantitative explanation of the appearance of the lines of H_2O, CH_3D and GeH_4 remains to be done. In this spectral region great difficulties exist in assessing the continuum absorption provided by the wings of strong nearby bands. The presence of haze of unknown composition and particle size distribution may complicate matters further. However, the Voyager spectra with their radiometric accuracy (although at moderate spectral resolution) in conjunction with radiative transfer and molecular absorption theory will certainly advance our understanding of the Jovian atmosphere.

The displayed sample spectra reflect only a small fraction of the available data. I have no time to dwell on the interpretation of the spectra. However, I hope to have conveyed to you the important relationship which must exist between the interpretation of planetary spectra and laboratory as well as theoretical spectroscopy. If researchers in both fields, that is in astronomy and in molecular science, pay attention to each others' needs, science as a whole will be well served. It is the purpose of this workshop to establish better communication between both disciplines.

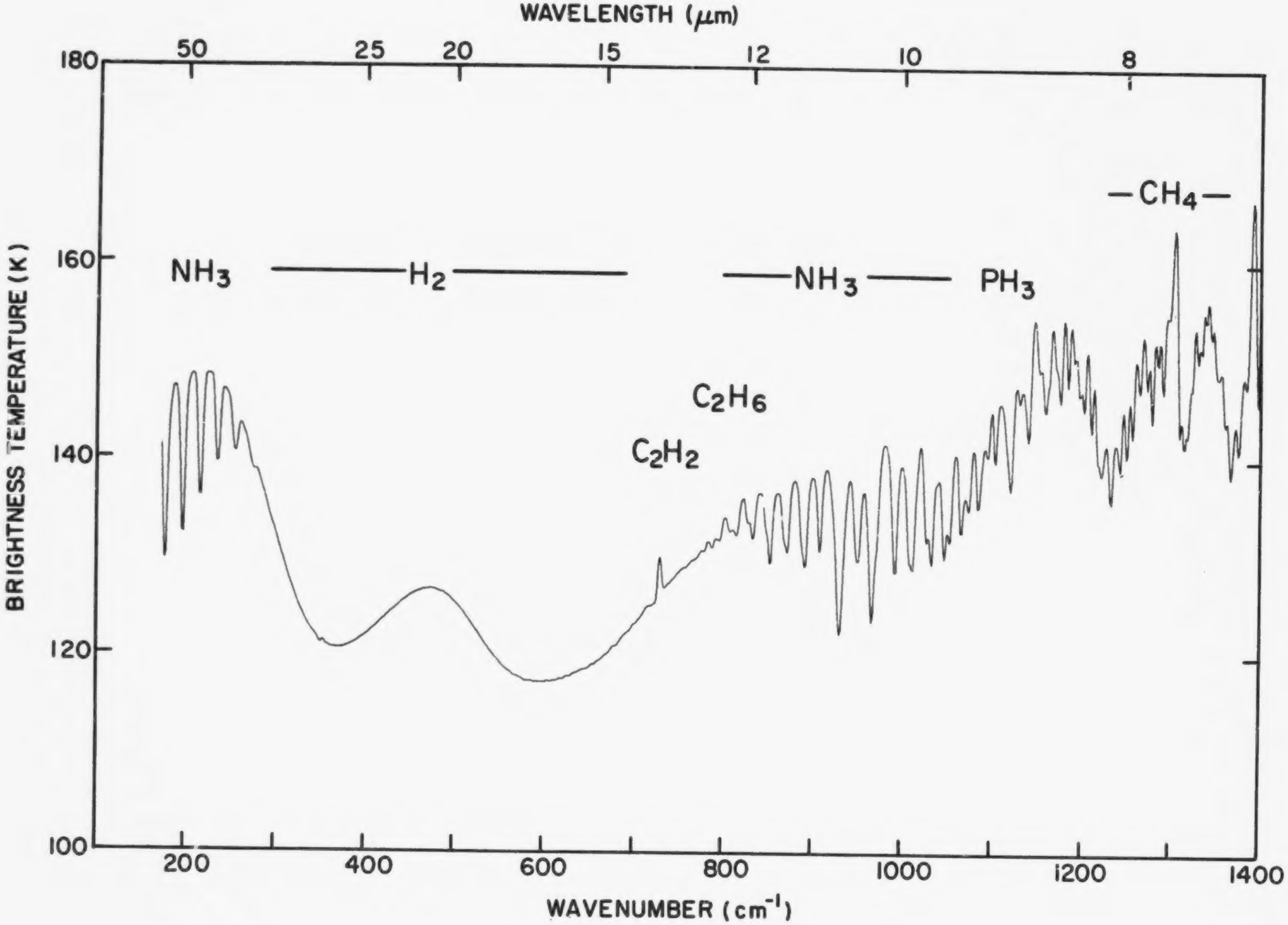

Figure 7. Thermal emission spectrum of Jupiter between 200 and 1400 cm^{-1} recorded by Voyager 1 in March 1979.

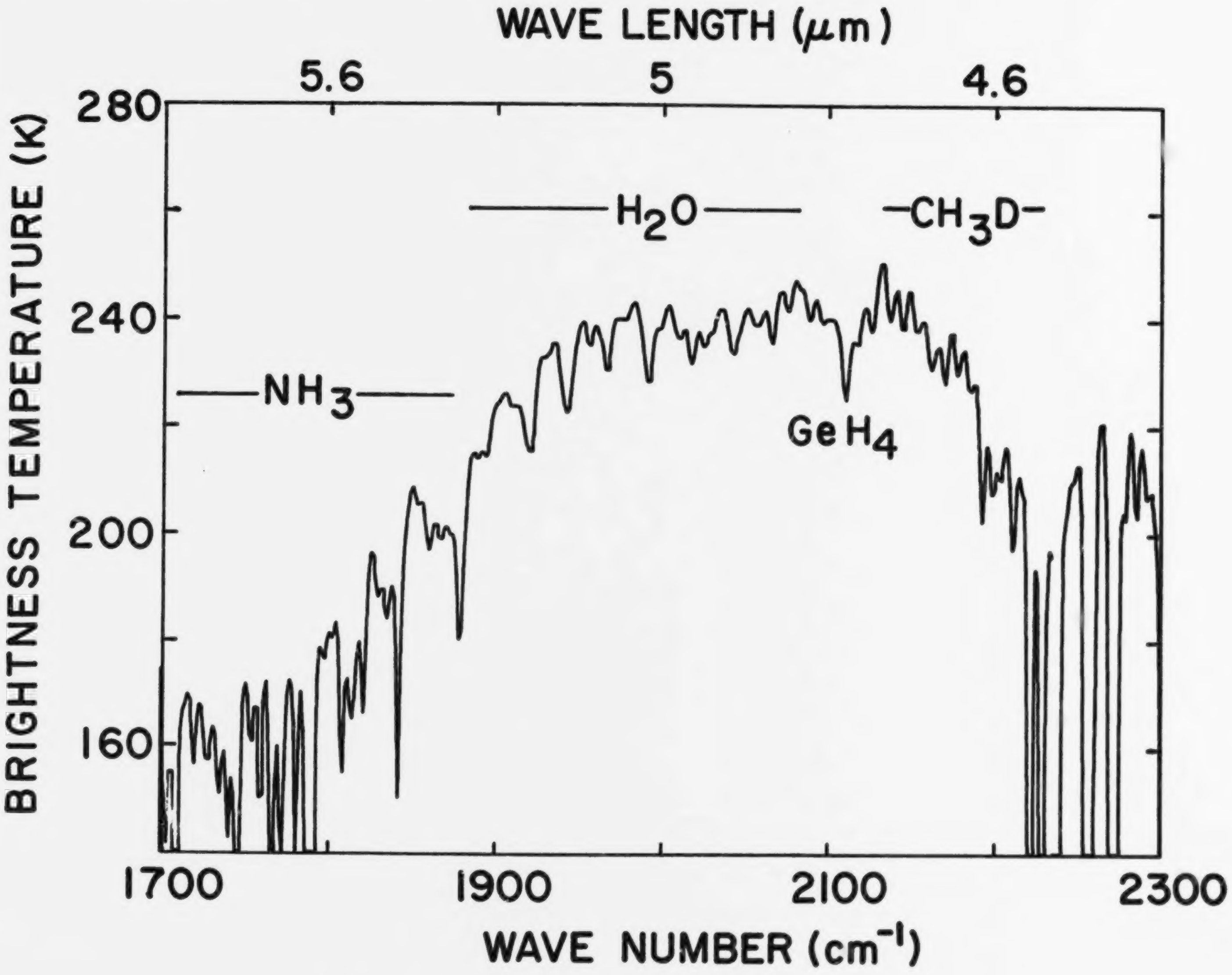

Figure 8. Thermal emission spectrum of Jovian "Hot Spot" between 1700 and 2300 cm^{-1} recorded by Voyager in March 1979.

References

Conrath, B. J., Hanel, R. A., Kunde, V. G. and Prabhakara, C., "The Infrared Interferometer Experiment on Nimbus 3", J. Geophys. Res., Vol. 75, No. 30, pp. 5831-5856, 1970.

Conrath, B., Curran, R., Hanel, R., Kunde, V., Maguire, W., Pearl, J., Pirraglia, J., Welker, J. and Burke, T., "Atmospheric and Surface Properties of Mars Obtained by Infrared Spectroscopy on Mariner 9", J. Geophys. Res., Vol. 78, No. 20, pp. 4267-4278, 1973.

Deepak, A., ed. "Inversion Methods in Atmospheric Remote Sounding", Academic Press, 1977.

Hanel, R. and Conrath, B., "Interferometer Experiment on Nimbus 3: Preliminary Results", Science, Vol. 165, pp. 1258-1260, 1969.

Hanel, R., Schlachman, B., Clark, F. D., Prokesh, C. H., Taylor, J. B., Wilson, W. M., and Chaney, L., "The Nimbus III Michelson Interferometer", Appl. Opt., Vol. 9, No. 8, pp. 1767-1774, 1970.

Hanel, R. A., Schlachman, B., Rodgers, D., and Vanous, D., "The Nimbus 4 Michelson Interferometer", Appl. Opt., Vol. 10, pp. 1376-1381, 1971.

Hanel, R. A., Schlachman, B., Breihan, E., Bywaters, R., Chapman, F., Rhodes, M., Rodgers, D., and Vanous, D., "Mariner 9 Michelson Interferometer", Appl. Opt., Vol. 11, pp. 2625-2634, 1972.

Hanel, R. A., Conrath, B. J., Kunde, V. G., Prabhakara, C., Revah, I., Salomonson, V. V. and Wulford, G., "The Nimbus 4 Infrared Spectroscopy Experiment: 1. Calibrated Thermal Emission Spectra", J. Geophys. Res., Vol. 77, pp. 2639-2641, 1972a.

Hanel, R. A., Conrath, B. J., Hovis, W. A., Kunde, V. G., Lowman, P. D., Pearl, J. C., Prabhakara, C., Schlachman, B., "Infrared Spectroscopy Experiment on the Mariner 9 Mission: Preliminary Results", Science, Vol. 175, pp. 305-308, 1972b.

Hanel, R., Conrath, B., Hovis, W., Kunde, V., Lowman, P., Maguire, W., Pearl, J., Pirraglia, J., Prabhakara, C., Schlachman, B., Levin, G., Straat, P., and Burke, T., "Investigation of the Martian Environment by Infrared Spectroscopy on Mariner 9", Icarus, Vol. 17, pp. 423-442, 1972c.

Hanel, R., Conrath, B., Gautier, D., Gierasch, P., Kumar, S., Kunde, V., Lowman, P., Maguire, W., Pearl, J., Pirraglia, J., Ponnamperuma, C. and Samuelson, R., "The Voyager Infrared Spectroscopy and Radiometry Investigation", Space Science Reviews, Vol. 21. 129-157, 1977.

Hanel, R., Conrath, B., Flasar, M., Kunde, V., Lowman, P., Maguire, W., Pearl, J., Pirraglia, J., Samuelson, R., Gautier, D., Gierasch, P., Kumar, S. and Ponnamperuma, C., "Infrared Observations of the Jovian System from Voyager 1", Science, Vol. 204, 972-976, 1979a.

Hanel, R., Conrath, B., Flasar, M., Herath, L., Kunde, V., Lowman, P., Maguire, W., Pearl, J., Pirraglia, J., Samuelson, R., Gautier, D., Gierasch, P., Horn, L., Kumar, S., and Ponnamperuma C., "Infrared Observations of the Jovian System from Voyager 2", Science, Vol. 206, No. 4421, 952-956, 1979b.

Hanel, R., Crosby, D., Herath, L., Vanous, D., Collins, D., Creswick, H., Harris, C. and Rhodes, M., "Infrared Spectrometer for Voyager", Applied Optics, Vol. 19, pp. 1391-1400, 1980.

Kunde, V. G., and Maguire, W. C., "Direct Integration Transmittance Model", J. Quant. Spectrosc. Radiat. Transfer, Vol. 14, pp. 803-817, 1974.

Kunde, V. G., Conrath, B. J., Hanel, R. A. Maguire, W. C., Prabhakara, C. and Salomonson, V. V., "The Nimbus 4 Infrared Spectroscopy Experiment: 2. Comparison of Observed and Theoretical Radiances from 425-1450 cm^{-1}", J. Geophys. Res., Vol. 79, No. 6, pp. 777-784, 1974.

Maguire, W. C., "Martian Isotopic Ratios and Upper Limits for Possible Minor Constituents as Derived from Mariner 9 Infrared Spectrometer Data", Icarus, Vol. 32, pp. 85-97, 1977.

Pearl, J., Hanel, R., Kunde, V., Maguire, W., Fox, K., Gupta, S., Ponnamperuma, C., and Raulin, F., "Identification of Gaseous SO_2 and New Upper Limits for Other Gases on Io", Nature, Vol. 280, No. 5725, pp. 755-758, 1979.

Prabhakara, C., Rodgers, E. B., Conrath, B. J., Hanel, R. A., Kunde, V. G., "The Nimbus 4 Infrared Spectroscopy Experiment: 3. Observations of the Lower Stratospheric Thermal Structure and Total Ozone", J. Geophys. Res., Vol. 81, No. 36, pp. 6391-6399, 1976.

Wark, D. Q., and Hillary, D. T., "Atmospheric Temperature: Successful Test of Remote Probing", Science, Vol. 165, pp. 1256-1258, 1969.

Editors' Note: The tape recording of discussion following this talk was defective, and no transcript of Discussions is available.

Radiative Transfer and Remote Sensing

Barney J. Conrath (NASA/GSFC)

Introduction

Radiative transfer is the basic theoretical tool for the quantitative interpretation of planetary infrared spectra such as those discussed in the preceeding paper. It links the remotely sensed data to the properties of the atmosphere (composition, thermal structure, dynamics, etc.) which we wish to infer. This paper gives a brief overview of the remote sensing problem as it pertains to the interpretation of planetary spectra. The presentation is tutorial rather than exhaustive.

First, an outline will be given of the basic theoretical formulation generally used in calculating the spectral radiance from a planetary atmosphere, followed by a discussion of how this formulation is used in interpreting measured spectra, both through the use of model atmospheres and by means of inversion methods. The information content of spectral measurements will then be examined. Finally, examples of applications to planetary data will be presented.

The Remote Sensing Problem

Examples of thermal emission spectra of Jupiter measured by the Voyager infrared spectrometer (IRIS) are shown in Fig. 1 (Hanel et al., 1979). The remote sensing problem is basically that of using data such as these to infer information on the atmosphere of the planet. With a knowledge of line positions of candidate species, it may be possible to make qualitative identifications of many spectral features. However, to quantitatively infer information on thermal structure and the abundances and vertical distributions of gases, it is necessary to have a theoretical representation of the spectral radiance in terms of the relevant atmospheric parameters. Such a representation is provided through radiative transfer theory.

The spectral radiance $I_\nu(\mu)$ at frequency ν and emission angle $\cos^{-1}\mu$ at the top of a plane-parallel atmosphere can be obtained from solutions of the

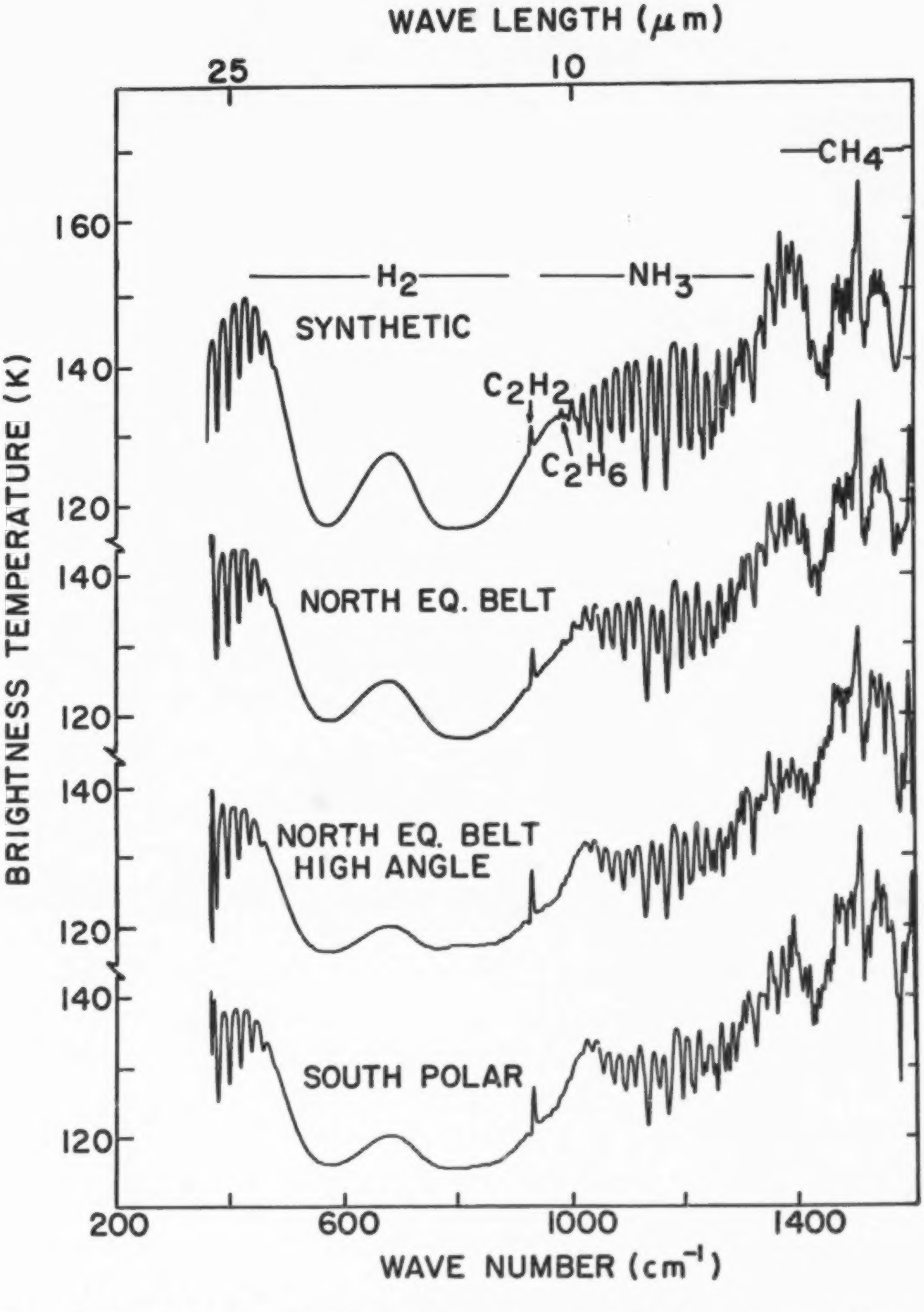

Figure 1. Spectra from selected areas on Jupiter obtained from the Voyager infrared spectroscopy experiment (Hanel, et al., 1979). A synthetic spectrum calculated from a model atmosphere is shown for comparison. Spectral features associated with several gaseous constituents are identified.

radiative transfer equation, which for purposes of this discussion can be written in the form

$$I_\nu(\mu) = \frac{\mu_o}{\pi} A_\nu F_\nu e^{-\left(\frac{1}{\mu_o} + \frac{1}{\mu}\right) \tau_\nu (z_b)}$$

$$+ \ (1-A_\nu) B_\nu (\theta_b) e^{-\tau_\nu (z_b)/\mu}$$

$$+ \int_{z_b}^{\infty} B_\nu [\theta(z)] \frac{\partial}{\partial z} [e^{-\tau_\nu(z)/\mu}]dz. \qquad (1)$$

The geometry is illustrated in Fig. 2. The solar flux F_ν is incident at the top of the atmosphere at solar zenith angle $\cos^{-1} \mu_o$. A_ν is the albedo of the lower boundary of the observable atmosphere (cloud or planetary surface), $\tau_\nu(z)$ is the perpendicular optical depth of the atmospheric column between altitude z and the top of the atmosphere, and the subscript b denotes values at the lower boundary. It has been assumed that local thermodynamic equilibrium (LTE) holds, and the source function is given simply by the Planck radiance $B(\theta)$ at the kinetic temperature θ. This assumption is reasonable for many applications involving medium resolution spectra, but with the advent of ultra-high resolution planetary spectroscopy such as heterodyne techniques, interesting non-LTE situations have been found. However, for simplicity, only cases for which LTE holds will be considered here.

The first term on the right hand side of equation (1) represents the contribution to the outgoing radiation of the direct solar flux reflected from the lower boundary, attenuated by absorption along the two-way path through the atmosphere. The second term is the thermal emission from the lower boundary at temperature θ_b, also attenuated by the atmospheric absorption. The third term represents the thermal emission from the atmosphere. The diffuse radiation field associated with particulate and molecular scattering would contribute additional terms to (1); however, these have been omitted in the interest of simplicity.

The radiance measured by an instrument with finite resolution can be related to the monochromatic radiance of (1) by

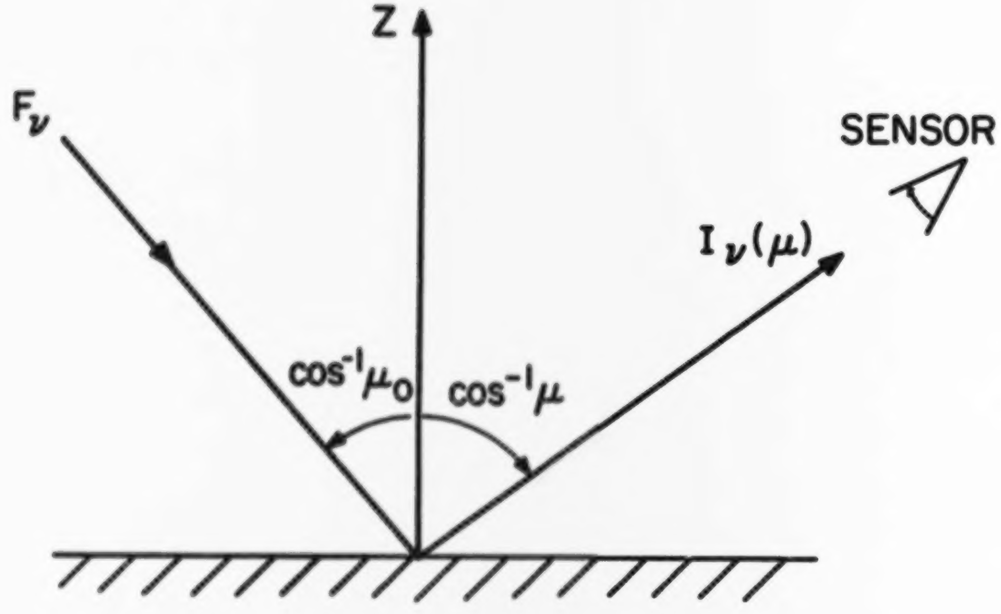
Z
F_ν
SENSOR
$I_\nu(\mu)$
$\cos^{-1}\mu_0$
$\cos^{-1}\mu$

Figure 2. Geometry of the radiative transfer formulation discussed in the text. The atmospheric radiance is measured at emission angle $\cos^{-1}\mu$ by a sensor above the atmosphere. The solar flux is incident at angle $\cos^{-1}\mu$.

$$I_{\bar{\nu}}(\mu) = \int_{\Delta\nu} \phi(\bar{\nu},\nu) I_{\nu}(\mu)\, d\nu \qquad (2)$$

where $\phi(\bar{\nu},\nu)$ is the normalized spectral response of the instrument, which defines a pass band of width $\Delta\nu$ with central frequency $\bar{\nu}$.

The physical parameter which links the state of the atmosphere to the measured radiance is the absorption coefficient $k(\nu)$. The optical depth for gaseous absorption is given by

$$\tau_{\nu}(z) = \int_{z}^{\infty} \sum_{i} k_i(\nu)\, \rho_i(z')\, dz' \qquad (3)$$

where k_i and ρ_i are respectively the absorption coefficient and density of the i-th gas, and the summation is taken over all optically active gases. The absorption coefficient for a molecular absorption band can generally be written in the form

$$k_i(\nu) = \sum_{j} S_{ij}\, f(\nu;\, \alpha_{ij},\, \nu_{ij}) \qquad (4)$$

where S_{ij} is the strength of the j-th line of the i-th gas, and ν_{ij} and α_{ij} are respectively the central frequency and half-width. The summation is taken over all lines which contribute to the absorption at frequency ν. Thus, to specify the absorption coefficient at a given point in the spectrum, it is necessary in principle to specify the strength, position and shape for every line of every constituent active in that portion of the spectrum. This of course is where laboratory and theoretical spectroscopy come into the picture.

For interpreting sufficiently low resolution measurements, it may be possible to use models of the gaseous transmittance which take into account only the average properties of the lines within an interval, but do not consider each line individually. As planetary measurements have become available at higher spectral resolution, increasing use has been made of direct line-by-line calculations. This requires a compilation of line parameters, usually on magnetic tape, which can be combined with information on line shape, and can then be inserted into equation (1) to calculate a synthetic spectrum from a given model atmosphere. The calculation involves summations over individual lines and constituents, integrations over atmospheric slant paths for essentially monochromatic radiation, and finally convolution with the instrument response function. This is a formidable computational problem. Although large amounts of computer time may be required, the problem is usually tractable.

To illustrate certain aspects common to most remote sensing problems, the specific problem of retrieving vertical temperature profiles of a planetary atmosphere from remotely measured infrared spectra will be considered. Let us assume the measurements are within an absorption band for which the atmospheric transmittance can be specified: that is, the vertical distribution of the relevant absorbers and their line strengths and widths are known. It will also be assumed that the reflected solar component and lower boundary emission terms in (1) are negligible. The theoretical expression for the measured radiance then becomes

$$I_{\bar{\nu}}(\mu) = \int_0^\infty B_{\bar{\nu}}[\theta(z)] \frac{\partial T_{\bar{\nu}}(\mu)}{\partial z} dz \tag{5}$$

where the atmospheric transmittance is defined as

$$T_{\bar{\nu}}(\mu) = \int_{\Delta\nu} \phi(\bar{\nu},\nu) e^{-\tau_\nu/\mu} d\nu, \tag{6}$$

and it has been assumed that the variation in the Planck function over the spectral interval $\Delta\nu$ is negligible. From a set of measurements of I as a function of $\bar{\nu}$ within the absorption band or as a function of emission angle $\cos^{-1}\mu$ or both, we would like to infer information on the temperature profile $\theta(z)$. For purposes of illustration we will consider here an inference based only on the dependence on $\bar{\nu}$. To estimate the sensitivity of $I_{\bar{\nu}}$ to $\theta(z)$, we shall consider perturbations $\Delta\theta(z)$ about a reference profile $\theta_o(z)$. The resulting perturbation of the measurements $\Delta I_{\bar{\nu}}$ is then given to first order by

$$\Delta I_{\bar{\nu}} = \int_0^\infty K(\bar{\nu},z) \Delta\theta(z) dz \tag{7}$$

where

$$K(\nu,z) = \left[\frac{dB_{\bar{\nu}}}{d\theta}\ \frac{dT_{\bar{\nu}}}{dz}\right]_{\theta_o(z)} . \tag{8}$$

The kernel or "weighting function" K is evaluated using $\theta_o(z)$, as indicated. Examples of weighting functions for Jupiter as given by Conrath and Gautier (1980) are shown in Fig. 3. Those with maxima at levels deeper than 100 mbar are associated with the S(0) and S(1) pressure induced hydrogen lines while the upper three correspond to selected points in the ν_4 CH_4 band centered near 1304 cm^{-1}. The calculations were made for a spectral resolution of 4.3 cm^{-1}. The weighting functions associated with strongly absorbing spectral regions peak higher in the atmosphere while those from regions of weaker absorption have maxima deeper in the atmosphere. Thus, a set of measurements from selected points in the spectrum can provide information on the thermal structure over a vertical range of the atmosphere which in this case extends from approximately 1 mbar down to 500 mbar.

A fundamental property of the radiative transfer process is illustrated in Fig. 3. The weighting functions are broad and strongly overlapping; thus, the radiative transfer process acts essentially as a low pass filter which prevents retrieval of fine scale information in the vertical structure. The high spatial frequency components are weakly represented in the measurements, and in the presence of realistic instrument noise they are inaccessible. The measurement process as it pertains to the remote sensing problem is illustrated schematically in Fig. 4. Information on the atmospheric structure and composition is degraded by the low pass filtering of the radiative transfer process and the introduction of instrumental noise and systematic errors. The problem then is to take advantage of whatever information is contained in the measurements of $I_{\bar{\nu}}$ while recognizing their intrinsic limitations.

Methods of Solution

The two general approaches to the inference of quantitative atmospheric information from measured thermal emission spectra are direct modelling and inversion. The basic objective of both approaches is of course the same, i.e., to find a set of physically meaningful atmospheric parameters which yield theoretical radiances in agreement with the measured radiances to within some specified level of tolerance. The philosophies of the two approaches are, however, somewhat different.

The direct modelling approach is illustrated schematically in Fig. 5. Several candidate models are defined based on plausibility, a priori information, etc. These models are used with the radiative transfer equation in direct calculations of synthetic spectra. These spectra are then compared with the measured spectrum, and a "best fit" is chosen based on some arbitrarily defined set of criteria. If necessary the chosen model may be fine tuned by introducing small changes in the parameters and repeating the procedure. An example of the comparison of model calculations with a Mariner 9 IRIS spectrum used to obtain water vapor abundance in the Martian atmosphere is shown in Fig. 6.

The inversion approach is illustrated schematically in Fig. 7. The measured radiances are introduced directly into the radiative transfer equation, forming an integral equation for the unknown atmospheric profile. An inversion algorithm is then used to solve the integral equation to obtain vertical profiles of temperature or composition. The limitations on the information content of the measurements can be analyzed and dealt with explicitly in the inversion approach. As discussed previously, the filtering action of the radiative transfer process surpresses information on small vertical scale structure in the profiles. As a result, the solutions are non-unique, in the sense that to any solution we can add high statial frequency components of arbitrary amplitude and still satisfy the integral equation to within the noise level of the measurements. For this reason all successful inversion algorithms introduce filtering constraints, either explicitly or implicitly, which exclude spurious high frequency components from the solutions. For a given set of weighting functions and known measurement noise level, formulations exist for the analysis of information content in terms of vertical resolution and error propagation (see for example Conrath, 1972; Twomey, 1977). Several inversion algorithms are currently in use for the analysis of remotely sensed data, but these will not be reviewed here. The interested reader is referred to inversion conference summaries

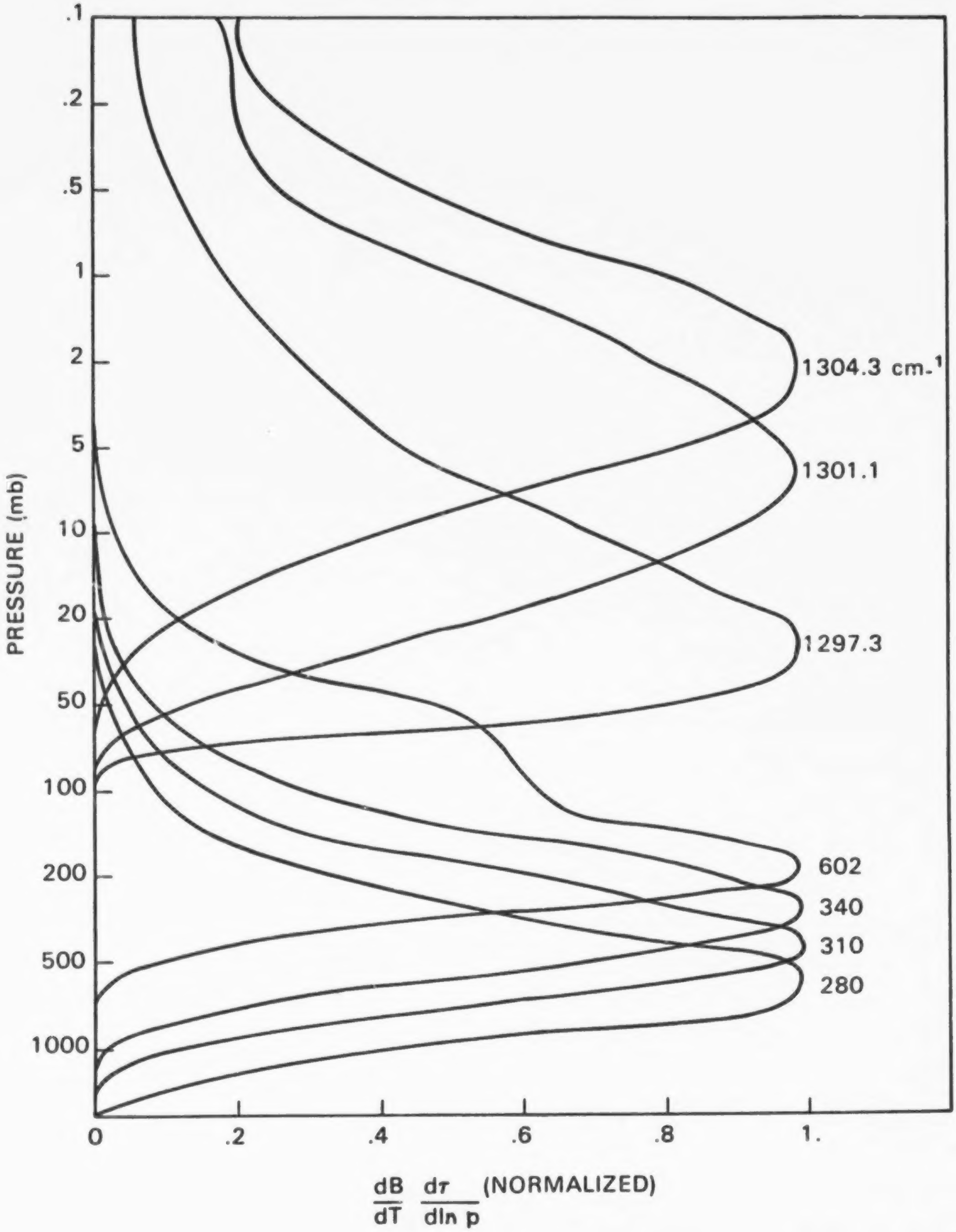

Figure 3. Weighting functions used for the retrieval of vertical temperature profiles on Jupiter from Voyager IRIS measurements (Conrath & Gautier, 1980). Those with maxima below 100 (mb) pertain to spectral intervals within the S(0) and S(1) pressure induced hydrogen lines. Those above 100 mb are from the ν_4 methane band.

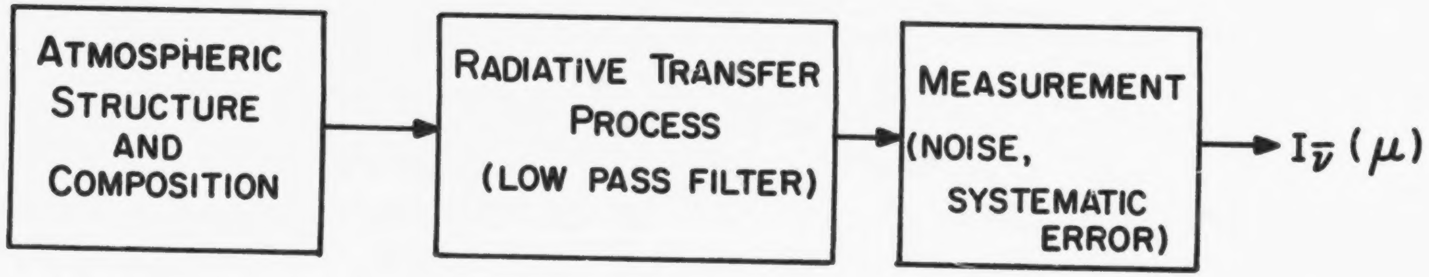
ATMOSPHERIC STRUCTURE AND COMPOSITION
RADIATIVE TRANSFER PROCESS (LOW PASS FILTER)
MEASUREMENT (NOISE, SYSTEMATIC ERROR)
$I_{\bar{\nu}}(\mu)$

Figure 4. Schematic of the measurement process as it pertains to the remote sensing problem. The radiative transfer process acts as a low pass filter on atmospheric structure, and the information content of the measurements is further degraded by noise and other instrumental effects.

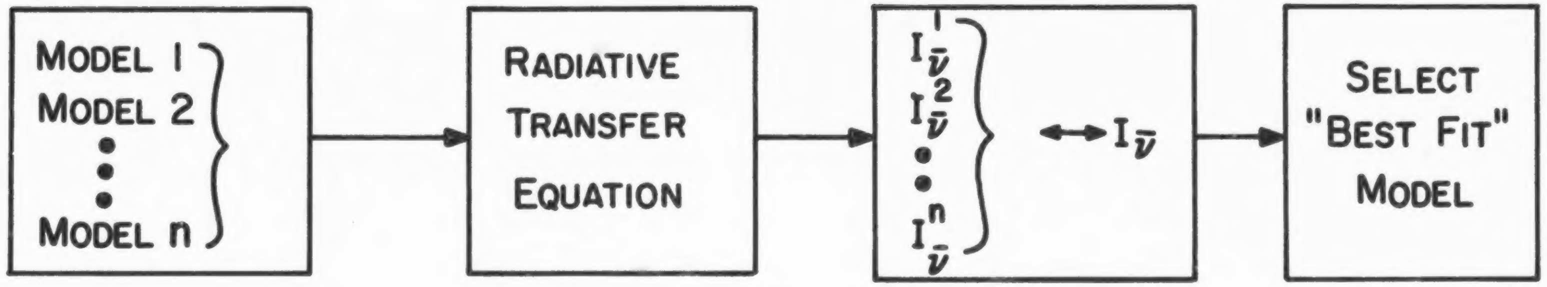
MODEL 1
MODEL 2
MODEL n
RADIATIVE TRANSFER EQUATION
$I_{\bar{\nu}}^{1}$
$I_{\bar{\nu}}^{2}$
$I_{\bar{\nu}}^{n}$
$I_{\bar{\nu}}$
SELECT "BEST FIT" MODEL

Figure 5. Schematic of the direct modelling approach to the retrieval of information from remote radiation measurements. A "library" of model atmospheres is used to calculate synthetic data which is compared with the measurements. On the basis of this comparison a best fit model is chosen.

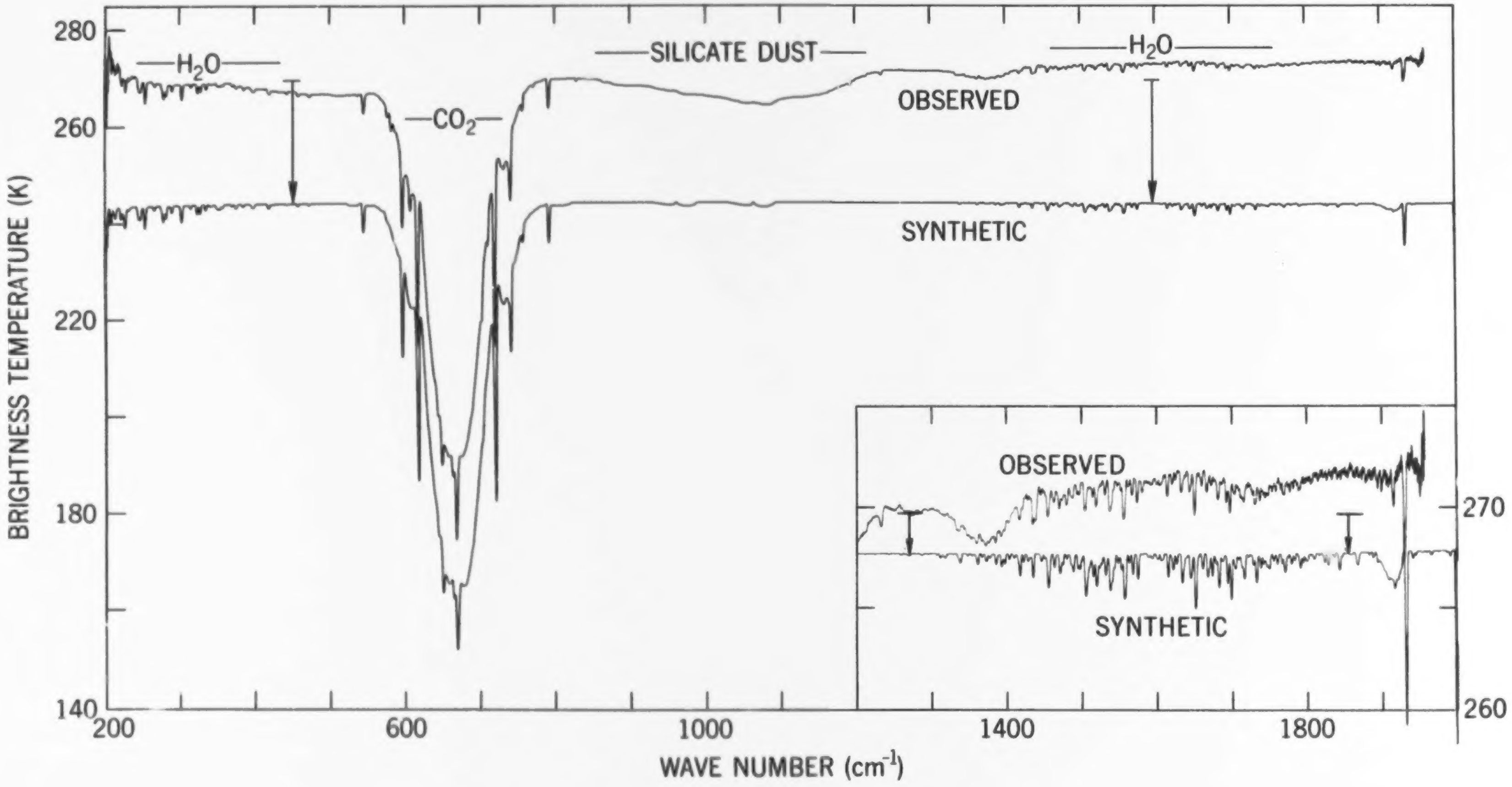

Figure 6. Example of the inference of water vapor abundance on Mars by comparison with synthetic data calculated from a model. The data in this case are from the Mariner 9 infrared spectroscopy experiment.

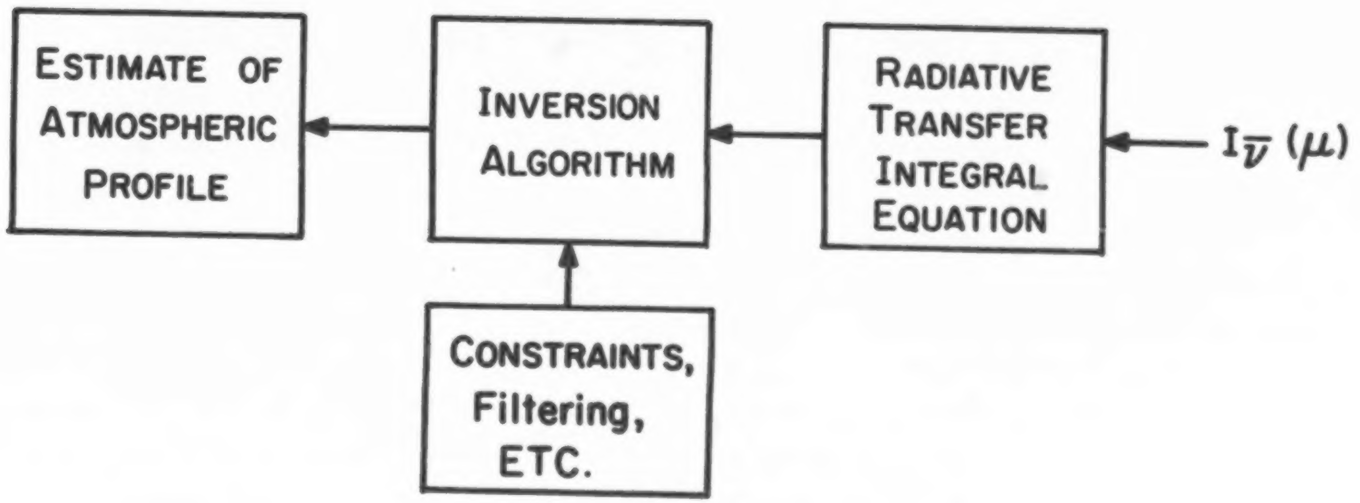
ESTIMATE OF ATMOSPHERIC PROFILE
INVERSION ALGORITHM
RADIATIVE TRANSFER INTEGRAL EQUATION
$I_{\overline{\nu}}(\mu)$
CONSTRAINTS, Filtering, ETC.

Figure 7. Schematic of the inversion approach to the retrieval of information from remote radiation measurements. The measured radiances are employed in an integral equation which is then solved. To prevent spurious features in the solution, the algorithm makes use of appropriate constraints based on a knowledge of the filtering introduced by the radiative transfer process and the instrument noise level (see Figure 4).

edited by Colin (1972) and by Deepak (1976) which contain review papers on the various techniques. Examples of Jovian temperature profiles retrieved from Voyager IRIS data are shown in Fig. 8.

Both the direct modelling and inversion approaches are extensively used. The inversion technique has found its widest application in the inference of atmospheric thermal structure and to a lesser extent in the retrieval of gaseous profiles. Direct modelling is especially useful in situations where the formulation of an explicit integral equation may be difficult or inconvenient, eg., in the inference of information on haze or cloud particles. With either approach it is imperative that the limitations on the information content of a given set of measurements be fully understood, otherwise, serious misinterpretation of the data may result.

Concluding Remarks

The use of radiative transfer theory for the quantitative interpretation of planetary spectra, both by direct modelling and through inversion techniques, requires a knowledge of gaseous absorption coefficients appropriate to the spectral region employed. It is not possible to make general statements concerning the uncertainties in the absorption coefficients which can be tolerated in remote sensing applications. Rather this question must be treated on a case-by-case basis. The sensitivity of temperature retrievals to absorption coefficient errors depends on the atmospheric lapse rate, the temperature range, and the spectral region. For example the inference of upper stratospheric temperatures from measurements within the Q-branch of the ν_4 CH_4 band is relatively insensitive to absorption coefficient errors because of the low lapse rate in this portion of the atmosphere. However, the use of the P- or R-branches of this band to infer C/H puts greater demands on absorption coefficient accuracy. In any event, determination of sensitivity to absorption coefficient errors should form a part of any complete remote sensing analysis, along with determination of information content of the measurements.

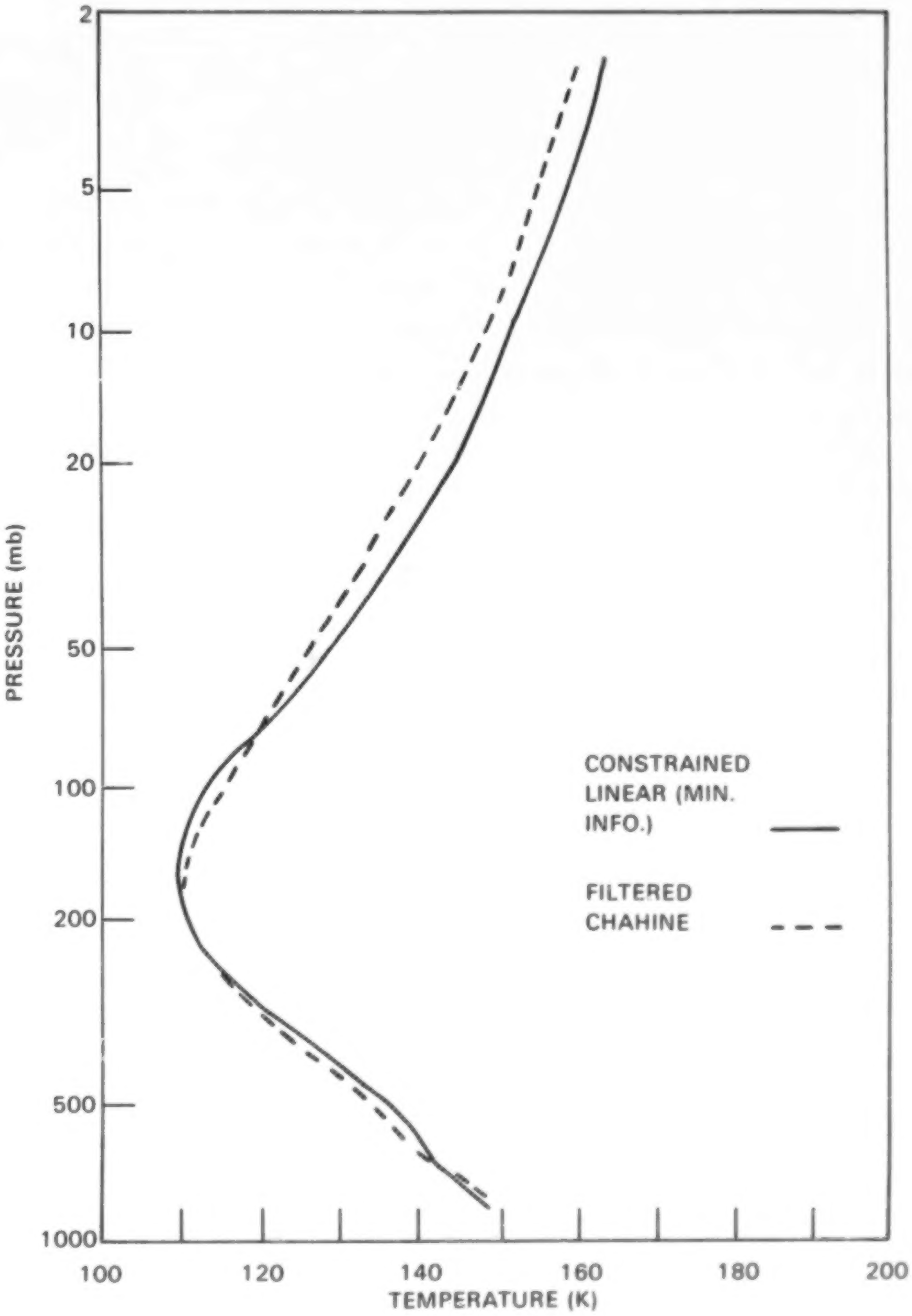

Figure 8. Examples of temperature profiles on Jupiter retrieved by inversion of Voyager IRIS measurements (Conrath & Gautier, 1980). The same data were inverted using two different algorithms as indicated.

References

Colin, L., editor, Proceedings of a Workshop on the Mathematics of Profile Inversion, NASA TM X-62, 150 (1972).

Conrath, B. J., Vertical resolution of temperature profiles obtained from remote radiation measurements, J. Atmos. Sci., 29, 1262 (1972).

Conrath, B. J., and D. Gautier, Thermal structure of Jupiter's atmosphere obtained by inversion of Voyager 1 infrared measurements, in Remote Sensing of Atmospheres and Oceans, A. Deepak, editor, Academic Press, New York (1980).

Deepak, A., editor, Inversion Methods in Atmospheric Remote Sounding, Academic Press, New York (1977).

Hanel, R. A. et al., Infrared observations from the Jovian system from Voyager 1, Science, 204, 972 (1979).

Twomey, S., Introduction to the Mathematics of Inversion in Remote Sensing and Indirect Measurements, Elsevier, Amsterdam (1977).

RAYLEIGH, RAMAN AND PARTICULATE SCATTERING

William D. Cochran
Astronomy Department and McDonald Observatory
University of Texas
Austin, TX 78712

In analyzing the visible and near infrared spectra of planetary atmospheres, it is absolutely essential to consider the multiple scattering of photons within the atmosphere. Within this spectral region, virtually all of the photons detected are solar photons which have been scattered by the gas and particles in the planetary atmosphere. This is seen clearly in Figure 1 which shows the incident and emitted fluxes for a hypothetical planet with an effective temperature of 100 K. Here I have plotted λB_λ vs log λ so the area under the curve is proportional to the total flux. For this hypothetical planet, which radiates the same amount of energy it receives, all of the light at wavelengths less than about 8 microns is scattered solar light. For a planet like Jupiter, the dividing point between scattered solar flux and emitted thermal flux is at a somewhat shorter wavelength since Jupiter radiates about twice the energy it receives from the sun and has an effective temperature of 125 K.

In order to begin to understand the information contained in the absorption spectrum of a planetary atmosphere we must first understand the various scattering processes these photons undergo within the atmosphere. There are three different physical processes we must worry about: Rayleigh scattering and Raman scattering by the gas molecules, and scattering by any cloud or dust aerosol particles in the atmosphere.

Let us briefly examine the physics of each of these processes.

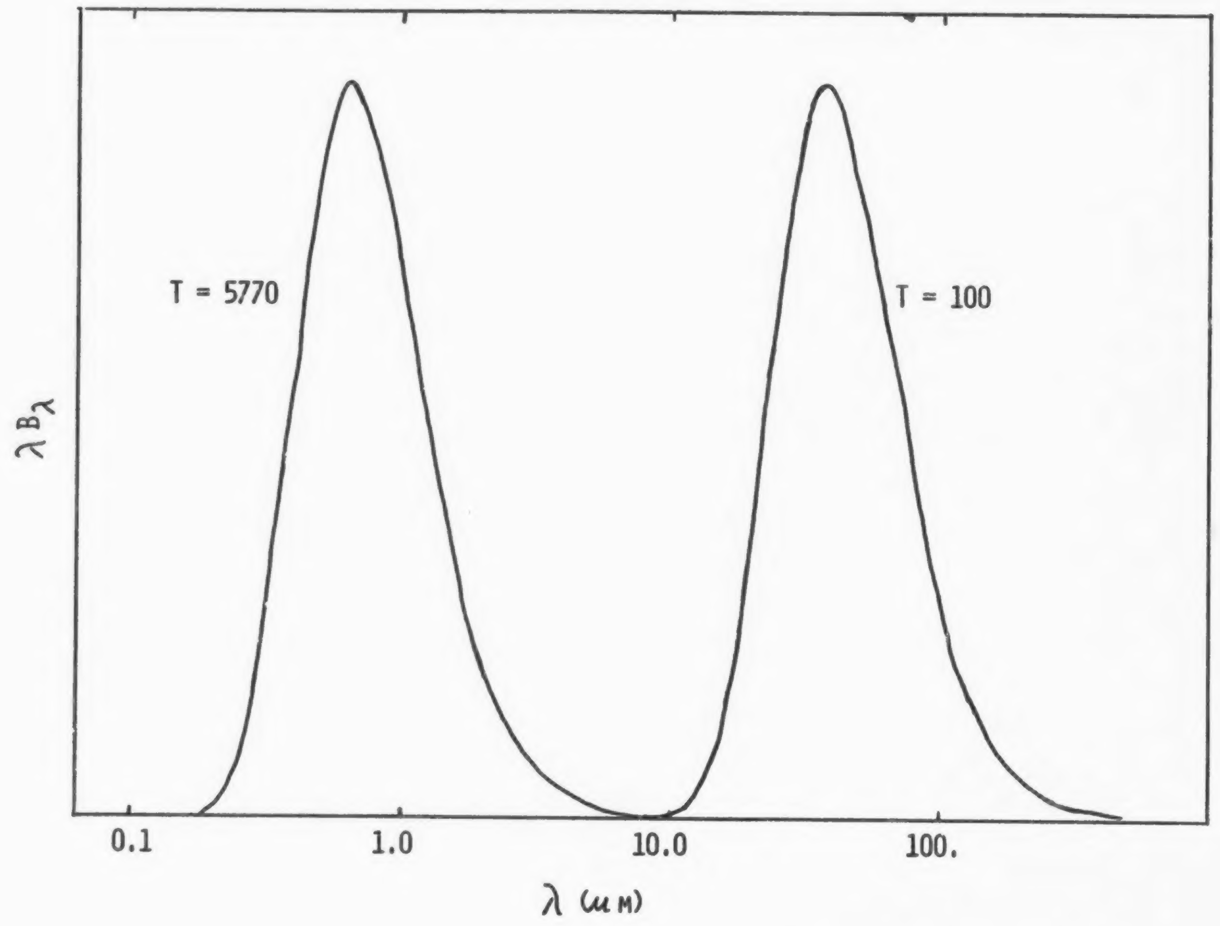

Figure 1. Incident and emitted fluxes of solar photons for a hypothetical planetary atmosphere with an effective temperature of 100 K.

Rayleigh Scattering

Rayleigh scattering is the scattering of radiation at a nonresonance frequency by any system which possesses an electric dipole polarizability. The size of the cross section depends on the polarizability of the particle within the radiation field, and thus depends on the index of refraciton. The classical Rayleigh scattering cross section is given in Table 1. We note that there is a λ^{-4} dependence of the cross section on wavelength. This increase in cross section with decrease of wavelength does not, of course, continue indefinitely. The scattering cross section will level off at a value of twice the geometric cross section as the wavelength approaches the physical dimension of the particle. Rayleigh scattering will result in some absorption if there is an imaginary part of the index of refraction.

On the lower part of the table we see the Rayleigh scattering cross section for molecular hydrogen given by Victor, Browne, and Dalgarno (1967, Proc. Phys. Soc., 92, 42). The constant terms are the same as for particles, but Victor et al. are able to calculate the polarizability and anisotropy as a function of wavelength. Similar calculations have also been made by Ford and Browne (1973, Atomic Data, 5, 307).

The Rayleigh scattering cross section for a molecule is fairly small, but for a deep atmosphere or for ultraviolet radiation, Rayleigh scattering can be a significant effect. A good rule of thumb is that the molecular hydrogen Rayleigh scattering optical thickness at 4000Å is about 0.01 per km-amagat. Table 2 shows the Rayleigh scattering optical thickness per kilometer-amagat of several common gases.

Table 1
Rayleigh Scattering

FOR PARTICLES:

$$\sigma_S = \frac{128\,\pi^5}{3\,\lambda^4}\;A^6\left|\frac{M^2-1}{M^2+2}\right|^2$$

$$\sigma_A = -\;\frac{8\,\pi^2\,A^3}{\lambda}\;\mathrm{IM}\left(\frac{M^2-1}{M^2+2}\right)$$

M = INDEX OF REFRACTION

A = PARTICLE RADIUS

FOR H_2

$$\sigma = \frac{128\,\pi^5}{9\,\lambda^4}\left(3\alpha(\lambda)^2 + \frac{2}{3}\gamma(\lambda)^2\right)$$

α = POLARIZABILITY

γ = ANISOTROPY

Table 2
Rayleigh Scattering Optical Thickness per Kilometer-Amagat

λ(A)	H_2	He	CH_4	CO_2	N_2	Ar
2000	0.1520	0.0094	1.3632	1.5604	0.6944	0.6256
4000	0.0095	0.0006	0.0852	0.0975	0.0434	0.0391
6000	0.0019	0.0001	0.0168	0.0193	0.0086	0.0077
8000	0.0006	-	0.0053	0.0061	0.0027	0.0024
10000	0.0002	-	0.0022	0.0025	0.0011	0.0010

Raman Scattering

Raman scattering is an incoherent nonresonance scattering of photons. An incident photon of frequency ν_0 is scattered and emerges at frequency $\nu_0 + \Delta\nu$ where $\Delta\nu$ is the frequency of the Raman transition of the molecule. The cross sections for rotational and vibrational Raman scattering by H_2 are shown in Table 3. We see the same λ^{-4} dependence on wavelength as in Rayleign scattering. This is to be expected since the physical processes are very similar.

Brinkmann (1968, *Ap. J.*, **154**, 1087) first realized that Raman scattering could have a detectable influence on a planetary spectrum when he identified rotational Raman scattering by N_2 and O_2 as the cause of the filling in of Fraunhofer lines in the spectrum of the Earth's daytime sky. Since then, several papers have been published by various authors discussing the influence of Raman scattering on the visible spectra of the planets. Raman scattering fills in the cores of the solar lines and causes Raman shifted ghosts of the solar spectrum to appear in the planetary spectrum. It also has a strong influence on the shape of the UV albedo curve.

Particulate Scattering

Scattering by anything other than molecules or very small particles is lumped into the category of aerosol scattering. This includes scattering by dust or haze particles as well as condensate and chemical cloud crystals or droplets. Aerosol scattering is the dominant source of scattering in most of the planetary atmospheres, and yet it is the process we understand the least. We have no way of predicting, *a priori*, the scattering properties of most of the cloud or dust layers we may expect in a planetary atmosphere. In fact, we have to turn the problem around and use the observational data to place constraints on the

Table 3
Raman Cross Sections for H_2

S (J) $$\sigma(J \rightarrow J+2, \lambda) = \frac{128\pi^5}{9\lambda'^4} \frac{(J+1)(J+2)}{(2J+3)(2J+1)} \gamma(\lambda)^2$$

O (J) $$\sigma(J \rightarrow J-2, \lambda) = \frac{128\pi^5}{9\lambda'^4} \frac{J(J-1)}{(2J-1)(2J+1)} \gamma(\lambda)^2$$

VIBRATIONAL $$\sigma(V \rightarrow V+1, \lambda) = \frac{128\pi^5}{9\lambda'^4} \left[3\alpha'(\lambda)^2 + \frac{2}{3}\gamma'(\lambda)^2\right] \frac{(V+1)h}{8\pi^2 \mu \nu_E}$$

scattering properties of the aerosols. From these scattering properties we try to determine the physical characteristics of the aerosols.

There are two major methods of incorporating aerosol scattering in radiative transfer calculations. The first is to assume an aerosol single scattering albedo and a convenient functional form of the scattering phase function. The phase function is then expanded in either Legendre polynomials or a Fourier cosine series, depending on the radiative transfer calculation scheme. The most popular functions are shown in Table 4.

The simplest and unfortunately a quite commonly used phase function is the isotropic case. The great advantage of this phase function is that many radiative transfer problems may be solved analytically and be reduced to Chandrasekhar X and Y functions. The disadvantage is that it is unrealistic. There is no particle in nature that I know of which scatters isotropically.

The easiest way to add some anisotropy to the phase function is to add a cosine Θ term. This is sometimes called the Euler phase function. This phase function is easy and convenient to use, but has the disadvantage that it cannot represent strongly anisotropic scattering. The maximum value of the asymmetry parameter (the mean value of the scattering angle, Θ) is only 1/3.

One of the most commonly used phase functions was developed by Henyey and Greenstein (1941, Ap. J., **93**, 70) in a study of interstellar grains. It has a somewhat complicated functional form, but the asymmetry parameter G may vary all the way from 0 to 1. The major disadvantage of this phase function is that it is strongly forward scattering, with no backscattering lobe. This problem is easily alleviated by using a simple linear combination if two Heyney-Greenstein functions, one with positive G and the other with negative G. This will result in both forward- and back-scattering lobes in the phase function.

Table 4
Scattering Phase Functions

1) ISOTROPIC

$$P(\theta) = 1$$

2) EULER

$$P(\theta) = 1 + X \cos(\theta)$$

$$0 \leq X \leq 1$$

$$\langle \cos\theta \rangle = X/3$$

3)
A) HENYEY - GREENSTEIN

$$P(\theta, G) = \frac{1 - G^2}{(1 + G^2 - 2G\cos(\theta))^{3/2}}$$

$$0 \leq G \leq 1$$

$$\langle \cos(\theta) \rangle = G$$

B) DOUBLE HENYEY - GREENSTEIN

$$P(\theta, G_1, G_2) = A P(\theta, G_1) + B P(\theta, G_2)$$

$$A + B = 1$$

$$G_1 G_2 < 0$$

Tomasko, West, and Castillo (1978, Icarus, 33, 558) have found this double Henyey-Greenstein function to be quite useful for parametrizing the scattering properties of the clouds of Jupiter.

The second approach in dealing with aerosol scattering is to assume the physical characteristics of the particles and then to calculate the phase function for these particles. The usual technique here is to guess at the index of refraction and particle size distribution and then use Mie theory to calculate the single scattering albedo, phase function and, if polarization is included in the calculations, the Stokes parameters. The index of refraction and size distribution are then adjusted so that the calculated model will fit the observed data. The use of Mie scattering makes the assumption that the scattering particles are spheres. This is probably a valid assumption for Venus, but it is quite doubtful for the outer planets and Titan.

Scattering Models

1) Reflecting Layer Model

How do we incorporate these various types of scattering into our radiative transfer models? The easiest way is to simply ignore all of the scattering. This is known as the reflecting layer model. In this model, a clear gas layer in which Rayleigh and Raman scattering are not considered sits above a reflecting surface. This surface is considered to be the top of a dense cloud deck or the actual surface of the planet. The only interaction of photons with the gas is molecular absorption. This is a very simple model that we can all easily compute with a hand calculator. The only problem is that when we apply it to any body in the solar system which we know definitely has an atmosphere, the reflecting layer model does not work. In the case of Venus and the outer planets it fails miserably. It gives the wrong variation of equivalent widths with position on the disk and solar phase angle. The gas abundances derived depend on the strength of the feature observed. The reflecting layer model even gives incorrect results for the thin atmosphere of Mars. We have learned by bitter experience that scattering must be included in the analysis of spectra of any planetary atmosphere. The only excuse for publishing a reflecting layer model today is to place upper limits on possible atmospheres of bodies such as Triton and Pluto.

2) Inhomogeneous Models

Now that we have been forced to include multiple scattering in our models, how do we go about doing it? It is possible to analytically calculate homogeneous multiple scattering models using many of the techniques developed by Chandrasekhar. Unfortunately, most planetary atmospheres are strongly inhomogeneous. We can have clear gas layers which fade into clouds, which then end at some altitude, etc. Fortunately, with the wide availability of large, high-speed scientific computers we may now calculate radiative transfer models of atmospheres with virtually any vertical inhomogeneity. There are a large variety of different radiative transfer techniques in use: doubling and adding, Monte Carlo, invariant imbedding, and Markov chains to name a few. FORTRAN programs have been published for many of these methods, and tested codes may be easily obtained for most of them. In fact, these codes are so widely available now that there is little excuse for not using some sophisticated radiative transfer technique.

It should be fairly evident that these inhomogeneous anisotropic scattering models have a large number of free parameters. We must specify the abundances of all of the gases, as well as the position, optical thickness, single scattering albedo, and phase function of all of the cloud layers. Obviously, a single spectrum can not constrain all of these parameters simultaneously. We must use a wide variety of data to constrain our models.

The largest difficulty in interpreting spectra is trying to simultaneously constrain both the gas abundances and the cloud scattering parameters. In order to illustrate this point, I would like to present the results of some calculations we have recently made of the profile of the 6190Å methane band in the Jovian atmosphere. Figure 2 shows the variation of the equivalent width of the band as a function of optical thickness of the upper ammonia cloud. Curves are shown for four different methane mixing ratios ranging from the value expected from a solar C/H ratio to four times that value. We can easily get the same equivalent width for this band by having a large methane abundance and a thick cloud or by having a low methane abundance and a thin cloud. In fact, since these curves turn over at low τ, a given methane abundance may result in the same equivalent width for two different optical thicknesses.

If we consider the cloud single scattering albedo instead of the optical thickness, we have a similar problem as shown in Fig. 3. We can obtain a desired equivalent width with a bright cloud and a low methane abundance or with a darker cloud and a higher methane abundance.

A single measurement of the equivalent width of the band will tell us nothing about the methane abundance or the cloud scattering properties. Additional data is needed to constrain one or the other of these properties of the atmosphere. Such additional data could be a continuum limb darkening curve or observations of the center-to-limb variation of the band. With the large number of free parameters, we must analyze a great deal of observational data to constrain a full inhomogeneous scattering model.

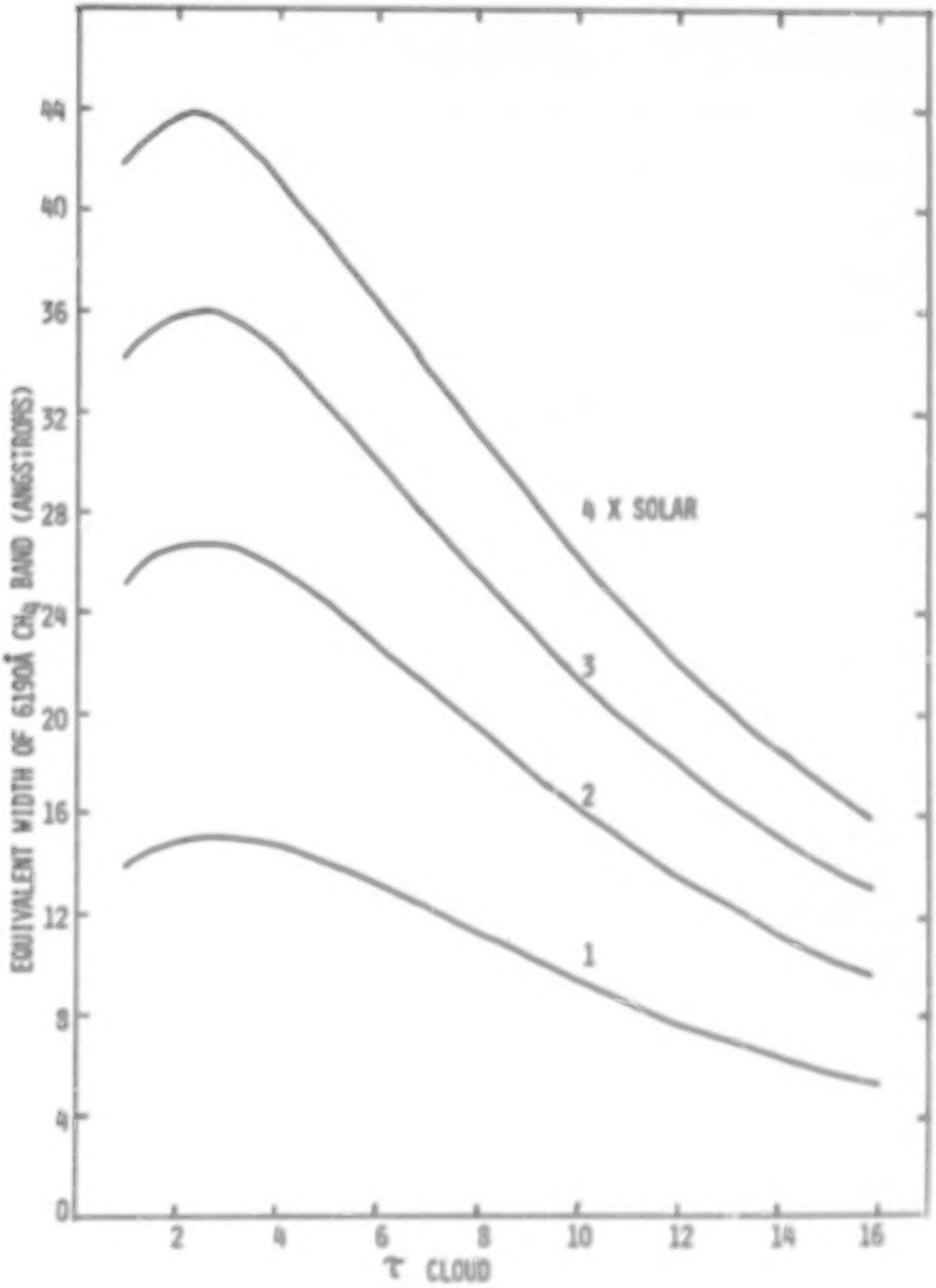

Figure 2. Variation of equivalent width of 6190A CH_4 band as function of optical thickness of NH_3 cloud in Jovian atmosphere.

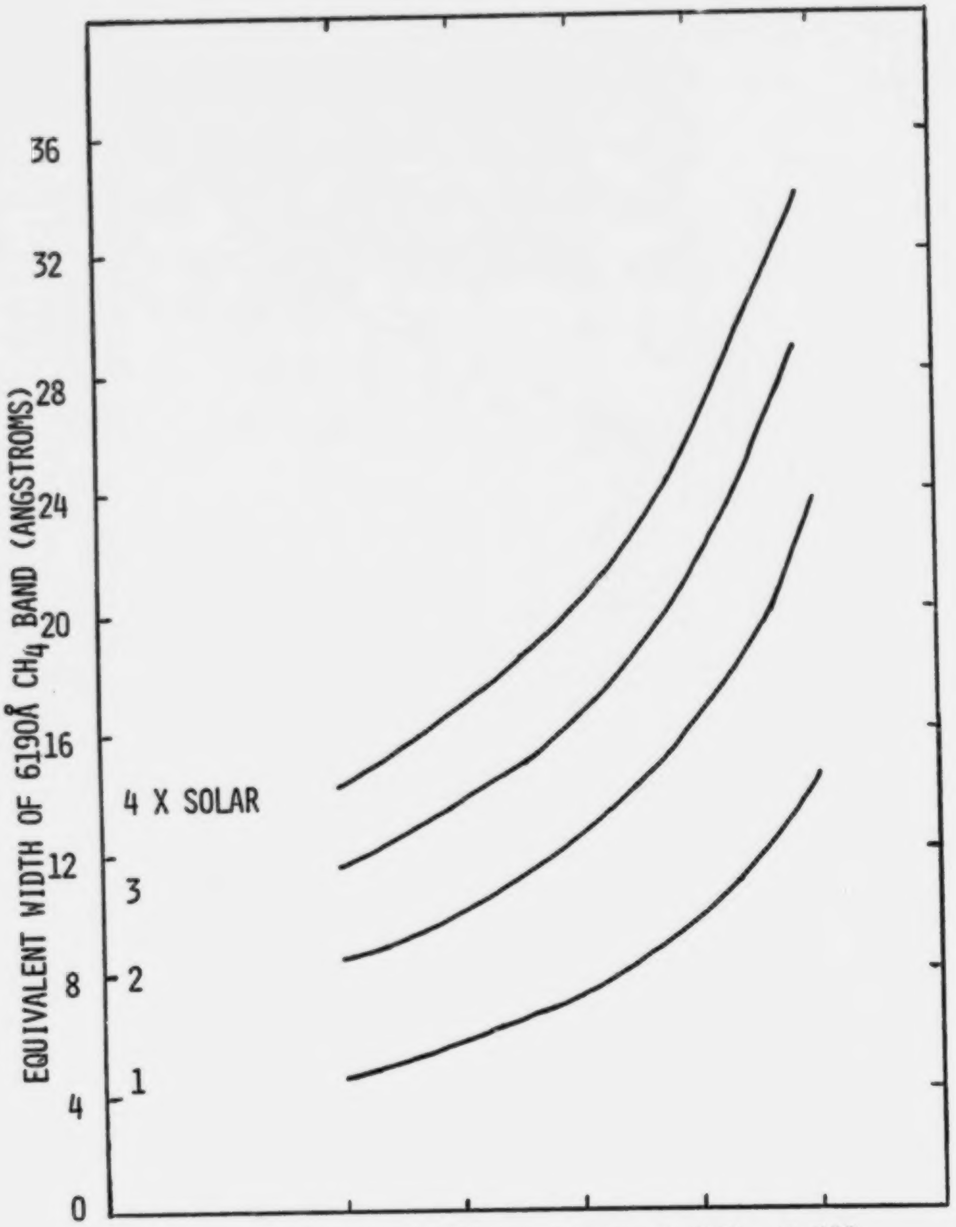

Figure 3. Variation of equivalent width of 6190A CH_4 band as function of NH_3 cloud single scattering albedo in Jovian atmosphere.

The method we have just discussed works quite well if our goal is to determine the cloud scattering structure as well as the gas abundances of a planetary atmosphere. An excellent example of this type of thorough analysis is the recent study of the Jovian atmosphere by Sato and Hansen (1979, J. Atmos. Sci., 36, 1133). We should note that abundances determined in this manner are still model dependent. We certainly use all available data to constrain the models, but we are still bound by the limitations of that model.

Alternative Models

The calculation of a full inhomogeneous scattering model clearly requires a large amount of data and is a lot of work. However, our goal is not always to derive a new model for the atmosphere. Often, we wish to determine the abundance of a newly detected atmospheric constituent, or we wish to use new laboratory data to redetermine the abundance of some gas. For these investigations, there is no point in calculating a full inhomogeneous scattering model. Our new data will not tell us anything new about the cloud structure.

One approach to this type of problem is to assume someone else's published cloud structure model and then calculate the abundance of the gas in question. This is a perfectly valid approach, but it does have a few drawbacks. First, the derived abundance is still model dependent. Secondly, no matter how fully and carefully you justify your selection of a particular model, there will probably be disagreement as to which published model is the best.

An alternative approach which avoids these problems was recently summarized by Combes and Encrenaz (1979, Icarus, 39, 1). They describe a method of deriving abundance ratios which completely detours the entire process of calculating a scattering model. This method has been used in various forms by several different investigators.

Let us consider two lines or bands formed by two different absorbers. If these two lines or bands are properly chosen and fulfill a set of four conditions, then a ratio of the abundances of these two absorbers may be derived which is valid regardless of the scattering process involved. The four conditions we impose guarantee that the scattering process has been the same for both lines and that the only difference between the lines is the abundance of the absorber.

The four conditions are shown in Table 5. The first condition is that the lines or bands considered be at the same, or nearly the same, wavelength. As we saw earlier, the Raman and Rayleigh scattering cross sections have a λ^{-4} dependence. Particulate scattering cross sections usually vary about as λ^{-1}. This first condition insures that the scattering cross sections will be about the same at the wavelength of the two features considered.

The second condition requires that we compare features of equal strength. This is the most crucial of the four conditions. It requires that the two lines fall at the same position on the curve of growth. Multiple scattering within a planetary atmosphere has a strong influence on the shape of the curve of growth. Weak lines are more affected by multiple scattering than are strong lines. For weak lines the photon may be scattered several times before a molecular absorption occurs. For strong lines, the absorption usually occurs on the first scattering. This condition guarantees that the photon mean free path has been the same for both lines.

The third condition is that the abundance ratio of the two gases, which is what we want to determine, is constant with altitude in the visible portion of the atmosphere. The species under study should not be condensable, or if they are both condensable they should follow the same depletion law. In other words, determination of an ammonia to hydrogen ratio on Jupiter is risky, but measuring $^{15}NH_3/^{14}NH_3$ is allowed.

Table 5
Combes and Encrenaz Conditions for Determining Abundance Ratios

1) LINES OR BANDS AT THE SAME WAVELENGTH

2) LINE DEPTHS MUST BE THE SAME

3) N_1 / N_2 CONSTANT WITH ALTITUDE

4) α_1 / α_2 CONSTANT WITH ALTITUDE

$$1, 2, 3, 4 \Rightarrow N_1 \alpha_1 = N_2 \alpha_2$$

$$\text{OR} \quad N_1 / N_2 = \alpha_2 / \alpha_1$$

The fourth condition is that the ratio of the two absorption coefficients is constant with altitude. This means that the line formation processes must have the same dependence on pressure and temperature. This is usually satisfied fairly well at line centers, as long as we are not considering pressure induced lines.

Of these four conditions, the second and the third are the most important. Reasonable deviations from the first and the fourth will not invalidate the conclusions. If these four conditions are met, the abundance ratio we wish to determine is just the reciprocal of the ratio of the absorption coefficients.

Conclusions

From all of these examples, we have seen that line formation in the visible spectra of the planets is dominated by multiple scattering in inhomogeneous atmospheres. The physics of some of the scattering processes such as Rayleigh and Raman scattering is well understood. Scattering by aerosol particles may be treated only by a parametrization process. Techniques exist for making radiative transfer calculations in vertically inhomogeneous atmospheres with anisotropic scattering. These atmospheres may be either plane parallel or spherical. Little progress has been made on including horizontal inhomogenieties in the calculations. A large amount of data is needed to constrain these multiple scattering models. For the much more limited goal of determining abundance ratios, we do not need to calculate such a fancy model. By adhering to a set of conditions which guarantee that the scattering has been the same for both lines in question, a model independent abundance ratio may be calculated directly.

This work has been supported by NASA Grant NGR 44-012-152.

Discussion

Comment (L. Wallace): It seems to me that Combes and Encrenaz have left out a fifth condition: that the line shapes should be the same. The mathematics screws up totally if you try to compare hydrogen quadrupole lines which are pressure narrowed with methane lines which are pressure broadened.

Response: That condition is folded in here, "the line formation process must be the same," so that would include line profiles.

Comment (L. Wallace): So this technique would basically be limited to methane isotopes.

Response: In their paper, they go through an argument for deriving ratios against ammonia. I'm not sure it is correct but they word it fairly convincingly. The method is for isotopes, or any other new constituents we may detect in the future. But in the visible part of the spectrum, you are right: all we can really see is methane, ammonia and hydrogen, unfortunately.

Comment (A. Goldman): Is it possible to get a new continuum from the Rayleigh and Raman scattering?

Response: Rayleigh and Raman scattering will determine the shape of the continuum quite definitely, for the ammonia bands in the ultraviolet. In fact, Raman scattering causes a peak in the albedo near 2400Å due to the shape of the solar spectrum.

Comment (R. Beer): I agree with Lloyd Wallace's comment. There are very few species for which the Combes and Encrenaz method is applicable. For all the really interesting species you want to look at, you don't really have a way of solving the problem. I also want to ask a question. It's been proposed that on Venus there is a haze of very, very small particles, called mode 0, and this wonderful haze somehow or other is much more strongly absorbing in the infrared than in the visible. How does that go along with this strong wavelength dependence? The particle sizes are supposed to be hundredths of a micron or 100 angstroms plus.

Response: For scattering by visible light, particles of that size would be in the Rayleigh regime.

Comment (R. Beer): Well, what they're telling us is exactly the reverse.

Response: I think that's probably telling us something about these particles; they may perhaps not be of that size. It is hard to get the scattering properties of aerosol particles to differ drastically between the infrared and the visible, because the scattering cross-sections just don't vary that fast.

Comment (M. Tomasko): You normally think that if a particle is not very important in the visible, then it's even less important at longer wavelengths, in the infrared. But that is true only if you have approximately the same index of refraction in both regions. Some species, like sulphuric acid, have whopping imaginary parts in the infrared but don't do much in the visible. That's one way you can make it work. There are a lot of other objections to these small particles, but at least in principle you can have stronger scattering in the infrared.

Response: Yes, you can change the absorption coefficient by adjusting the imaginary part of the index of refraction, even though the scattering cross section isn't going to vary much.

Comment (M. Mumma): Your very elegant talk seemed to me a pretty damning indictment against the abundance determinations in the visible.

Comment (L. Wallace): That is absolutely right.

Comment (M. Mumma): You are saying that you really want to go as far into the infrared as feasible.

Comment (L. Wallace): We only want to do that until we learn the problems in that region.

Comment (M. Mumma): There certainly will be problems there, but the Rayleigh scattering problem will be absent.

Response (W. Cochran): I don't think that spectroscopy in the visual region is as hopeless as you seem to feel it is. I agree that it is difficult to determine model-independent abundances from visible spectra. What you really determine from the visible spectra are the cloud scattering properties, since cloud scattering is dominating all that can be seen. In the infrared, where the scattering is due to molecular rather than aerosol processes, we may learn about the abundance, temperature, and pressure of gas. In order to fully understand the structure of an atmosphere, we must study both the aerosol and gas properties.

Comment (G. Orton): I'd like to make the same point. I'm not sure I believe any scattering models or abundance determinations made on the basis of the analysis of near-visible spectra, unless we know what the real temperature dependence of all these things are.

Comment (B. Lutz): Switching from the visible to the infrared is not necessarily a panacea; as soon as you do that, you don't know what the continuum is. You don't know where you are, until you start model fitting everything.

Response: I agree. You still end up with model-dependent abundances in the infrared.

Comment (J. Caldwell): A couple of comments on what people have said. I came to the same conclusion that Mike Mumma stated: the visible is a tough place to work. If you go into the ultraviolet, you can handle Rayleigh scattering. If you go into the infrared, there are advantages you can at least attempt to apply. In this connection, the 10-micron spectra of Saturn and Titan are instructive. On those two planets the continuum seems to be quite depressed with respect to the emission bands from the stratosphere, even more so than on Jupiter. On both these planets there is an immense ethane emission feature, methane sticks up quite nicely above the continuum, and on Titan you can even see traces of ethylene. When you are dealing with the emission from the stratosphere there is a good chance that you are away from particle scattering effects, although the absolute abundance that you derive depends on the temperature profile, as Barney Conrath illustrated in his talk yesterday. Relative abundances in that regime, between species like ethylene, ethane, methane and so on, offer some potential for really good results.

Blank Page

REVIEW OF THEORETICAL AND EXPERIMENTAL SPECTROSCOPIC METHODS

Page

Prediction of Molecular Infrared Band and Line Intensities – Willis B. Person 89

New Theoretical and Experimental Methods for Pressure-Broadened Linewidths and Their Interpretation – Jack J. Gelfand 125

Laboratory Molecular Spectroscopy – Jack Margolis 149

Microwave Rotational Spectroscopy – H. Pickett 171

Blank Page

PREDICTION OF MOLECULAR INFRARED BAND AND LINE INTENSITIES

Willis B. Person
Department of Chemistry
University of Florida
Gainesville, Florida 32611

ABSTRACT

The general problem of predicting infrared intensities is examined, with an introduction intended to define the problem to be considered and also the concepts involved. After some rather non-specific discussion of the problem of predicting line intensities, attention is focussed specifically on the problem of predicting vibrational strengths (or total band intensities). Two methods are considered: predictions based on ab initio quantum-mechanical calculations, and predictions based on the transfer of atomic polar tensor parameters from small model molecules to the molecule of interest. Comparisons of predicted spectra with experimental spectra are shown for CH_3OH, CH_3OCH_3, C_2H_5OH, and $HOC\ell$. It is suggested that the most important application of this work may be to the prediction of intensities for free radicals, ions, and reactive intermediates so that the infrared spectrum can be used in the quantitative analysis for these interesting species.

INTRODUCTION

Although this audience is familiar with traditional studies of infrared intensities, it is still perhaps worthwhile to take a few minutes to review a few elementary concepts and define the problem of predicting infrared intensities. First of all, it is worth remembering that literally hundreds of thousands of low resolution survey infrared spectra have been recorded for all kinds of molecules that occur in the laboratory. Figure 1 shows an example in the form of a survey spectrum showing the infrared absorption of a gaseous sample of SF_6.[1] This spectrum shows the two allowed fundamental absorption bands (ν_3 at 950 cm^{-1} and ν_4 at 615 cm^{-1}) in SF_6 as very strongly absorbing features, with a few other weak absorption bands due to some of the allowed combination bands. This low resolution spectrum (spectral slit width about 1 cm^{-1}) nevertheless serves to pose the primary question to be answered by a prediction of infrared intensities; namely, why is the absorption by ν_3 so very strong, and why is that by ν_4 so weak (not much stronger, in fact, than some of the absorption by combination bands)?

We all know that we can look at one of these absorption bands with higher resolution and see much more detail about the band. For example Figure 2 shows the ν_4 band near 615 cm^{-1} as observed[2] with a Nicolet Fourier transform infrared (FTIR) spectrometer at a resolution of 0.05 cm^{-1}. We see there that the nice smooth envelope from ν_4 seen in Figure 1 is misleading, and that it is due to the convolution in this region of a very large number of individual vibration-rotation lines with the large spectral slit width. A number of other complications begin to show up at higher resolution: for example, the Q-branch absorption by $^{34}SF_6$ is marked, and we see a set of hot bands at about 614 cm^{-1} and a number of sharp Q-branches from other hot bands superimposed on the main 0 → 1 Q-branch at 615 cm^{-1}, as well as the weaker vibration-rotation hot band peaks between the strong sharp vibration-rotation lines for the main 0 → 1 transition. At this

BLANK

PAGE

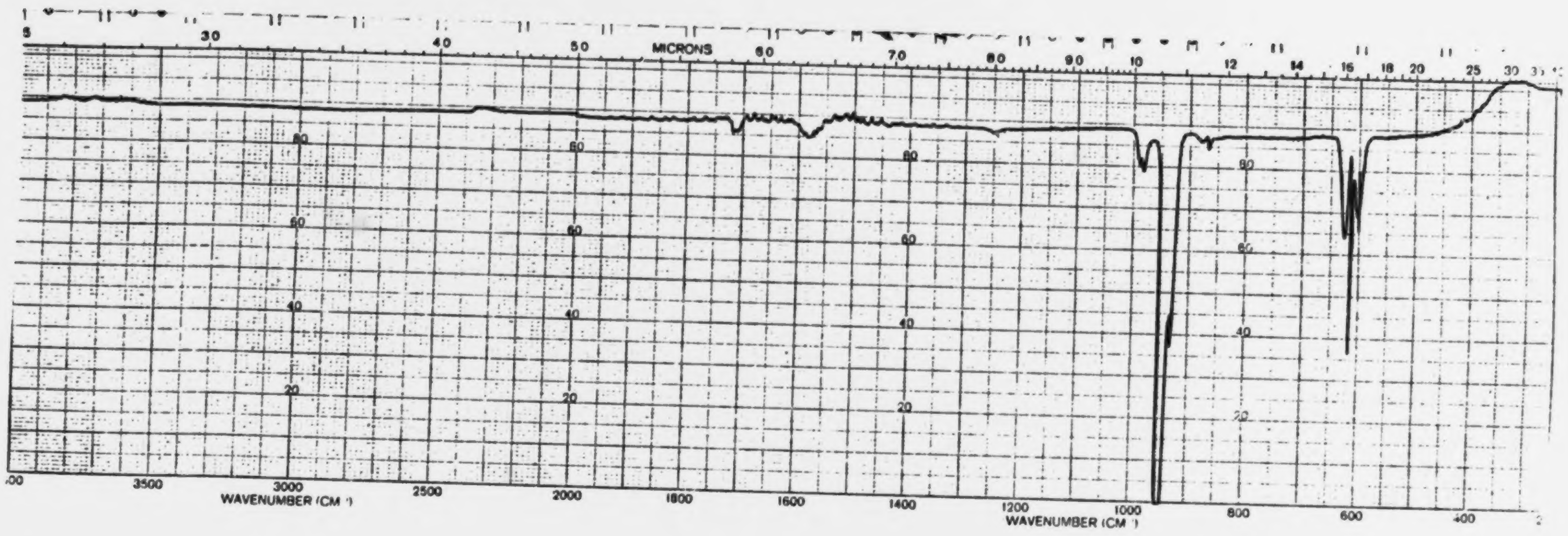

Figure 1. Survey infrared spectrum of SF_6 gas (about 2 torr, in a 10 cm cell) taken with a Perkin-Elmer Model 457 grating spectrometer at about 1 cm^{-1} resolution. (Figure taken from Perkin-Elmer Infrared Bulletin 36.[1] We are grateful to the Perkin-Elmer Corporation for permission to reprint this figure.)

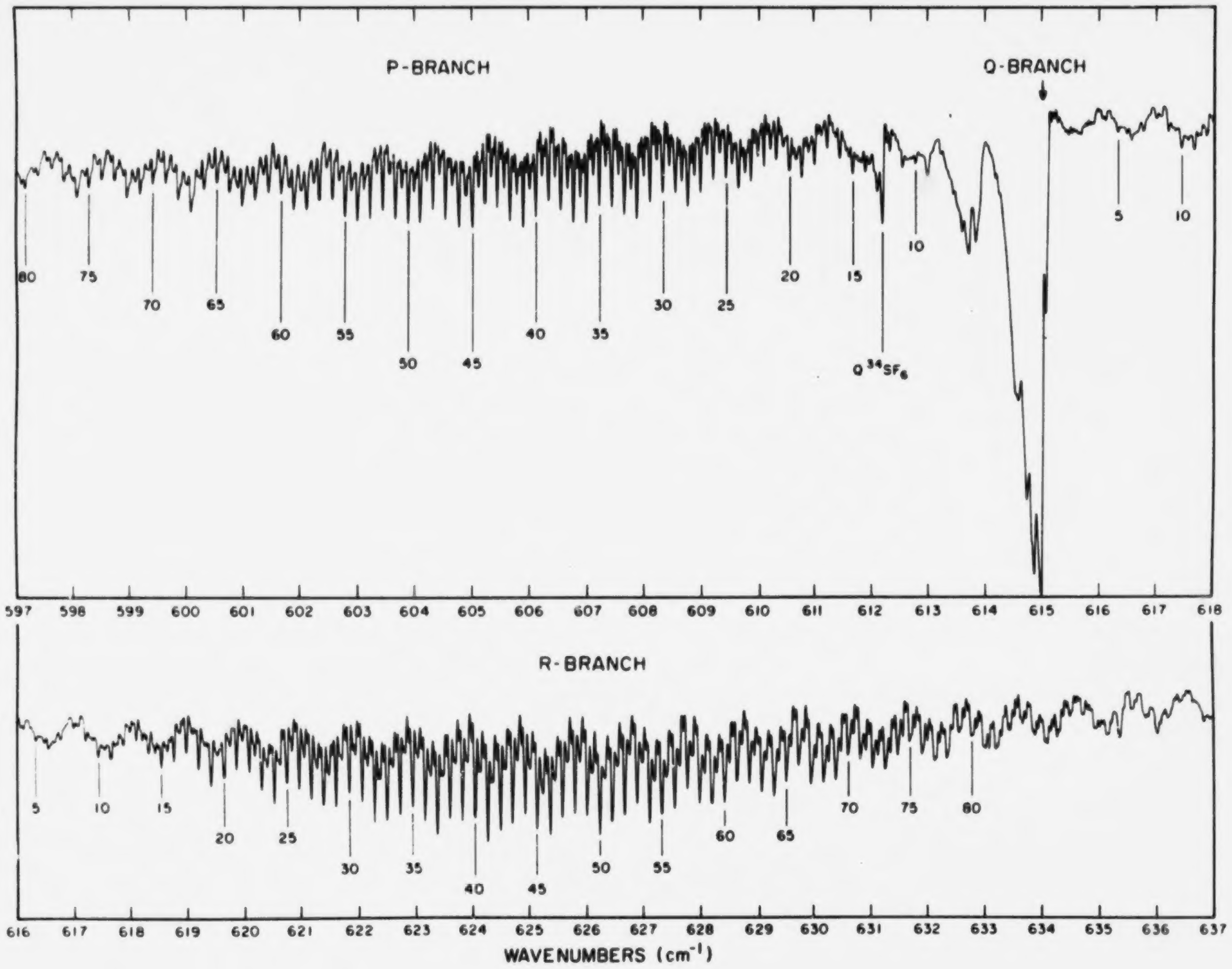

Figure 2. Infrared spectrum of SF_6 gas in the ν_4-region (near 615 cm^{-1}) taken with a Nicolet FTIR Spectrometer at 0.05 cm^{-1} resolution. (Figure taken from Fig. 2 of reference 2, with permission from J. Mol. Spectrosc.)

BLANK
PAGE

level of resolution, we see that we might want the theory to predict not only the total absorption intensity due to all the individual lines in the band, but also we might want to predict the intensity of each individual vibration-rotation line or the intensity of each of the different "hot bands" (transitions ($v_4 = 0 \rightarrow 1$) occurring in molecules which already have one or two (or more) quanta of excitation in vibrational modes -- for example, a molecule excited in the state with $v_6 = 1$ may absorb a 16 μm photon to reach the state with $v_6 = 1$ and $v_4 = 1$).

As complicated as this spectrum may seem, we find that the situation becomes even more interesting when the spectrum is examined with an infrared diode laser with a spectral resolution of about 10^{-5} cm^{-1}. Figure 3 shows the appearance of one of the vibration-rotation "lines" (P(39)) when it is examined with a diode laser.[2] Now we see that the "prediction" of intensities must concern itself not with the intensity of just one vibration-rotation "line," but instead with the intensity of each of the many components of this line.

Hence, we see from these three figures that the "prediction" of infrared intensities must be considered on several different levels of sophistication, depending upon the quality of the experimental data. At the present time, intensity theory is primarily concerned with predicting the total band intensities of Figure 1, but we shall outline here some ideas on how this kind of prediction can be extended to predict the "line" intensities of Figure 2, or even to predict the "component" intensities in Figure 3.

DEFINITIONS

The term "infrared intensity" is used here to indicate the integrated molar absorption coefficient

$$A = (1/C\ell) \int_{band} \ell n(I_0/I)d\nu. \qquad (1)$$

Here C is the concentration in moles/liter (for gases C = p/RT, where p is

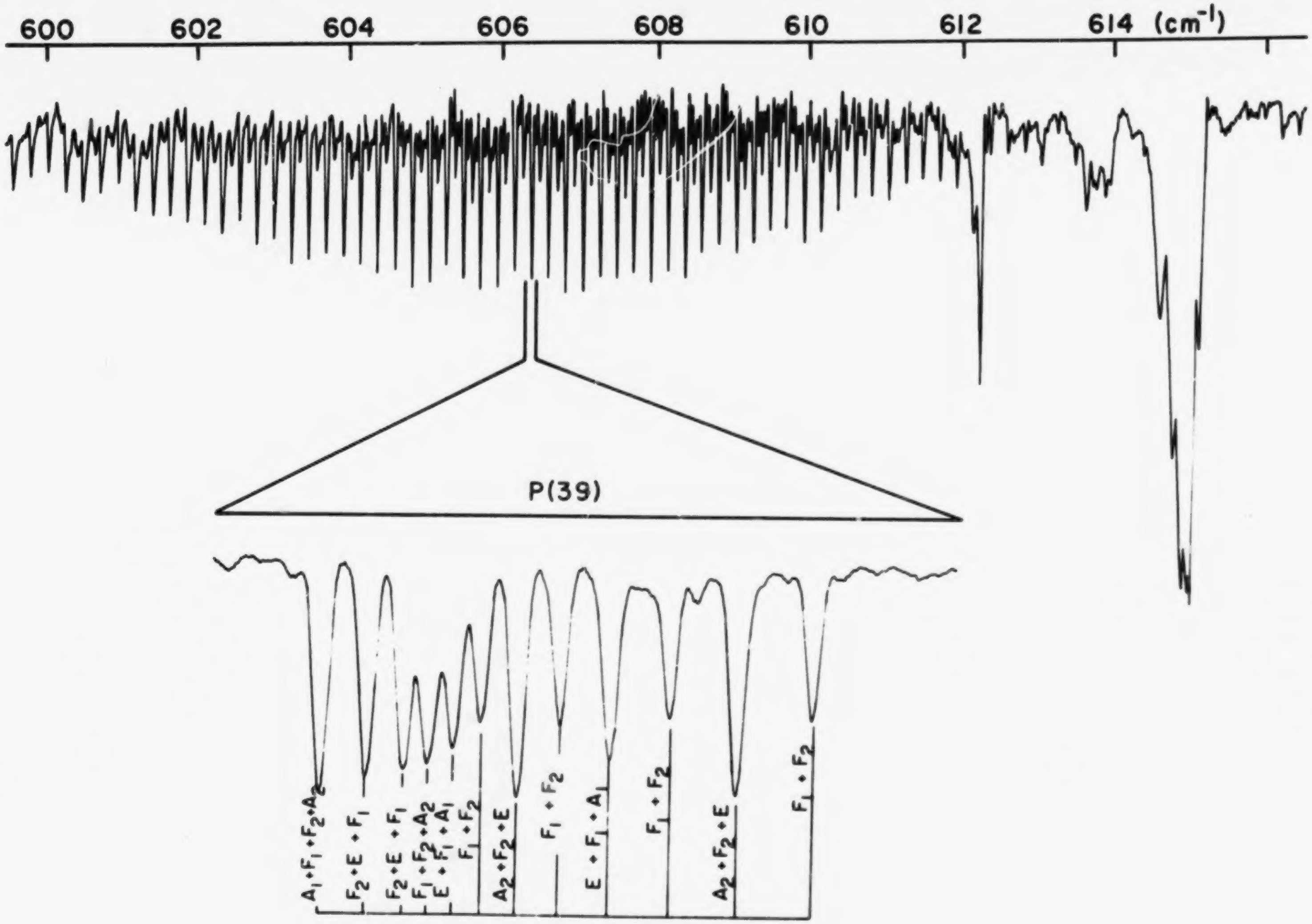

Figure 3. The absorption spectrum in P(39) of ν_4 of gaseous SF_6, taken with a 16 μm diode laser at about 10^{-5} cm^{-1} resolution. (Figure taken from Fig. 4 of reference 2, with permission from J. Mol. Spectrosc.)

BLANK

PAGE

pressure in atm , T is temperature in K, and R is 0.08205 ℓ-atm K^{-1} $mole^{-1}$), ℓ is the pathlength in cm, ν is the wavenumber in cm^{-1}, and the integration is carried out over each individual component of Figure 3 to get a "line component intensity," over all the components in a line to get the "line intensity," or over all the lines in the entire band to get the total "band intensity." Note that the total band intensity in general includes the intensity contributions from all the hot bands, as well as the contribution from the 0 → 1 transition, but the individual line intensity measures intensity for a single rotational transition for the 0 → 1 vibrational transition (for example). Hence the intensity of the latter depends on the population of molecules in the ground vibrational state (hence also on the temperature) while the total band intensity includes all contributions from all the molecules (vibrationally excited as well as ground state molecules), and so is independent of temperature.

The units of A from Eq. 1 are cm $millimole^{-1}$ (or "darks"); this value of A(cm $mmole^{-1}$) can be converted to A(km $mole^{-1}$) by dividing by 100: A(km $mole^{-1}$) = (1/100)A(cm $mmole^{-1}$) = [A(cm^{-2} atm^{-1}) at T °K)] × (RT × 10^{-5}), with R = 82.05 cm^3-atm K^{-1} $mole^{-1}$. Other conversion factors are given, for example, by Pugh and Rao.[3]

Another commonly used measure of intensity is Γ defined by[4]

$$\Gamma = (1/C\ell) \int_{band} \ell n(I_0/I)\, d(\ell n\ \nu). \qquad (2)$$

For many theoretical applications this measure of intensity is preferred[4] over A. These two quantities are related: $10^5 \times A(\text{km mole}^{-1}) \approx [\nu_0(\text{cm}^{-1})] \times \Gamma(\text{cm}^2\ \text{mole}^{-1})$, where ν_0 is the band center. In most of the rest of this article we shall mean A in km $mole^{-1}$ when we refer to the "intensity," and we shall specify whether it is band, line, or component intensity that we mean.

Experimentally, the total integrated band area, A, is obtained not by integrating over each line in Figure 2 and summing, but by pressure broadening the lines by adding several atmospheres of inert, transparent gas (for example, 10-50 atm of N_2) so that the lines overlap and give a smooth envelope of absorption over the entire band so that the integrated absorbance can then be measured accurately.[4,5] Otherwise, curve of growth methods[4,5] can be used to obtain experimental band intensity values.

LINE INTENSITIES

In principle the integrated line intensity value for the transition from state i to state f is related to the quantum mechanical transition dipole matrix element μ_{ij} (= $<v_jR_j|\hat{\mu}_F|v_iR_i>$) by:

$$A_{ij} = S_{ij} = \frac{K'8\pi^3 N_{av}\nu_0}{3\,hc}\;\frac{\nu}{\nu_0}\;\frac{(1-e^{-hc\nu_0/kT})}{Z_v}\;\frac{g_i e^{-Bhc\,J(J+1)/kT}}{Z_R} \times |<v_jR_j|\hat{\mu}_F|v_iR_i>|^2. \tag{3}$$

Here ν_0 is the wavenumber of the band center in cm^{-1}, ν is the wavenumber for the $i \rightarrow j$ transition, Z_v and Z_R are the vibrational and rotational partition functions, g_i is the degeneracy of the i state, B is the rotational constant, J is the rotational quantum number, v_jR_j designates the wavefunction for the upper state of the transition, $\hat{\mu}_F$ is the F component of the dipole moment operator in a space-fixed coordinate system, K' converts units to consistent values, and the other symbols have their usual meanings. If A_4 (or $S_{01}(v_4)$) is given in km $mole^{-1}$ and the transition dipole is in eÅ, the constants in the expression on the right hand side must be $K = K'8\pi^3N_{av}/3\,hc = 173.3$. This expression, obviously, is applicable to a diatomic molecule, where $E_J = B\,J(J+1)$.

The F component of the dipole moment operator is related to the components of a dipole moment operator expressed in molecule-fixed axes, α, by the direction cosines $\Phi_{F\alpha}$ between each pair of axes in the two coordinate systems:

$$\hat{\mu}_F = \sum_{\alpha} \hat{\mu}_\alpha\, \Phi_{F\alpha}. \tag{4}$$

Hence the transition moment integral can be expressed as a sum of products:

$$<v_jR_j|\hat{\mu}_F|v_iR_i>^2 = \sum_{\alpha} <v_j|\hat{\mu}_\alpha|v_i><R_j|\Phi_{F\alpha}|R_i>. \tag{5}$$

and

$$|\langle v_jR_j|\hat{\mu}_F|v_iR_i\rangle|^2 = \sum_\alpha |\langle v_j|\hat{\mu}_\alpha|v_i\rangle|^2 \; |\langle R_j|\Phi_{F\alpha}|R_i\rangle|^2. \qquad (6)$$

Substituting into Eq. 3, we obtain finally

$$S_{ij} = K\nu_0 \; \frac{\nu}{\nu_0} \; \frac{(1-e^{-hc\nu_0/kT})}{Z_v} \; \frac{g_i e^{-Bhc J(J+1)/kT}}{Z_R} \; \times [f(J,K)]S_v^{\,0}. \qquad (7)$$

$$= \text{Population Factors} \times \text{Line Strength} \times \text{Vibrational Strength}$$

Here the line strength factor f(J,K) is the contribution to the total transition moment from the integral of the direction cosines over the rotational wave functions. In principle it is known (or can be evaluated) from the theory of rotational spectroscopy.[6] The vibrational strength factor, $S_v^{\,0}$ related to the vibrational transition moment $\langle v_j|\mu_\alpha|v_i\rangle$, is obtained from the total integrated intensity over the entire vibration-rotation band, as discussed below.

Unfortunately, the integrated line strengths (S_{if}) in a real vibration-rotation band for any real molecule usually do not obey the simple theory outlined here and summarized in Eq. 7. This is because the energy levels are perturbed by interaction with nearby energy levels from other vibration-rotation states. This perturbation means that the simple harmonic-oscillator-rigid-rotor wavefunctions in Eq. 5 are no longer correct, and the correct wavefunction for the v_jR_j state (for example) is

$$|v_jR_j\rangle = a|v_a^{\,0}R_a^{\,0}\rangle + b|v_b^{\,0}R_b^{\,0}\rangle. \qquad (8)$$

Here $|v_a^{\,0}R_a^{\,0}\rangle$ and $|v_b^{\,0}R_b^{\,0}\rangle$ are the zero order wavefunctions for the two interacting states and a and b are their coefficients in the perturbed wavefunction. In general

$$b = X_{ab} \,/\, (E_a^{\,0} - E_b^{\,0}); \qquad\qquad a^2 + b^2 = 1. \qquad (9)$$

Here X_{ab} is the matrix element for the Hamiltonian operator; its non-zero value causes the perturbation between levels a and b. For the Coriolis interaction between vibration-rotation levels of ω_3 and those of ω_4 in tetrahedral or octahedral molecules[7] (like CH_4 or SF_6, for example)

$$b = -[4B\zeta_{34}\ (\omega_3\omega_4)^{1/2}/(\omega_3^{\ 2} - \omega_4^{\ 2})]m. \tag{10}$$

Here m = -J for P-branch transitions, m = J+1 for R-branch transitions or m = 0 for Q branch transitions; B is the rotational constant, and ζ_{34} is the Coriolis coupling constant.

Hence, the transition moment integral in Eq. 5 is

$$<v_jR_j|\hat{\mu}_F|v_iR_i> = a<v_a^{\ 0}R_a^{\ 0}|\hat{\mu}_F|v_iR_i> + b<v_b^{\ 0}R_b^{\ 0}|\hat{\mu}_F|v_iR_i>. \tag{11}$$

Substituting into Eqs. 5-7, we find

$$S_{if} = K\nu_0(\nu/\nu_0)\ \frac{(1-e^{-hc\nu_0/kT})}{Z_v}\ \frac{g_i e^{-Bhc\ J(J+1)/kT}}{Z_R}\ [f(J,K)]\,S_v^{\ 0}\ F(m). \tag{12}$$

The correction factor F(m) for line intensities in the ν_4 band due to the Coriolis interaction in this example is

$$F(m) = [1 + [4B\zeta_{34}\ (\omega_3\omega_4)^{1/2}/(\omega_3^{\ 2}-\omega_4^{\ 2})](P_3/P_4)m]^2. \tag{13}$$

Here P_s is the dipole moment derivative with respect to dimensionless normal coordinates, $\partial\mu/\partial q_s$, and the other terms have been defined previously.

This example illustrates the effect of one kind of perturbation on the line intensities. Similar treatments are required for all possible perturbations. In general, the situation can be very complicated, indeed, especially if a transition is perturbed by more than one of the nearby states. In principle, all these complications can be treated, so that line intensities could be predicted, using Eq. 12, for any line, provided that the value of the vibrational strength $S_v^{\ 0}$ is known.

Without any intent to minimize the difficulty of this calculation of line intensities, however, let us now focus our attention on this vibrational strength factor $S_v^{\ 0}$. Our point of view for the remainder of this survey is that if we can predict $S_v^{\ 0}$, we can in principle predict the individual line strengths using Eq. 12.

VIBRATIONAL STRENGTH, $S_v^{\ 0}$

The relationship between the vibrational strength, $S_v^{\ 0}$, and the transition moment integral is given by:

$$S_v^{\ 0} = A(\mathrm{km\ mole}^{-1}) = K\nu_0|\langle 1_i|\hat{\mu}|0\rangle|.^2 \tag{14}$$

It has been shown[4,8] that A (the total integrated band intensity, including the contributions from all the hot bands) is just equal to $S_v^{\ 0}$. Hence we can obtain $S_v^{\ 0}$ experimentally either by measuring the total band intensity[4] or by measuring the intensities of several individual vibration-rotation lines[9] and evaluating $S_v^{\ 0}$ from Eq. 12. If all the measurements are done properly and if the vibration-rotation theory has been properly worked out (particularly so that F(m) is known) then the two experimental techniques provide the same value for $S_v^{\ 0}$.[10]

To go the other way, and predict the vibrational band strength, we must evaluate the transition moment integral. For harmonic oscillator wavefunctions, and after expanding the dipole moment in a Taylor's series in the normal coordinates:

$$\mu = \mu^0 + \Sigma(\partial\mu/\partial Q_i)Q_i + (1/2)\sum_i\sum_j(\partial^2\mu/\partial Q_i\partial Q_j)Q_iQ_j + \ldots, \tag{15}$$

neglecting second (and higher) order terms, we find that

$$\mu_{01} = \langle 1_i|\hat{\mu}|0\rangle = (10^{16}h/8\pi^2c)^{1/2}\ [(\partial\mu/\partial Q_i)/\nu_0^{\ 1/2}]. \tag{16}$$

Hence

$$S_v^{\ 0} = 976.6\ |\partial\mu/\partial Q_i|^2. \tag{17}$$

Here $S_v^{\ 0} = A$ is in units of km mole^{-1} and $\partial\mu/\partial Q_i$ is in esu$^{-1/2}$.

The dipole moment derivative $\partial\mu/\partial Q_i$ is different for each molecule; substitution of a deuterium atom for a hydrogen atom, for example, changes the form of Q_i, and thus $\partial\mu/\partial Q_i$ changes. Thus, it is useful to transform from normal coordinates to cartesian coordinates to determine dipole derivatives ($\partial\mu/\partial x_\alpha$, etc.) that are well defined for all atoms in a molecule. The reason to do this is that we might expect to be able to evaluate the change in dipole moment for movement of the H atom, for example, in a CH bond in methane and then have some expectation that the same change might be produced for the same movement of an H atom in a CH bond in ethane.

There are a number of possible coordinate systems that could be chosen, but it turns out that expressions in space-fixed cartesian coordinates for each atom are particularly useful. These derivatives form a tensor, called the "atomic polar tensor" by Biarge, Herranz, and Morcillo,[11] who first introduced this concept. The atomic polar tensor for the _α_th atom is:

$$\underset{\sim}{P}_X{}^{\alpha} = \begin{pmatrix} \partial\mu_x/\partial x_\alpha & \partial\mu_x/\partial y_\alpha & \partial\mu_x/\partial z_\alpha \\ \partial\mu_y/\partial x_\alpha & \partial\mu_y/\partial y_\alpha & \partial\mu_y/\partial z_\alpha \\ \partial\mu_z/\partial x_\alpha & \partial\mu_z/\partial y_\alpha & \partial\mu_z/\partial z_\alpha \end{pmatrix}. \qquad (18)$$

The total 3 x 3N polar tensor for all the atoms in the molecule is formed by juxtaposition of the individual atomic polar tensors:

$$\underset{\sim}{P}_X = \left\{ \underset{\sim}{P}_X{}^1 \,\vdots\, \underset{\sim}{P}_X{}^2 \,\vdots\, \cdots \,\vdots\, \underset{\sim}{P}_X{}^{\alpha} \,\vdots\, \cdots \,\vdots\, \underset{\sim}{P}_X{}^N \right\}. \qquad (19)$$

The experimental data are, of course, the values of A_s (or the vibrational strengths for each of the fundamental vibrations of the molecule). These values (or their square roots) can be arranged in a "polar tensor" in normal coordinate space:

$$\underset{\sim}{P}_Q = \begin{pmatrix} \partial\mu_x/\partial Q_1 & \partial\mu_x/\partial Q_2 & & \partial\mu_x/\partial Q_{3N-6} \\ \partial\mu_y/\partial Q_1 & \partial\mu_y/\partial Q_2 & \cdots & \partial\mu_y/\partial Q_{3N-6} \\ \partial\mu_z/\partial Q_1 & \partial\mu_z/\partial Q_2 & & \partial\mu_z/\partial Q_{3N-6} \end{pmatrix} \qquad (20)$$

These derivatives are obtained from the experimental values of $S_v{}^0$ (A_s) using Eq. 17, and the signs are determined as described below. If the molecule has some symmetry, then the cartesian coordinates can be chosen parallel to the principal axes of inertia, and we can expect at most only one component in each column in Eq. 20 to be non-zero.

The relationships between the polar tensor in normal coordinate space ($\underset{\sim}{P}_Q$) and that in the space-fixed cartesian coordinate space ($\underset{\sim}{P}_X$) were described in detail elsewhere[11,12] and we summarize them below:

$$\underset{\sim}{P}_X = \underset{\sim}{P}_Q \underset{\sim}{L}^{-1} \underset{\sim}{B} + \underset{\sim}{P}_\rho \underset{\sim}{\beta} \tag{21}$$

and

$$\underset{\sim}{P}_Q = \underset{\sim}{P}_X \underset{\sim}{A}\, \underset{\sim}{L} \tag{22}$$

Here $\underset{\sim}{L}$ (and its inverse, $\underset{\sim}{L}^{-1}$) is the normal coordinate transformation matrix, $\underset{\sim}{R} = \underset{\sim}{L}\underset{\sim}{Q}$ (or $\underset{\sim}{Q} = \underset{\sim}{L}^{-1}\underset{\sim}{R}$); and $\underset{\sim}{B}$ is the transformation matrix between the 3N-6 internal coordinates ($\underset{\sim}{R}$) and the 3N cartesian coordinates ($\underset{\sim}{X}$):

$$\begin{pmatrix} \underset{\sim}{R} \\ \hline \underset{\sim}{\rho} \end{pmatrix} = \begin{pmatrix} \underset{\sim}{B} \\ \hline \underset{\sim}{\beta} \end{pmatrix} \underset{\sim}{X} \tag{23a}$$

and

$$\underset{\sim}{X} = (\underset{\sim}{A} \,\vdots\, \underset{\sim}{\alpha}) \begin{pmatrix} \underset{\sim}{R} \\ \hline \underset{\sim}{\rho} \end{pmatrix}. \tag{23b}$$

Here $\underset{\sim}{\rho}$ is the 6 x 1 column matrix of translations and rotations and $\underset{\sim}{\rho} = \underset{\sim}{\beta}\underset{\sim}{X}$ is the statement of the six Eckart conditions. The $\underset{\sim}{P}_\rho \underset{\sim}{\beta}$ term in Eq. 21 is the "rotation correction" term; see references 11 and 12 for definitions and further discussion.

PREDICTION OF INTENSITIES

Basically, there are two different approaches that can be made to the prediction of infrared intensities. The first is to use quantum mechanics to calculate the transition dipole moment (or perhaps to calculate μ as a function of atom position to obtain a quantum mechanical prediction of $\partial\mu_x/\partial x_\alpha$, for example). The second is to evaluate the atomic polar tensor elements for the H atom, for example, from experimental studies of CH_4, and then assume that the atomic polar tensor for the H atom in C_2H_6 is the same and transfer the H atom polar tensor from CH_4 to predict intensities for C_2H_6.

A slight modification of the latter approach, which is the one that we use, is to use the quantum mechanical calculation to help us choose the correct sign for $\partial p/\partial Q_i$ (or to choose signs for those parameters that give signs for the derived atomic polar tensors that agree with those from the quantum mechanical calculation). This "sign choice" is a very important step in analyzing experimental data to get atomic polar tensors to transfer to other molecules.

The quantum mechanical calculations help, also, in testing to see whether or not we can expect the atomic polar tensor to transfer from the simple molecule to the more complicated molecule. For example, we know that the hydrogen atom attached to the oxygen in CH_3OH is chemically different from the hydrogen atoms attached to the carbon atom. We might expect to be able to transfer the H-atom polar tensor from CH_4 to the CH_3 hydrogen atoms, but not to the OH atom. A quantum mechanical calculation can help us predict how much change to expect in the polar tensors for the two different hydrogen atoms. These "calibration" quantum mechanical calculations can be very important in helping us to understand the intensity parameters (atomic polar tensors) in different molecules.

Method for Predicting Intensities, based on Quantum-Mechanics. -- The "*ab initio*" quantum mechanical calculation of infrared intensities can be done in principle by calculating the wavefunctions and thus the dipole moment at equilibrium:

$$\mu_0(R_e) = \langle 0|\hat{\mu}|0\rangle_{R_e}. \tag{24a}$$

Here $|0\rangle_{R_e}$ is the ground state wavefunction evaluated at the equilibrium configuration. Solving the quantum-mechanical problem again at a different configuration, R (for example, move atom H_1 in the positive x direction by 0.02 Å), gives

$$\mu(R) = \langle 0|\hat{\mu}|0\rangle_R, \tag{24b}$$

so

$$(\partial\vec{\mu}/\partial R)_{R_e} \simeq \Delta\vec{\mu}/\Delta R = \frac{\langle 0|\hat{\mu}|0\rangle_R - \langle 0|\hat{\mu}|0\rangle_{R_e}}{R - R_e} \qquad (25)$$

For our example above, $\Delta R = \Delta x_{H_1} = 0.02$ Å, and we would have calculated $\partial\vec{\mu}/\partial x_{H_1}$.

Most of our calculations[13] have been made in this rather cumbersome manner. Recently much more elegant schemes have been introduced[14] for making these calculations, so that it is not necessary to do complete quantum-mechanical calculations at several configurations to obtain *ab initio* values for $\Delta\mu/\partial R$. Even so, the inelegant procedure we have used can give calculated values for all the atomic polar tensor elements for CH_3OH, for example, using the Gaussian 70 program[15] with a 4-31G basis set,[16] with a few minutes of computer time on a CDC-7600 (or equivalent) computer.

Having obtained "*ab initio*" predictions for the atomic polar tensor elements for the different atoms in the molecule, the values of the $\partial p/\partial Q_i$'s are predicted using Eq. 22, and the intensities then are predicted using Eq. 17. Some examples are shown below.

Method for Predicting Intensities by Transferring Intensity Parameters. -- The other approach to the prediction of infrared intensities is to evaluate intensity parameters from studies of simple molecules, and then use these parameters for the same atoms (or bonds, or functional groups) when they occur in similar chemical environments in more complicated molecules. We believe that atomic polar tensor elements are particularly useful parameters for transferring, partly because the space-fixed cartesian coordinates are well-defined, and there is no "rotation correction" needed (beyond that defined in Eqs. 21 and 22) when we use H-atom intensity parameters to predict the intensities for the corresponding deuterated molecules, for example. (Other intensity parameters may not exhibit this property; see reference 17.)

Other workers use other intensity parameters in their predictions. The most commonly used of these other parameters are the "electro-optical parameters" introduced by Gribov[18] and used also by Sverdlov and coworkers[19] in Russia, and also extensively by the Italian group (Zerbi, Gussoni, and coworkers)[20] in predictions, for example, of intensities in polyethylene.[21] We prefer to use approximate atomic polar tensors in our attempts to transfer parameters because there are fewer parameters involved than in the use of electrooptical parameters. Our choice may result in errors in the predicted spectra, when compared with experiment, but it has the advantage of simplicity. Several examples of spectra predicted in this way are presented in the following section.

COMPARISON OF PREDICTED SPECTRA WITH OBSERVED SPECTRA

We began our predictions with the series of fluoromethane molecules, CF_xH_{4-x}.[22] We extended the predictions to SF_6 and UF_6[23] and to XF_5 molecules.[24,25] These predictions were remarkably successful, even for UF_6, using the F and H atom polar tensors from CH_3F. This work was reviewed previously.[26]

At the time we first began to report these results, we were told by our friends that we should have expected to find such good transferability for the F-atom polar tensor. "After all, everyone knows that fluorine is so electronegative that it does not matter (in its electronic properties) just what atom it is attached to." In order to meet this kind of criticism, we decided to look at the problem of predicting infrared intensities for other kinds of molecules. We chose to study oxygen-containing organic molecules: alcohols, ethers, ketones and aldehydes. This work has been done by Jerry Rogers[27] in our laboratory, and I should like to preview it briefly for your information. Certainly, no one has ever said that we should expect H-atom polar tensors in these molecules to be successfully transferable, and the oxygen atoms might surely be expected to be different. Hence these molecules provide a severe test of the concept of transferable polar tensors.

The first molecule in this study was CH_3OH. Figure 4 shows the spectrum predicted for CH_3OH vapor (at 3.04k Pa (=22.8 torr) pressure in a 10.2 cm cell) compared with the survey experimental spectrum measured under those conditions with a Nicolet Model 7199 FTIR spectrometer. This prediction is based on ab initio atomic polar tensor elements calculated for the hydrogen, carbon and oxygen atoms using the Gaussian 70 program with a 4-31G basis set[28] using the normal coordinate transformation[29] generated from the force constants given by Mallinson.[30] We see in Figure 4 that our predicted intensities are really in very good agreement with the experimental spectrum. The intensity predicted for the OH stretching fundamental near 3667 cm^{-1} (22 km $mole^{-1}$) agrees perfectly with the experimental value (22 ± 1 km $mole^{-1}$). The prediction overestimates (by about a factor of two) the intensity in the C-H stretching region near 3000 cm^{-1} and also overestimates that in the C-O stretching region near 1000 cm^{-1}, and the distribution of intensities in the CH_2 bending region near 1400 cm^{-1} may not be exactly perfect, but the overall agreement is gratifying, indeed. It is important to emphasize here that even though the predicted values for A_s differ from the experimental values by factors of two or three in some cases, still the pattern predicted for the spectrum as shown in Figure 4 is in very close apparent visual agreement with the experimental spectrum.

In Figure 5, we show the comparison between the spectrum predicted for CH_3OH using atomic polar tensor elements for the H atoms in the CH_3 group transferred from CH_3F, APT's for the H and O atoms in the OH group transferred from H_2O, and obtaining the C atom polar tensor using

$$\sum_{\alpha} \underset{\sim}{P}_X^{\alpha} = \underset{\sim}{0}. \qquad (26)$$

Again the agreement between predicted and experimental spectra is most

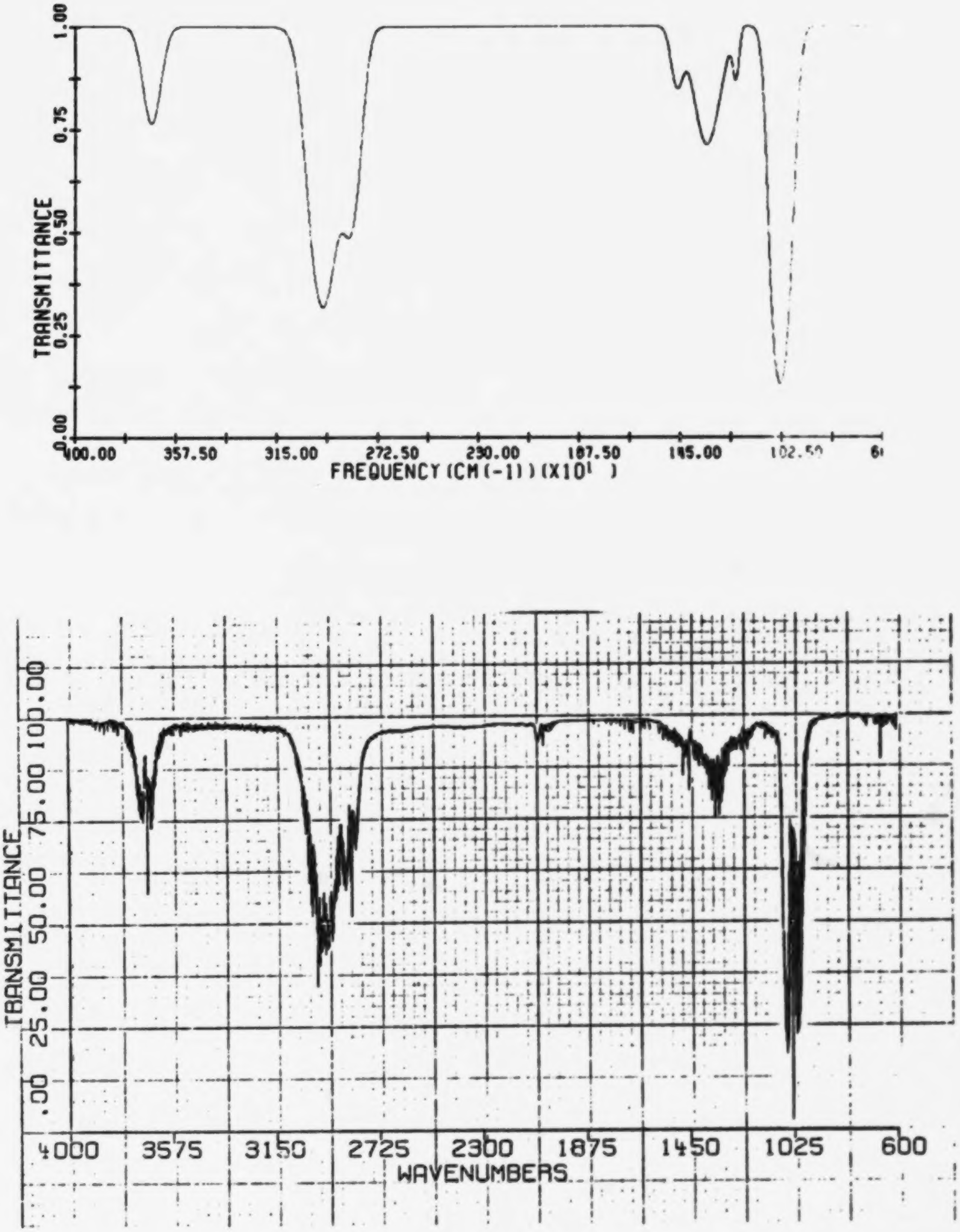

Figure 4. Predicted spectrum of CH_3OH (upper figure) based on ab initio quantum mechanical calculation compared with experimental spectrum (lower curve) of gaseous CH_3OH measured at 0.5 cm^{-1} resolution with a Nicolet FTIR spectrometer.

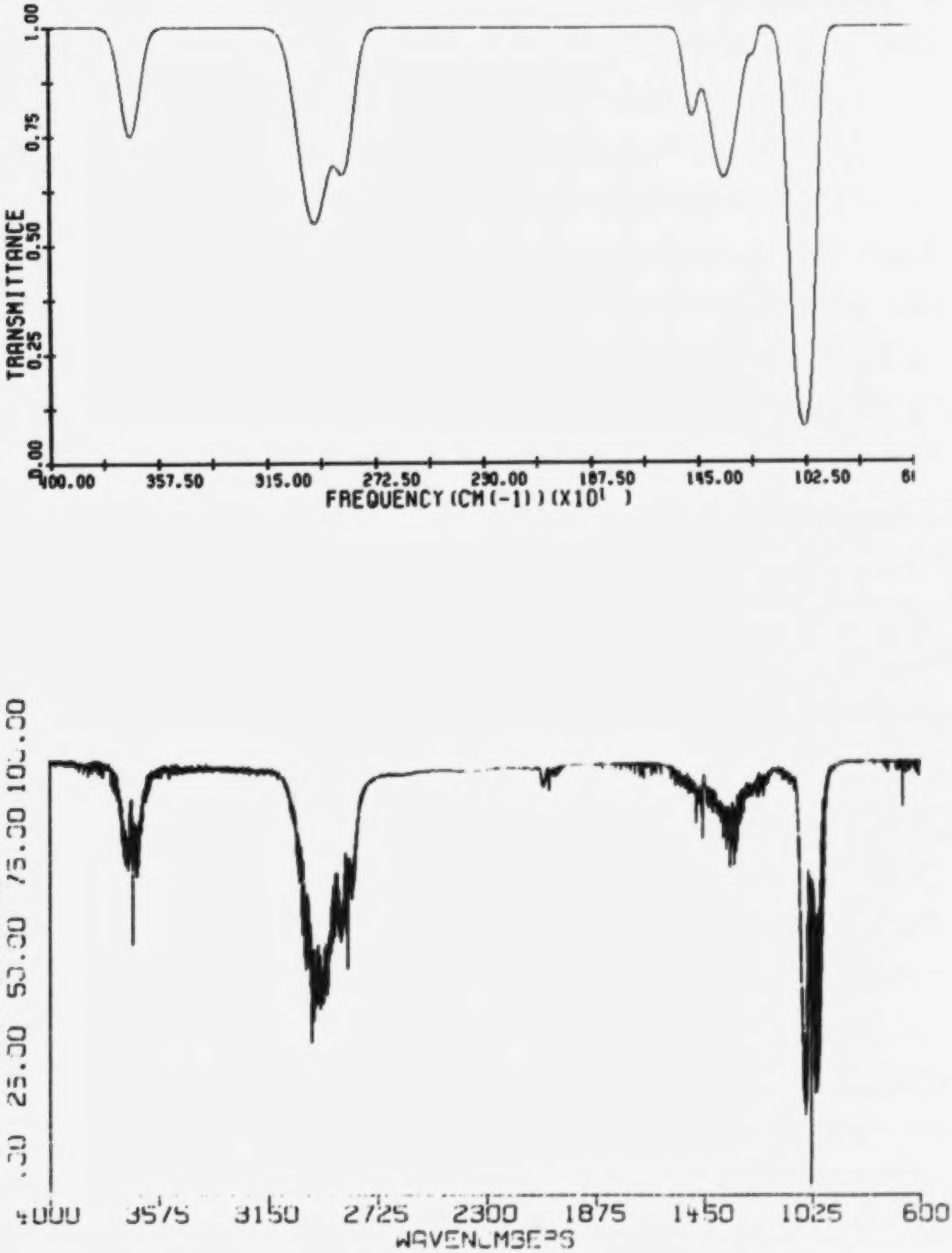

Figure 5. Predicted spectrum of CH_3OH (upper figure) based on transfer of APT's from CH_3F for methyl H atoms and from H_2O for O and H atoms (see text) compared with experimental spectrum of CH_3OH vapor (lower curve). See Figure 4, and text.

satisfying. Certainly this agreement is good enough that we can believe that we have the correct signs for the calculated dipole derivatives (especially since the signs of all the APT's from the 4-31G ab initio calculation agree with all those for the APT's obtained by transfer of APT's from CH_3F and H_2O).

Although the agreement between the predicted and experimental spectra for CH_3OH is pretty good for either prediction, it is not perfect (factor of two errors in A_s). Some of the discrepancy is probably due to a real non-transferability of APT's all the way from CH_3F and H_2O to CH_3OH. Hence, it seemed to us to be appropriate to evaluate "experimental" APT's for CH_3OH from the experimental intensities (which we had also remeasured[27]) using the separation of intensities from the overlapping bands proposed by Serrallach, Meyer and Gunthard.[31] These "experimental" APT's for the C and H atoms in the CH_3 group in CH_3OH were then used to predict the intensities for CH_3OCH_3. (The APT for the O atom was obtained using Eq. 26.) Figure 6 compares the predicted spectrum with the experimental spectrum for CH_3OCH_3. We have used the force field given by Levin, Pearce and Spiker[32] to obtain the normal coordinate transformation matrices needed in the prediction.

Once again, the agreement between the predicted spectrum and the experimental spectrum seems quite satisfactory. We note that there are discrepancies: for example, the relative intensities in the CO stretching region (near 1000 cm^{-1}) is not quite correct. Nevertheless, this agreement (again typical of "factor-of-two" agreement between the numerical values predicted for the intensities and those measured for the intensities) is good enough to give a pattern for the predicted spectrum that is close enough to the observed spectrum to be useful in verifying assignments, etc. It is not clear at present whether the remaining discrepancies are due to errors in the assumption of transferability or to errors in the normal coordinate calculation.

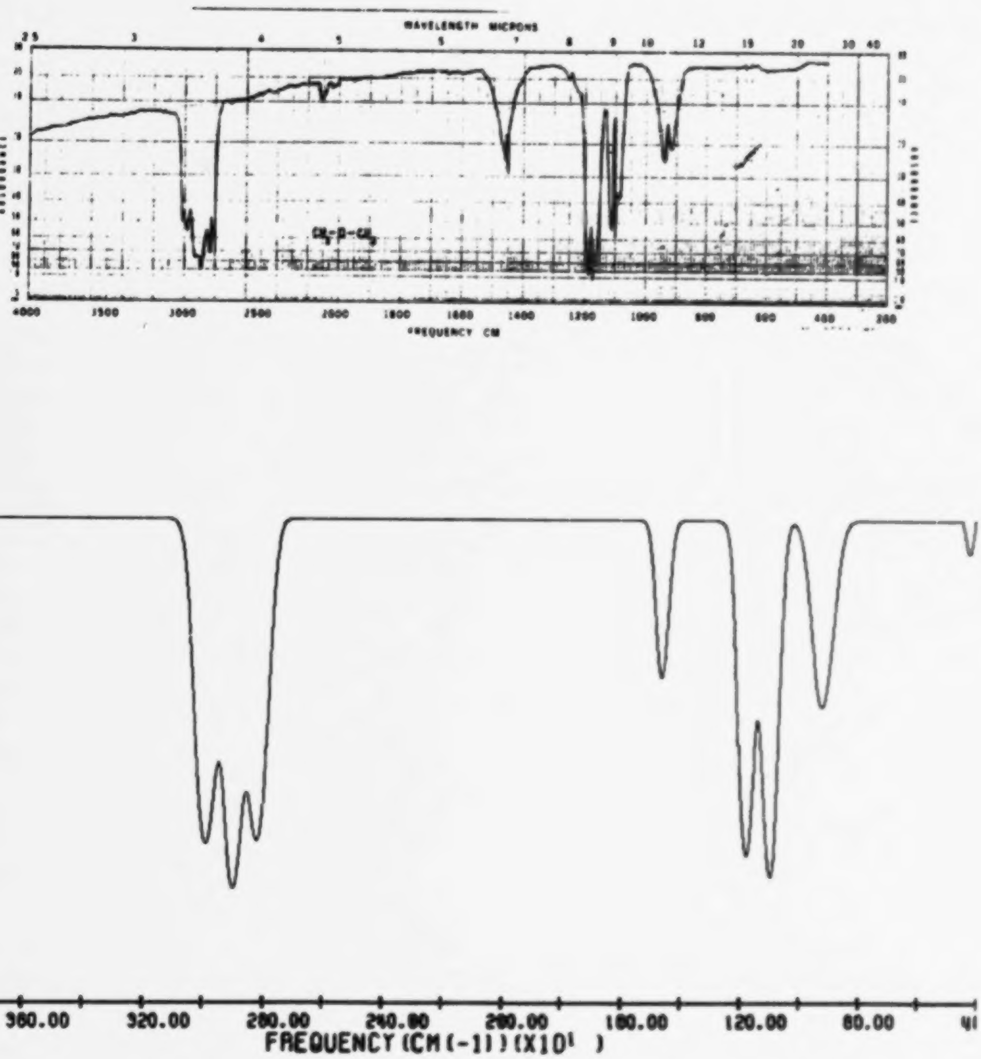

Figure 6. Predicted spectrum of gaseous CH_3OCH_3 (lower curve) based on transfer of CH_3 APT's from CH_3OH compared with experimental survey spectrum (taken from Sadtler collection, with permission).

The ethanol molecule (C_2H_5OH) forms another test case. Here we have some problems in finding a good normal coordinate analysis (and thus a reliable force field) in the literature. We found one force field by Zemlyanukhina and Sverdlov,[33] based on assumed transferability of force constants from similar molecules. Using that force field and transferring APT's for the C and H atoms in the CH_3 group from ethane, APT's for the OH atoms from CH_3OH (and also transferring the H atom polar tensor for the CH_2 group), adjusting the C-atom polar tensor in the CH_2 group by Eq. 26, we calculated the predicted spectrum. Before comparing it with experiment, we wanted to examine the effect on the predicted spectrum of a change in the force field assumed for the normal coordinate calculation. Hence, we deduced our own force field by examining the "*ab initio*" force fields calculated by Blom, Otto and Altona[28] for CH_3OH and by Blom and Altona[34] for CH_3CHCH_2. We transferred the appropriate force constant from these two molecules to the CH_3CH_2OH molecule, adding about 5 more from the Zemlyanukhina-Sverdlov field[33] for the interaction constants between CH_3 and OH groups (for example, the force constant for the CCO bend). The new force field fit the experimental frequencies very well, and its use with the same APT's used in the other C_2H_5OH calculation gave the predicted spectrum shown compared with the experimental spectrum in Figure 7. The effect of the different normal coordinate treatments can be seen in Figure 8 which compares the two predicted spectra. The normal coordinates do indeed have an effect on the predicted intensities (see especially the region near 1450 cm^{-1} in Figure 8). Nevertheless, the general pattern predicted from either set of assumed force constants (Figure 8) is within "factor-of-two" agreement with the experimental spectrum (see Figure 7).

One more example of the kind of agreement that can be expected between either kind of prediction (*ab initio* or transferred APT's) and experimental

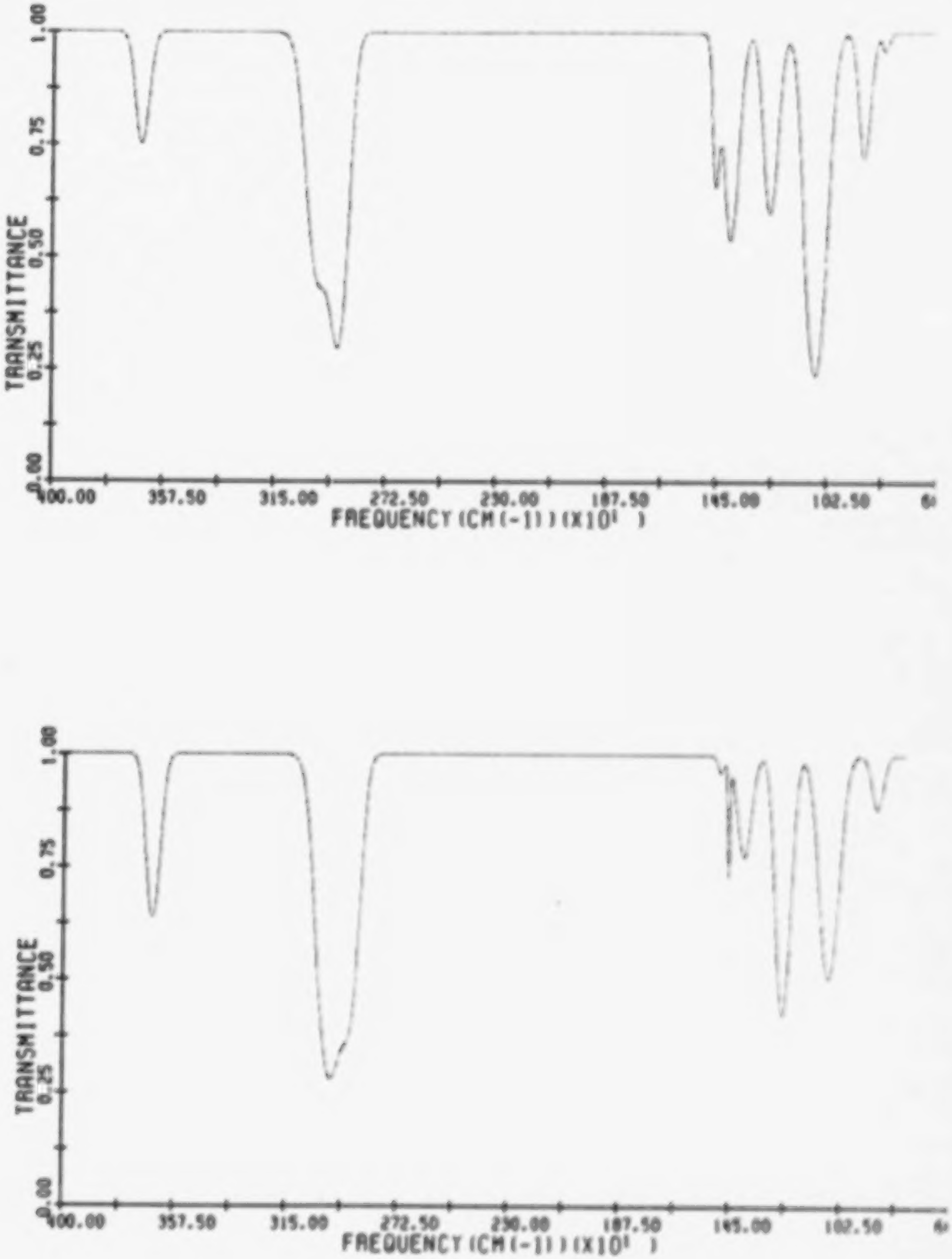

Figure 7. Predicted spectrum of gaseous C_2H_5OH (lower curve) based on our force field and APT's transferred from CH_3CH_3 for CH_3 and from CH_3OH for H-atoms on CH_2 and for OH APT's compared with simulated experimental spectrum (from a computer fit to survey spectrum on Nicolet FTIR).

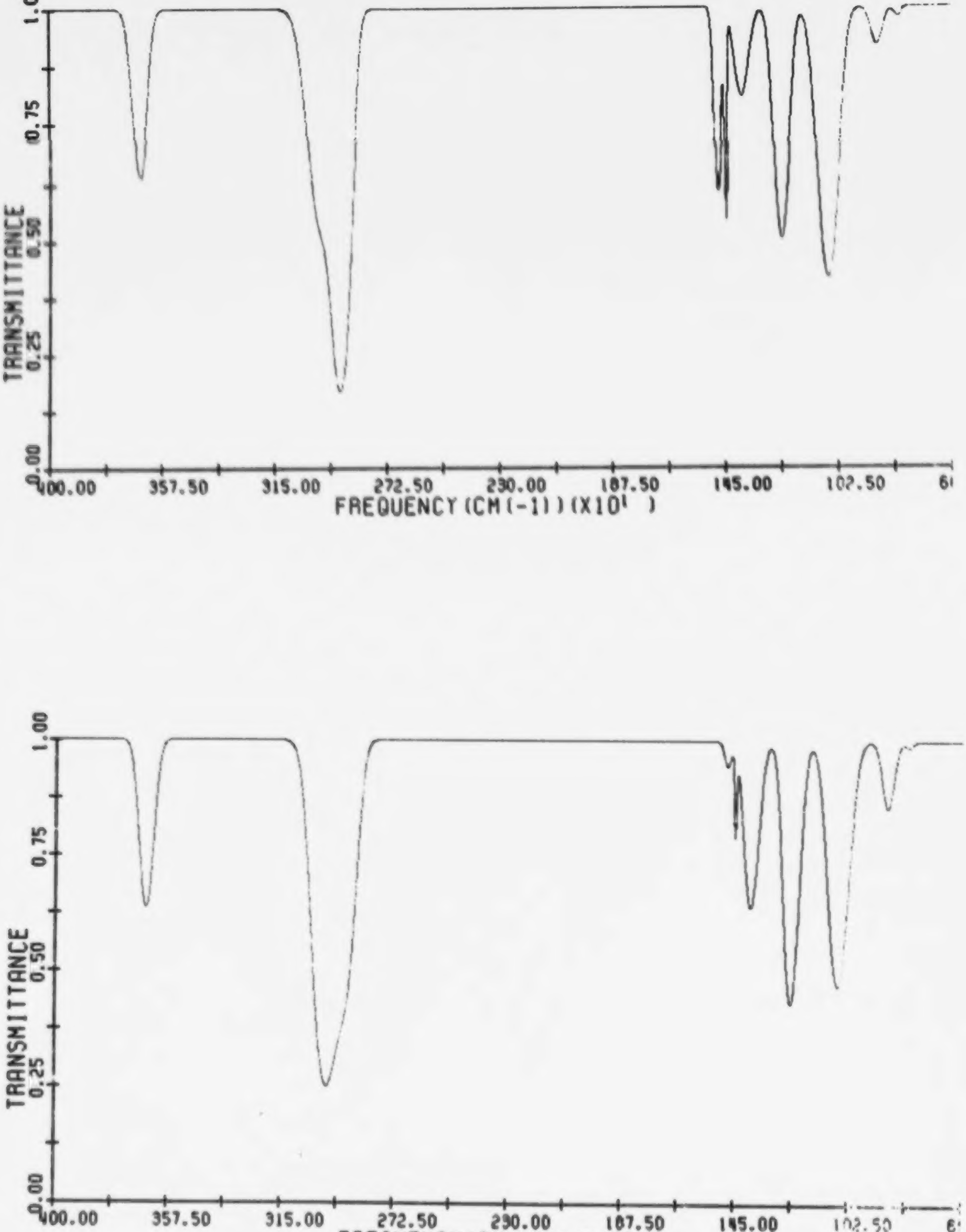

Figure 8. Predicted spectrum of gaseous C_2H_5OH (upper curve) based on Zemlyanukhina-Sverdlov force field[33] with APT's as in Figure 7, compared with predicted spectrum (lower curve) based on our force constants and described also in Fig. 7.

spectra is provided by the HOCℓ molecule,[35] which is of somewhat more interest to this group. For HOCℓ, the intensities have been calculated by Komornicki and Jaffe[14] in an ab initio quantum mechanical calculation using their elegant new technique with a fairly large gaussian basis set, including polarization functions on the oxygen atom. Their predicted spectrum, plotted out in our standard format, is compared with the simulated experimental spectrum (from Su, Calvert, Lindley, Uselman and Shaw[36]) in Figure 9. Just to show what can be done using transferred APT's, we show in Figure 10 the comparison between the experimental spectrum of HOCℓ and that predicted using the force field given by Schwager and Arkell[37] and transferring the H atom APT from H_2O and the Cℓ atom APT from CℓCN.[38] Neither prediction (in Figures 9 and 10) agrees very well with the experimental spectrum, but both predictions are within "factor-of-two" agreement. One is off in one direction, the other prediction was off in the other direction. Either one gives better than "order-of-magnitude" estimates for the intensities of the three fundamental vibrations of HOCℓ.

As impressive as these comparisons may be, the object of predicting infrared intensities is not to predict values to compare with spectra that can be measured more accurately in the laboratory. We believe that the most important contribution the predictions can make is in reasonably reliable predictions of infrared intensities for species which are hard to study in the laboratory. For example, we think it is possible to predict spectra of free radicals, of free gaseous ions, or of other reactive intermediates that will be as accurate as are the predictions for spectra of molecules shown here in this survey. Using these predicted integrated molar absorption coefficients (A) we can then measure the infrared spectrum of the free radical ("on the fly" with an FTIR instrument in the course of a reaction, perhaps, or maybe trapped in an argon matrix at low temperatures) and determine its concentration. I know of no

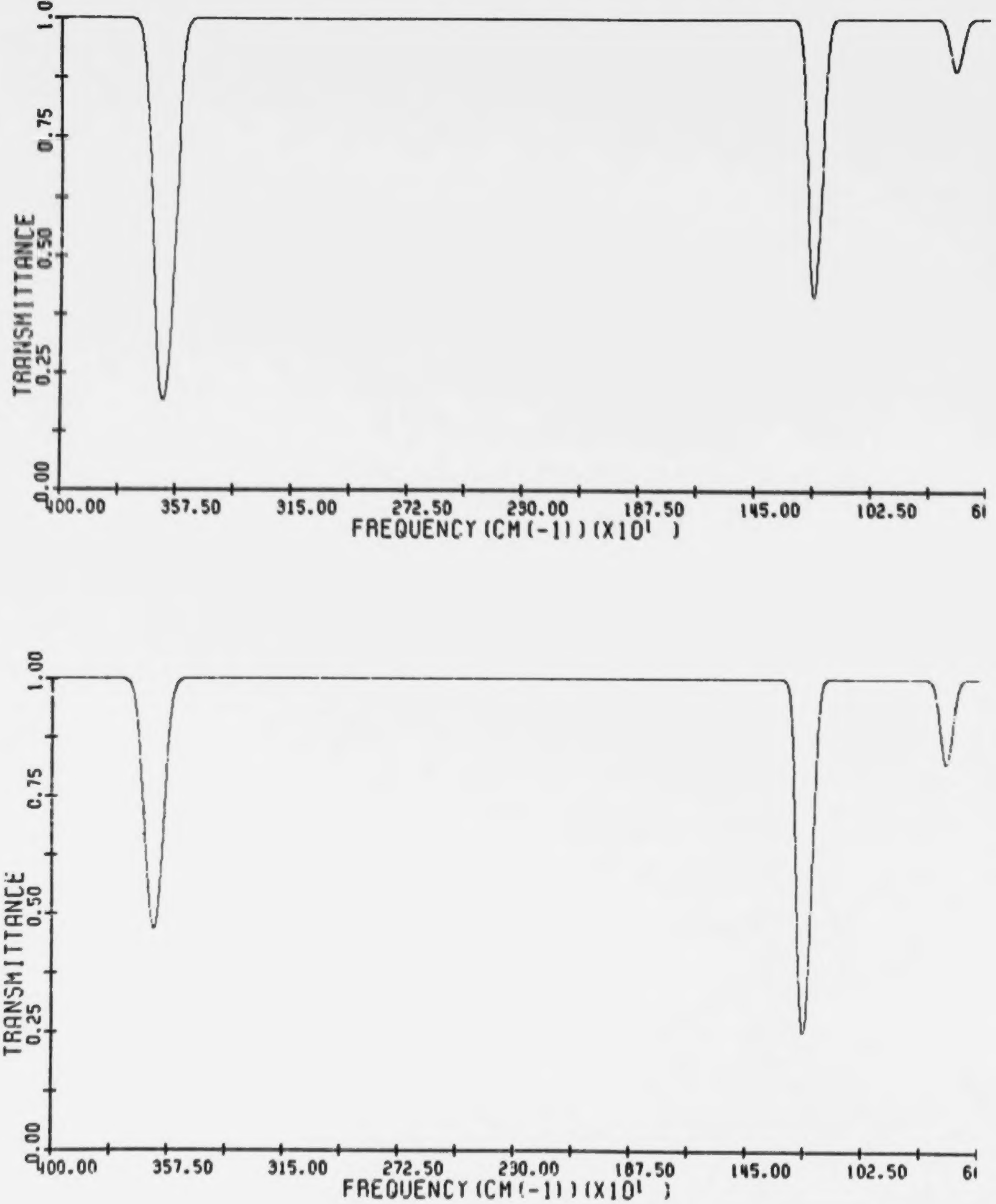

Figure 9. Predicted spectrum of gaseous HOCl (upper curve) based on ab initio quantum mechanical calculation reported by Komornicki and Jaffe[14] compared with simulated experimental spectrum (lower curve) based on results reported by Su et al.[36]

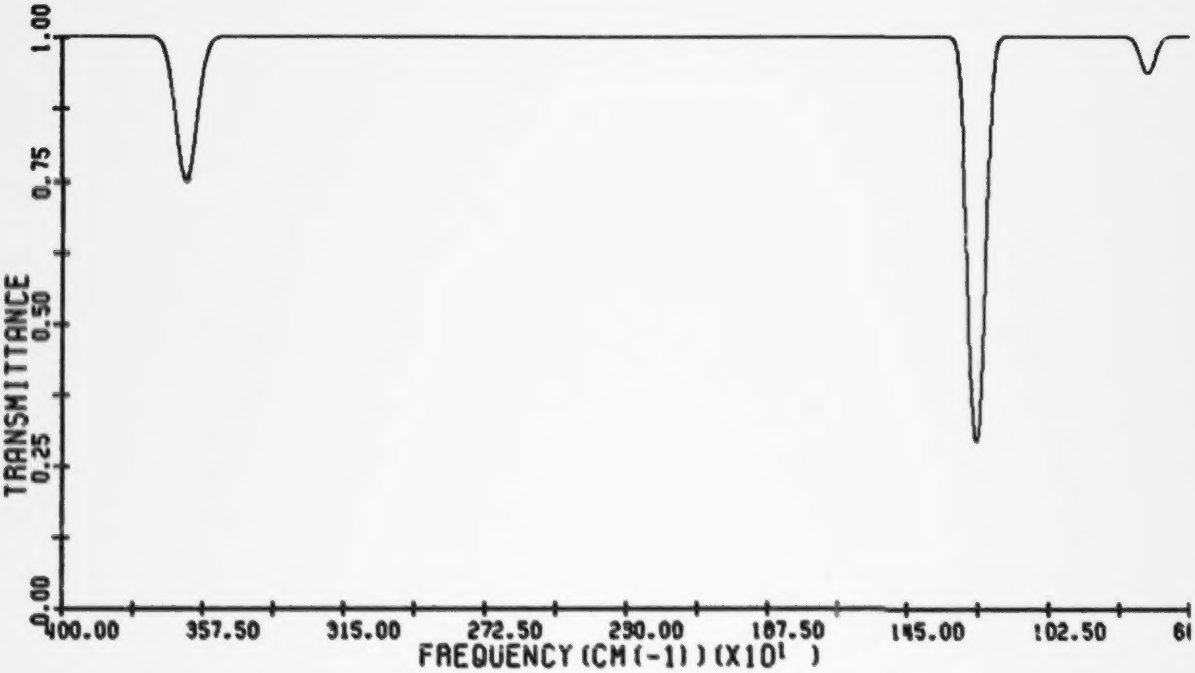

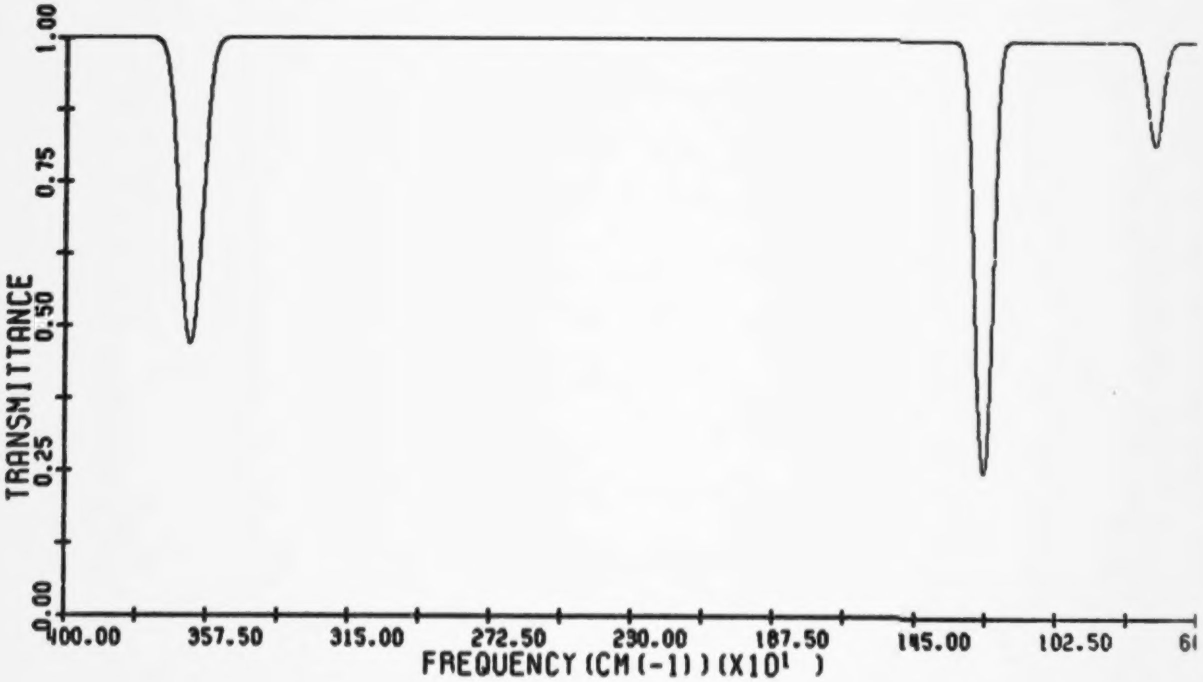

Figure 10. Predicted spectrum of HOCl vapor (upper curve) based on transfer of Cl atom APT from ClCN and H atom APT from H_2O compared with simulated experimental spectrum for HOCl vapor (lower curve) based on results reported by Su et al.[36]

other way to get this kind of information about these reactive molecules.

We have previously published[39,40] an illustration of this technique applied to the spectrum of CF_2 and CF_3 radicals trapped with the final CF_4 product molecule in an Ar matrix after uv photolysis of CF_2N_2 molecules in the matrix.[41] We have already reported this procedure in sufficient detail[40] that we do not need to repeat the description here. Suffice it to say that we believe it would be entirely feasible to determine the concentrations of these radicals accurate to better than a factor of two, by using the predicted intensities.[40] Surely this kind of ability to predict intensities for this kind of reactive species has potentially interesting applications in the study of photochemistry occurring for example in planetary atmospheres.

ACKNOWLEDGEMENTS

Partial support for the predictions reported here from the National Science Foundation (Grant No. CHE-7818940) is gratefully acknowledged. I am grateful to Jerry Rogers and to Roberto Maia for permission to "preview" unpublished results from their Ph.D. theses for this audience.

REFERENCES

1. Taken from Perkin-Elmer Infrared Bulletin 36, "Reference Spectra of Gases," by M.V. Zeller and M.P. Juszli, October, 1973.

2. Taken from K.C. Kim, W.B. Person, D. Seitz and B.J. Krohn, J. Mol. Spectrosc., 76, 322 (1979).

3. L.A. Pugh and K.N. Rao, in Molecular Spectroscopy: Modern Research, (K.N. Rao, Ed.) (Academic, New York, 1976) Vol. II, chap. 4.

4. For a review of many of these basic concepts and techniques see J. Overend, in Infrared Spectroscopy and Molecular Structure, (M. Davies, Ed.) (Elsevier, New York, 1963) chap. 10.

5. S.S. Penner, Quantitative Molecular Spectroscopy and Gas Emissivities (Addison-Wesley, Reading, Mass., 1959).

6. For example see H.C. Allen, Jr. and P.C. Cross, Molecular Vib-Rotors (Wiley, New York, 1963).

7. A.G. Robiette and I.M. Mills, J. Mol. Spectrosc., 77, 48 (1979); see also W.B. Person and B.J. Krohn, to be published.

8. I.M. Mills and D.H. Whiffen, J. Chem. Phys., 30, 1619 (1959).

9. For example, see R.A. Toth, L.R. Brown and R.H. Hunt, J. Mol. Spectrosc., 67, 1 (1977).

10. See W.B. Person and K.C. Kim, J. Chem. Phys., 69, 1764 (1978); see also K. Kim, R.S. McDowell and W.T. King, J. Chem. Phys., in press.

11. J.F. Biarge, J. Herranz and J. Morcillo, An. R. Soc. Esp. Fis. Quim., Ser. A 57, 81 (1961); see also W.B. Person and J.H. Newton, J. Chem. Phys., 61, 1040 (1974) for a rephrasing of these ideas in the present formulation.

12. J.H. Newton and W.B. Person, J. Chem. Phys., 64, 3036 (1976).

13. Our calculations began with CNDO calculations; (a) see the review by W.B. Person and D. Steele, Molecular Spectroscopy, 2, 357 (1974) (in the Specialist Periodical Report of the Chemical Society, (London)); (b) see also W.B. Person, K.G. Brown, D. Steele and D. Peters, "Ab Initio Calculations of Vibrational Properties of Some Linear Triatomic Molecules. I. Intensities", to be submitted to J. Chem. Phys.

14. A. Komornicki and R.L. Jaffe, J. Chem. Phys., 71, 2150 (1979); see also A. Komornicki and J.W. McIver, Jr., J. Chem. Phys., 70, 2014 (1979).

15. W.J. Hehre, W.A. Latham, R. Ditchfield, M.D. Newton and J.A. Pople, "Gaussian 70", program 236, Quantum Chemistry Program Exchange, Indiana University (1971).

16. For example, see R. Ditchfield, W.J. Hehre, and J.A. Pople, J. Chem. Phys., 54, 724 (1971); ibid., 56, 2257 (1972).

17. See M. Gussoni and S. Abbate, J. Chem. Phys., 65, 3439 (1976); also P.L. Prasad, J. Chem. Phys., 69, 4403 (1978).

18. L.A. Gribov, Intensity Theory for Infrared Spectra of Polyatomic Molecules, English translation (Consultants Bureau, New York, 1964); see also L.A. Gribov, M.E. Elyashberg and M.M. Raikhshtat, J. Mol. Struct., 53, 81 (1979).

19. Reviewed in L.M. Sverdlov, M.A. Kovner, and E.P. Krainov, Vibrational Spectra of Polyatomic Molecules, IPST English translation (Wiley, New York, 1974).

20. Reviewed by M. Gussoni, in Vibrational Intensities (W.B. Person and G. Zerbi, Eds.) (Elsevier, Amsterdam, to be published 1980) chap. 5; see also G. Zerbi, ibid., chap. 15.

21. S. Abbate, M. Gussoni, G. Masetti and G. Zerbi, J. Chem. Phys., 67, 1519 (1977).

22. a) J.H. Newton, R.A. Levine and W.B. Person, J. Chem. Phys., 67, 3282 (1977); b) J.H. Newton and W.B. Person, J. Phys. Chem., 82, 226 (1978).

23. W.B. Person and J. Overend, J. Chem. Phys., 66, 1442 (1977).

24. B.J. Krohn, W.B. Person and J. Overend, J. Chem. Phys., 65, 969 (1976).

25. B.J. Krohn, W.B. Person and J. Overend, J. Chem. Phys., 67, 5091 (1977).

26. W.B. Person and J.H. Newton, J. Mol. Struct., 46, 105 (1978).

27. J. Rogers, Ph.D. thesis, University of Florida (1980). Parts of this work have been reported in preliminary talks also at the Symposium on Molecular Spectroscopy, Columbus, June, 1979; at the European Congress of Molecular Spectroscopy in Frankfurt, September, 1979; and at the Meeting of the American Chemical Society in Washington, September, 1979.

28. Our calculation is more or less equivalent to the one reported by C.E. Blom, L.P. Otto, and C. Altona, Molec. Phys., 32, 1137 (1976).

29. Our calculations were made using Program CHARLY obtained from J. Overend at the University of Minnesota and adapted by G. Sanchez for use on the University of Florida IBM computers.

30. P.D. Mallinson, J. Mol. Spectrosc., 58, 194 (1975); see also P.D. Mallinson and D.C. McKean, Spectrochim. Acta, 30A, 1133 (1974).

31. A. Serrallach, R. Meyer and H.H. Gunthard, J. Mol. Spectrosc., 52, 94 (1974).

32. I.W. Levin, R.A.R. Pearce and R.C. Spiker, Jr., J. Chem. Phys., 68, 3471 (1978).

33. I. Ya. Zemlyanukhina and L.M. Sverdlov, Opt. Spectrosc., 36, 391 (1974).

34. C.E. Blom and C. Altona, Mol. Phys., 31, 1377 (1976).

35. The results previewed here are taken from R. Maia, Ph.D. thesis, University of Florida (1980).

36. F. Su, J.G. Calvert, C.R. Lindley, W.M. Uselman and J.H. Shaw, J. Phys. Chem., 83, 912 (1979).

37. I. Schwager and A. Arkell, J. Am. Chem. Soc., 89, 6006 (1967).

38. Taken from reference 13b.

39. J.H. Newton and W.B. Person, J. Chem. Phys., 68, 2799 (1978).

40. J.H. Newton and W.B. Person, Applied Spectrosc., 32, 290 (1978).

41. a) D.E. Milligan and M.E. Jacox, J. Chem. Phys., 48, 2265 (1968); b) D.E. Milligan, D.E. Mann, M.E. Jacox and R.A. Mitsch, J. Chem. Phys., 41, 1199 (1964); c) M.E. Jacox, private communication.

DISCUSSION

Question (R. Beer): I have two questions. The first is, how much work is it to do one of these computations? Is it something you can do in minutes, hours, days or months?

Response: The problem is that you have to know the normal modes, which takes several days or months of computation and experiment. If those are known for a molecule from prior work, prediction using the transferred polar tensors takes just a few minutes. The prediction via an *ab initio* calculation takes quite a bit longer: a few days.

Question (R. Beer): My second question is, can you reverse the procedure? If I give you a spectrum, can you identify the molecule?

Response: I don't know. In principle, it should be possible. We'd have to try it.

Comment (Uwe Fink): In your *ab initio* calculations you need some parameters. You use normal coordinates, so you have to have a set of fundamental frequencies, you also need the interaction force constants. What sort of experimental data are needed for these so-called *ab initio* calculations?

Response: In principle, you can tell the computer what atoms are in the molecule and their approximate locations. Then you do a set of calculations at several different geometries to find the one with lowest energy, which is supposedly also the equilibrium geometry. During this search we shall have generated information to get predicted force constants, hence the normal modes. So in principle you can do the *ab initio* calculation without any data, and compare with experiment at the end, provided you have enough computer time. Of course, one should be cautious about these procedures.

Question: Can you comment on the calculation of the individual line shapes that go into the band shape?

Response: We haven't looked into that problem very carefully. We just fit the overall envelope by a function that approximately matches its shape.

Question (H. Pickett): The *ab initio* calculations generally overestimate the dipole moments. Does the same thing happen with the derivatives?

Response: Yes, the numerical values of the derivatives are usually not predicted correctly; sometimes they are over-estimated, but sometimes underestimated. There is a reason for that: for the calculations to be practicable you must use fairly small basis sets. Even when the calculated dipole moments are wrong, however, the derivatives may be in better agreement with experiment. The errors in the derivatives are not correlated one-to-one with errors in moments. I would expect the calculated vibrational band strength to be within a factor of two of the correct value, but it could be high or low.

Question: When you determine atomic polar tensor matrix elements from experimental data, is there any sign ambiguity?

Response: Yes, there is a problem in determining signs.

Question: Can the ab initio calculations help to resolve the sign ambiguities?

Response: Yes, we think that they are a big help in determining signs. If the basis set is too small or if configuration interaction calculations are not made, the predicted signs can be wrong. However, we believe the ab initio predictions of signs for dipole derivatives will be correct most of the time. The sign problem is one reason that transferability of intensity parameters was never expected to be possible. In the early days (20 years ago), there were so many sign possibilities that had to be considered in analyzing experimental data that it never seemed possible to decide which of them was right.

Question: Can you comment on the prospect of improving the accuracy of the predictions of vibrational strengths? Do you think we can get them within 10%?

Response: I think so. However, I don't really understand why things work as well as they do already. In order to study this question, we now try to compare the transferred polar tensors with the polar tensors that were calculated by ab initio methods, and then try to understand any discrepancies. When we transfer a polar tensor, we are assuming that the atom has the same environment (as far as its electrical and vibrational properties) in both the old and new molecules. In the HOCℓ molecule, the chlorine probably affects the environment of the hydrogen atom differently than another hydrogen would, so the hydrogen in HOCℓ is in a slightly different environment from that in H_2O. If we can understand this kind of effect and build it into the way we transfer polar tensors, we can improve the accuracy of the prediction to ± 10 percent.

Blank Page

NEW THEORETICAL AND EXPERIMENTAL METHODS FOR PRESSURE-BROADENED LINEWIDTHS AND THEIR INTERPRETATION

Jack J. Gelfand (Princeton Univ.)

In this presentation I will attempt to review recent progress in the theory of collisional line broadening, particularly the impact of recent advances in collision dynamics calculations. Also, I will discuss some new approaches to the interpretation of experimentally measured linewidths and their impact on planetary atmosphere research. Finally, I will mention some new experimental techniques which may have some advantage in providing pressure broadening data at very low temperatures.

As we all know, pressure broadening is caused by collisions that interrupt the emission or absorption of a photon. The calculation of pressure broadened linewidths then must involve some form of collision dynamics computation. During the course of this workshop many investigators have expressed dissatisfaction with the available data on pressure broadened linewidths, especially with regard to their behavior at low temperatures. I believe that recent advances in the ability to perform the necessary collision dynamics computations should help this situation in the near future.

An upsurge in computational capabilities has paralleled the development of very large computer systems in the past few years. The impetus for the development of computing techniques in collision dynamics in particular, along with the necessary funding, has been provided by a number of very practical applications to lasers, laser induced chemistry, and combustion. There has been, for some time, a moderate amount of activity in the modelling of many of the collisional interactions that are believed to be important for understanding the interstellar medium. This is because the molecular systems encountered are quite simple. In addition, the interstellar environment is at an extremely low temperature where very few rotational states are populated and the kinetic energies are small. These factors make the problem relatively simple. The spectra encountered in planetary atmospheres, on the other hand, involve molecules that are somewhat more complex than those that have been studied in interstellar medium. Furthermore, pressure broadening in planetary atmospheres usually involves molecule-molecule collisions and the temperatures encountered are high enough such that an appreciable number of rotational states are accessible. These factors make the total number of state changes encountered much larger than in interstellar medium problems. For this reason, the ab initio calculation of linewidths for systems of interest to planetary scientists has been typically beyond the capabilities of available computer systems and computational techniques. I feel, however, that the recent advances in the capability to do complex dynamical and intermolecular potential calculations will make its impact felt in these areas in the near future.

I would like to briefly review some of the important concepts involved in the capabilities and limitations of the present state of theory in collision dynamics. This review is by no means meant to be comprehensive, rather I will discuss these topics using some representative examples chosen to illustrate certain tradeoffs and capabilities. The important points to be made here are not in the specific examples, but rather, in outlining in broad terms where present limitations overlay the needs of planetary astronomers.

Pressure broadened linewidths are obtained by starting out with a potential function for the collision partners of interest. This potential function is substituted into the Schrodinger equation, and the Schrodinger equation is then solved to obtain state-to-state cross sections for the collision processes that are the components of the desired linewidth. By appropriate summing and averaging, collisional rates are computed. These rates can then be used to obtain the linewidth.

Some simplifications are usually made in order to make this problem more tractable. In the linewidth computation method due to Anderson one considers only long range electrostatic multipole interactions.[1] An arbitrary cut-off is usually made for the short range intermolecular potential. Furthermore, one assumes straight line classical trajectories for the collision path and a perturbation theory approach is used in solving the Schrodinger equation. This procedure works moderately well for highly polar molecules, but begins to break down in non-polar systems. It has also been found to give unsatisfactory predictions of the temperature dependence of collision broadening.

It is possible at present to do fully quantum mechanical calculations for systems that include up to about 100 states which are accessible in the collision process. This limitation is dictated by the size of the basis set that must be used. More than 100 states presently strain the capabilities of available computing systems to perform the matrix operations involved. Investigators are attempting to develop computational schemes that may allow for computations with as many as 1000 rotational sub-states. These restrictions on the size of the basis set translate to a limitation of temperature and the complexity of rotational structure of the systems involved. Molecules with many rotational levels at higher temperatures obviously have more states populated and therefore their collision dynamics are much more difficult to calculate.

A further complication arises in the need for accurate intermolecular potential surfaces. It appears that the most accurate intermolecular potential functions can be obtained for those cases where the potential can be calculated entirely ab initio. Gordon-Kim or electron gas type potential function calculations have been found to be satisfactory for systems where of the collision partners has as many as four atoms.[2] The limitation is in the number of points at which the potential must be calculated in order to accurately specify the intermolecular potential surface. This number of points grows rapidly with the number of individual parameters needed to specify the system. For a diatomic molecule colliding with an atom, one need only know the potential surface as a function of the distance between the collision partners, the vibrational spacing of the diatomic molecule, and the angles needed to specify the orientation of the collision partners. One can see that the dimensionality of the problem increases rapidly as one goes to molecules with a larger number of atoms. Satisfactory surfaces have been generated for formaldehyde-atom collisions and ammonia-atom collisions, as well as for some diatomic molecule-diatomic molecule systems.[3,4,5]

From the above discussion we see that there are limitations in the capabilities of both dynamical calculations and potential surface calculations. These translate into the complexity of the system that can be handled, i.e. the number of atoms in each of the collision partners, the rotational level structure, and the temperature. A survey of the literature indicates that the complexity of the systems for which dynamical calculations have been made exceeds that of the available ab initio potentials. For example, dynamical calculations have been made on the CH_4-He system to test certain features of methane-helium scattering, but a best guess intermolecular potential was used simply to demonstrate the effect and the capabilities of the computation.[6] However, accurate quantum mechanical calculations utilizing the best possible intermolecular potentials do exist for systems in which there is sufficient practical interest. For example, some good calculations exist for the collision dynamics in the HF-HF system for which a pressing need exists in the design of powerful HF chemical lasers.[7]

In summary, the capability exists to perform satisfactory fully quantum mechanical computations of the component collision processes of pressure broadened linewidths for many systems that would be of interest to planetary astronomers. The appropriate intermolecular potential functions, however, are not available in the literature simply because of a lack of overlap between these systems and systems that have been of interest to the collision dynamics, laser design or combustion community. Another problem exists in that computations in the literature are usually not user oriented. Most dynamical calculations are done to demonstrate some particular effect or calculate some small number of rates of interest. It is necessary to compute the rates for all of the collisions which interrupt the absorption of a photon for both the upper and lower states of the spectral transition. You cannot just thumb through the Journal of Chemical Physics and say, "Ah-ha, here are all the component rates for my line in a methane band, and I'm going to put in this pressure broadening coefficient." It is encumbent, then, upon the planetary physics community to encourage the appropriate workers in the collision dynamics community to first produce calculations of intermolecular potentials for the systems that are important in planetary atmospheres and, second, to do dynamical calculations which are sufficiently complete and user oriented so that they can be employed in generating the pressure broadening linewidths that are needed.

Other possible approaches to producing linewidth data exist and I would like to discuss a method which may be of some benefit in the areas discussed in this workshop. Two important problems seem to arise repeatedly in many different applications in the interpretation of spectra in planetary atmospheres. One is the generation of band shapes or low resolution spectra from individual line parameters and the other is the extrapolation of pressure broadening data at or near room temperature to other temperatures, especially lower temperatures. We discussed in the first section of this talk approaches to calculating pressure broadening data which involve full quantum mechanical calculations along with the necessity of calculating or measuring very accurate intermolecular potential functions. Some work that I am doing in the area of collision dynamics and linewidths may have some bearing on simplifying this task.

As I discussed earlier in this presentation, those phenomena which immediately precede the generation of pressure broadened linewidths are the state-ot-state rates of the component collision processes. Utilizing a procedure developed by DePristo and Rabitz it is possible to actually obtain state-to-state rates by direct inversion of appropriately measured linewidth data.[8] Having the appropriate set of rates and other dynamical factors obtained in this fashion, it may become possible to generate information from experimental measurements which can then be used to generate other needed linewidths and aid in extrapolating the linewidths to other temperatures.

The determination of any individual collision transition rate from a single bulk experiment, such as pressure broadening, has been considered difficult in the past because the pressure broadened linewidth is not very sensitive to any one component rate. In this approach to the inversion of linewidths to yield state-to-state rates, we are utilizing recently developed scaling relationships which fix the ratios of many rates within a family to a fundamental rate in that class, e.g., rotation-rotation or rotation-translation collisions.[9] The small number of fundamental rates can then be determined by a small number of independent linewidth measurements. Also determined are dynamical factors which allow one to calculate the elastic contributions such as dephasing, and the change in the various contributions to the linewidth with the vibrational excitation of the collision partners.

An example of the results of such a study are shown in Figure 1.[10,11] The experimental points are the pressure broadened linewidths for self-broadening in HCl. The fitted points are those generated by the component rates and dynamical factors derived from the inversion of the experimental data. An examination of the experimental points in Figure 1 reveals that the magnitude and form of the variation of the pressure broadening coefficient within a branch change as one goes from the fundamental to the higher overtone bands. One can see that within each branch that the peak valuse of the pressure broadening diminishes and the shape of the curve becomes flatter. The pressure broadening shows a peak because of the predominant contribution of near resolution R-R collisions. Because both collision partners must be in nearby rotational states, the probability of these types of collisions is controlled by the Boltzmann distribution and the degeneracy of the rotational states. The pressure broadening then varies in a manner which is similar to the probability function for the states of the collision partners. The lower peak pressure broadening coefficient and flattening of the curves for the higher overtone bands qualitatively indicates a diminished contribution of these types of collisions as the vibrational excitation of the spectrally active collision partner increases.

The results of the qualitative discussion above are confirmed by the actual rates some of which are displayed in Figure 2. These rates are for collisions between HCl molecules in the $j = 6$ rotational state and HCl molecules in the ground vibrational state as a function of the rotational state, j_2, of the collision partner.

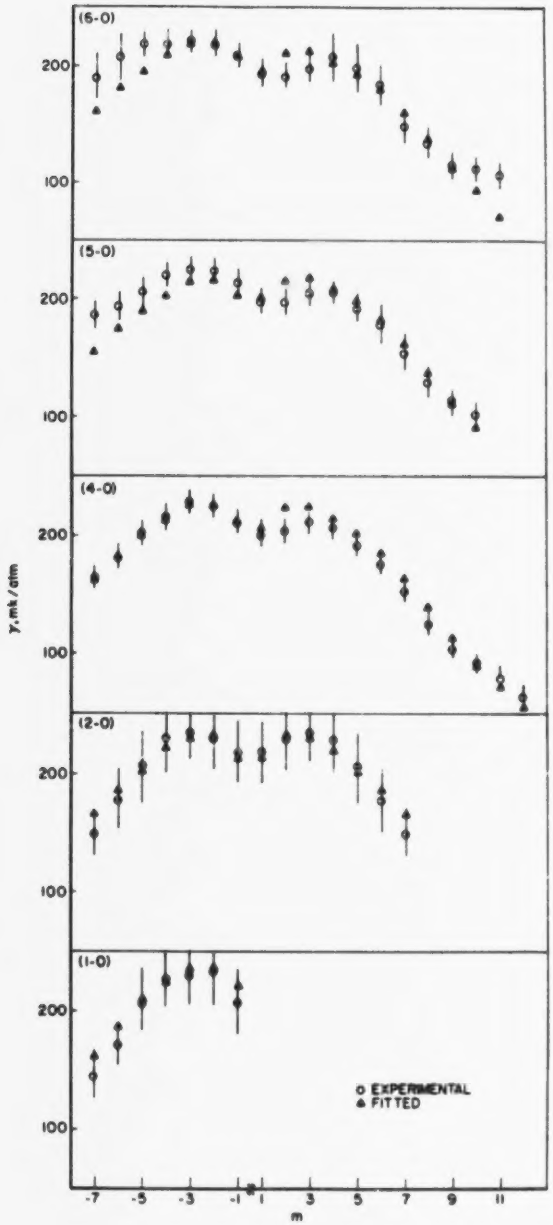

Figure 1. Experimental and fitted linewidths for the fundamental and 2-0, 4-0, 5-0, and 6-0 overtone bands of HCl.

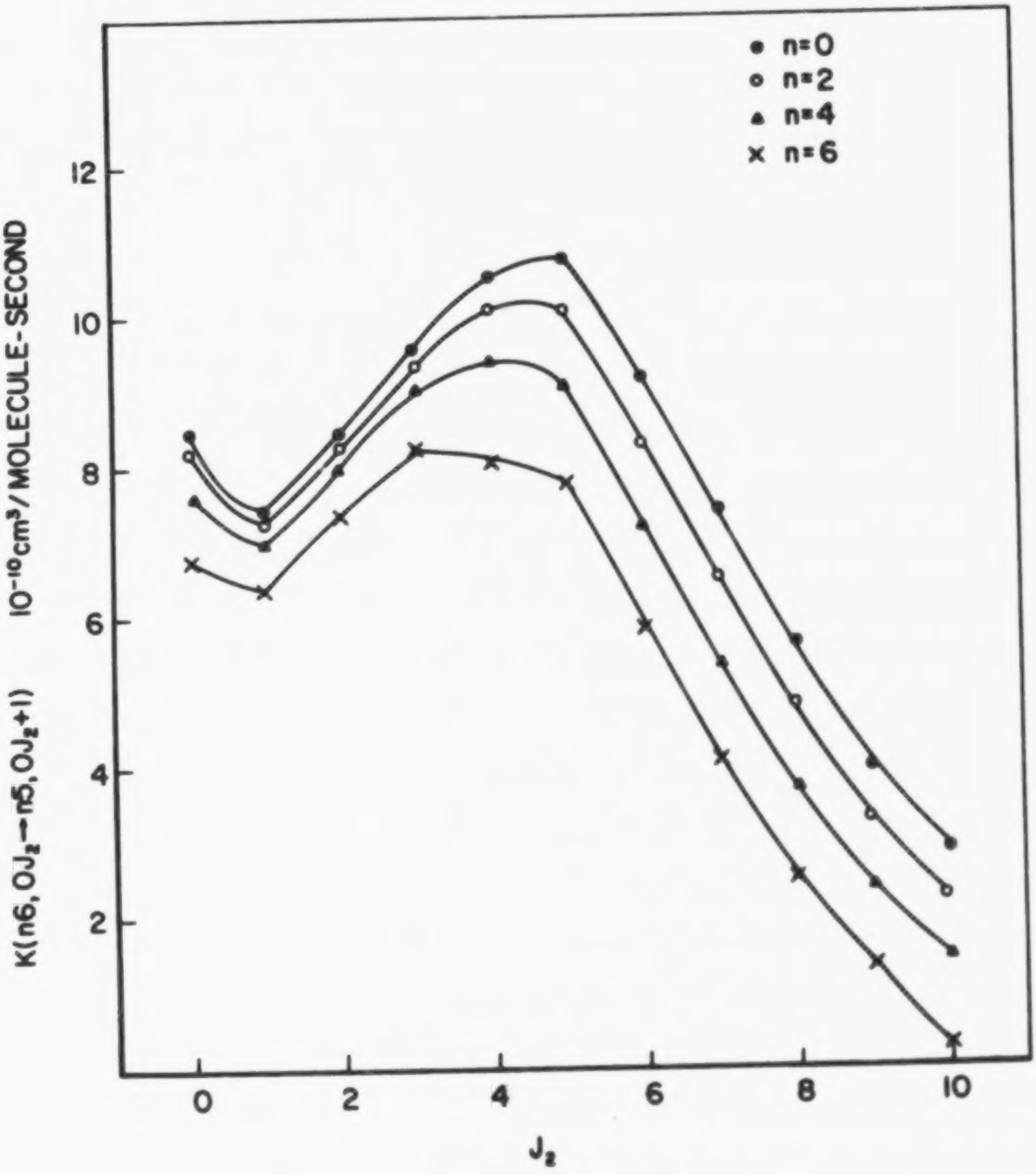

Figure 2. Representative state-to-state rotation-rotation rates extracted by inverting the 4–0 through 6–0 band linewidth data shown in Figure 1. These rates are for collisions between molecules in the j=6 state of the n=0, 2, 4 or 6 vibrational level and molecules in the j_2 rotational state of the ground vibrational level.

Curves are shown for the molecule in j = 6 in various vibrational states from the ground state to the sixth vibrationally excited state. As pointed out in the discussion above, the rates peak for the resonant collision of the molecule in j = 6 colliding with the molecule j = 5. We can also see that these rates diminish with the vibrational excitation of the j = 6 collision partner. This might be expected because the rotational spacing in HCl diminishes with vibrational excitation thereby making collisions with molecules in the adjacent rotational state less energetically resonant.

I would like to speculate on how the procedure which I have just outlined might be of some help in atmospheric modelling problems. If it is possible,utilizing a number of linewidths in a particular vibration-rotation band,to generate all of the component rates, then a set of basic information is available to generate other linewidth data for that band. This could be of great help in generating band shapes and synthesizing low resolution spectra. But more importantly, I think it may become possible to use these underlying rates as a basis for providing practical temperature scaling and temperature interpolation information.

The change in pressure broadening with temperature arises because of the change in the Boltzmann distribution of the energies of the collision partners. In computing the pressure broadened linewidth, it is necessary to calculate cross sections for collisions over the entire energy range of the Boltzmann distribution at that temperature. Different energy ranges are required as the temperature changes. An approximate way of doing this is simply to assume that the cross sections have no energy dependence and to scale the linewidth as a function of the average collision frequency. This results in the familiar $T^{1/2}$ gas kinetic linewidth dependence. The possibility of breaking linewidths down into their component collisional mechanisms may allow for a much more sophisticated temperature scaling of pressure broadening. Having obtained the individual rates one may scale each with its own temperature dependence. This may become possible due to recent progress in formulating simple energy scaling relations for the underlying cross sections.[12] This treatment may in the future provide a very elegant way of generating linewidths for atmospheric modellers over a wide range of conditions.

It is obvious from what I have reviewed up to this point that the kind of information that astronomers want at low temperatures for all of the systems needed will not be available immediately. Some day you will be able to ask someone to give you a pressure-broadening coefficient at 95° Kelvin for methane colliding with H_2, but at present if we want to get information in this area we are going to have to do some measurements. It is very difficult, however, to make these measurements on gases at temperatures where their vapor pressures are so low that there is hardly enough material in the cell to produce a detectable absorption. One of the answers to this problem may be the sensitive techniques that have been developed in various applications of laser spectroscopy. Some of these techniques were reviewed here at this workshop by Margolis in an earlier talk.

In the various direct absorption methods, one modulates a laser incident on an absorption cell. This can be frequency modulation, or one can simply switch back and forth between a gas cell and a reference cell, or one can modulate the gas employing the Stark effect. Some workers have produced direct laser absorption measurements with sensitivities equivalent to absorption coefficients in the vicinity of 10^{-5}/cm.[13]

Another method which was developed originally for air pollution measurements is the photoacoustic technique. A typical configuration is diagrammed in Figure 3. A cell is placed inside the cavity of a laser which is modulated at audio frequencies. The molecules in the cell are excited by absorption. They can receive either rotational, vibration-rotation or electronic excitation. As they collide with each other they relax producing a slight increase in the translational energy in the cell. This is then detected as an increase in pressure by a microphone. Patel at Bell Laboratories has pushed this experimental technique about as far as I think it can go, and he has been able to measure absorptions down to the vicinity of 10^{-10} per cm.[14] Microphones have been made which work at liquid nitrogen temperatures as well as for corrosive gases. One uses the intracavity configuration to take advantage of the high circulating power in the laser cavity. Not much power is being absorbed and one needs many incident photons to produce a detectable signal. Typical intracavity circulating powers are on the order of tens of watts, and for absorption coefficients of 10^{-6} cm^{-1}, about ten microwatts of energy are deposited in the cell. This level can easily be detected by the microphone.

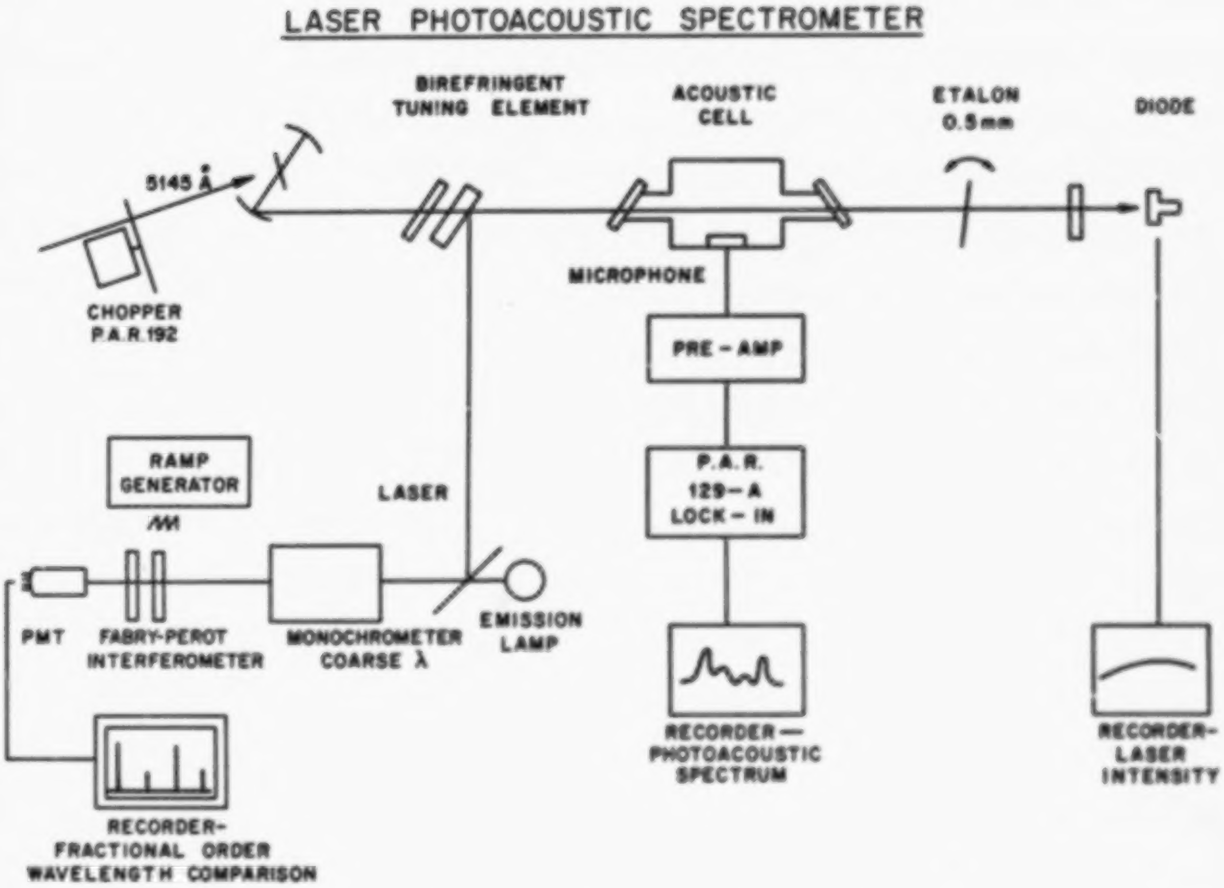
LASER PHOTOACOUSTIC SPECTROMETER
BIREFRINGENT TUNING ELEMENT
ACOUSTIC CELL
ETALON 0.5mm
DIODE
5145 Å
CHOPPER P.A.R.192
MICROPHONE
PRE - AMP
P.A.R. 129—A LOCK — IN
RAMP GENERATOR
LASER
PMT
FABRY-PEROT INTERFEROMETER
MONOCHROMETER COARSE λ
EMISSION LAMP
RECORDER — PHOTOACOUSTIC SPECTRUM
RECORDER-LASER INTENSITY
RECORDER-FRACTIONAL ORDER WAVELENGTH COMPARISON

Figure 3. Schematic diagram of the laser photoacoustic spectrometer.

Another advantage of the laser based system in addition to high sensitivity is that you can perform very accurate wavelength calibrations. One can use fractional order wavelength comparisons with emission lamps, for example. Pressure broadening measurements can be easily done using photoacoustic spectroscopy.[15] Figure 4 shows an example of some unpublished spectra of the so-called $5\nu_1$ band of NH_3 at 6450 Å taken at various pressures.

Question: Does the high intensity of the laser beam affect the shape of the line?

Response: No, we are not anywhere near the power-broadened regime for the absorption. The reason is that the laser is not focussed. The photoacoustic signal that you get does not depend upon whether the beam is small or fills the entire cell; it just depends on the deposition of energy. So if one were worried about multiphoton absorption or other kinds of nonlinear effects, one could simply expand the laser beam such that the energy density would be low enough to avoid these effects.

There is another method which is similar to photoacoustic spectroscopy, but uses the detection of the change in index of refraction to monitor the translational energy. This technique, developed by Davis and known as Phase Fluctuation Optical Heterodyne Spectroscopy, uses a Mach-Zender interferometer configuration.[16] A beam from a single mode He-Ne laser is divided into two parts at the input beam splitter. The reference beam passes through one arm of the interferometer to a photodetector. The other beam is routed through the other arm of the interferometer, through the gaseous sample under study and is recombined at the photodetector

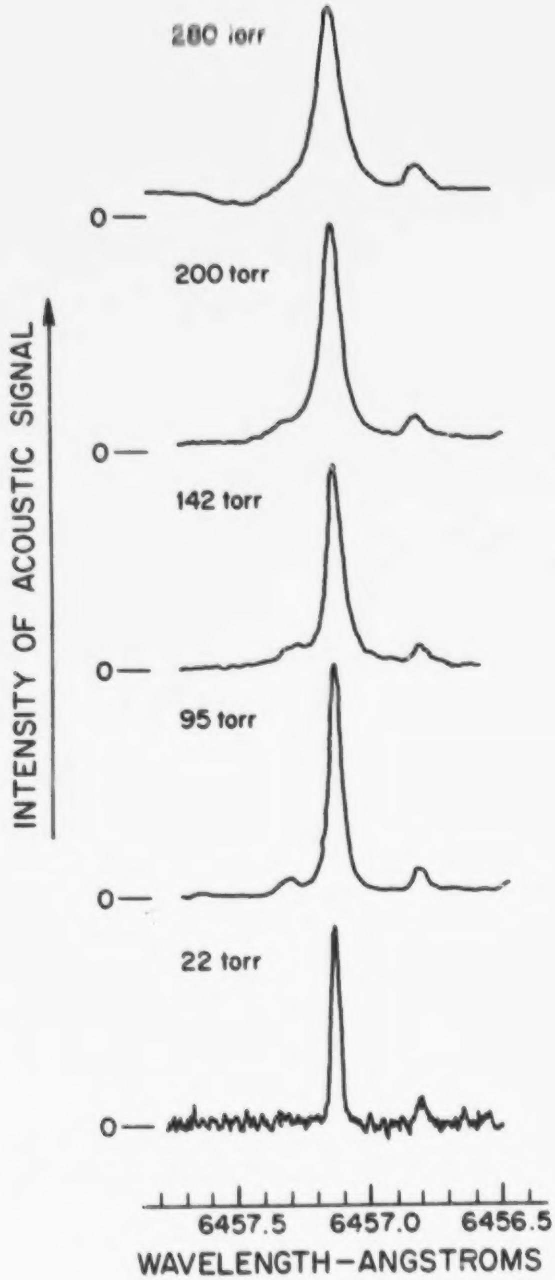

Figure 4. Photoacoustic spectra of a portion of the 6450A ammonia band taken at various pressures from 22 to 280 torr.

with the reference beam. The sample must of course be transparent to the probe laser. Another laser, collinear with the probe laser, is tuned to the spectroscopic transition being studied. As before, absorption of energy eventually produces a change in the translational energy which causes a change in the gas density. This gas density change produces a phase modulation on the probe beam which is detected by detecting the frequency side bands in the heterodyne detector. Index of refraction fluctuations smaller than 10^{-11} can be detected with this method and this translates into a limiting equivalent absorption coefficient which is comparable to photoacoustic spectroscopy, about 10^{-10} per cm.

Many of the laser detection techniques have been utilized successfully primarily because they have been mated with tunable dye lasers at visible wavelengths. As was stated in Jack Margolis' presentation earlier, tunable dye lasers are very well behaved sources. It would be nice to utilize some of these sensitive laser detection techniques further out into the infrared, especially to get to the fundamentals of some of the ammonia and methane bands for example. Though, pulsed tunable laser sources are available which operate in these regions, they are not as suitable for quantitative spectroscopic measurements as CW lasers, primarily due to poor pulse-to-pulse amplitude and frequency stability problems.

I would like to briefly mention that there have been some new developments at Bell Laboratories on a laser source capable of providing tunable CW radiation over the range from approximately 8000 Å to 3.5 microns wavelengths. This source, known as an F-center laser, utilizes color centers generated in alkali-halide crystals as the active medium.[17] Defects can be produced in alkali-halide crystals which absorb light in the visible and fluoresce in the infrared. Laser action is initiated by pumping the F-center crystal with either a visible or near infrared laser and tuning it in a cavity in much the same way as one operates a CW dye laser. One set of crystals with defects known as $F2^+$ color centers can tune from about 8000 Å all the way out to 2 microns. Substitutional color centers can go all the way to about 3.5 microns. These lasers appear to work as well as dye lasers in that they have good narrow frequency output behavior and smooth tuning characteristics. One of the drawbacks is that the color center crystals are expensive to produce and must be stored at liquid nitrogen temperatures. Rapid development is proceeding on this device and it appears that room temperature crystals which lase in the infrared will be produced in the near future. We have done some preliminary work on the spectrum of methane in the region of 9800 Å and find that this laser system works quite satisfactorily.

Sensitive measurements at wavelengths longer than approximately 3 microns are still the domain of direct absorption studies with diode lasers and very good Fourier transform machines. I do think, however, that there will be some developments in far infrared mixing schemes in the near future. Unfortunately all of the laser techniques suffer from very small tuning ranges. For an F-center laser or especially a diode laser one has to work through a particular absorption band one piece at a time.

References

1. P. Anderson, Phys. Rev. 76, 647 (1949).
2. Y. Kim and R. Gordon, J. Chem. Phys. 61, 1 (1974).
3. B. Garrison and W. Lester, J. Chem. Phys. 66, 531 (1977).
4. S. Green, J. Chem. Phys. in press (1980).
5. J. Prissette, E. Cochanski, D. Flower, Chem. Phys. 27, 373 (1978).
6. L. Smith, D. Malik and D. Secrest, J. Chem. Phys. 71 (1979).
7. M. Alexander, J. Chem. Phys. in press (1980).
8. A. DePristo and H. Rabitz, J. Chem. Phys. 68, 1981 (1978).
9. A. DePristo, S. Augustin, R. Ramaswamy and H. Rabitz, J. Chem. Phys. 71, 850 (1979).
10. M. Zughul, J. Gelfand and A. DePristo, J.Q.S.R.T. in press (1980).
11. A. DePristo, J. BelBruno, J. Gelfand and H. Rabitz, J. Chem. Phys. in press (1980).
12. A. Eslava, L. Eno and H. Rabitz, J. Chem. Phys. in press (1980).
13. A. Hordvik, Applied Optics 16, 2877 (1977), and references therein.
14. C.K.N. Patel and R. Kerl, Appl. Phys. Letts. 30, 578 (1977).
15. J. Gelfand, W. Hermina and W.H. Smith, Chem. Phys. Letts. 65, 201 (1979).
16. C. Davis, Appl. Phys. Letts. in press (1980).
17. L. Mollenauer, "Color Center Lasers", Ch. 6 in C.L. Tang, ed., Methods of Experimental Physics, Vol. 15B, Academic Press, New York (1979).

DISCUSSION

Comment (K. Fox): There may be an intermediate position; for a particular band, get measurements on several or a few key lines, to interpolate and extrapolate.

Response: That's right. We need appropriate interaction between the experimentalists and the theoreticians in this area. The theoreticians may have some particular relationship they feel can be extrapolated over some temperature range. They can come to the experimentalists, and say, "If you can give me a certain number of lines in this band, I can work out a generalization." I think that kind of interaction is necessary to crack the problem.

Question (B. Lutz): What were the conditions for the ammonia spectrum at 6475?

Response: The cell had a five centimeter path length, and the intracavity power in the laser was probably in the vicinity of five watts.

Question: You mentioned a sensitivity of 10^{-10} cm^{-1}. Is that difficult to achieve?

Response: Yes, that is with a signal-to-noise ratio of unity, and a lot of work. Realistically, you can get 10^{-8} cm^{-1}. Anyone can build preamplifiers and utilize fairly common microphones and put a photoacoustic cell together and achieve a sensitivity equivaleng to an absorption coefficient of 10^{-8} cm^{-1}.

Question: Do the windows limit your sensitivity?

Response: That depends on the scattered light in the cell. The windows scatter a very small fraction of light, which then hits the walls and produces a small amount of heat. This masks itself as an absorption. So it is very difficult to make good continuum measurements, although you can do it, if you are careful.

Question: What was your effective resolution on that ammonia spectrum?

Response: Probably 0.5 Å. That resolution was achieved with just one intercavity etalon and a birefringent tuning element. In contrast to spectrographs, with lasers you don't lose power as you narrow the linewidth to get better resolution. For each intracavity element inserted, you lose maybe 10 or 20% in intensity, but the resolution goes up by a factor of ten. It's just that life becomes extremely difficult because when there are intercavity elements in the laser cavity, you have to synchronize all the tuning and its a real show. You have stepping motors all over the place, and need some sort of microprocessor to control it all.

Question: When you do photoacoustic measurements you get out a photoacoustic signal, which bears a nonlinear relationship to the intensity. How reliably can you deduce the pressure broadening of the optical absorption from the pressure broadening of the photoacoustic signal?

Response: It's not nonlinear. The photoacoustic signal is linearly related to the energy deposited in the gas. The spectrum that you get is certainly good to within 5% of the true spectrum, by examination. Experiments are in progress in my lab at the present time to find out what the limiting accuracy is. I have spectra that were taken at Kitt Peak in the HCl overtone bands with 20,000 to 1 signal-to-noise ratio. I'm going to compare them to photoacoustic spectra. There is no reason why the photoacoustic spectrum can't be an exact reproduction of the optical absorption; it's not nonlinearly related, it's linearly related to the energy deposited. But I'm not going to stand here and tell you that it's going to be perfect. People have pushed it to where they can say that it's good to within 1% of the true spectrum. I haven't seen anybody who's bothered to take the trouble to really push it further than that. I have the need in my own measurements to work at this level so I am investigating this at present.

Question (H. Pickett): In connection with the last question, there will be a problem in getting the broadening, because the photoacoustic line profile will depend on the process that converts the optical absorption to heat, and not only on the shape of the optical absorption.

Response: Yes, the absorption has to be converted to heat. You have to be very careful about cell design, and chopping frequency. The cell must be large enough so that excited molecules do not diffuse to the wall and do not relax on the way. (That's a big problem at low pressures.) You also have to make the chopping time slow enough so that you allow for the total relaxation of the molecules. If you want to try to do a photoacoustic spectrum of hydrogen, it can be a problem because hydrogen relaxes extremely slowly. But for molecules like ammonia and methane, which have very fast relaxation times, it's not much of a problem.

Question: Is any work done in the time domain?

Response: Doing it in the time domain is another problem altogether. It is also a very active area of research.

Question: Are the scaling relations recursion relations?

Response: They are not recursion relations. You always use the same fundamental rate in the scaling relationship.

Question: With what accuracy can you scale these rates?

Response: We call it a "working-man's theory". It's good to approximately 10%.

Question (G. Birnbaum): I'm puzzled about the rates. You don't use potentials. But a transition probability per unit time is calculated quantum mechanically by taking matrix elements of the potential. If only one part of the potential is important for a particular rate, that rate can be scaled. So you need different rates for each part of the potential.

Response: That's right. What I showed was a relationship containing a fundamental rate. You need a fundamental rate for every family of interactions. So you need a fundamental rate for the rotation-to-rotation transitions, which depend upon the long range dipole part of the potential. For example, in HCl you have about six or seven fundamental dynamical quantities, but you have about 20 linewidth values, so the problem is well determined.

Question (G. Birnbaum): If you have one rate per piece of potential function, I grant that it can be scaled. But you still have the problem which has always been central to pressure broadening calculations. How would you relate the various rates, phase shifts, and the very strong perturbations: during the close part of encounters the perturbations become huge. All of these things have to still be solved to get a linewidth.

Response: Each of these types of interactions has a fundamental rate associated with it or dynamical factors which specify its contribution to the linewidth. That is the power of this procedure. For a full treatment on this subject, I refer you to a paper by Andy DePristo at the University of North Carolina, which will appear shortly in the Journal of Chemical Physics.

Blank Page

LABORATORY MOLECULAR SPECTROSCOPY

Jack Margolis (JPL)

I'd like to comment briefly on the relationship between astronomers and spectroscopists. It has been usual for astronomers to prefer to have spectroscopists try to simulate planetary atmospheres in the laboratory under conditions spectroscopically similar to those on the planet. This is a satisfactory procedure only for a crude analysis of observational data since all conditions of spatial and thermal inhomogeneity cannot practically be re-created in a real laboratory. Because of the obvious physical constraints of the laboratory environment, what they must deliver to the astronomers is enough spectral data so that the complete planetary atmosphere can be simulated in some other way, presumably a numerical simulation in a computer. In many ways this is a preferable procedure. The computer simulations can be used in several different ways, for example:

1. Various different atmospheric models can be calculated to compare simulated measurements with actual observations. The consistency between these can be used to deduce information about the physical parameters of the atmosphere.

2. The spectral data can be inserted into different atmospheric models in order to best design strategy for experiments, instruments or observations.

These are really kind of obvious remarks, but they point out the importance of completeness. In order to synthesize an atmosphere, what you need is all the information about the spectrum in some particular spectral region. This is actually an immense task and one which is not commonly undertaken. For example, if you look at the details of the spectrum in the vicinity of some particular vibration-rotation band, there may be many more than just a few infrared-active bands. In the case of methane, which is an interesting molecule to atmospheric scientists, there may be literally thousands of bands in a given spectral region, interacting in a complicated way and passing through each other. Admittedly, for some purposes complete spectroscopic information isn't necessary, but it certainly is important to matters like radiometric studies of atmospheres.

The traditional mode of operation for spectroscopists is to analyze a single band or a single set of interacting bands at a time. This produces a set of assignments and vibration-rotation parameters and this is what has scientific value to the spectroscopic community, whereas a simple listing of the lines in a given spectral region has little value although that may be exactly what the astronomers are after. Looking at a single band or a group of bands tends to leave out lots of probably weak lines which may add up to a lot of opacity in the atmosphere, or may contribute importantly to the signal in some sort of correlation spectrometer, or perhaps contribute to the signal in some other kind of instrument in some unexpected way.

These preceding remarks are significant because the spectroscopic methods which are of the most general value to the astronomers are those which acquire and can handle large volumes of spectra in digital form, or in a form which is compatible with computer analysis, and in a form which is at least internally consistent. Not all spectroscopic instruments do that sort of thing, and the ones that do may not be adequate to make the kinds of measurements that are desired and necessary. Also, in order to get the kinds of data that are important in the planetary sciences, there are certain combinations of instruments and devices which are necessary, and these combinations only rarely appear together.

Now I'd like to make some preliminary remarks about the spectroscopic state of the art. First of all I will discuss the precision that is required to make the necessary measurements. The remarks are directed specifically to vibration-rotation spectra rather than continuum absorptions. The ultimate precision that's required for line positions is related to the width of the lines which may be no narrower than the Doppler width. It is really necessary to know the position of the lines to some small fraction of the Doppler width in order to characterize the way in which lines are blended together when they do blend together (and that is a very common spectroscopic situation). That requirement means that the line position precision must be some small fraction of about 0.01 cm^{-1} at one micron (that is the Doppler width for moderately heavy molecules which appear in the atmosphere), or about 0.001 cm^{-1} at ten microns for those same kinds of molecules. That is a very tough requirement for line positions in the thermally interesting region around ten microns. Perhaps even higher precision is required to measure parameters like pressure shifts of the lines. Pressure shifts haven't been addressed so far, but they may be important in looking at winds, which can be detected and measured accurately to a few meters/sec by observing Doppler shifts in some sensitive way. This may be done for stratospheric and higher winds where pressures are low enough that the lines are not broadened much. At the present time absolute line positions are generally being determined consistently with accuracies within a small integer times a milli-wavenumber throughout the entire one to ten micron spectral range.

There does not seem to me to be any natural limit to the precision with which strengths need to be measured. It seems to me, though, that if individual lines can be measured to 5 percent, that's probably good enough for most applications, and well within the state-of-the-art for many kinds of spectroscopic instruments these days. It doesn't really strain the state-of-the-art for the best spectroscopic methods to do that job. Continuum absorption is difficult to measure; Dr. George Birnbaum will tell you about that later.

Line widths in the infrared are being determined these days to about 5 percent, and normally only at room temperatures. In all cases the precision of the measurements is much higher in those cases where the spectrum is open and unblended. That's a satisfactory situation for the very sparse spectrum of hydrogen. For most other molecules of interest, there is frequently lots of blending going on to make things complicated. and the kind of precision needed for determining the physical parameters of interest depends on just how thoroughly the lines are blended. They can be seriously blended, indeed, for molecules like acetylene, methane, ammonia, carbon dioxide, and water.

A frequently used technique for clearing up the spectra is to cool the gas. This reduces the strength of the hot band lines as well as high J lines. But coolable absorption cells with long optical paths are rare.

The most versatile kind of instrument for laboratory spectroscopy is a Fourier transform spectrometer. This has the special, desirable attributes that were brought out before by Dr. Rudi Hanel. It multiplexes the spectrum so that a wide wavelength range can be covered with a high signal-to-noise ratio, with the highest spectral through-put. It has a high potential resolution, which can be extended to the Doppler limit or almost to the Doppler limit in atmospherically interesting spectral regions simply by extending the mirror motion to lengths that are not really unreasonable with today's technology. The data is acquired automatically in digital form, and in a form which is suitable for manipulation in the computer. There are few examples of really high quality Fourier transform spectrometers and laboratory spectrometers now existing, and I apologize for not mentioning every one and not mentioning everybody's work. There are several in France; one at Meudon which has acquired spectra with a spectral resolution of 5 milliwavenumbers and better. There's one at Orsay which has gotten down to 5 milliwavenumbers. There's one at Air Force Geophysical Laboratories with a spectral resolution of 10 milli-wavenumbers, and one at Kitt Peak which operates at 10 milliwavenumbers and has been made to operate at 5. There are lots of others around the world and in this country which operate at .02 wavenumbers. These instruments have been remarkably prolific in producing spectral data of value to the atmospheric sciences. For example, an immense amount of work on methane molecules has been produced, but not all at the ultimate quality. Let me illustrate the quality that can be attained with FTS instruments by giving an example of a spectrum that was obtained at Kitt Peak observatory. This is a spectrum of hydrogen, the 4-0 line. Notice that the transmission covers a range of only 0.1%. The signal-to-noise in the line itself is greater than 50 to 1 and this was acquired with about 3 atmospheres of hydrogen in the absorption cell, at approximately 1/2 km of path length.

Question: What is the integration time required for the S/N obtained?

Answer: That represents 25 scans of the FTS at about 7 min/scan integration time. Another qualification I should make about that too--not every spectrum that comes out of there has that quality.

Talk resumes: The signal-to-noise in the continuum is something like 10^5 to 1; That may be the world's record for FTS instruments. The Kitt Peak device can be coupled to a number of short cells, including the 1 meter baselength White cell and a 6 meter baselength White cell, with paths up to about 1/2 km. The reason I bring this up is because the high signal-to-noise ratio, which is possible with the FTS, obviates some of the need for very long path lengths; the very long path lengths which are necessary to observe really weak absorptions like the quadrupole absorption in hydrogen, and which become spectroscopically important in planetary atmospheres which can have very extensive absorption paths. The instrument at Meudon can be coupled to a temperature controllable White cell, which has an 80 cm path length, and has been run down to 150° Kelvin.

There are a number of grating instruments which are competitive in resolution to the best FTS devices. These exist in various places around the country: at Ohio State, University of Texas, Florida State, the NBS, and also at the Herzberg Institute in Canada. These instruments have gained strongly by resolution enhancement, that is, the deconvolution of the instrumental function from the observed spectra. That's done, however, at the expense of signal-to-noise. Also, because of the way the gratings are driven in real spectrometers, the wavelength precision in grating spectrometers may not be as good as an FTS instrument. The wavelength calibration is a function of grating position in grating instruments, whereas all that is necessary for the absolute calibration of the wavelengths for an FTS instrument is the accurately known position of a single line. Even if this is not available, the relative positions of the FTS measured lines are well determined. This is an important advantage of the FTS.

There are a few other high resolution incoherent techniques: Fabry-Perot etalon, SISAM instruments, Hadamard transform instruments, and also a number of laboratories use correlation spectroscopy.

I'd like to go on to talk about laser methods. There are a few laser methods which operate over the interesting IR wavelength range, primarily lead salt diode lasers, which operate from 15 microns to about 3 microns. There are a number of disadvantages to working with diode lasers; I'll mention these before I get to the advantages. First of all, they need to operate at very low temperatures, that is, temperatures below about 100° Kelvin. They tune continuously within a single mode only over a very short wavelength range; typically the wavelength tuneability in a single mode is about a wavenumber. It's frequently less than that--infrequently more. That's true especially at the longer wavelengths where they are most useful, because of their high resolution and because the FTS instruments are most inadequate there. They also have a very complex mode structure (that is, complex in frequency as well as spatially) and they frequently emit several modes simultaneously, which creates a spectral purity problem. They don't tune linearly, and they tune non-linearly differently in different modes. That's a problem for frequency calibration. However, a group at the NBS recently used heterodyne methods (that is, heterodyning the diode laser against a stable CO_2 laser) to directly measure the frequency of the 10 micron diode laser; that sort of wavelength calibration can be carried out with very high accuracy. Diode lasers are noisy, especially when several modes are being emitted simultaneously, and they're delicate. Those are the disadvantages. They do possess a number of characteristics which are so attractive that they frequently offset the disadvantages. First of all, they have extremely high resolution when they're properly operated; you can get absolutely Doppler-limited spectra using them even at 10 microns and longer. They can be tuned at high speed, in fact, at a kiloHertz rate, and that makes it possible to do derivative spectroscopy. This is an attractive mode of operation, because it makes it easy to measure or detect weak absorption. The record for weak absorption measured in this way is an absorption of one part in 10^5 (that was measured by a group at McMaster University in Canada, using diode lasers), and that sensitivity has also been achieved at JPL. You can see how being able to detect weak absorption sensitively is an advantage in reducing the size of absorption cells. Sometimes the diode lasers can generate modestly high power; milliwatts at the short wavelengths, and a tenth of a milliwatt or so at the longer wavelengths. The amount of power that they produce appears to be unpredictable; the construction of diode lasers evidently appears to still be an art, not a science. They may be developed to the point of being suitable for quiet operation; if so, they can then be used as local oscillators in heterodyne detectors. This sort of operation has been demonstrated and is very desirable from the standpoint of achieving quiet detection in the IR.

Comment: In fact, it's in general use.

At shorter wavelengths there are dye lasers which have been extensively used for spectroscopic purposes from the very near IR to the UV. They can be made to operate in a single mode and very quietly. Their operation in this wavelength range, however, is competitive with the FTS which is superior in several respects:

1. wavelength coverage
2. calibration and internal consistency
3. data format

However, dye lasers may be superior in terms of the ultimate S/N obtainable, and therefore, the weakest absorption detectable. That's important in the short wavelength region, because we are really dealing with high overtone and combination bands there, which are intrinsically weak. Because they can emit a great deal of power in a single mode (a few hundred milliwatts is not difficult to achieve) and can be made to be fairly noise free, they can approach photon noise statistics. It has been shown that the ultimate sensitivity may be a few powers of 10 of the number of detectable molecules.

The best application of dye lasers to the kind of spectroscopy of interest to this meeting may be the Allan Pine beat frequency parametric oscillator. He beats a single mode stabilized dye laser against an argon ion laser in a temperature tuned LiN_bO_3 crystal. This limits his frequency of operation to 2.2 μm $\leq \lambda \leq$ 4.2 μm, and his output power to submultiples of μwatts. Nevertheless, with good InSb detectors (which have NEP's $\lesssim 10^{-11}$ watts $\sqrt{Hz}$) and reasonably short integration times, Pine is able to get marvelously high signal-to-noise ratios, on the order of 10^4, and moderately long tuning range per mode. A high signal-to-noise ratio is the key to getting really good frequency calibrations at high sensitivity. This method produces absolutely Doppler-limited spectra at these wavelengths, and Pine gets very good frequency calibrations, on the order of a milliwavenumber, and really superior line strength determinations. The precision of his line strength determinations is at least on the order of a percent, probably much better than that, and they are obtained just by measuring the peak height. These strength determinations are among the best ones around.

An interesting application of laser methods in high sensitivity detectors is opto-acoustic spectroscopy. This has been carried out with high sensitivity at Bell Labs by Patel, who has claimed a sensitivity on the order of 10^{-10} per cm. This sort of thing is being carried out in other places as well, namely, at Princeton University and at Washington University in St. Louis, where there is some effort being made to apply the method to molecules of planetary atmospheric interest. Frequently, the opto-acoustic detector is operated in an inter-cavity mode in a dye laser, and that's most useful for the short wavelength bands which show up in extensive planetary atmospheres and which are weakly absorbing. What's attractively advantageous about this technique is that the opto-acoustic cells are really small physically, and so it's much easier to control the temperature, for example, and determine the temperature dependence of the parameters of interest.

The prospects for using lasers directly for high sensitivity detection in weak absorptions are intriguing; I'll give an example of that. Modern detectors are available in all wavelength ranges these days, with small NEP, and sometimes with a large dynamic range. With laser sources of even modest power, the controlling noise is in the laser itself. As the lasers are improved, the ultimate limit will be the quantum statistical noise of the photons themselves. The signal-to-noise ratio will then increase as $\sqrt{\text{intensity}}$ and can get to be very large even for a small laser intensity. Although real lasers always possess greater noise power than the quantum limit, some of them do pretty good. For example, a Canadian group at McMaster University claims to have detected an absorption of $\sim 10^{-5}$ using an exceptionally quiet single mode diode laser and a 2nd derivative method. Shimoda has used a CO_2 laser to obtain

Stark modulated spectra of CH_3Cl and indicated that his ultimate sensitivity was $\sim 10^6$ molecules.

There appears to be no good reason why correspondingly high sensitivity should not be achieved in other spectral ranges covered by different tuneable lasers, for example FCL, beat frequency lasers, dye lasers or TEA CO_2 lasers.

A numerical example will illustrate the kind of measurements it may be possible some day to do:

> R(1) of the $3\nu_3$ band of CH_4 has a strength of 10^{-5} cm^{-2} atm^{-1}. The peak absorption of an unbroadened line in a 10 cm cell at 0.1 atm pressure will be $\alpha_{peak} \approx 0.5 \times 10^{-3}$.

The quantum statistical signal-to-noise for a 1μ watt laser at 1.0μm is $\sim 2 \times 10^6$. This implies that, even for a noise power 100x greater than the quantum statistical noise limit the R(1) line could be detected in an absorption cell of very modest proportions. This kind of sensitivity greatly alleviates the requirements on long absorption cells and large amounts of sample material. [Samples can become very expensive when some rare isotopes are considered, and these are almost invariably lost.] The smaller physical size will, as mentioned earlier, alleviate the difficulties of varying the temperature in the absorption cell.

Let me talk about prospects, dividing them into long-term and short-term without really saying how long or how short.

It seems to me that the best short term prospects for obtaining spectra of the highest quality over wide spectral ranges are those using conventional methods and especially the FTS method. The best FTS instruments are, in fact, capable of producing data for almost any of the problems proposed for planetary atmospheric spectroscopy, and there appears to be no inherent difficulty in extending their capabilities. For the short wavelength ranges starting at about 1 1/2 micron, a one meter total path instrument is adequate to resolve the Doppler widths of any atmospheric molecule. For wavelengths longer than 1 1/2 microns, where high resolution is required to resolve the line widths, many of the difficulties in making the instruments decreases, e.g. the precision requirement on knowing the moving mirror position is relaxed as are the optical quality requirements.

The best long term prospects I think are with laser spectroscopy. I don't really know how to prove the truth of that statement; I'm merely stating it as a matter of faith more than of knowledge. Nevertheless, the technology of high-power tunable low noise single mode lasers or laser devices continues to be improved, and to be applied to interesting problems in spectroscopy. These applications are important to the production of high quality, high resolution, high sensitivity spectra. As the power of these devices increases, their signal-to-noise increases, and the speed advantage of conventional multiplex spectrometers decreases. This leads to a serious problem for both the conventional and laser spectroscopists, namely, that as the volume of spectrum production increases, it reaches a limit beyond human capabilities to analyze it. In fact, the modern FTS instruments already produce a data rate that surpasses an individual's capacity to examine it at each stage. The best FTS produce data at such a rate that even a small group of people can't really keep up. So I would like to conclude by saying it is really going to become necessary to wed the spectrum to a computer, in order to comprehend it. The detection and the determination of the frequency of spectral lines is already carried out at high speed this way, for the great mass of FTS spectral data produced. At present, efforts are being made to extend this kind of computer analysis to the determination of shapes and strengths. The method seems to work well for isolated lines, and I think needs to be improved for blended line widths.

Discussion

Comment: Everything you said about certain types of instrumentation and spectroscopic techniques is in some sense true, and it points out that you need to look at them not as individual methods, but to look at them in a coordinated sense. Your diode laser is a good example. When you are looking at diode laser spectra, you like to have either high resolution FTS or grating spectra to compare with, and that's an indirect comparison. Another is, of course, to connect the diode laser with one of these instruments, an FTS or grating, as was done at Ohio State. That combines the best of two worlds. My second comment applies to your closing statements about the volume of spectroscopic information. If you think of what you do when you have a set of data of varying accuracies, either intensity or frequency, you weight them by roughly the square of the accuracy. That means that as resolution and accuracy on intensity and frequency improve linearly, the spectral information content improves quadratically, and when coupled with the broad band width attainable with an FTS instrument, it's not surprising that things are getting out of hand. Of course, that doesn't mean we want to stop! There is much more spectral information in the high resolution, high accuracy data obtained today, and automated data handling and data bases are important.

Comment (M. Mumma): I think we can go further than that. In the past, say more than five years ago, there was a kind of public works project for spectroscopists. Measurements were primarily instrumentation limited, meaning that with each improvement in the instrumentation one might re-do the spectroscopy, re-do the calculation of band constants and strengths and so forth, and get an improvement. Now we're at the point where we can really do definitive spectroscopy on many molecules, spectroscopy that doesn't have to be re-done. We can fully resolve the lines and get absolute line frequencies to an accuracy that's sufficiently good for any purpose you can imagine. Line strengths can be measured to the accuracy with which you can determine the pressure and cell length. We've got an opportunity now to do the fundamentals once and for all, and to begin on the overtones and intercombination bands, as you pointed out, and from that standpoint I think spectroscopy is changing right now. The number of diode laser systems that have been sold in the past five years is really phenomenal; tremendous numbers of articles are appearing in print, reporting what I call "final spectroscopy" on many of these band systems.

Response (J. S. Margolis): I'd like to say something about the diode laser systems. They do produce Doppler-limited spectra, but it really is difficult to calibrate them in frequency. I think we really want to know the line positions to do something on the order of a tenth of the Doppler width. That's tough to do with diode lasers.

Comment (M. Mumma): Well, we're working on that problem; a number of clever approaches have been developed recently, but I think we're a long way from solving it. You mentioned heterodyning against a known laser line; that's one approach. A second is varactor mixing: the gas laser is mixed with a microwave oscillator and a tunable diode locked to a particular line. The third is reference to standard lines. You're quite right in highlighting the problem, but I think it's well on its way to solution.

Comment (B. Lutz): I am afraid what you said about the FTS or other good spectrometer obviating the necessity for longer paths is not always true. It is true if you consider single isolated lines, but when you start looking at manifolds or places where the line density is high, you can't tolerate three atmospheres or even one atmosphere. In the case of ammonia, you can't tolerate 50 torr or even 10 torr. You need very, very low pressure and then also very long path length.

Comment (L. Brown): But you don't need to get the maximum optical density by using long path lengths at high pressure. You can put in long paths at low pressure and still get good sensitivity.

Response: You can detect very weak absorption by virtue of having very high signal-to-noise ratio.

Comment (B. Lutz): But I think you still have cases where you need long paths. With very, very weak absorptions you can't get enough column density in a single path cell, even with a 6 meter cell.

Response (J. Margolis): Well, by having high signal-to-noise ratio, you can reduce the required path.

Comment: But you increase the pressure broadening.

Comment (L. Wallace): You didn't mention line shapes; line shapes are a very important problem these days.

Response: I am not biased against line shapes, but I don't have much to say about them.

Comment (A. Tokunaga): You mentioned Indium Antimonide detectors having an NEP of 10^{-12}, or approaching that anyway. I have noticed a tendency for laboratory spectroscopists to use techniques which are not truly optimized, in the background-limited-sense that astronomers use. It would be interesting to know if you have a flux-limited experiment in a lab.

Comment: I am interested in experiments at high pressure. Are the current intra-cavity opto-acoustic detection systems capable of working at high pressures?

Response: Yes. They work better at high pressures. They have been used up to atmospheric pressure.

Question: And above?

Response: They can be made to work; it's just a matter of keeping the windows on. I don't know of anybody who operates at above atmospheric pressure.

Comment (J. Caldwell): I think most of the comments I've heard just recently are from people who are loosely called spectroscopists. Let me make an astronomical comment. I would like to take sharp disagreement with one of your introductory remarks about whether or not laboratory people should attempt to simulate conditions in a planetary atmosphere when they take their data. I could cite numerous activities where not doing this caused an error. The alternative you suggest, simulating a band on a computer, I think is not desirable; I just don't have confidence that you guys know enough to do that correctly. I have here a viewgraph I would just love to show you, of a band which as far as I know nobody predicted. It was observed first in planets. This is a spectrum of liquid methane, but it happens to correspond very nicely to gaseous methane. The important feature here is that the temperature is 96 Kelvin. This little feature is the wing of the well-known 8800 Angstrom band out here, and you see it is very strong indeed. There is a real feature here. This spectrum was taken in 1977. At that time the existing methane spectra were essentially all at room temperature (at least all of the ones my colleagues knew about), so the high-J line was populated out here and there was no way in the world anybody could tell that there was something extra here. Now this feature does exist: you can see it in the spectrum of Titan. 96K is a fairly good representation of the middle atmospheric temperature on Titan. One could imagine planetary scientists going through all kinds of trouble trying to interpret this feature in terms of an exotic molecule, when in fact it's just methane, which everybody knows is there in copious amounts. There are many other molecules that people have tried to fit to so-called unidentified features. The whole point is that if you were working at room temperature, you would miss this feature. I don't know of anybody who could predict this feature on a computer. My point is that in trying to simulate the planet, you can get insights about temperature effects like this.

Response: Let me make my remark again and add a qualification that I missed the first time. What the spectroscopists should report to the astronomers is a complete set of data, including the line positions, the strengths, and the temperature dependence of the strengths.

Comment: That normally requires an analysis computed to know the ground state energies and the transitions.

Response: Generally, it's good enough to know the ground state energies approximately, and these can be determined simply be measuring the strengths at, say two temperatures.

Comment (R. Beer): That isn't going to help you with the kind of extra feature Caldwell was talking about.

Response: Well, if you knew the temperature dependence of the strengths of the lines you would know what the appearance of that band is going to be.

Comment (R. Beer): Isn't Caldwell's point that this extra feature can't even be seen at room temperatures, because too much else is emitted near it?

Comment (K. Fox): Well it's not as bad as that. It's possible to scale the spectrum by temperature...

Comment (M. Mumma): If you know the constants and all that.

Comment: That's more efficient than trying to simulate all conceivable conditions.

Comment (L. Brown): If you have a quantitative and complete list of molecular constants or temperature dependences, you really can predict the spectrum under different conditions. You can satisfy the needs of people looking at a lot of different atmospheres this way. Now your case involves a spectral region that hasn't been well investigated. If you had been looking instead at the 7-micron region, I think you can predict more of what's going to pop up at a lot of different temperatures.

Comment (K. Fox): And that could also be done if an astronomer requested a focus on a certain spectrum or band.

Comment (J. Caldwell): If you don't know something is there, you can't request such a focus. Those who request the focusing are probably going to be diffuse about what they want.

Comment (K. Fox): That's right, but you must have had a clue.

Comment (J. Caldwell): No, we didn't.

Comment (R. Beer): Part of a spectrum can have a little bump, a little wiggle in it somewhere. That is in fact the intent of my question to Willis Person: If I give you a spectrum, can you tell me what it's made of? Otherwise, all we can say is "Gee whiz, we've got a new molecule." Unless you can give me a lab spectrum pertaining to conditions that at least approximate those I'm seeing, how am I ever going to proceed?

Comment (P. Varanasi): You didn't have time to mention a couple of aspects which have remained problems all the while that sources and detectors were being improved. These aspects are important in the measurement of intensities, line widths, shapes, and so on. In determining the intensities from the data (even at high resolution), there is a question of noise, not only in the sources and detectors, but also in the conditions of the gas. Even if you know the frequency and intensities very precisely, you may not know very accurately how much ammonia you have, or its pressure, or whether the temperature is the same everywhere in the cell. Especially if you have a cell of very large volume, the ammonia will stick to the walls of the cell. Where do we stand on these problems?

Answer: We all suffer from these problems. I don't know how to answer that question. It's a tough problem.

Comment (K. Fox): I think we'll come back to some of these same questions throughout the workshop. They are liable to pop up again.

Comment (U. Fink): To come back to this problem of simulating atmospheric conditions, you do need actual data; calculations are not enough. You might think that methane in the 7-micron region is a good counter-example. We know all the fundamentals. There are very few new bands that you think can happen there, but I can show you some methane spectra at three or four kilometer-amagats which show bands in absorption which you have never predicted before.

Blank Page

Microwave Rotational Spectroscopy

H. Pickett (JPL)

I will concentrate on two topics. First, I want to urge you to take advantage of the region upward of 1 millimeter, which hasn't been discussed much at this conference. Second, I want to describe applications of this region: how microwave, millimeter and submillimeter spectra (the so-called rotational spectra) can fruitfully interact with infrared spectral measurements.

Figure 1 shows that frequently the rotational bands of molecules can be quite strong, compared with vibrational bands. I have plotted a typical rotational absorption coefficient for a linear molecule in a low-J state with a dipole moment of about one Debye. The solid curve represents an absorption coefficient at a pressure which is high enough to produce the pressure-broadened limit, (I assume that the spectral resolution is great enough to resolve the line), and the broken curve represents the absorption coefficient in the Doppler limit. The vibrational case was chosen similarly: the transition dipole moment used for the vibrational case is typical of CO at the peak of its rotational distribution. This is a moderately fair comparison of strong absorptions in both regions. The low pressure curves show that, in the high atmosphere (clouds), the rotational spectrum has the potential for giving much greater sensitivity because of the larger absorption coefficient. Rotational spectra can also provide much information on high altitude parameters that often cannot be obtained from higher frequency spectra.

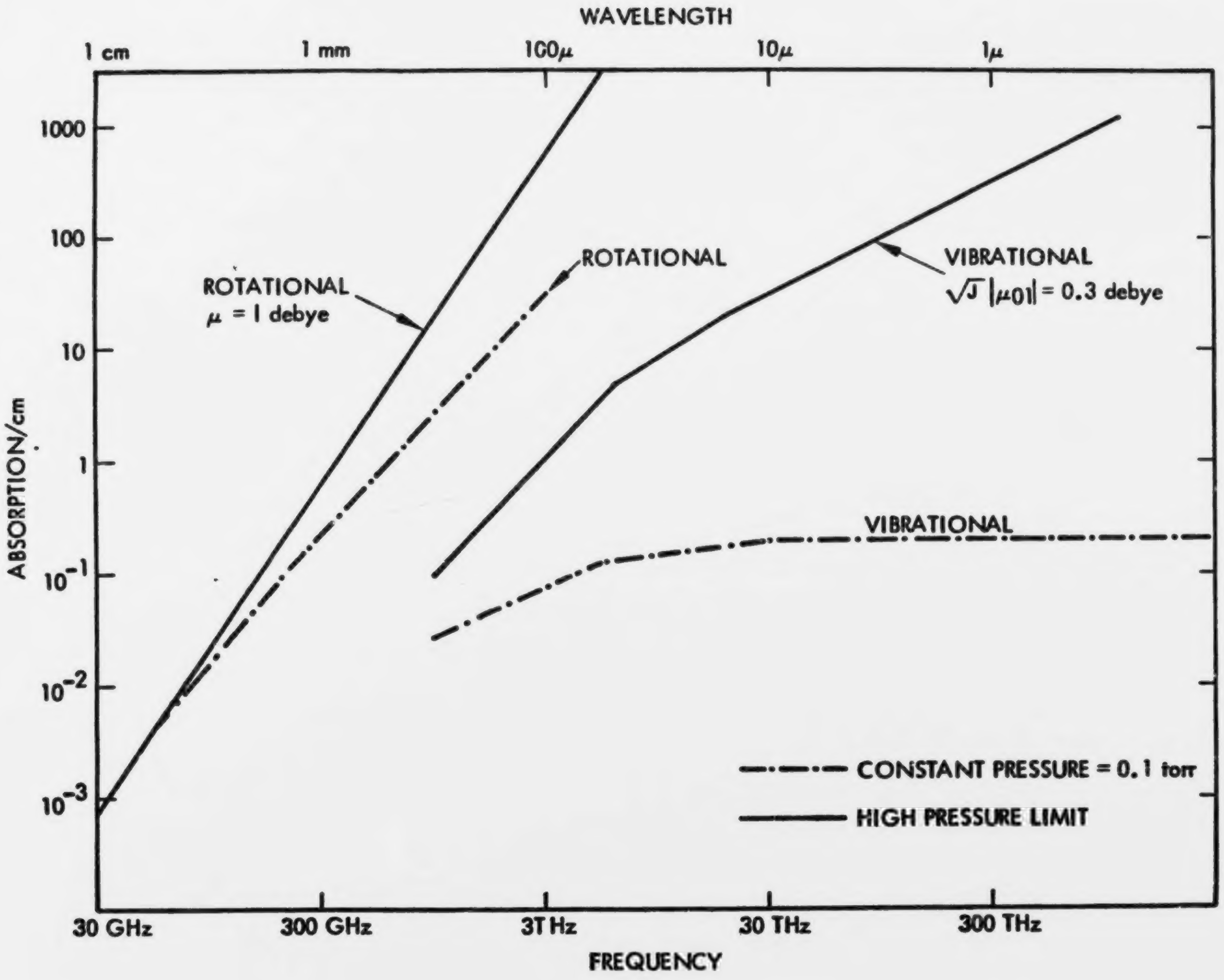

Figure 1. Strengths of molecular rotational and vibrational bands in the pressure-broadened and Doppler-broadened Regimes.

Figure 2 shows the transition from the pressure-broadened limit to the Doppler-broadened limit, at a variety of frequencies. At pressures near 0.1 atmosphere, the 10 μm shapes are already going into the Voigt and Doppler profiles. It would be difficult to get information about the composition and temperature at low altitudes from this infrared spectrum, whereas such information would be obtainable from the rotational spectrum, which is in the pressure-broadened limit. Since the pressure cross-over value scales directly with the frequency, by a wavelength of 1 millimeter the half-width has become very small.

On the other hand rotational spectra also give information on trace species at high altitudes. In particular, they are useful for measuring photochemical trace species at higher altitudes. The resolution needed for this would probably require a heterodyne system, for example. For heterodyne detection of thermal emission you have to use a modified Planck function, namely, the Planck function multiplied by the square of the wavelength.

Figure 3 shows the modified Planck function as a function of frequency. It provides a measure of the efficiency with which temperature can be determined from the input power. At about 10 microns only 10% of the power at a particular temperature will be effective, compared to the efficiency at lower frequencies. Combined with the absorption this can tell you about absorption in the submillimeter region by species in the upper atmosphere.

To be fair, I should mention some of the disadvantages of the submillimeter region. Absorption by the Earth's atmosphere is large enough to force you to use an airplane, balloon or spacecraft platform. Also, the

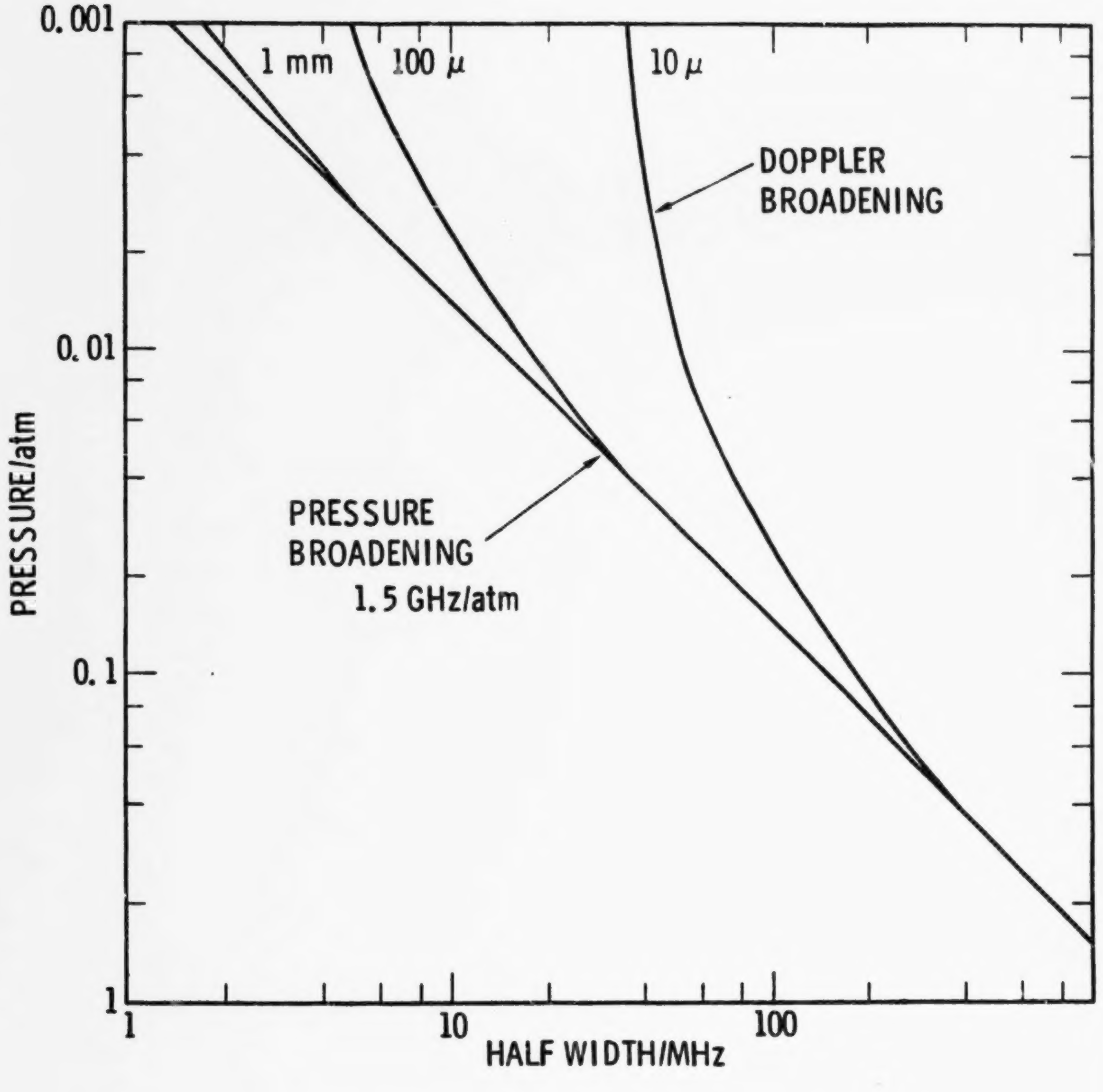

Figure 2. The transition from Doppler-broadened to pressure-broadened lines as a function of wavelength and pressure.

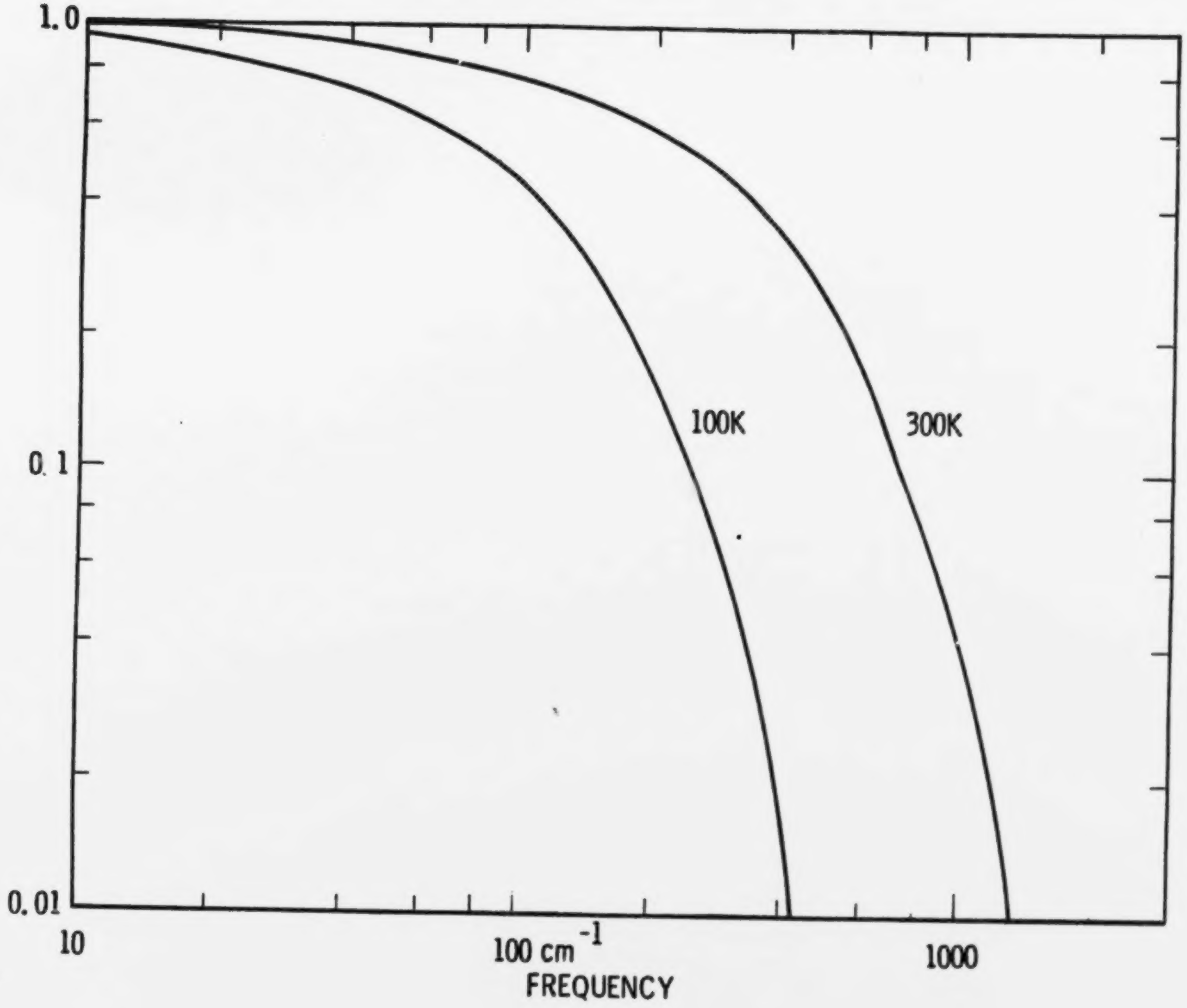

Figure 3. The normalized effective Planck function seen by heterodyne receivers (see text).

development of local oscillators and heterodyne mixers is much less advanced in the far infrared or the submillimeter region than it is for lower or higher frequencies.

Now I'd like to switch to my second topic: how laboratory spectroscopy in the lower frequency region can interact quite favorably with infrared measurements, as well as being a help to astronomers using the lower frequency region.

Table 1 shows some parameters for NO, which can be considered to be a planetary molecule if we include the Earth in our list of planets, derived from our work on the pure rotational lines resolving the hyperfine structure of NO up to 500 GHz. Surprisingly enough, we were able to use the same Hamiltonian that is used in the infrared; it is quite uncommon to be able to do so. The parameters of this Hamiltonian are compared in Table I with those derived from a very high quality Fourier transform spectrum in the infrared. We get rather good agreement with the infrared data. Moreover, the pure rotation data determine the parameters of the four-frequency fit much more precisely than the infrared data can.

Another example is the spectrum of CH_3D (Fig. 4). This molecule has a dipole moment of about 5×10^{-3} Debyes for this transition, very weak and also (because the dipole moment is small) hard to modulate. The peculiar shape is an artifact of the different way in which absorption coefficients are measured in this region. My point is that it is possible to measure species like this. Its rotational spectrum, and therefore the ground-state energies can be determined quite accurately. Using molecular constants derived from Fourier

Table 1
$^{14}N^{16}O$ Parameters (MHz)

	This Work	Amiot et al.[4]	Adjusted From Hallin et al.
A_o	3691453. (assumed)	3691453. (4)	3691438. (16)
B_o	50849.2276 (20)	50849.24 (11)	50849.22 (5)
A_{Do}	10.4217 (11)	10.421 (9)	10.43 (8)
D_o	0.16415 (8)	0.16400 (17)	0.1637 (12*)
p	-350.34512 (16)	-350.44 (24)	--------
q	-2.85507 (8)	-2.850 (22)	--------
p_j	-0.000228 (4)	0.	
q_j	-0.0000420 (12)		

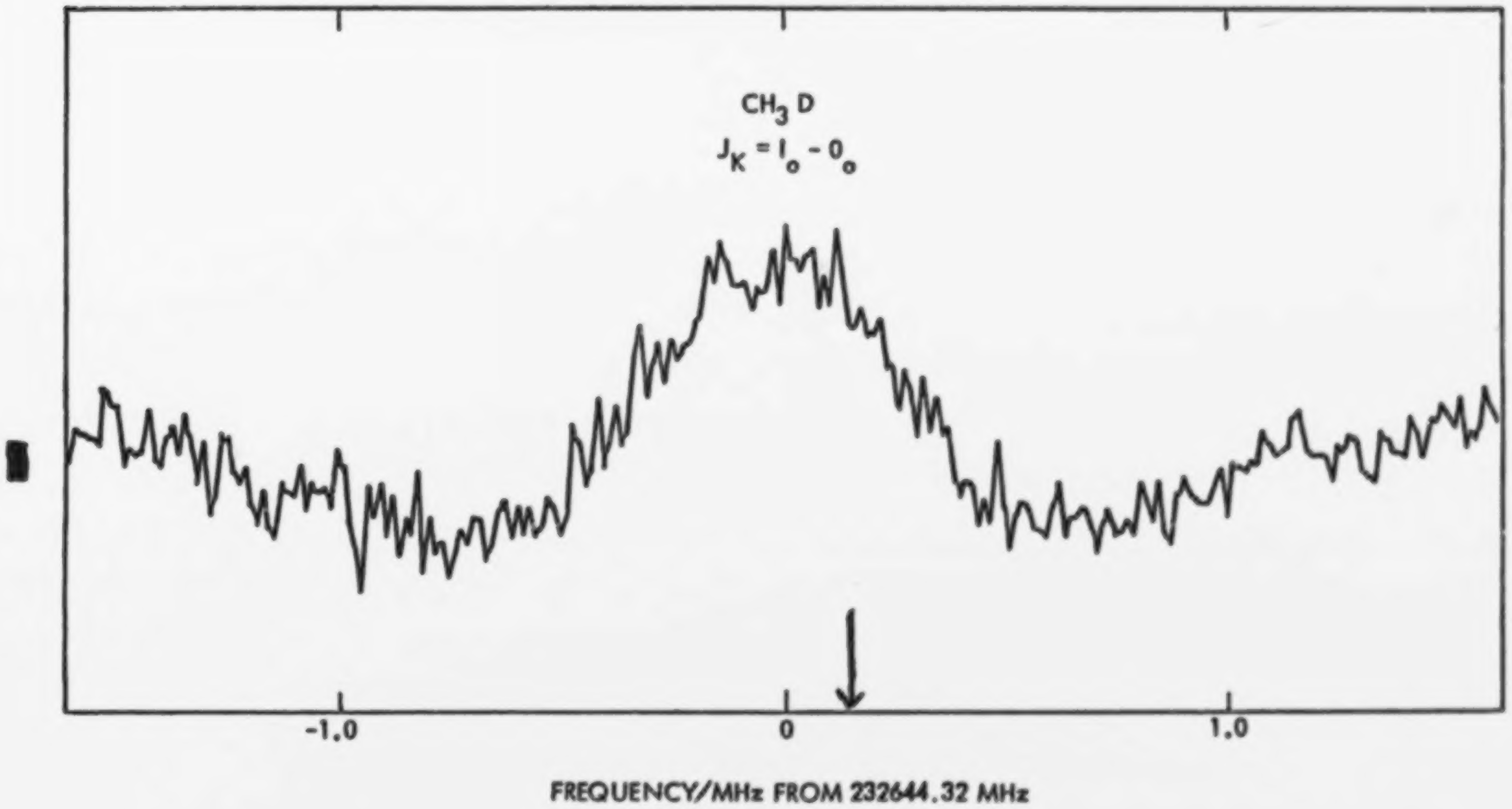

Figure 4. Laboratory measurement of sub-millimeter rotational line of CH_3D. Arrow indicates predicted position based on infrared data of Chackerian (Ref. 6).

transform measurements in the infrared, Chackerian[6] was able to predict the frequency of the central line (Fig. 4). Their prediction is shown by the arrow, only 40 KHz away from the measured microwave transition. At least for frequency determinations, the values determined by the high-accuracy Fourier instruments and the precision microwave frequency measurements have converged in the last five years or so. Note that the whole of Figure 4 covers a range of only about 0.0001 cm^{-1}.

Figure 5 shows an example of what can be done with trace species by using the rotational region of the spectrum. Fig. 5 is a spectrum of the ClO radical. This was taken at 649 GHz, the highest frequency at which a free radical has been observed using microwave techniques. The splitting is about 6 MHz and is due to lambda doubling in the $^2\pi_{3/2}$ state. At lower frequencies we have also measured the temperature dependence of the line width of $C\ell O$ for pressure broadening by nitrogen. An advantage of the microwave region for free radical trace species, is that once the dipole moment is known, the line strength can be calculated accurately, without having to make absolute measurements of the density.

Figure 6 is a spectrum of phosphine. It shows the J=K=0 to J=1, K=0 transition at 266 GHz. The spectrum appears on our spectrometer as one line, but the rf modulation gives it the shape seen in the figure, the result being essentially a coarse-grained second derivative. We have developed a new procedure for fitting line widths when working with these modulated spectra. We take the low pressure spectrum and convolve it with a Lorentzian, adjusting the width and shift of the Lorenzian until the result agrees with the high pressure spectrum. Then we plot the residual to evaluate how well the

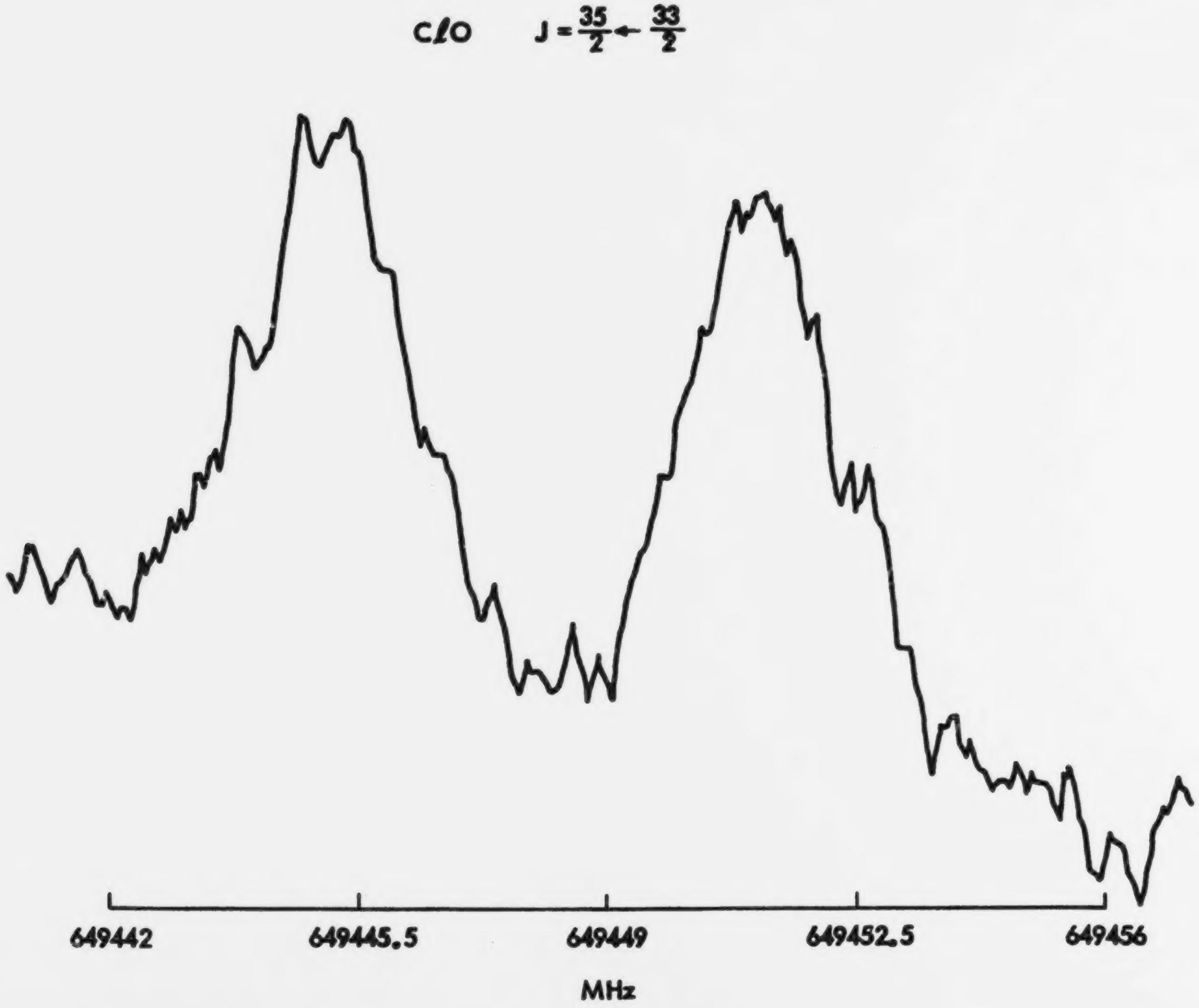

Figure 5. Laboratory measurement of lambda splitting in ClO ($^2\pi_{3/2}$) state near 461 μm.

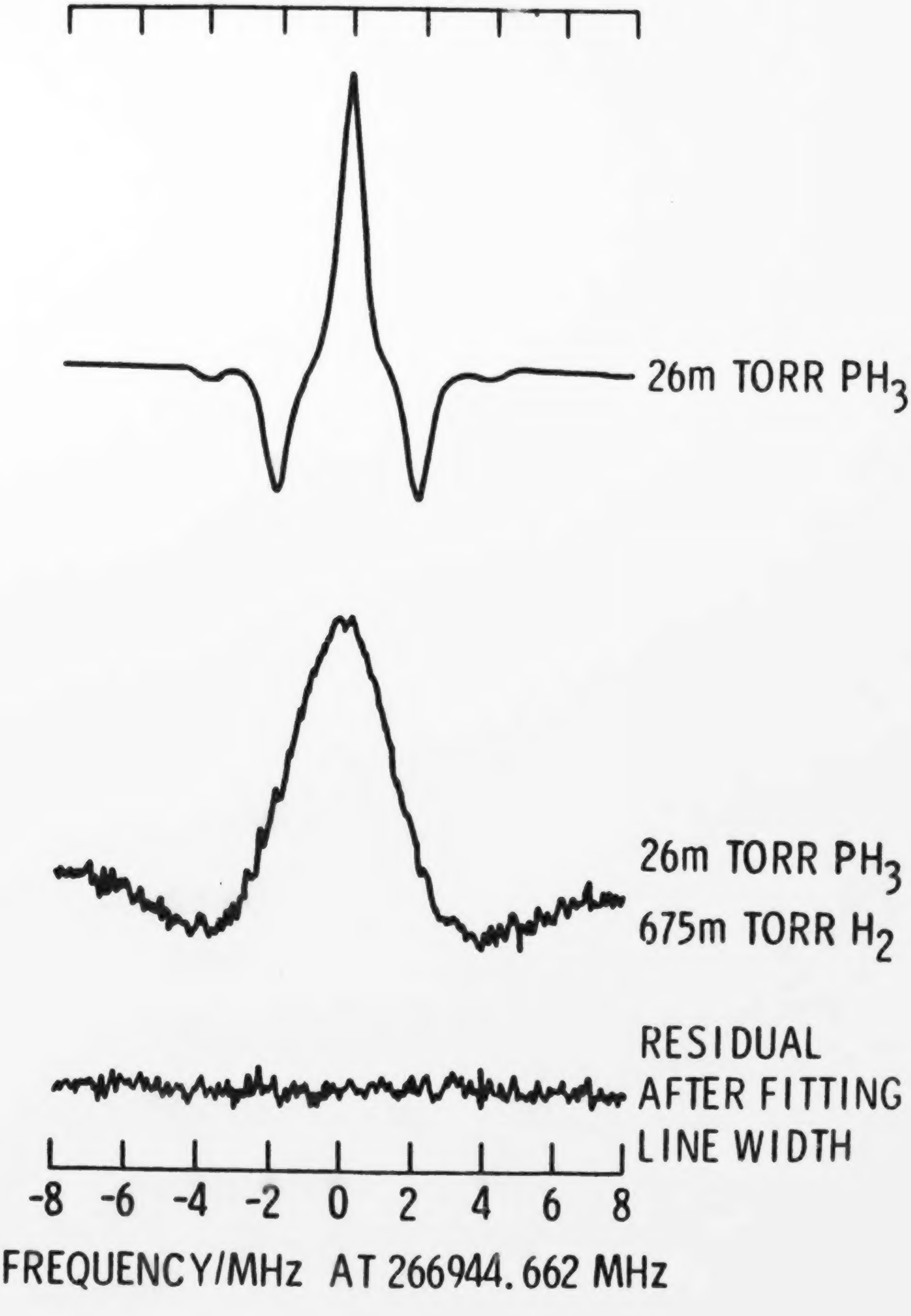

Figure 6. Illustration of measurement of pressure-broadening of PH_3 by H_2.

synthetic high pressure spectrum agrees with the low pressure spectrum. This method doesn't require any knowledge of the form of the modulation we use (the instrument function, so to speak), or the amount of Doppler broadening.

Table 2 shows some results of our measurements on phosphine (to about 5% accuracy) and (to a little bit better accuracy) for phosphine with hydrogen and helium broadening. These measurements were taken only at room temperature, but it certainly would be possible to measure them at lower temperatures. Note that the hydrogen broadening in this case is not much larger than the phosphine self-broadening. To repeat a warning that I made yesterday, the line shift for this transition for phosphine self-broadening is only a factor of 10 smaller than the width.

Finally, a simple expression for line widths, valid in both the microwave and the infrared region is: line width $=\langle 1-S_{ii}S_{ff}^{*}\rangle$. It involves a scattering S-matrix for the initial and final states. Without going into details, it can be seen that the S matrix (and therefore the width) is an average over the vibrational state: an expectation value of sorts. Therefore the microwave line width is expected to be the same as an infrared line width with similar rotational quantum numbers to the same level of accuracy that a P-branch width is similar to an R-branch width involving the same rotational quantum numbers. As a rule of thumb, this typically is accurate to better than 5%.

Gas	Differential pressure (mtorr)	Width (MHz)	Shift (MHz)	Width/pressure (MHz/torr)	Shift/pressure (MHz/torr)
PH_3	26.	0.146	0.0098	5.615	0.392
	102	0.576	0.0450	5.647	0.441
	152	0.852	0.0943	5.605	0.620
			average:	5.62	0.56
				±0.02	±0.08
H_2	112	0.495	0.001	4.42	0.009
	225	0.951	-0.013	4.23	-0.058
	335	1.448	-0.005	4.32	-0.015
	445	1.945	+0.004	4.37	0.009
	550	2.417	0.012	4.39	0.022
	675	2.996	0.023	4.44	0.034
			average:	4.39	0.000
				± .06	±0.033
He	83	0.177	0.0017	2.135	0.020
	164	0.354	0.0013	2.161	0.008
	272	0.613	0.0046	2.252	0.017
	3790	0.856	0.0116	2.258	0.031
	485	1.101	0.0070	2.278	0.014
	585	1.340	0.0093	2.291	0.016
	787	1.798	0.0121	2.284	0.015
	1021	2.335	0.0197	2.277	0.019
			average:	2.24	0.017
				±0.08	±0.007

Table 2
Phosphine Broadening and Pressure Shift

References

1. H. M. Pickett, E. A. Cohen, and T. G. Phillips, "Deuterated Methane: Laboratory Rotational Spectrum and Upper Limits for Its Abundance in OMC-1", Astrophys. J. (Letters), 236, L43-44 (1980).
2. H. M. Pickett, "Determination of Collisional Linewidths and Shifts by a Convolution Method", Applied Optics, 19, 2745-2749 (1980).
3. H. M. Pickett, R. L. Poynter and E. A. Cohen, "Pressure Broadening of Phosphine by Hydrogen and Helium," J. Quant. Spec. and Rad. Transf. 26, 197-198 (1981).
4. C. Amiot, et al., Can. J. Phys. 56, 251-265 (1978).
5. K-E. J. Hallin, et al., J. Mol. Spec. 74, 26-42 (1979).
6. C. Chackerian (private communication).

DISCUSSION

Comment: A general lesson can be learned here, about CH_3D in particular, but also about other molecules. According to molecular theory, it is possible to use regions of the spectrum where certain instruments can obtain highly accurate molecular constants, and then use these constants to calculate other regions of the spectrum which may not be accessible. The ground state of methane is an example.

Response: Another example is the spectrum of vibrationally excited states. Vibrationally excited states can often be measured in the microwave region, and rotational parameters can be obtained for those excited states.

Question (K. Rao): Can you comment on the difference between your results and the Soviet results for the frequencies of CH_3D lines?

Response: We have found a number of cases where frequency calibrations have been important for frequency measurements with this number of significant figures. For our calibrations, we run our frequency counter directly out of the wall from the hydrogen maser at JPL. So I am confident that our frequency measurements are quite good. Frequency calibrations may or may not play a role in the particular discrepancy you mentioned.

Question (K. Rao): You showed some very nice phosphine and $^{14}N^{16}O$ spectra. Do you have similar information for ^{15}NO and $N^{18}O$?

Response: We plan to work with $N^{15}O$ and we are planning to look at the vibrationally excited states.

Comment: I agree that the line widths of the microwave lines are similar to those for the vibrational lines, with one possible exception: that is, at certain temperatures or for particular transitions of non-polar broadeners.

Response: Very peculiar exchange affects can occur for non-polar broadeners, particularly for self-broadening. We have also glossed over the collisional phase shifts between the upper and lower state. These will affect the line shift more than the widths. These phase shifts enter as a sine in the former and as a cosine in the latter.

Comment (B. Lutz): How do molecular constants obtained by your group agree with those found by other groups. Both Alan Tokunaga and I feel that there is far too little critical inter-comparison of results obtained by different groups working on the same molecule.

Response: For a molecule like NO we had difficulty comparing our results to their results. The signs of some of the parameters are ambiguous in the literature, particularly for large molecules where the sign depends on whether the interacting state is assumed to be a sigma plus or a sigma minus state. To properly inter-compare infrared and microwave results, the data itself must be involved in the fitting. A co-variance matrix is not usually available from the previous author's data.

Comment: For several molecules, such as phosphine, no two sets of measurements give the same values of the molecular constants.

Response: There is no hope of reconciling molecular constants based on different measurements unless error bars are published with the measurements. Papers on vibrational transitions often give the difference between observed frequencies calculated from molecular constants, but hardly ever show error bars on either.

Question: With the accuracy currently available, are the pure rotational experiments sensitive to the pressure, and the temperature? Can you detect pressure shifts?

Response: Yes.

Comment (A. Young): This seems to be one of the first places where pressure shifts have really come up for discussion. Mike Mumma mentioned a situation a little while ago, where you really need absolute frequencies in order to get Doppler effects, e.g., when you are talking about wind speeds on the order of meters per second. In these cases the pressure shifts can be comparable to the meters-per-second Doppler effects that you are trying to measure, so you do need to take them into account.

Question (K. Rao): Do you have plans to go into higher frequency regions?

Response: We can routinely work up to 650 GHz and have made several measurements to 850 GHz.. We run into a stone wall there, because our multiplier and detector both die at that point.

Blank Page

SPECTROSCOPIC DATA COMPILATIONS

Page

The JPL Millimeter, Sub-Millimeter, and Microwave Line Catalog – Herbert Pickett 191

The AFGL Molecular Line Atlases – Laurence Rothman 195

Blank Page

The JPL Millimeter, Sub-Millimeter, and Microwave Line Catalog

Herbert Pickett (JPL)

Our catalog includes molecules of interest in the interstellar medium, in planetary atmospheres and in the Earth's atmosphere.

We use slightly different units than those on the AFGL tape, but they contain much the same information. For citing line frequencies in the microwave region, we decided to include on the tapes either the experimental errors or the propagation of errors from the fit. This gives an estimate of how accurate the frequencies are. The intensity units are defined as follows: the logarithm of the intensity unit is the cross-section times the frequency in MHz. This is essentially the same unit as on the AFGL tape, but contains fewer factors of the speed of light. We don't list line widths, but we do include the upper-state degeneracy. The upper-state degeneracy is an important quantity, since the spin degeneracy must be properly taken into account when calculating the Einstein A-coefficients from the intensities. Table I shows some of the molecules presently on the tape.

The catalog is available to the scientific community either as a tape or on microfiche (filmed in frequency-sorted and molecule-sorted format). The upper frequency limit in our fitting calculation is 100 cm^{-1}.

DISCUSSION

Question: What is the lower cut-off on line strengths for a line to be included in the catalog?

Response: The cut-off for the line strengths varied from molecule to molecule. For every molecule, there's a write-up which includes the strength cut-off and a cut-off in J (if one was used). It also includes the partition function that would be used at 300°K; in considering resolved line structure, you have to make sure that everybody agrees on the partition function, and that the values of the dipole moment appear correctly.

Question: Are you planning to include line widths in the future?

Response: We didn't include line widths because we are interested in both atmospheric and planetary applications, and we couldn't decide which broadening gases to use.

Question: How can you get copies of the catalog?

Response: We do not have a mailing list. If you write to us we'd be glad to tell you how to obtain a copy. For a tape copy, you would send us a clean tape, and we'll send you back a tape, 9-track, blocked in 720 characters, ASCII. Microfiche will also be available; this is actually a very convenient form.

Question: Can you possibly fit 90,000 lines on microfiche?

Response: The lines fit on 8 fiche at 42X reduction.

Table 1
Index of Species

1001	H-Atom
2001	D-Atom
3001	HD
12001	C-Atom
13001	C-13-Atom
14001	N-Atom
14002	N-Atom-D-State
16001	O-Atom
17001	HO
17002	NH3
17003	CH3D
18001	DO
18002	N-15-H3
18003	H2O
18004	NH2D
18005	H2O-ν2
19001	HO-18
19002	HDO
27001	HCN
27002	HNC
28001	CO
28002	HC-13-N
28003	HCN-15
28004	DCN
28005	HNC-13
28006	HN-15-C
28007	DNC
29001	C-13-O
29002	HCO+
29003	CH2NH
30001	CO-18
30002	HC-13-O+
30003	DCO+
30004	H2CO
30005	C-13-H2NH
30006	CH2N-15-H
30007	CH2ND
30008	NO
31001	HCO-18+
31002	H2C-13-O
32001	O2
32002	O2-v1
32003	CH3OH
32004	H2CO-18
34001	O-18-O
34002	H2S
34003	PH3
34004	H2O2
35001	HDS
36001	HCl
38001	HCl-37
40001	CH3CCH
41001	CH3CN
41002	CH3CC-13-H
41003	CH3C-13-CH
41004	C-13 H3CCH
41005	CH3CCD
41006	CH$_2$DCCH
42001	CH3CN-15
42002	CH2CO
43001	CHDCO
44001	CS
44002	SiO
44003	CH3CHO-A
44004	N2O
44005	CH$_3$CHO-E
45001	C-13-S
45002	Si-29-O
45003	NH2CHO
46001	CS-34
46002	Si-30-O
46003	H2CS
46004	C2H5OH
46005	HCOOH
47001	H2C-13-S
47002	HC-13-OOH
47003	DCOOH
47004	HCOOD
48001	SO
48002	SO-v1
48003	H2CS-34
48004	O3
48005	O3-ν2
48006	O3-ν1,3
50001	S-34-O
50002	SO-18
50003	O3-SYM-O-18
50004	O3-ASYM-O-18
51001	HCCCN
51002	ClO
52001	HCCC-13-N
52002	HCC-13-CN
52003	HC-13-CCN
52004	HCCCN-15
52005	DCCCN
52006	HOCl
53001	C2H3CN
53002	Cl-37-O
54001	CH2CHC-13-N
54002	CH2C-13-HCN
54003	C-13-H2CHCN
54004	CH2CDCN
54005	HOCl-37
55001	C2H5CN
56001	CH3CH2C-13-N
56002	CH3C-13-H2CN
56003	C-13-H3CH2CN
56004	C2H5CN-15
56005	CH2DCH2CN-S
56006	CH2DCH2CN-A
60001	OCS
60002	SiS
61001	OC-13-S
61002	O-18-CS
62001	Si-29-S
62002	O-18-CS
62003	Si-30-S
62004	SiS-34
63001	HNO3
64001	S2
64002	SO2
75001	HCCCCCN
76001	HCCCCC-13-N
76002	HCCCC-13-CN
76003	HCCC-13-CCN
76004	HCC-13-CCCN
76005	HC-13-CCCCN
76006	HCCCCCN-15
76007	DCCCCCN
80001	HBr-79
82001	HBr-81
95001	Br-79-O
97001	Br-81-O

Blank Page

The AFGL Molecular Line Atlases

Laurence Rothman (AFGL)

I will describe the current status of the AFGL line compilations. For those of you who may not be familiar with them, there are two compilations extant, the main Atlas and the Trace Gas Atlas. The main Atlas has been available for about five or six years, and includes the major absorbers in the Earth's atmosphere approximately in the wavenumber region shown in Table 1. There have been several updates. The present version is distributed for us by the National Oceanographic and Atmospheric Administration in Asheville, North Carolina.

Currently, the main Atlas includes about 150,000 lines (the Trace Gas Atlas is 30-40,000 at the moment). The information on each Atlas is essentially a card image per line, which includes the frequency (in vacuum wavenumbers) of the transition, the line strength at a standard temperature of 296 Kelvin (given in cm^{-1} per molecule per square centimeter), and the half width of the line. The lower-state energy is the fourth parameter, E", shown in the last line of Table 1 (a -1 is put in place of E" for transitions which have not been identified as yet, so that people using transmission/emission codes have a flag to avoid incorrect temperature extrapolation). Then there is

Table 1
AFGL Data Bases

- MAIN ATLAS

AFGL ATMOSPHERIC ABSORPTION LINE PARAMETERS COMPILATION

MAJOR TERRESTRIAL ABSORBERS FROM 0-20000 cm^{-1}

(H_2O, CO_2, O_3, N_2O, CO, CH_4, O_2)

- TRACE GAS ATLAS

POLLUTANTS, UPPER ATMOSPHERE, PLANETARY ATMOSPHERES, LABORATORY

(NO, SO_2, NO_2, NH_3, HNO_3, OH, HYDROGEN HALIDES, ClO, ETC.)

INFORMATION PER TRANSITION

ν_i, $S_i(T_o)$, $\alpha_i^L(T_o)$, E_i'' , QUANTUM IDENTIFICATION, DATE, ISO, MOL.

a quantum identification field, giving the vibrational transitions, rotational information, and other quantum index information such as electronic level or splitting code. Finally there is a data code that provides a means of referencing a particular line, and finally an isotope and a molecule code. For calculating transmission and emission strengths in LTE conditions, only the first four parameters and the molecule identification are needed to determine whether corrections to the molecular parameters are needed.

The work currently in progress has mainly been driven by water (see Table 2). In the case of updates on pure rotation, we found quite a number of strength discrepancies in the vibrationally excited ν_2 rotation, and we are in the process of regenerating the eigenvectors for that transition. This is a rather tricky problem since we must avoid the bad minima in the least-squares fitting process, but we expect to have it finished shortly. By the way, I hope to have both the main compilation and the trace gas compilation out by the summer of 1980. (At that time, there will be the third meeting of a workshop that is being held under the auspices of the Upper Atmospheric Division of NASA. A great deal of input on the trace gases has been coming out of workshops of this type). In the case of the 6.3, 2.7, 1.9 and 1.4 micron regions, we

Table 2
Updates to Main AFGL Data Base for 1980 Version

1. H_2O
    - (010-010) PURE ROTATION
    - 6.3μ: ν_2 , $2\nu_2-\nu_2$, $\nu_1-\nu_2$, $\nu_3-\nu_2$
    - 2.7μ: $2\nu_2$, ν_1 , ν_3
    - 1.9μ: $3\nu_2$, $\nu_1+\nu_2$, $\nu_2+\nu_3$
    - 1.4μ: $4\nu_2$
    - (181): $\nu_1+\nu_2$, $\nu_2+\nu_3$

2. CO_2
    - UPDATED CONSTANTS
    - CORRECT PI-LEVELS FOR ASYMMETRIC SPECIES

3. O_3
    - 10μ: ν_1 , $\nu_1+\nu_3-\nu_1$, $2\nu_3-\nu_3$, $\nu_2+\nu_3-\nu_2$, ν_3 , $\nu_1+\nu_2-\nu_2$
    - 5μ: $2\nu_1$, $2\nu_3$, $\nu_1+\nu_2$

4. N_2O
    - HOT BANDS

Table 2
Updates to Main AFGL Data Base for 1980 Version (Continued)

5. CO
   - PURE ROTATION ISOTOPES
   - ALL BANDS RECALCULATED

6. CH_4
   - 7.7μ
   - 3.3μ
   - 2.3μ
   - CH_3D

7. O_2
   - 1.27μ: α's

are incorporating the data of the French, which Camy-Peyret, Flaud, and Toth have analyzed. We are comparing these to the data on the AFGL tape, replacing them when necessary or updating the frequencies of certain AFGL transitions that the French data did not include (very weak lines, generally of the type $\Delta K=5$, and so on). An example of the kind of shifts this comparison yields, especially in the fundamental, is shown in Figure 1. This is not a comparison of observations, unfortunately; instead it shows a direct comparison of the two theoretical extrapolations. But it does show the large shifts that result from comparing the French frequencies to what was previously on the tape; the frequency scale is in wavenumbers, so we expect quite an improvement. The shift is actually more than 3 wavenumbers for the bars truncated on Figure 1a. You're dealing with a whole band of lines here. For example, the center of the second plot is a strong domain, around the center of the band. The scale represents ratios. This band - the fundamental band of ν_1- is one of the bands that required updating on the tape. We've already seen quite an improvement from the change we've made in ν_2. Recent measurements at 800K by Jimmy Sakai at our lab have shown that using the French ν_2 for water gives quite a substantial high resolution improvement, and we're about to put those on the tape. We consider this region (6.3μm) now to be in

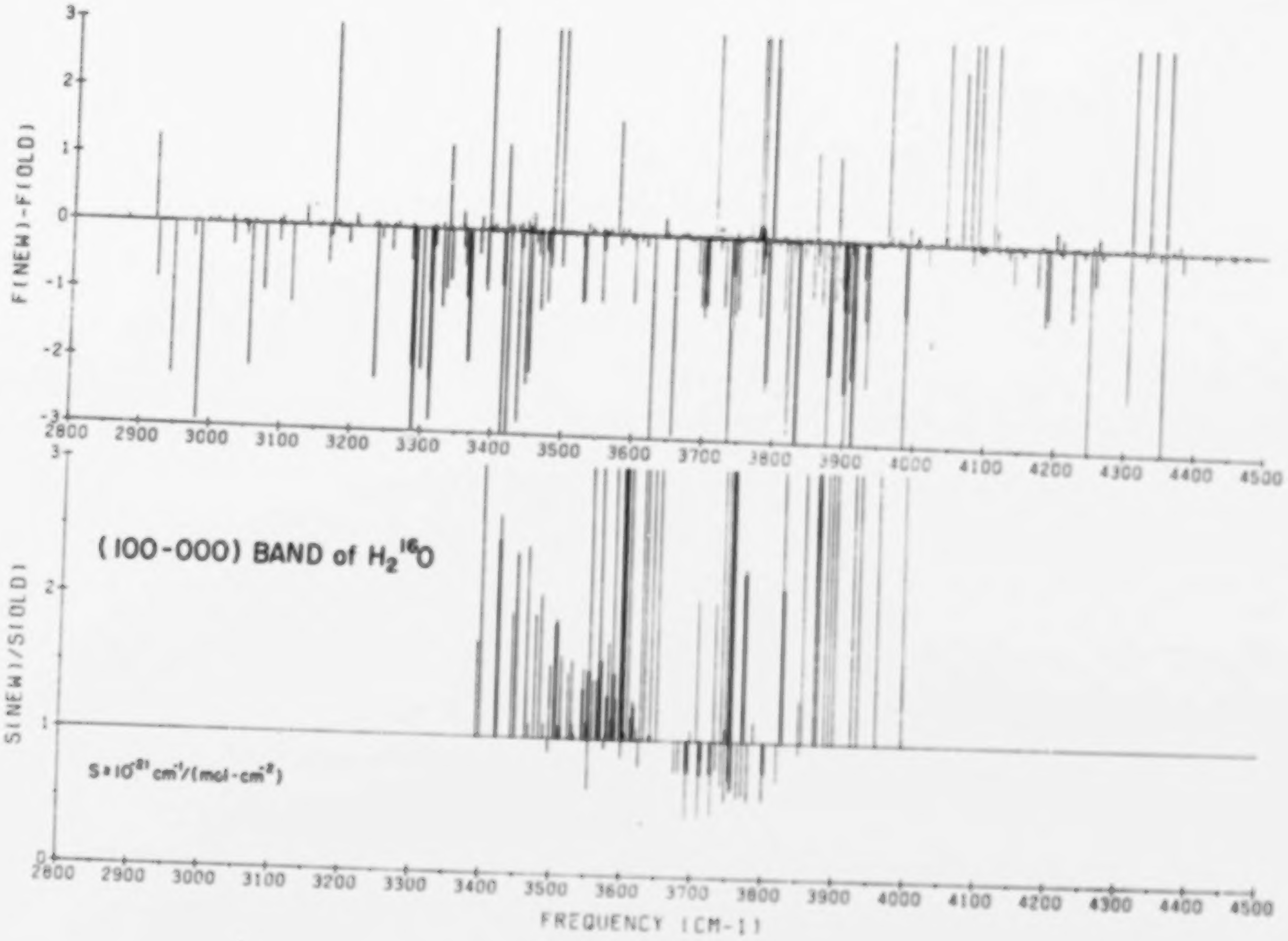

Figure 1a. (above) Difference between frequencies for ν_1 band of H_2O, 1980-1978.
1b. (below) Ratioof line strengths for ν_1 band of H_2O, 1980/1978.

pretty good shape. The transition, $4\nu_2$ in Table 2, was just recently observed by the French; it was not previously on the tape. To my knowledge, it has never been observed before. The last item for H_2O, $\nu_1 + \nu_2$ of $H_2{}^{18}O$ is also a new addition to the tape.

In the case of CO_2, the people at NASA/Goddard recently pointed out to me that the asymmetric species (628-627) has an alternating error in the lines that involve pi-levels. Since it is a major effort to get the correction onto the tape, we're updating the constants with the correction at the same time. We try to bootstrap; we take recent measurements of fundamentals and fix the molecular constants, then apply them to the laser transitions and so on, and work our way up. Everything is coupled; we have about 560 bands, counting the isotopes, on the main compilation.

For ozone I recently updated the two regions shown in Table 2, again with measurements by the French, at the University of Reims. Some of these ozone absorptions were never on the compulation before, for example the two overtones $2\nu_1$ and $2\nu_3$. We feel this represents quite an improvement over the fourth-order expansion work, which is quite old.

In the case of nitrous oxide there is quite a bit of work that will be done. I hope by this summer to get some improvement on the hot bands of nitrous oxide. There is another set of results that was published by Amiot, which we might be able to get on tape.

In the case of carbon monoxide (Table 2), we've re-done all the old work on the tape. We've lowered the cut-off so there are now a few more transitions than heretofore. Also we were missing isotopic variations and pure rotation transitions, and they have been included in the new update.

I will not say much about methane here since many people will be discussing it later. But I should mention a few items about methane. Presently available to me is some work in the 7.7μm region that Glenn Orton has provided, and at the moment it is the best I have available. I know there is a lot of other work being done in this region, but this data is already in the AFGL format and is therefore easy to add to the Atlas. Two band areas, 2.3 and 3.3μm, are awaiting more identification work. I know Bob Toth and Linda Brown have been working on monodeuterated methane; I don't know if it will actually be ready in time for inclusion in the 1980 tape. We hope to get it on shortly.

There is a minor improvement to be made with the half widths of oxygen in the 1.27μm region.

I think the updates to the constituent data base will be of interest to many of the people here (see

Table 3
Updates to Constituent Data Base
for 1980 Version

8. NO
   - (2-0) BAND
   - ISOTOPES
   - REMOVE DUPLICATE LINES

9. SO_2
   - PURE ROTATION

10. NO_2
    - CORRECT $S-\nu_2$

11. NH_3
    - $S-\nu_2$

12. HNO_3
    - PURE ROTATION
    - $2\nu_9, \nu_5$
    - ν_4
    - ν_2

13. OH
    - PURE ROTATION
    - $\Delta V = 1$ SEQUENCE
    - OVERTONES

Table 3
Updates to Constituent Data Base for 1980 Version (Continued)

14. HF
    - PURE ROTATION
    - FUNDAMENTAL, OVERTONES
15. HCl
    - PURE ROTATION
    - FUNDAMENTAL, OVERTONES
16. HBR
    - PURE ROTATION
    - FUNDAMENTAL, OVERTONES
17. HI
    - PURE ROTATION
    - FUNDAMENTAL, OVERTONES
18. ClO
    - FUNDAMENTAL

Table 3). We have added data on the overtones of nitric oxide, and have corrected some errors in the pure rotation transitions that were on an earlier version of the tape. The new version of this second compilation should appear at the end of the summer of 1980.

In the case of NO_2 there was an intensity error in the ν_2 band; it has been corrected.

For NH_3 there seems to be a serious question about the band strength of ν_2. What has been published and put on the tape is quite different from what some groups have found. It would be nice to have this issue resolved. Obviously, if we could get ν_4 and some of the other bands, it would be of great interest for studies of planetary atmospheres.

For nitric acid, we now have pure rotation, $2\nu_9$, ν_4, and ν_2 on the tape, and we are trying to separate out from the $2\nu_9$ region some of the ν_5 lines.

We hope to soon have included the hydroxyl radical; eventually the whole sequence of bands.

For the case of hydrogen halides I have all of the information in the AFGL format, and am still working on some compromise for the half-widths of molecules 16 and 17. The fundamental of ClO was provided to me by Jack Margolis of JPL.

In addition to these molecules, it is likely that we will have formaldehyde and possibly methyl chloride included in the compilation in the near future.

There are a few things I want to mention in closing. It is essential for people to send us their data. We don't have a large group of people working on the AFGL catalog, so it would be very helpful if it were sent to us in the AFGL format. We would also like to be notified when you find discrepancies between your measurements and what is on the AFGL tape, so we can make corrections as soon as possible.

In the future, I hope to get out a newsletter similar to that put out by NASA/Ames, to find out where there is data available, which molecules are of interest to the atmospheric science community and other communities, and to review the data that come out of the various workshops, and get them on the tape so that they can be used efficiently.

DISCUSSION

Question: For CO_2 and CO with carbon 13, are the intensities on the tape measured intensities, calculated intensities, or are they simply scaled by some factor?

Response: Some of both. The weaker bands are scaled. A lot of the strengths come from prehistoric times, and their basis rests with Prof. Benedict.

Comment (K. Fox): Some recent measuremnts on methane taken at the University of Tennessee disagree with the conventional wisdom. I am working on a theory that may help to explain intensities that vary from band to band for $^{12}C/^{13}C$.

THE TERRESTRIAL PLANETS – CURRENT KNOWLEDGE

Page

Thermal Balance of Venus – Martin Tomasko 211

Neutral Species in the Atmosphere of Venus – Andrew Young 229

Transient Species on Mars and Venus – Yuk L. Yung 243

Blank Page

THERMAL BALANCE OF VENUS

Martin Tomasko (University of Arizona)

The Pioneer Venus mission measured several parameters of the atmosphere of Venus which pertain to its temperature structure and thermal balance. Among them are the temperature profile, the composition of the atmosphere, the solar fluxes throughout the atmosphere, and the thermal fluxes throughout the atmosphere.

Figure 1 is a plot of the temperature structure of Venus compiled by A. Seiff, who has the atmospheric structure experiment on Pioneer Venus. The main thing to notice is that the atmosphere is essentially adiabatic below about 35 or 40 km, but from there up to the bottom of the lower cloud (at ~47 km altitude) there is a subadiabatic region. For reference, the dashed line is an extension of the adiabatic profile of the lower atmospheres to higher altitudes. In the middle and lower clouds there is a second adiabatic region, followed by a second radiative region above ~55 km.

In addition to the temperature structure, the Pioneer Venus Sounder Probe contained an experiment to measure the solar flux. The solar zenith angle at the Sounder probe entry site was about 67°. The easiest place to measure the net solar flux is right at the ground, because there the upward flux is low, the downward flux is significant, and one needn't work with the difference between nearly equal numbers. It is interesting to compare the Pioneer Venus flux measurements at the ground with fluxes measured by Veneras 8 through 12. Figure 2 shows how the net solar flux varies with the cosine of the solar

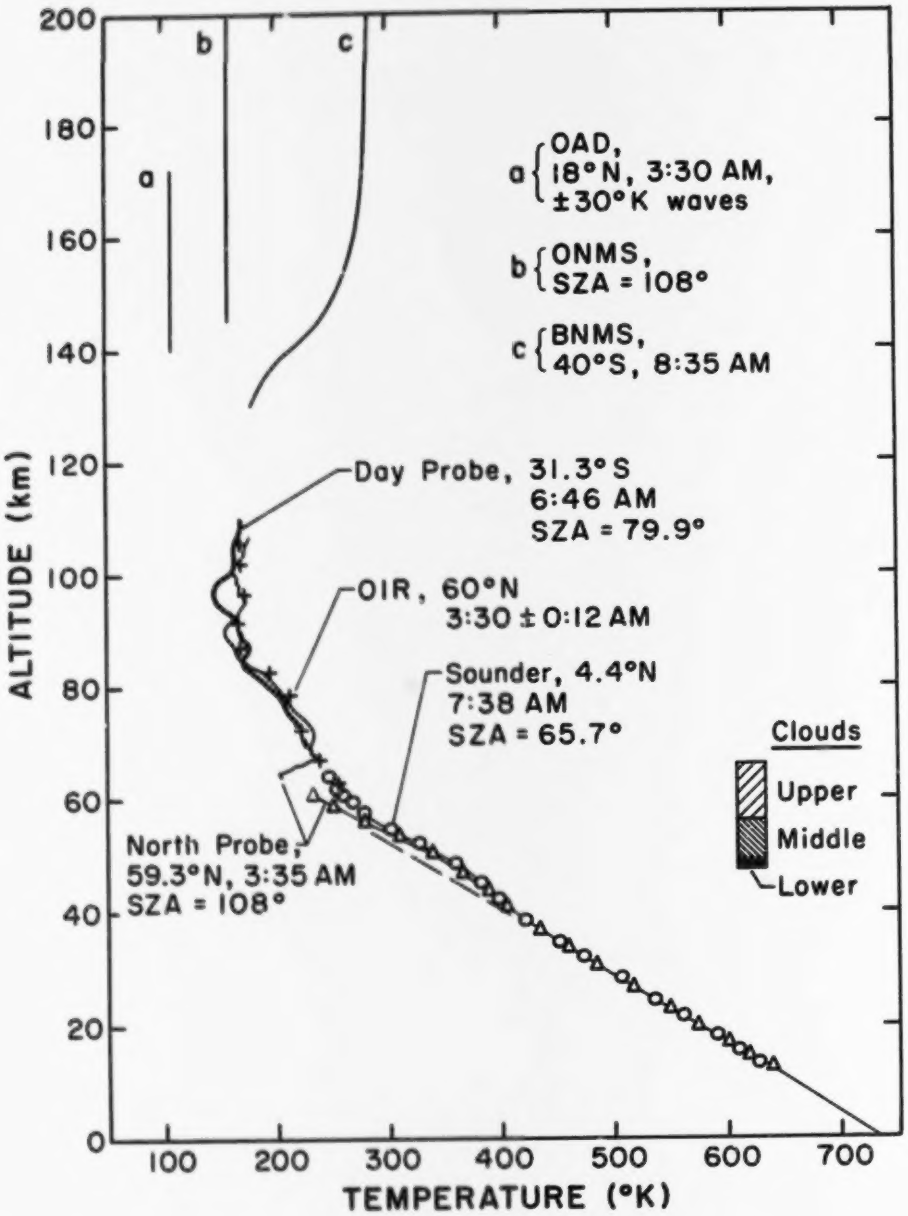

Figure 1. Temperature profiles measured by various Pioneer Venus instruments as indicated – Atmosphere Drag experiment (OAD), Orbiter Neutral Mass Spectrometer (ONMS), Bus Neutral Mass Spectrometer (BNMS), Orbiter Infrared Radiometer (OIR), and the Atmospheric Structure experiments on the probes.

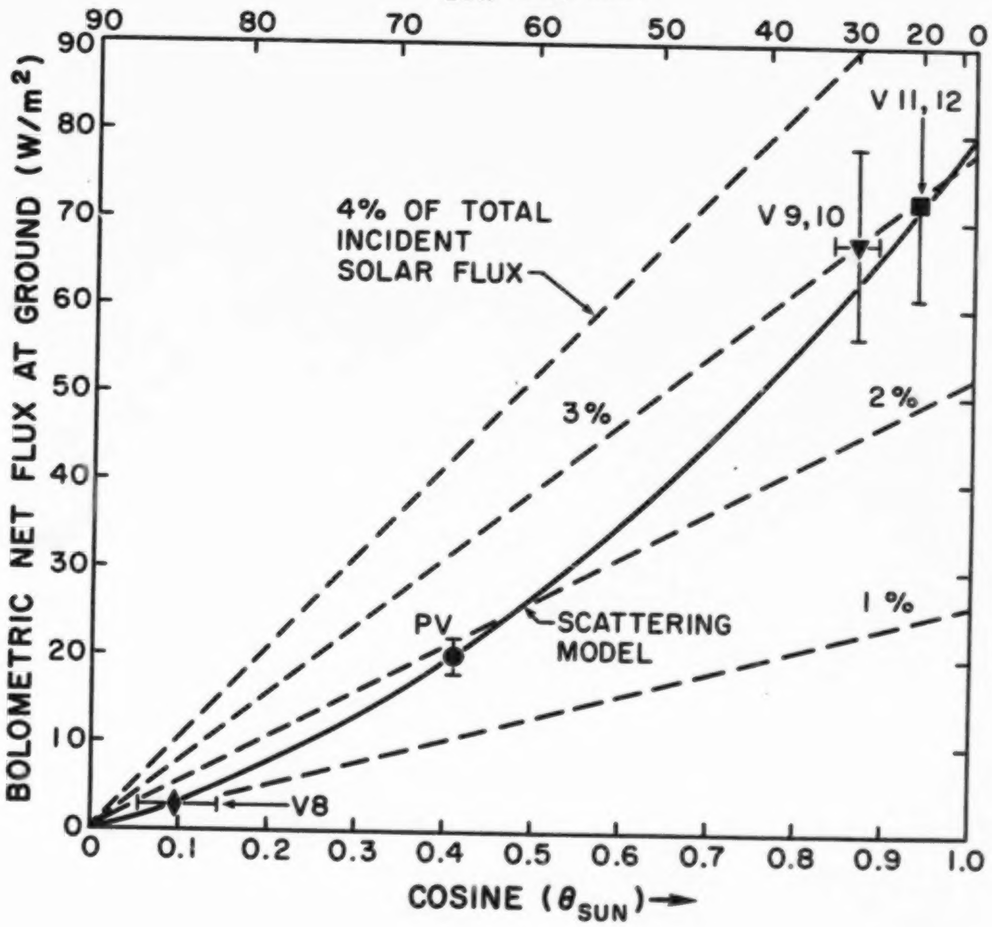

Figure 2. Net solar flux at the surface of Venus as a function of the cosine of the solar zenith angle. Dashed lines represent constant fractions of the incident solar flux as indicated. The solid line represents the variation computed for a forward scattering cloud model adjusted to pass through the Pioneer Venus measurement at the Sounder probe site (labeled PV). This measurement and those measured at the Venera 8 (labeled V8), Venera 9 and 10 (V9, 10) and Venera 11 and 12 (V11, 12) sites are quite consistent as discussed in the text.

zenith angle. The dashed lines are constant percentages of the incident solar flux. Pioneer Venus found that a little less than 2% of the incident sunlight reaches the ground at this location. Venera 8 measured about 1% and Veneras 9 through 12, which landed much nearer the subsolar point, found about 3% of the incident flux reaches the ground. For forward-scattering clouds more of the incident flux is expected to reach the ground at the subsolar point than at the glancing geometries, where the solar zenith angle is smaller. In fact a scattering model which includes the forward scattering nature of the particles and is scaled to go through the Pioneer-Venus data point is remarkably consistent with the other measures. The amount of sunlight reaching the ground is thus pretty well known: averaged over the planet, about 2.5% of the sunlight incident on Venus is absorbed in the ground.

In addition to the net solar flux at the ground, measurements were also made of the net flux of sunlight as a function of altitude at the Sounder Probe entry site. Figure 3 shows the measured net solar flux plotted against altitude. The nominal calibration of the solar flux radiometer (LSFR) gives the lower curve. Considering the uncertainty in that calibration procedure, the solar flux profile probably is no higher than the upper curve.

The Pioneer Venus mission also measured the solar flux at the top of the atmosphere using the Orbiter; there are two separate measurements. A measurement of the albedo of the planet indicates the absorption of sunlight to be about 150 watts/m^2, averaged over the planet. There is also a measurement of the thermal emission from the planet. This gives a slightly higher value, although the size of error bars in the present data reductions are too large to allow strong statements about the presence or size of any

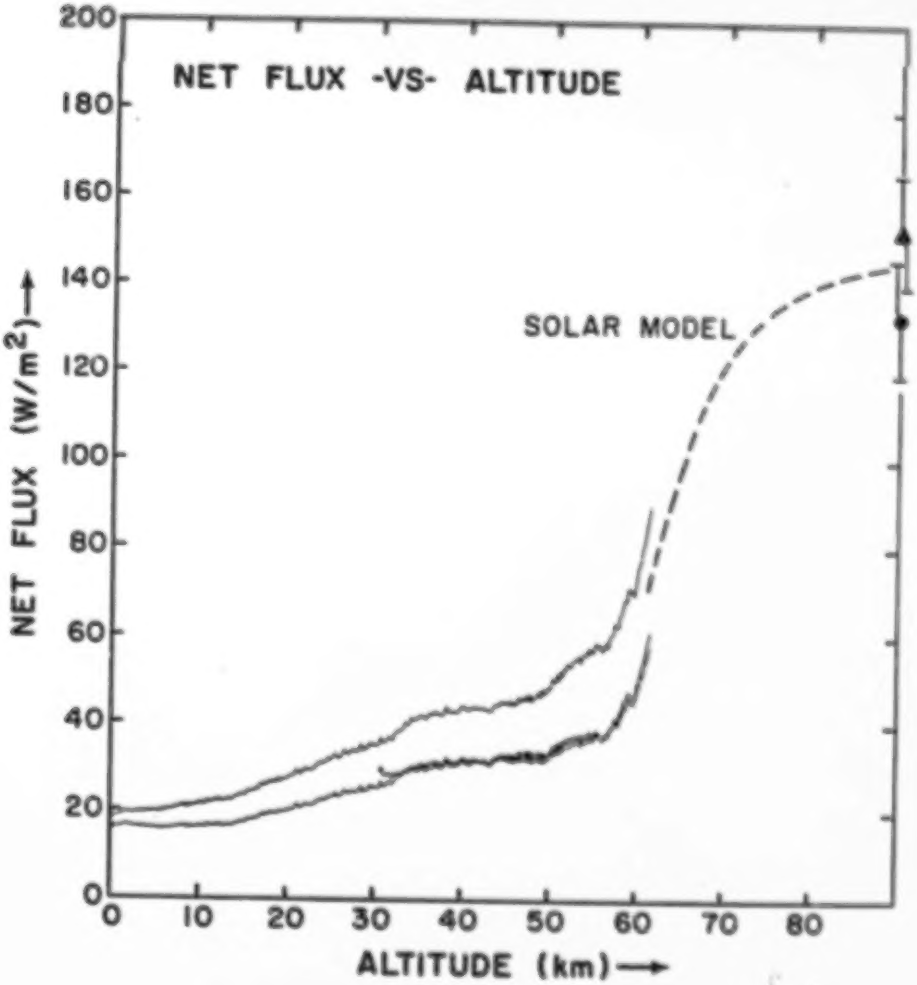

Figure 3. Globally averaged bolometric net solar flux versus altitude. The PV measurements in both the "broad-band" and "combined" channels (above 35 km altitude) each scaled up to include energy outside the LSFR filters and averaged over the planet using a forward scattering cloud model are shown in the curves (nearly superimposed) labeled "nominal solar". Also shown is the highest solar net flux profile (labeled "high solar") consistent with relative and absolute calibration uncertainties in the LSFR upward and downward looking detectors. The dashed curve above 60 km altitude is a model calculation. The triangle corresponds to the net thermal flux and the dot to the net solar flux measured for the top of the atmosphere by the orbiter.

energy imbalance. The dashed curve in Figure 3 shows the solar flux computed from a model consistent with the cloud structures observed from the probes. Notice that the amount of sunlight absorbed below 30 km altitude level is about 40 watts/m^2 or less.

It is interesting to compare the profiles of net solar flux with the profiles of net thermal flux measured on the probes. Verner Suomi's experiment on the three Pioneer Venus small probes had a broad passband that included both the solar and the thermal part of the spectrum. One of these probes landed on the daylight side of the planet, near the terminator. For this probe the solar contribution can be estimated from models and then subtracted off to estimate the thermal flux alone. The other two small probes landed on the night side, and give the thermal net flux directly.

The results of these measurements (shown in Fig. 4) are surprising in several respects. Firstly, the thermal flux profiles vary considerably - from 20 to 80 watts/m^2 at 30 km altitude, for example. If the measurements are right, the thermal opacity in the lower atmosphere must vary considerably from place to place. One possibility is that small variations in the abundance of some minor constituent might be effective in controlling the flux passing through window regions in the opacity due to CO_2. Another surprise is the fact that the average of the three thermal flux profiles exceeds the solar net flux profile. Taken at face value, this indicates that thermal radiation escapes from the deep atmospheric layers faster than it is replaced by the absorption of solar energy. I don't think such a conclusion is really justified on the basis of these three measurements of the thermal flux. For one thing, the variation in the three thermal profiles is so great that their

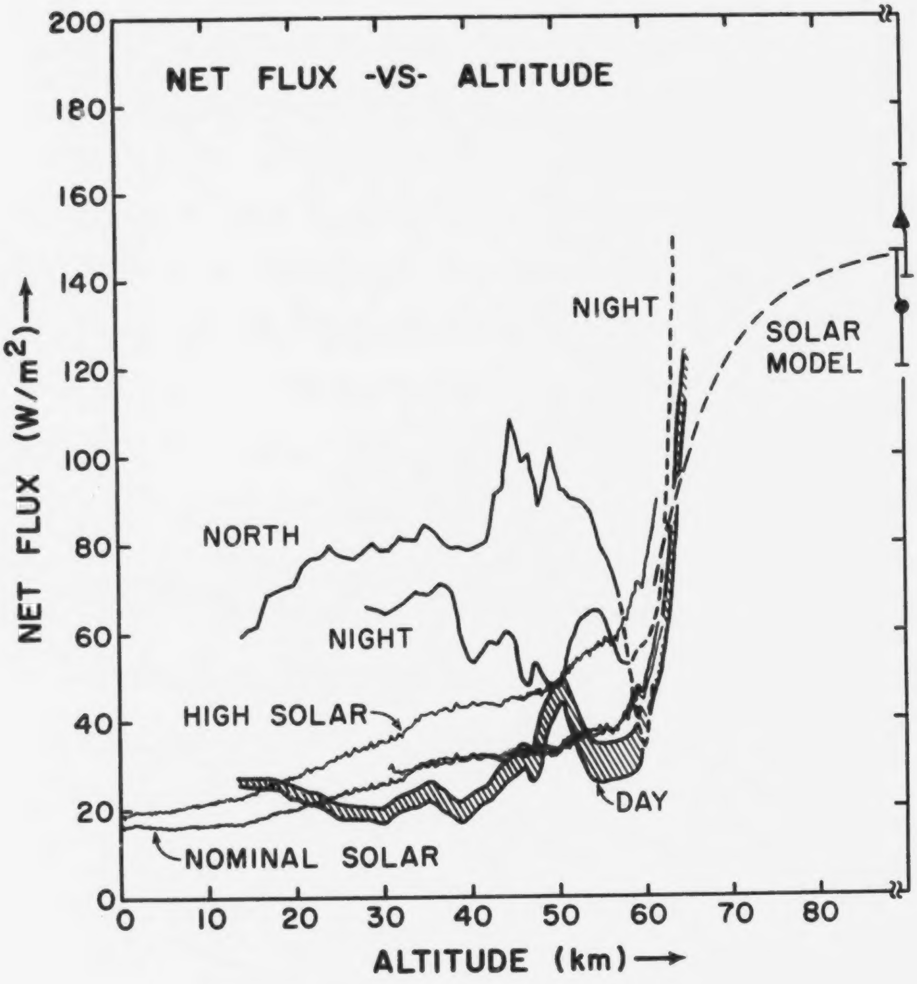

Figure 4. The SNFR thermal net flux measurements at the night, north, and day probe sites are compared with the globally averaged bolometric net solar fluxes as a function of altitude.

simple average is unlikely to be a good approximation to the true globally averaged thermal flux profile. Also, the globally averaged solar net flux profile could certainly differ somewhat from the one shown if the cloud structure varies over the planet.

It seems clear that the abundance of water must be very low to reproduce the high thermal fluxes measured. Figure 5 shows several estimates of the water mixing ratio plotted against altitude (or pressure). The water mixing ratios determined by the gas chromatograph (LGC) on the Pioneer Venus entry probe are shown by the three points, and the solid curve is a preliminary result from the optical spectrometer experiment on the Venera 11 and 12 probes. The Venera measurements are more than an order of magnitude smaller than those of the LGC. Calculations using the LGC water abundance give thermal fluxes that are very much smaller than the values Suomi has given. The Venera water measurements and small variations around them corresponding to curves 1, 2 and 3 on Fig. 5 lead to the thermal fluxes shown in Fig. 6. Here the dots are Suomi's measurements from the two probes that entered in the night side of the planet, the crosshatched band corresponds to the uncertainty in the thermal flux at the day probe site due to generous estimates for the uncertainty in the corrections for the net solar flux there. The three curves are the result of thermal flux calculations made using a thermal opacity table provided by Jim Pollack. The curve labelled "1" is for the nominal Venera profile that was shown in Fig. 5 while the curves 2 and 3 are for variations in the water mixing ratio of factors 3 to 5 about the nominal Venera profile as indicated on Fig. 5. For this particular opacity table rather large variations in the thermal flux can be obtained, depending on the water mixing ratio, including some profiles indicating even greater fluxes than appear in

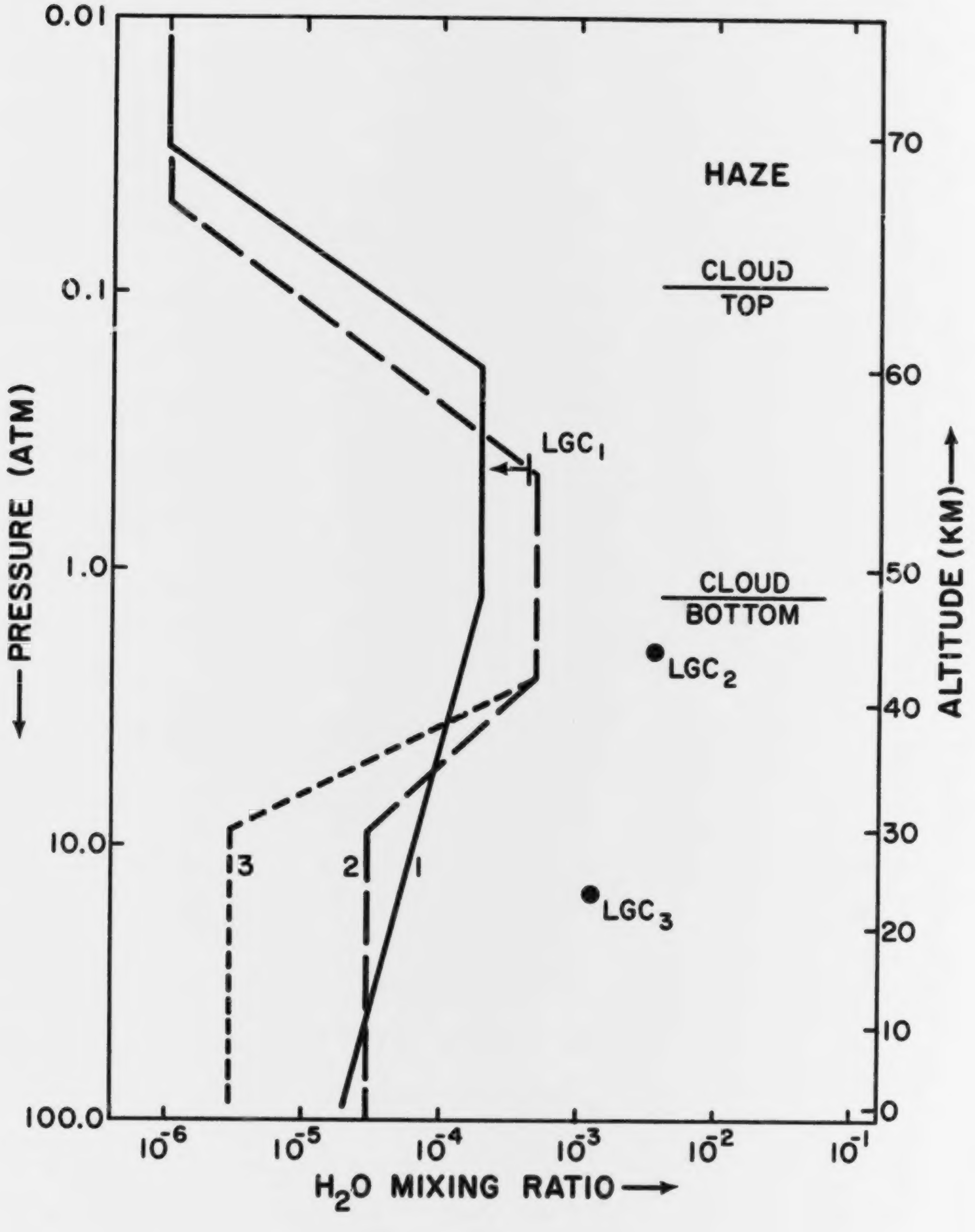

Figure 5. The Venera 11/12 water mixing ratio profile (1) and two variations (2 and 3) which are used to compute the sensitivity of the lower atmosphere to humidity changes. The Large Probe Gas Chromatograph (LGC) Measurements are shown for comparison.

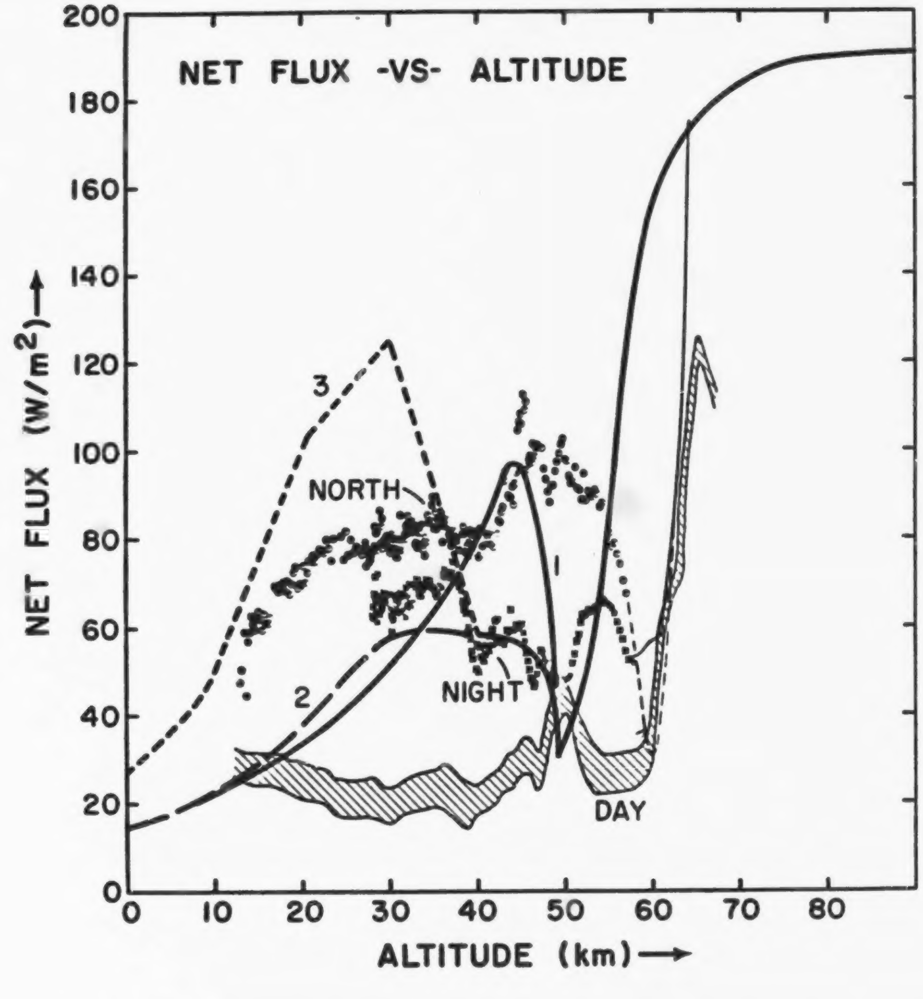

Figure 6. Thermal net fluxes predicted by the nominal model using the three water profiles of Fig. 12. The SNFR flux profiles are shown for comparison. Local variations in water abundance can make large changes in the thermal net flux and may explain the variability between the different small probe entry sites.

Suomi's measurements. However it is difficult to assess the accuracy of thermal flux calculations for the lower part of Venus' atmosphere because generally only relatively crude, broadband opacity tables are used. The tables are based on measurements at room temperature and don't include hot bands, which are potentially very important in the lower Venus atmosphere. It seems clear that the true thermal flux should be somewhat lower than these calculations, but how much lower? If not much lower, then the thermal flux measurements may still be correct with all they imply about new heat balance mechanisms on Venus. If the opacity of CO_2 along at high temperature were shown to be considerably higher than in the broadband models, the implication would be that the Venus thermal flux measurements are likely to be wrong. This is a good reason for measuring the opacity of CO_2 at high temperature and high pressure more completely than heretofore.

If the LGC water profile is used in the flux calculations, the computed thermal flux profile is much lower than any of the thermal flux measurements (see Fig. 7). In this case the thermal flux is easily low enough to allow the greenhouse mechanism to produce the observed surface temperature, but another serious problem results, as shown in Fig. 8. Here the solid curve is the observed temperature profile, and the model (based on the LGC water abundance) is represented by the dashed curve. Notice that the model is convective everywhere below the upper cloud. The radiative region represented by the kink in the observed profile below the clouds is not reproduced by this model, with its large thermal opacity.

On the other hand, calculations by Pollack using the Venera water profile and revised gaseous opacities (to include SO_2 and some improvements in the

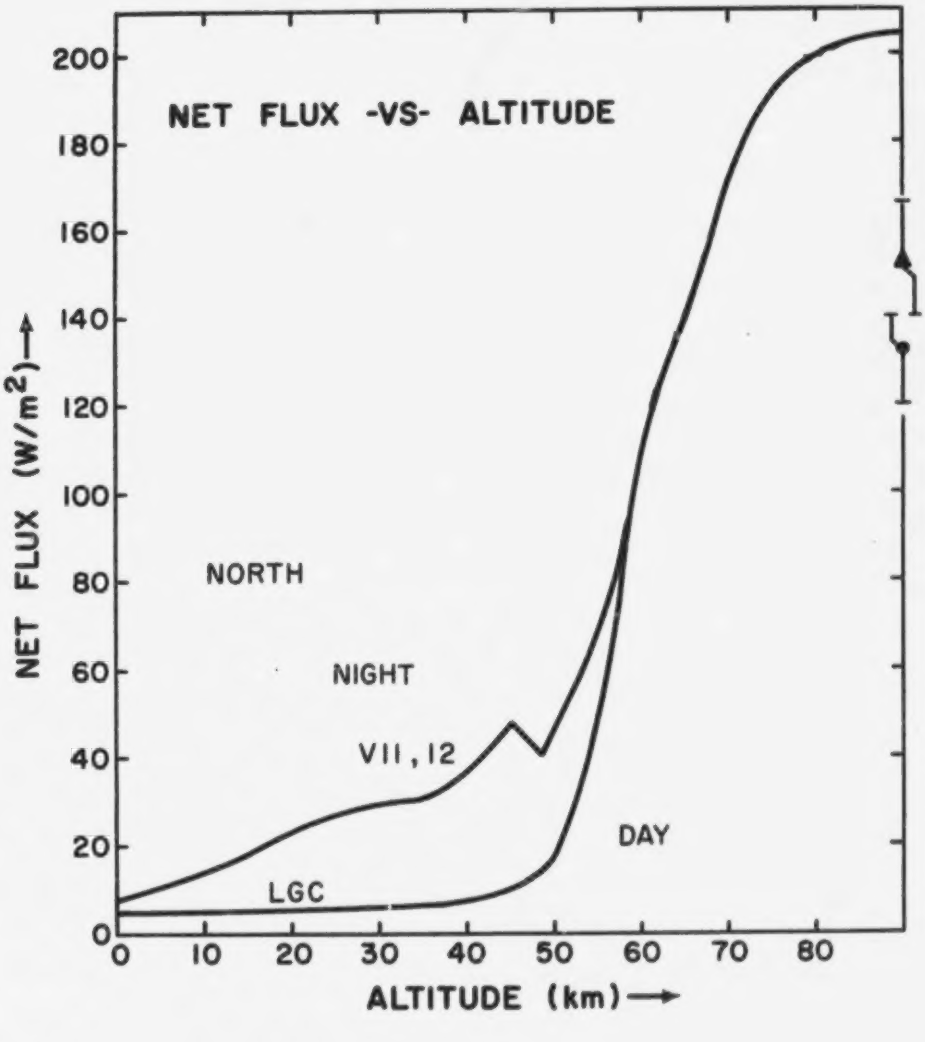

Figure 7. Thermal net fluxes predicted by the nominal atmosphere model are compared to the net flux profiles measured by the three SNFR's. The model predicts that 205 watts/m^2 is emitted to space compared to the value measured by the OIR (triangle) and the Bond albedo (circle). While the nominal model contains the water vapor abundances measured by Venera 11 and 12 (V 11, 12), the model has been rerun with the considerably larger PV water vapor abundances (LGC) for comparison.

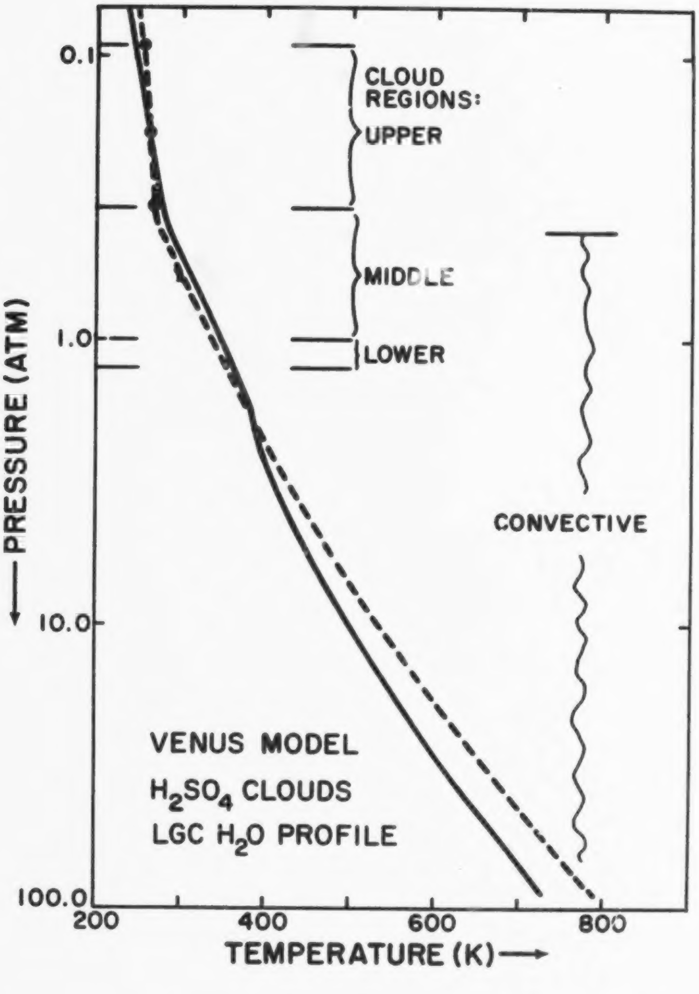

Figure 8. A 1-D radiative-convective greenhouse model is shown with the temperature profile adjusted such that the thermal net fluxes equal the solar net fluxes. Wherever the calculated lapse rate exceeds the adiabatic lapse rate, it is assumed that convective processes dominate. The LGC profile is used to evaluate the opacity due to water. Notice that the model is convective everywhere below the middle cloud.

treatment of water and CO_2) give the thermal fluxes labeled V11, 12 in Fig. 7. This set of opacities gives temperatures profiles as shown in Fig. 9 when used with the nominal or "high" solar net flux measurements as indicated. Notice that the models now reproduce the radiative region observed below the cloud bottoms as revealed by the kink in dashed curve between 35 and 50 km altitude, in addition to bracketing the observed ground temperature. The ability to reproduce the kink in the temperature profile may be a clue that the opacities used in this calculation are fairly reasonable, at least just below the clouds where the temperature is not much above room temperature. It would be nice to have similar confidence in the opacities at lower altitudes where the thermal flux measurements are so large and variable.

I would like to call your attention to one more problem in the Venus data. Notice that the calculations shown in Fig. 7 give ~200 watts/m^2 at the top of the atmosphere as opposed to the observed value of 140-150 watts/m^2. The calculations include CO_2, SO_2 and a very small amount of water above the clouds. A rather considerable amount of opacity still seems to be missing from the models. One proposal (Soumi, et al., 1980) is to add aerosols of a particular type to the upper atmosphere. The aerosols must be sufficiently small that their optical depth in the visible is not very large, to prevent them from conflicting with visible-region measurements made from the probes. Nevertheless, if they contain sufficient mass per unit area they may be able to provide significant opacity in the thermal infrared. Whether or not these particles will be able to account for all of the optical and thermal measurements is still very unclear, but unless a significant source of gaseous opacity has been overlooked, aerosol opacity may well be required to resolve the flux problems near the top of the atmosphere.

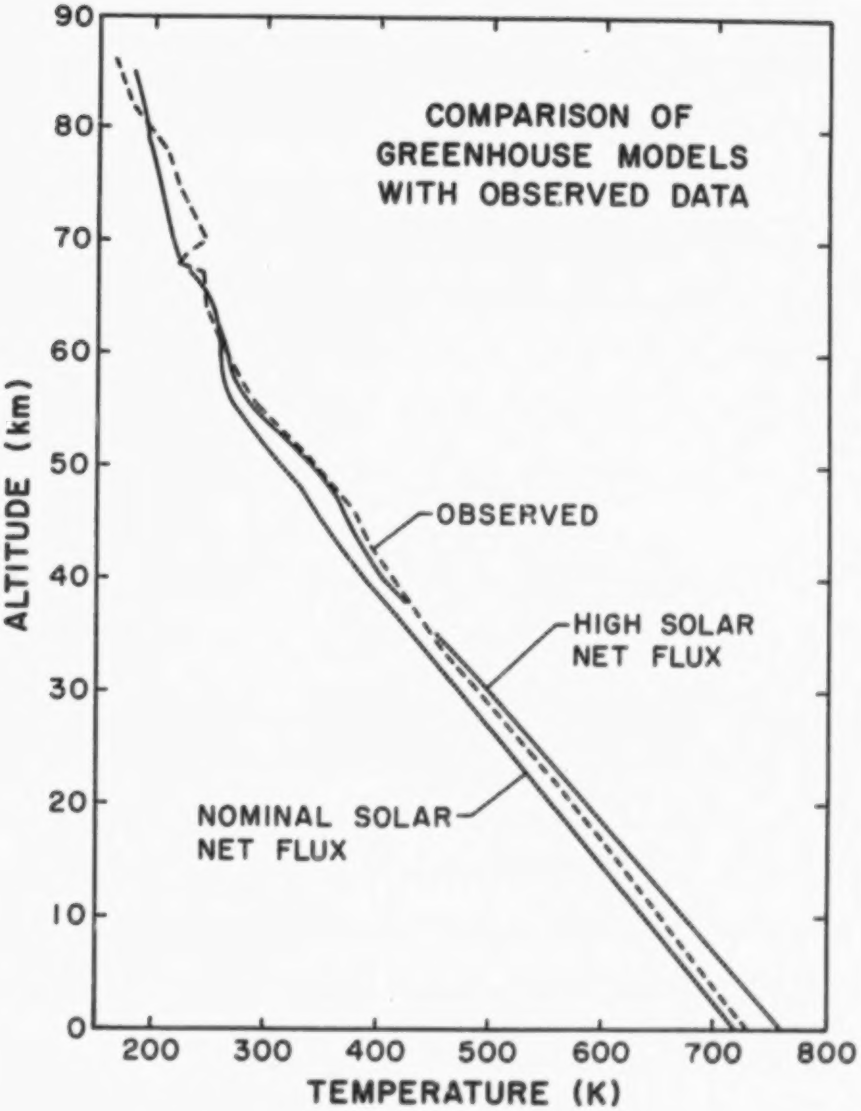

Figure 9. Similar to Fig. 6 but using the Venera 11/12 water profile. Both the nominal and the high solar net flux profiles are tried and compared with the temperature profile observed by PV at the large probe site (see Fig. 1). Notice that the model reproduces the radiative region observed between about 35 and 47 km. altitude.

DISCUSSION

Question: What is the source of your opacity tables?

Response: We got these opacity tables from Jim Pollack. The curves in Figs. 7 and 9 are due to some recent modifications he has made since the calculations in Fig. 6 were done. Still, a large portion of the flux in the lower atmosphere is carried in regions near 2.5 μm where many possibilities for hot bands exist, so I'm not at all sure that the actual fluxes should be as high as the calculations.

Comment: That whole region from 3.5 to 4 microns carries a very large fraction of the black body radiation spectrum escaping from the ground, and it is very important to read it carefully.

Comment (A. Young): Louise Young is working on these problems to some extent. She is calculating opacities for hot CO_2, and large paths appropriate to Venus; I already presented the first section of those results to the DPS meeting last fall. As far as the whole region is concerned, a much greater opacity has been derived by the Russians who have done this, and they find that they can make the greenhouse work just fine.

Response: A great deal of work is required to do the calculations properly, and so people have tended to wave their hands and say, "Oh, it will probably all work out and it will be okay; there is plenty of spectral overlap, there are plenty of hot bands, and they'll take care of everything." On the other hand, Suomi has his measurements, and he keeps saying there's nothing wrong with them. They give high fluxes. So you have one body of people who say CO_2 will have plenty of opacity, although they don't have quite the calculations all done in the way to prove it, and on the other hand, you have Suomi who says that his measurements are fine and that there are significant windows in the CO_2, with the opacity in these windows being controlled by minor constituents. I think it's interesting to figure out which of these two pictures is closer to the truth.

Question: If you put something else in there, do you get less opacity?

Response: We get more opacity with something else in there. The question is how much more. Is it enough to indicate that Suomi's measurements are incorrect?

Question (M. Tomasko to A. Young): How do you explain the fact that Suomi's measured thermal flux in the lower 20 km is variable by a factor of 4 from one place on the planet to another?

Response (A. Young): Because he's looking at the wake of his spacecraft and he can only see a couple of centimeters down there in CO_2. He's not seeing the free atmosphere. He's just seeing the flow pattern and the temperature distribution around the probe.

Response (M. Tomasko): You will have to argue with him about that. I'm not going to try to defend what he's seeing and what he's not. I'm not saying his measurements are right or wrong; I'm saying it's an interesting controversy.

Comment (A. Young): Well, I say they are wrong.

Blank Page

NEUTRAL SPECIES IN THE ATMOSPHERE OF VENUS

Andrew Young (Texas A&M)*

About 97% of the Venusian atmosphere is CO_2, with the balance comprised of various trace constituents. I will first discuss species other than CO_2 that have either been found in Venus' atmosphere or have been sought unsuccessfully, and then will return to problems connected with the spectrum of CO_2 itself.

Species Other than CO_2

A number of species - in particular, nitrogen and argon - have no dipole moment, and so cannot be detected by infrared spectroscopy. They can be detected by mass spectrometry and gas chromatographs. On Venus, nitrogen is present with a mixing ratio of about 3% (this number is uncertain by 50%), and argon with a mixing ratio of about 10^{-4}. Other species can be detected spectroscopically, and some of them have also been observed by direct sampling. These include SO_2, H_2O, CO, HCℓ, and HF.

SO_2 has been detected spectroscopically, although by its electronic (ultraviolet) rather than vibration-rotation transitions. It has also been detected by gas chromatographs and mass spectrometers. According to the gas chromatographs (and to a lesser extent, the mass spectrometers), the abundance of SO_2 is about $2x10^{-4}$ below the clouds, but the spectroscopic observations from outside the planet show that this mixing ratio falls very drastically with increasing altitude, i.e., through and above the clouds. The SO_2 is presumably drifting up from below and being converted into sulphuric acid by way of sulphur trioxide, by some chemical or photochemical processes that are still not well understood.

---

* Present address: San Diego State University, San Diego, CA 92182

Water has been observed on Venus. It was first measured by the Russian chemical experiments, below the clouds. It has also been measured spectroscopically at the top of the clouds, and most recently it has been measured (by Moroz' equipment) all the way down to the surface. Moroz[1] obtains a mixing ratio of about $2\text{-}3x10^{-4}$ in the clouds, and $2\text{-}3x10^{-5}$ at the surface. Louise Young and I re-analyzed these spectra in early 1981, and found the mixing ratio of water to be close to 10^{-4} throughout the lower atmosphere. (This will be reported in detail at the Ames conference on Venus, Fall 1981).

CO was detected very plainly in the Connes' spectra and the resulting analysis required a mixing ratio of about $2x10^{-5}$. More recently the CO mixing ratio has been studied extensively by microwave techniques: it is about 10^{-4} in the region from 90 to 100 km, and drops drastically at lower altitudes. CO is apparently being produced at high altitudes by the photodissociation of CO_2, and is consumed by thermal chemical reactions at lower altitudes. This may be related to the destruction of sulphuric acid: the oxygen that was added to SO_2 to make SO_3 and then H_2SO_4 may be transferred back to CO to make CO_2 in the hot lower atmosphere, but the details are not well understood.

The Connes' spectra also showed HCℓ and HF. This is the only published observation of these species: all we have is one spectrum, and these species are likely to have quite variable abundances. (The abundance of HF should be particularly variable, because HF reacts strongly with sulphuric acid). This one observation may give the order of magnitude for the abundances near the cloud tops: 4×10^{-7} for HCℓ and 10^{-8} for HF.

Some species have been searched for unsuccessfully: ozone, bromine, chlorine, NO_2, and other sulphur bearing molecules (see above for SO_2). At least above the clouds, the mixing ratio of ozone must be less than about 10^{-8}. Moroz has analyzed the short wavelength (electronic) absorption in his spectra, and finds upper limits of 10^{-10} for bromine, 10^{-8} for chlorine and 5×10^{-10} for NO_2, at least in the lower part of the atmosphere. One candidate for the ultraviolet absorption is sulphur, but sulphur forms so many different compounds that it is difficult to decide whether it is indeed responsible. Some little wiggles in Moroz[3] spectra were at about the right wavelength to be the 5200 Angstrom band of S_4, and there was a shoulder near 4000 Angstroms which might be S_2, S_3, S_6, S_8 or almost any sulphur molecule. These sulphur molecules have little or no dipole moment, so they are very difficult to observe in the infrared.

Some of these undetected species have been looked for in ultraviolet spectra taken from rockets and satellites, but unfortunately these spectra have all been taken at large phase angles (the phase angle is the angle at the planet between the Sun and the observer). The equivalent widths of spectral lines observed from outside the planet depend strongly on the phase angle. When the phase angle is small, Venus is fully illuminated but we see it on the far side of the Sun, where its apparent diameter is small. When the phase angle is near 180 degrees we see only a thin crescent, because Venus is then on the near side of the Sun.

CO_2

The dependence on phase angle, just discussed in connection with the undetected species, also occurs for the dominant species on Venus, CO_2. This is illustrated in Figure 1, which shows two spectra taken from the ground by our group.[2] In the spectrum taken at a small phase angle, the 7820 Angstrom band is very strong; in the spectrum taken at a phase angle of 165 degrees only a few CO_2 lines are still visible, and even those few are very much feebler. Expressed quantitatively, the strongest equivalent width would be about 0.30 Angstroms (i.e., about 0.050 cm^{-1}) in the small phase angle spectrum, and the strongest equivalent widths are of the order of 0.005 Angstroms (i.e., about 0.010 cm^{-1}) in the 165° phase angle spectrum. These lines appear to be quite weak when we see Venus illuminated tangentially.

As noted earlier, the phase dependence of the strengths points to a weakness in the oft-proposed strategy of trying to detect minor constituents by looking tangentially through the atmosphere. With tangential viewing, you only see the very top of the clouds - a high altitude, low pressure region. In such a region the lines are highly

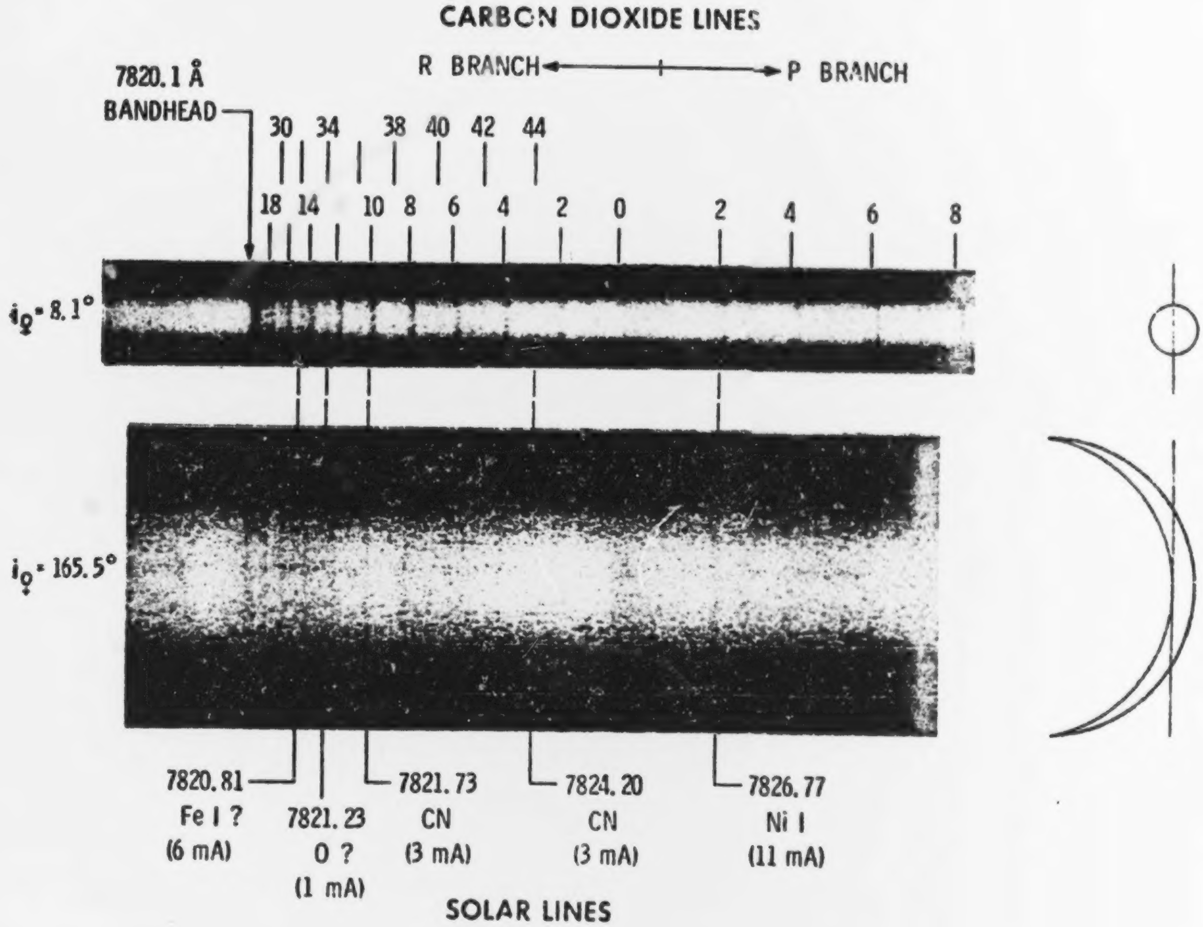

Figure 1. Spectra of Venus taken at phase angles of 8.1° and 165.5°. The sketches at the right show the phases and apparent diameters of Venus, with vertical lines indicating the positions of the spectrograph slit. The upper spectrum was taken near superior conjunction, and required a 40-minute exposure; the lower spectrum was taken near inferior conjunction, and required a 2 1/2 hour exposure. The solar lines at the bottom are due to iron, oxygen, cyanogen and nickel, each labeled by its equivalent width in milli-Angstroms.

saturated, so their equivalent widths are very small. The opposite situation, nearly vertical viewing is better. Although the geometric path in the cloud is shorter, you see down to regions of much higher pressure: the lines are broadened, and have nice equivalent widths. These two viewing extremes are illustrated in Figure 2. Bear in mind how faint the spectrum is at a phase angle of 165 degrees, for comparison with the spectra to be discussed next.

One of the weakest bands ever observed on Venus is a higher combination band at 7158 Angstroms - a shorter wavelength than the previous features. At small phase angles, it looks about like the 7820Å band at large phase (cf. Fig. 1). (At Kitt Peak I recently took some newer spectra of this band, with about five times the dispersion shown in Fig.1, and using a bigger telescope. Although the resolution is no better, the signal-to-noise ratio is much higher on the new spectra, and they show many lines). This weak band is very difficult to observe in the laboratory: when Herzberg studied it using a 5.5 km path length at 10 atmospheres, he was only able to see the band head! (Of course, at this high pressure the rotational structure is wiped out by pressure broadening, so individual lines can't be distinguished). But in the Venusian spectrum the band is quite observable, and is suitable for determining rotational constants.

This illustrates the fact that Venus is still the best absorption cell available for CO_2. It provides very low pressures (about 50 millibars) and very long path lengths: a couple of km-atmospheres of gas. A perfect combination: a tremendous amount of absorbing gas, at a pressure low enough to allow structure to be resolved. To really resolve all the

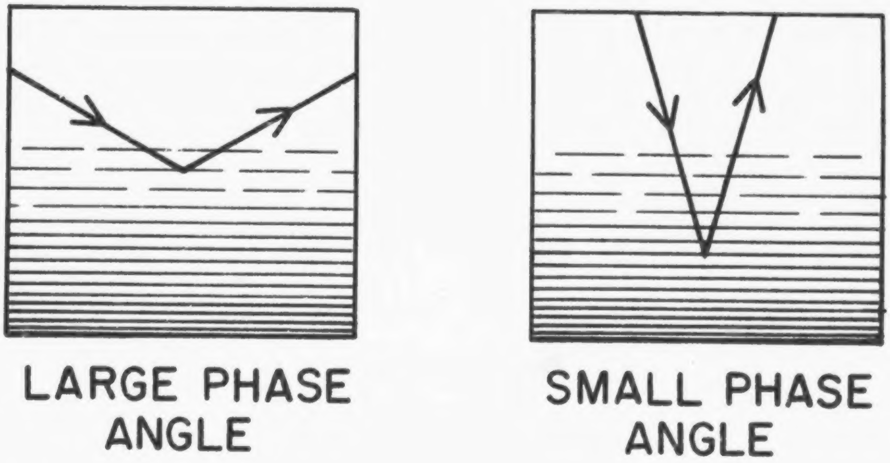
LARGE PHASE ANGLE
SMALL PHASE ANGLE

Figure 2. Schematic Representation of Depth of Penetration vs. Phase Angle.

structure (i.e. individual line shapes) in Venus' CO_2 spectrum would require an order of magnitude better resolution than in the current spectra. The current spectra show only the instrumental profiles, not the actual line profiles.

To contrast Venus with Mars, recall the Mars CO_2 spectrum in Rudy Hanel's paper, where various isotopic bands showed up as little blips. We see about a hundred times as much CO_2 above Venus' cloud tops as we see above the surface of Mars. The little blips from rare isotopic CO_2 molecules, would be big, black bands on Venus. This should be remembered in calculating the greenhouse effect. The amount of CO_2 above the surface of Venus is about a thousand times more than that above the clouds (the pressure is only about a tenth of an atmosphere above the clouds, while it is almost a hundred atmospheres at the surface). So, even the weak band at 7158Å is black at the surface of Venus. A tremendous amount of absorption by CO_2 occurs within and below the clouds of Venus.

More quantitatively, in a laboratory spectrum at 1 atmosphere, about a centimeter of CO_2 is sufficient to black out the spectrum at 15 microns, in the bending mode fundamental. The amount of gas above the surface of Venus is about 10^8 times greater. This means that in considering whether there are any holes in the greenhouse you have to include extremely weak bands in the lower atmosphere. For example, a band that is 10^{+4} times weaker (per molecule) than the fundamental, produced by a rare isotope with mixing ratio 10^{-4} will still be black. The hot bands are important for the same reason. At room temperature kT is about 1/40 eV, and the lowest vibrational transition for CO_2 is about 1/25 eV, so the Boltzmann factor strongly suppresses the higher states: the Boltzmann factor falls by roughly a factor of 20 for each successively higher vibrational state, at room temperature. At the surface temperature on Venus (750 degrees), kT becomes .06 eV, which is almost equal to the first vibrational quantum. The Boltzmann factor falls by only a factor of four for each successive harmonic. To compensate for a factor of 10^8 you have to go up 13 times the fundamental vibrational quantum. Admittedly, the partition function increases by about a factor of 10 in going to these high temperatures, so lets conservatively say that 11 or 12 vibrational states are important. If 10 or 12 hot bands are included for every fundamental, the spectrum fills up very quickly. Louise Young has been saying for years that CO_2 takes care of the greenhouse entirely by itself, and the Russians say that at most a mixing ratio for water of 10^{-5} is enough to plug all the holes in the greenhouse - and there is certainly that much water present. So the huge thermal fluxes and other peculiar features found by Suomis' Pioneer-Venus experiment are very implausible. Both the large fluxes and many of the other peculiar results of this experiment are readily explained if the instruments were seeing the thermal wake of the probe, rather than the atmosphere.[3]

Before closing, I want to convey to you Louise's request that the pure rotation spectrum of CO_2 be looked for on Venus. CO_2 is not ordinarily thought to have a pure rotation spectrum because the common isotopes ($^{12}C^{16}O_2$, $^{13}C^{16}O_2$, $^{12}C^{18}O_2$, etc.) give a symmetric CO_2 molecule. But CO_2 made from the less common isotopes (e.g. $^{13}C\ ^{16}O\ ^{17}O$) will have a small dipole moment, and should have a pure rotational spectrum. The long path length and low pressures on Venus should be ideal for detecting such spectra.

Discussion

Question: Does the 10-micron CO_2 window make a hole in the greenhouse on Venus?

Response: In Louise's calculation, the transmittance from 20 to 30 km altitude above the surface was only e^{-206}. The exponent register for the 20-bit floating point word on the CDC 6600 computer isn't big enough to express the tiny transmittances from below 20 km, so they come out as zero on the computer. Nothing is coming out of the "window" from below about 30 km.

Comment: Given the large amount of CO_2 on Venus, there are other sources of opacity besides isotopic bands and hot bands. You can have pressure-induced transitions, double vibrational transitions with CO_2+CO_2 or CO_2 and any minor species.

Response: Yes. Many transitions that are ordinarily forbidden can be important on Venus, e.g., quadrupole and hexapole radiation. We are just not used to an atmosphere 100 times as massive as the Earth's and made of an infrared-active gas.

Comment: I want to make two points in connection with the high thermal fluxes found by Suomi's Pioneer-Venus experiment. I agree that these thermal flux measurements seem remarkably high. A fair amount of work went into making those measurements, and a fair amount of work should now be done on greenhouse calculations, to close the loop. These calculations take a great deal of effort even for narrowly defined spectral regions; I hope someone will decide that they are worth doing. Now my second point. Although there is a tremendous amount of CO_2 opacity in the lower atmosphere, where the pressures are about 50 bars, the greenhouse tends to run into trouble not where the pressure is 50 bars, but higher up, in the clouds where the pressure is only 1 bar. To make the greenhouse work, CO_2 and other species have to be opaque at these altitudes.

Response: I agree. The problem is that the lab data don't provide the information we need to settle this issue. In the middle of the cloud, say between 55 and 60 km, a couple of kilometer-atmospheres of CO_2 at 1 bar are available as an absorber. The lab data are already becoming inadequate for such large amounts of absorber. Below the cloud all sorts of mechanisms (unobservable in the lab) contribute to the absorption.

Comment: (H. Pickett): Absorption from CO_2 containing O^{18} has now been observed in the laboratory. The cells were only 3 meters long and the gas was at 1/10 torr pressure. The permanent dipole moment turned out to be about a hundreth of a Debye.

Comment: (U. Fink): The kind of calculations described earlier by W. Person seem well suited to the questions we are discussing now. The band intensities of CO_2 are known for the major bands and for the simple hot bands, but those for the higher hot bands are very difficult to measure. I wonder how difficult it would be to predict them for Person's theory.

Question: (R. Beer): Aren't the pressures getting too high for extrapolations based on nearly-free molecules?

Comment: At 100 bars the corrections are not very important yet.

Response: (A. Young): The deviations from the perfect gas law are less than about 10%.

Question: (Y. Yung): Do you still think that the sharp kink in the profile of CO is due to its destruction by thermal chemistry below the clouds?

Response: (A. Young): I think it is likely.

Comment: (Y. Yung): But that disagrees with what is expected from strong vertical transport. If part of the CO profile is due to strong vertical transport then it will be well mixed and its profile will not have the sharp curvature that is observed. The only way I can see to produce such a curvature is by additional destruction just above the clouds.

Response: (A. Young): But the CO can't be destroyed photochemically at these depths. At altitudes just above the clouds all the short-wavelength ultraviolet has already been soaked up by CO_2, and isn't available for photochemistry.

References

1. V. I. Moroz, N. A. Parfentev and N. F. San'ko, Cosmic Research 17, 601-614 (1979).

2. A. T. Young and L. G. Young, Sky and Telescope 43, 140-144 (1972).

3. A. T. Young, Bull. Am. Astron. Soc. 12, 717 (1980).

Transient Species on Mars and Venus

Yuk L. Yung (Cal. Tech.)

Although my topic is transient species on Mars and Venus, I will often compare them to the Earth as well as to each other. The chemistry of the Earth's stratosphere has striking similarities to that of the atmosphere of Mars and the stratosphere of Venus.

The transient species in all three atmospheres are the offspring of the parent species listed in Table 1. Table 2 shows the transient species, and contains most of the substance of my talk. This table has been assembled from diverse sources, and I wish to disclaim responsibility for some of the entries. To emphasize this "caveat emptor," please regard Table 2 as a painful compromise between published results (some of which I do not believe) and my own guesses (which have not been worked out fully).

Our understanding of the transient species in Mars' atmosphere is fairly satisfactory, and the corresponding entries in Table 2 should be fairly reliable. The number densities of the important transient species on Mars are shown as functions of altitude in Figures 1 and 2. Note that the number densities of HO_x and NO_x compounds in Mars' atmosphere are comparable to those in the Earth's stratosphere. Our understanding of Venus' stratosphere is far less satisfactory, and will occupy the rest of my talk.

The most interesting classes of compounds in Venus' stratosphere are ClO_x and SO_x. Both classes have also received a lot of attention in the Earth's stratosphere. For comparison, Venus' atmosphere has about 500 parts per billion of chlorine, while the Earth's atmosphere has only about 2 parts per billion; there are about 8 parts per million of sulphur compounds of all types on Venus, compared with less than one part per billion on the Earth. Both classes are far

Table 1
Abundances of Parent Molecules[†]

	Venus (Stratosphere)	Mars	Earth (Stratosphere)
Altitude Range	> 60 km	> 0 km	> 20 km
Pressure	< 200 mb	< 6 mb	< 100 mb
Temperature	~ 250 K	~ 150 K	~ 200 K
O_2	$\leqslant$ 1 ppm	0.13%	20%
H_2O	1 ppm	100 ppm	5 ppm
H_2	100 ppm*	10 ppm	0.5 ppm
N_2	3.5%	2.5%	80%
HCl	600 ppb	-	1 ppb
SO_2	3 ppm	-	0.1 ppb

[†] Abundance given in volume mixing ratio, 1 ppm = 1×10^{-6}, 1 ppb = 1×10^{-9}.

Table 2
Maximum Concentrations of Transient Species†

		Venus (Stratosphere)	Mars	Earth (Stratosphere)
O_x	O	10^{11}	4×10^9	4×10^9
	O_3	10^8	2×10^9	5×10^{12}
HO_x	H	10^8	10^7	5×10^7
	OH	10^6	2×10^6	2×10^7
	HO_2	10^9	10^8	3×10^7
	H_2O_2	10^{11}	5×10^9	10^8
NO_x	NO	10^9	10^9	10^9
	NO_2	3×10^7	4×10^7	10^9
	HNO_3	1×10^6	5×10^4	6×10^9
ClO_x	HCl	3×10^{12}	-	1×10^9
	Cl	10^8	-	5×10^5
	ClO	10^8	-	10^8
FO_x	HF	6×10^9	-	10^8
SO_x	H_2SO_4	3×10^{12}	-	-
	SO	10^{10}	-	-
	SO_2	2×10^{13}	-	3×10^8
	SO_3	10^6	-	-
	H_2S	2×10^{13} ?	-	-

† Concentrations in molecules cm^{-3}.

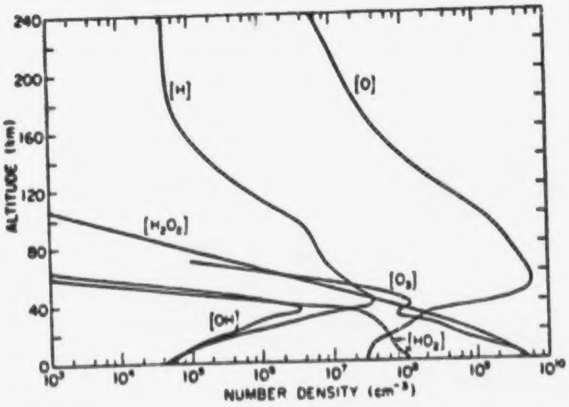

Figure 1. Number densities of O_X and HO_X species in the Martian atmosphere, taken from McElroy, Kong and Yung, J. Geophys. Res. 82, 4370, 1977.

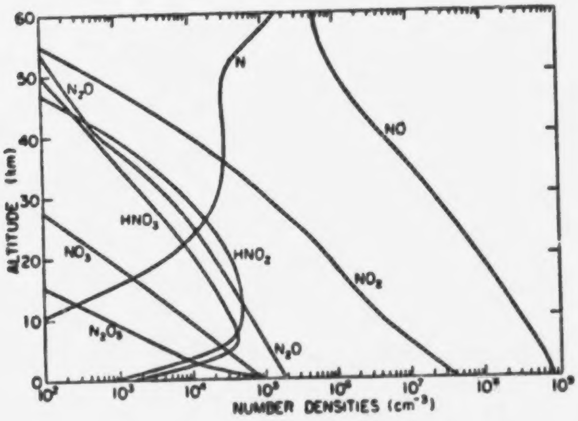

Figure 2. Number densities of NO_X species in the Martian atmosphere, taken from Yung, Strobel, Kong and McElroy, Icarus, 30, 26, 1977.

more abundant on Venus, so there are advantages in studying them on Venus.

The photochemistry of Venus' stratosphere was first studied by Prinn and McElroy, and Sze and Yung. Dissociation of HCℓ was recognized as playing a crucial role as a source of the HO_x radicals. The composition of the upper atmosphere now seems to be understood in a preliminary way. But unfortunately the coupling between the HO_x and $C\ell O_x$ families was subsequently found to be much stronger than originally assumed. This demands a drastic revision of the entire chemistry of the upper atmosphere, and the results are not entirely satisfactory yet.

To further complicate the picture, Stewart's group (Univ. of Colorado) showed that the SO_x family can couple with the oxygen chemistry. To show what difficulties this causes, I will briefly review some of his calculations; this will also give a good picture of the current state of Venus modelling. The abundance profiles of the sulphur compounds are shown in Figure 3. (The SO_2 profile was determined by Charlie Barth's group). There is as much SO_2 in Venus' atmosphere as there is ozone in the Earth's stratosphere. SO_2 can be oxidized to form sulphuric acid, by a chain of reactions. Stewart's model predicts 100 times more O_2 than the spectroscopic upper limit allows, because the model doesn't have enough hydroxyl radicals to turn the oxygen into H_2SO_4. One possible solution is to suppose that H_2 is present, with an abundance of about 100 parts per million. This number has been bruited about for a few months, but the data on Venus' chemistry is so bad that I don't know whether it should be believed or not. If this large H_2 abundance is true, it would save the hydroxyl radicals: Cℓ would react primarily with H_2 and leave the hydroxyl radicals alone, leaving them free to turn oxygen into H_2SO_4. But even if this solution is true, it does not solve the problem of the CO abundance in the lower part of Venus' atmosphere, namely, how to destroy CO after your chemical sources

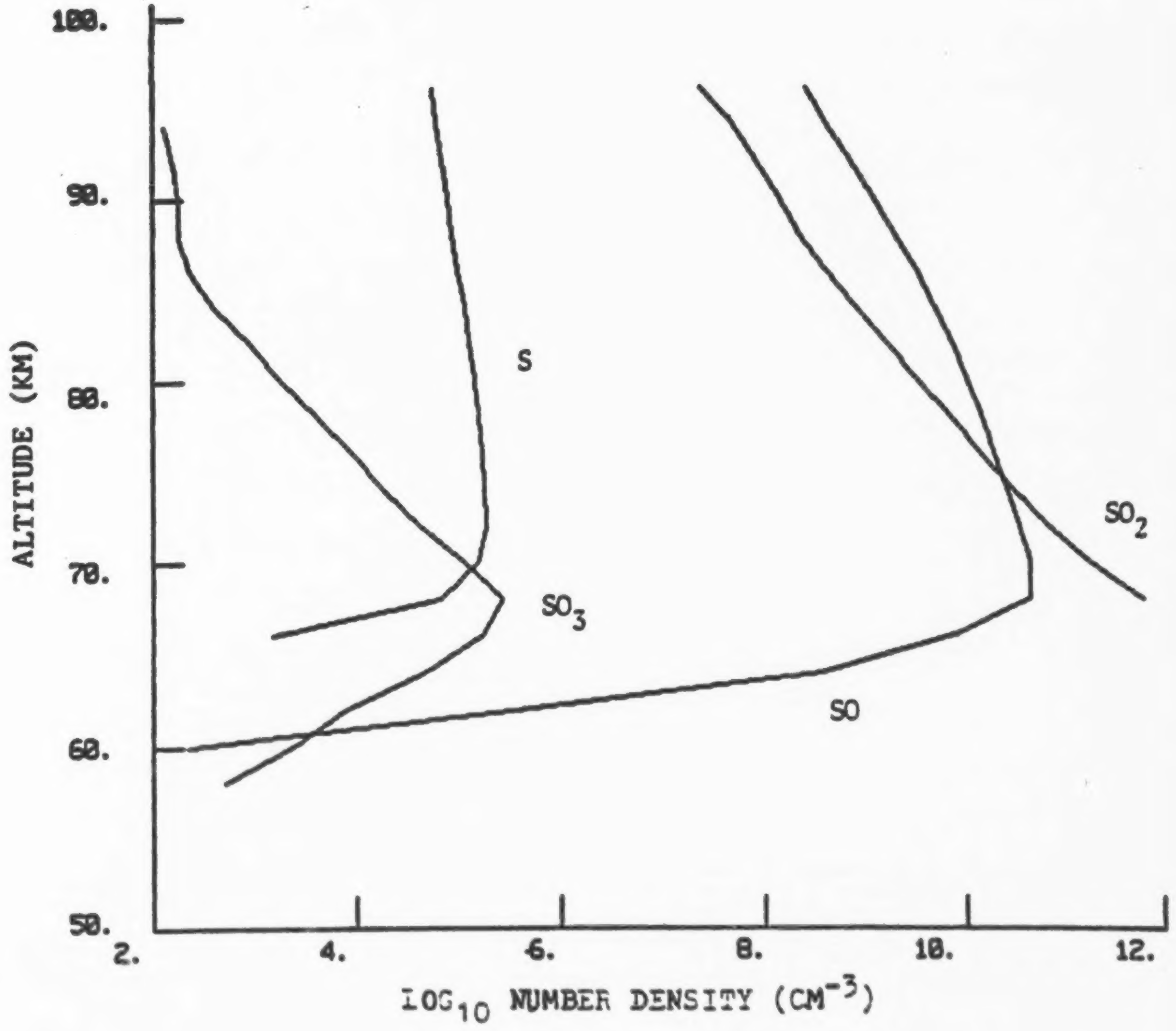

Figure 3. Number densities of SO_x species in the atmosphere of Venus, taken by kind permission from a preprint by Wimick and Stewart, submitted to J. Geophys. Res., 1980.

have been turned off.

Photochemical models can probably yield the other sulphur compounds satisfactorily. Starting with SO_2, oxidation yields SO_3. The SO_2 can also dissociate to give SO, which in turn can dissociate to give S.

DISCUSSION

Question (M. Mumma): When you say that the chemistry of Mars' atmosphere is well understood, are you claiming that all the species in Table 2 have been measured at the same abundances predicted by the models?

Response: Yes. Extensive work by M. B. McElroy's group at Harvard has given us a complete understanding of the photochemistry in Mars' atmosphere, and its evolution.

Question (M. Mumma): Do you then agree with Don Hunten on the abundance of peroxide on Mars?

Response: The peroxide abundance was definitely settled in the thesis of my colleague T. K. Kong at Harvard. Although Hunten is not here to verify my statement, I believe he agrees with Kong.

Comment (M. Mumma): I have a comment for the many spectroscopists in the audience. The test of any theory is a good experiment, and your talk has highlighted a number of species for which spectroscopic work is badly needed, both in the laboratory and in observations of Venus.

Response: I've listed about 15 species, both to indicate those of greatest interest and to roughly indicate their abundances, to encourage such observations.

Question (K. Fox): In the list of transient species in Venus' atmosphere, the maximum concentration quoted for H_2S is followed by a question mark. What is it trying to say?

Response: There are theoretical reasons for supposing H_2S to be present, but it hasn't been detected yet. The estimated value in Table 2 is based on a theoretical analysis by John Lewis. His model predicts H_2S, as well as OCS and CS_2 in the lower atmosphere.

Comment (A. Young): I'd like to comment on the estimate of three parts per million as the concentration of H_2S. Venus' atmosphere has about 200 parts per million of SO_2. Attributing to various oxidation states of sulphur all of the ultraviolet absorption observed at the bottom of the atmosphere, the Russian data give a mixing ratio of 2×10^{-8}; this assumes thermochemical equilibrium, which is probably not correct, but the result should be indicative, and in any case it agrees fairly well with the 2×10^{-8} just cited. These two estimates are at least two orders of magnitude below the mixing ratio for SO_2. Your estimate of H_2S claims that a still further reduced species will be more abundant than that. That is very implausible.

Blank Page

SPECTROSCOPY PERTINENT TO THE INNER PLANETS

Page

Gaseous Infrared Absorption in the Lower Atmosphere of Venus – C. Chackerian, Jr. and R. W. Boese 255

The Spectroscopy of Venus – Reinhard Beer...................... 271

Spectroscopic Measurements of Mars and Venus with Heterodyne Techniques – Albert Betz 277

Infrared Absorption by OH-Containing Compounds – John J. Hillman 295

Infrared Absorption of Sulfur-Bearing Compounds – Arthur Maki 311

Blank Page

Gaseous Infrared Absorption in the Lower Atmosphere of Venus

C. Chackerian, Jr. and R. W. Boese (NASA-Ames)

The recent Pioneer-Venus and Venera missions to Venus have provided us with a large body of information on that planet's atmosphere. These data include measurements of the vertical pressure-temperature profile and the mixing ratios for a number of atmospheric constituents. The vertical pressure-temperature profile has yet to be fully explained on the basis of theoretical modeling of the Venusian atmosphere. It has been shown, however, that the greenhouse effect is a dominant mechanism in determining this profile. Therefore, a knowledge of the infrared opacity of relevant atmospheric constituents in the mid- and far-infrared over the appropriate range of gas conditions (pressure = 90 bar to 200 mbar, temperature = 760 K to 220 K) is central to the theoretical modeling.

It is the object of this talk to identify the possibly important sources of infrared opacity in the Venusian atmosphere. The mixing ratios of various atmospheric constituents are shown in Table 1. We will see that CO_2, which is the major atmospheric constituent comprising about 97 percent of the atmosphere, is the dominant infrared opacity source. Not shown is N_2 which comprises about 3 percent of the atmosphere. The mixing ratio of water vapor varies considerably with altitude but falls in the range of about 20 to 200 parts per million (ppm). The mixing ratio of SO_2 falls in the range of 100-200 ppm. This number is about 5000 times larger than estimates obtained earlier via earth-based observations. The abundance of some of the other minor constituents is also shown. While these constituents are not important in the mid-infrared their importance for the opacity beyond 20 microns has not been established. Other minor constituents such as CO and HCℓ may not play a role in the greenhouse effect.

The first five figures show the development of the mid-infrared CO_2 spectrum at room temperature as the gas abundance is increased. In Fig. 1 we see

Table 1
Venus' Atmospheric Gases

CONSTITUENT	ABUNDANCE
CARBON DIOXIDE	950,000 PPM
WATER VAPOR	20 - 200 PPM
SULPHUR DIOXIDE	100 - 200 PPM
HYDROGEN SULFIDE	1 - 10 PPM
ETHANE	0.5 - 5 PPM
SULPHURIC ACID	
SULPHER TRIOXIDE	

the mid-infrared transmission spectrum of CO_2 at a pressure of 10 torr and a path length of 331 cm. In this case the mid-infrared is transparent except for absorption in the region of the bending and the asymetric stretching fundamental vibrations. In Figure 2 the pressure is increased by a factor of 10, and two hot bands near 1000 cm^{-1} and two combination bands near $\sim$ 1900 cm^{-1} already begin to contribute to the gaseous opacity. In Figure 3 the pressure is increased to 5 atmospheres and the normally infrared inactive Fermi diad near about 1350 cm^{-1} is seen to absorb. These bands are made infrared active by forces between molecules; their intensity is therefore proportional to the square of the density. The sharper line spectrum centered about 1600 cm^{-1} is due to uncancelled atmospheric water vapor. In Figure 4 the gas pressure is increased to 10 atmospheres. At this abundance the absorption intensity of the Fermi pressure-induced diad at 1350 cm^{-1} has become greater than the hot bands centered at 1000 cm^{-1}. Finally in Figure 5 we have increased the pressure to 20 atmospheres and the path length to 30.7 meters. The transmission windows remaining at this abundance will surely be closed in the lower reaches of the Venusian atmosphere where the pressures are greater than 20 atmospheres and the temperatures greater than 295 K.

The opacity for all the bands is expected to grow toward the lower frequencies as the temperature is increased. Nevertheless at appropriate altitudes in the atmosphere, windows in the CO_2 transmission will develop. It is likely that SO_2 can act as a "plug" for these windows. In the Table 2 we indicate the location for some of the absorption bands of SO_2. The intensity for some of these bands has been measured at room temperature, and on the basis of these measurements we can estimate the contribution of SO_2 to the 1150 cm^{-1} window at say the 20 atmosphere level. In Figure 6 we again look at the CO_2 room temperature spectrum recorded at a total pressure of 20 atmospheres and a

Table 2
Location of Some Sulphur Dioxide
Absorption Bands

2715 WAVENUMBERS (CM^{-1})

2500

2296

1876

1665

1535

1361

1151

1025

519

path length of 30.7 meters. We estimate the contribution of SO_2 at 1150 cm^{-1} assuming an abundance of 100 ppm and absorptivity data of Chan and Tien.[1] The dotted line indicates the contribution of SO_2 to the opacity if it alone were the absorbing species in this frequency region. We see that SO_2 effectively "plugs up this hole" in the CO_2 spectrum. The positions of other infrared active SO_2 bands are indicated by the horizontal lines. Some of these fall in other window regions. On the basis of this we would expect that SO_2 will make significant contributions to the Venusian mid-infrared opacity at appropriate altitudes. Water may also contribute significantly to the opacity in the 1600 cm^{-1} region of the spectrum at the higher altitudes.

Two of the molecules we have been talking about, namely CO_2 and SO_2, have significant opacity in the far-infrared. Figure 7 illustrates the far-infrared absorption coefficient of CO_2. Notice that the absorption coefficient is proportional to the square of the pressure. Since this is a pressure-induced feature we expect that the opacity will be influenced by the temperature. Figure 8 shows the far-infrared spectrum of SO_2 which was obtained by Larkin et al.[2] N_2 also has a pressure-induced spectrum in this region, but no data exist for the N_2-CO_2 system. CO_2 has a rather large quadrupole and the induced spectrum of N_2 could therefore be significant.

On the basis of the laboratory data that we now have, we anticipate that CO_2, SO_2, and H_2O will be the dominant contributors to the opacity in the mid-infrared. The far-infrared at frequencies less than 140 cm^{-1} will be dominated by SO_2 and CO_2. The importance of the N_2-CO_2 pressure induced spectrum to this region is unknown. At appropriate altitudes a window is expected to develop in the CO_2-SO_2 spectrum extending from about 200 to 400 cm^{-1}. Here H_2O and possibly HCℓ could be significant sources of opacity.

In conclusion the mid- and far-infrared opacity of the Venusian atmosphere is dominated by CO_2. SO_2 probably makes important contributions. Both of these molecules should be studied in the laboratory under conditions of elevated temperature (760 K) and pressure (90 bar). The opacity of H_2O is also needed, but here account should be taken of the distribution with altitude, and somewhat less extreme conditions are probably necessary.

References

1. S. H. Chan and C. L. Tien, Journal of Heat Transfer 93, 172 (1971).
2. R. J. Larkin, R. Lovejoy, P. Silvaggio, and R. Boese, J.Q.S.R.T. (submitted).

DISCUSSION

Question (A. Young): What temperature is used in obtaining your absorption spectra?

Response (C. Chackerian): These spectra were obtained at room temperature, and of course the Venusian surface temperature is on the order of 760^{K}. One should really take the data and somehow use them to predict the spectrum at higher temperatures or get higher temperature data.

Comment (A. Young): I just want to point out that the laboratory conditions for which you showed CO_2 spectra are only appropriate for the atmosphere above the cloud tops. On Venus, a thousand times more CO_2 lies underneath the cloud tops.

Comment (C. Chackerian): I would like to emphasize that we do not have laboratory data for CO_2 opacity which are appropriate to the low atmosphere of Venus; nevertheless Pollack, Toon, and Boese, in recently completed work, have reproduced closely the observed surface temperature and lapse rate structure using estimates for CO_2 opacity in their greenhouse model.

Question (K. Fox): Have you considered the collision-induced absorption induced in N_2 by CO_2?

Response (C. Chackerian): No. I do not know if laboratory data exist for the pressure-induced rotation-translation spectrum of N_2. The rotational constant of N_2 is about five times greater than that of CO_2 so it is possible that this spectrum of N_2 could contribute to the opacity shortward of the CO_2 rotational band. We know from Pioneer Venus that N_2 accounts for about three percent of the atmosphere.

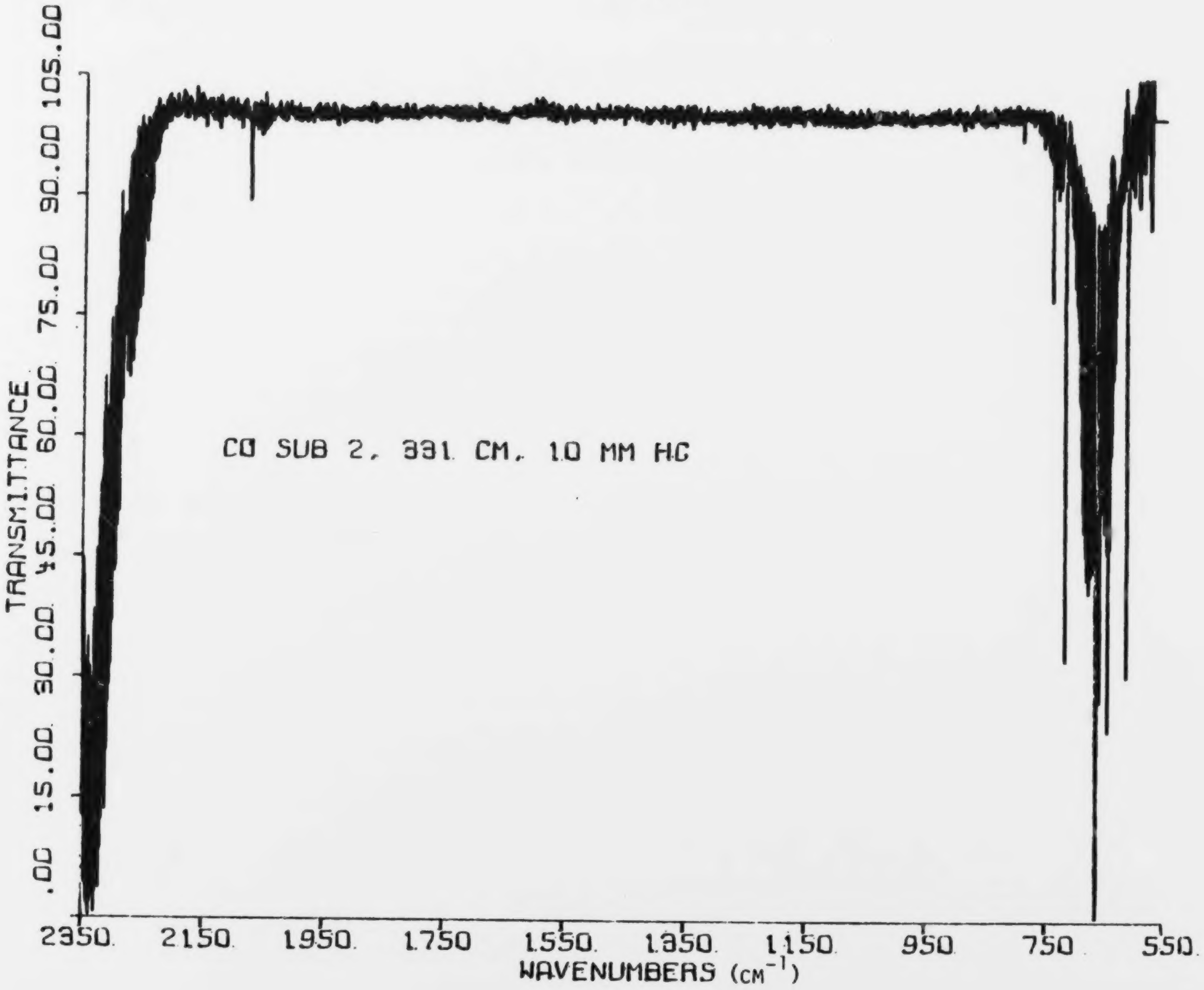

Figure 1. CO$_2$ spectrum.

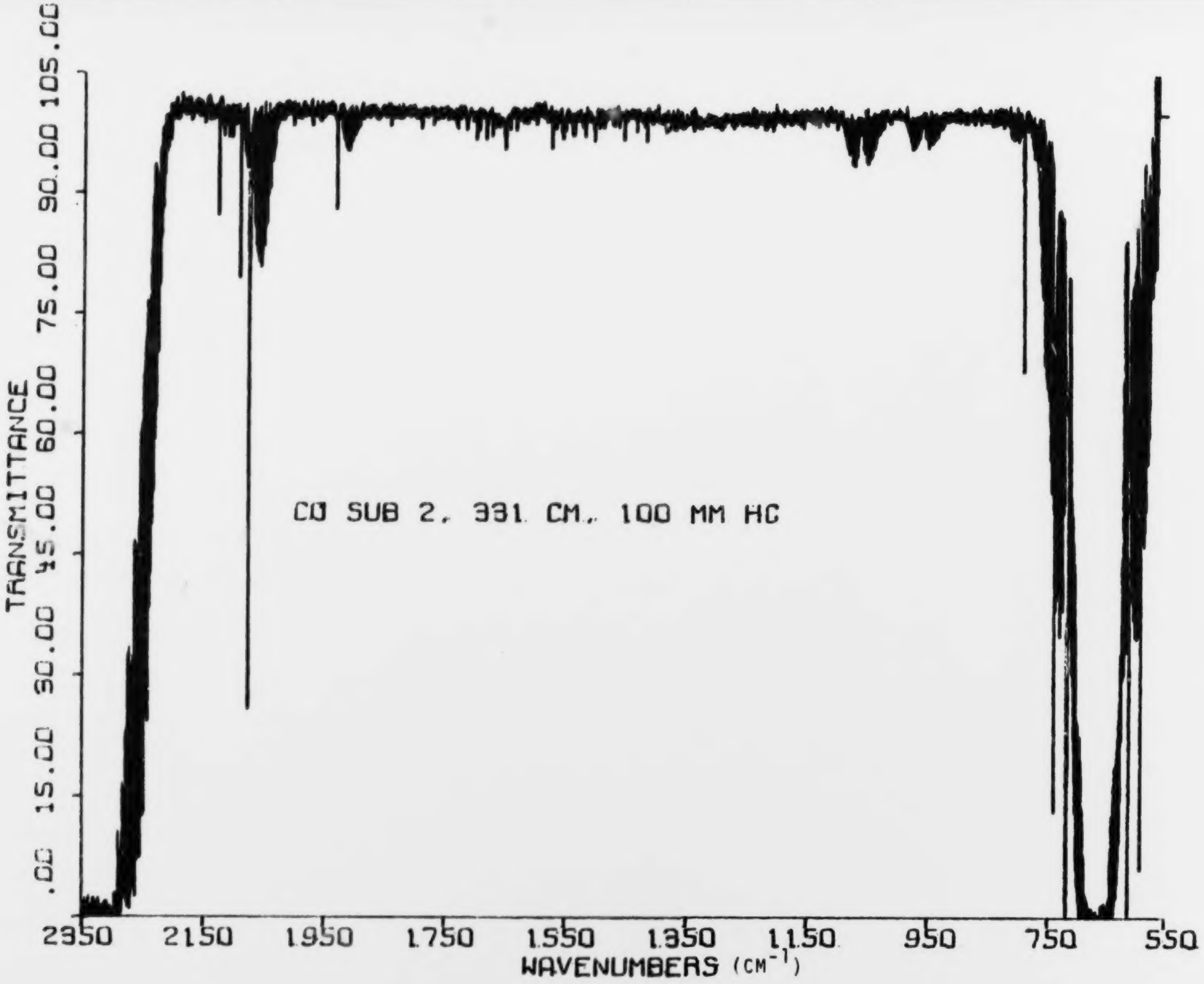

Figure 2. CO_2 spectrum.

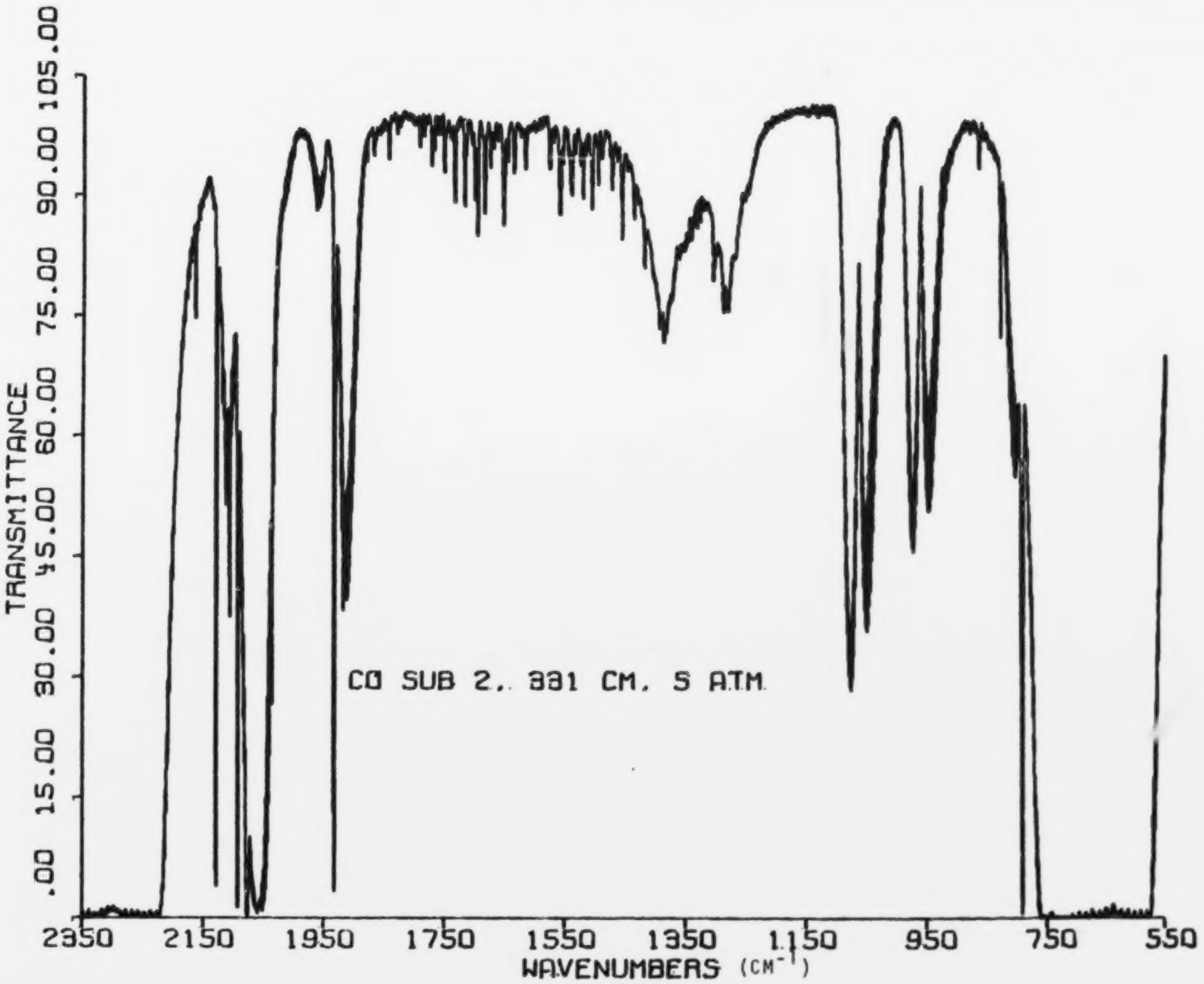

Figure 3. CO$_2$ spectrum.

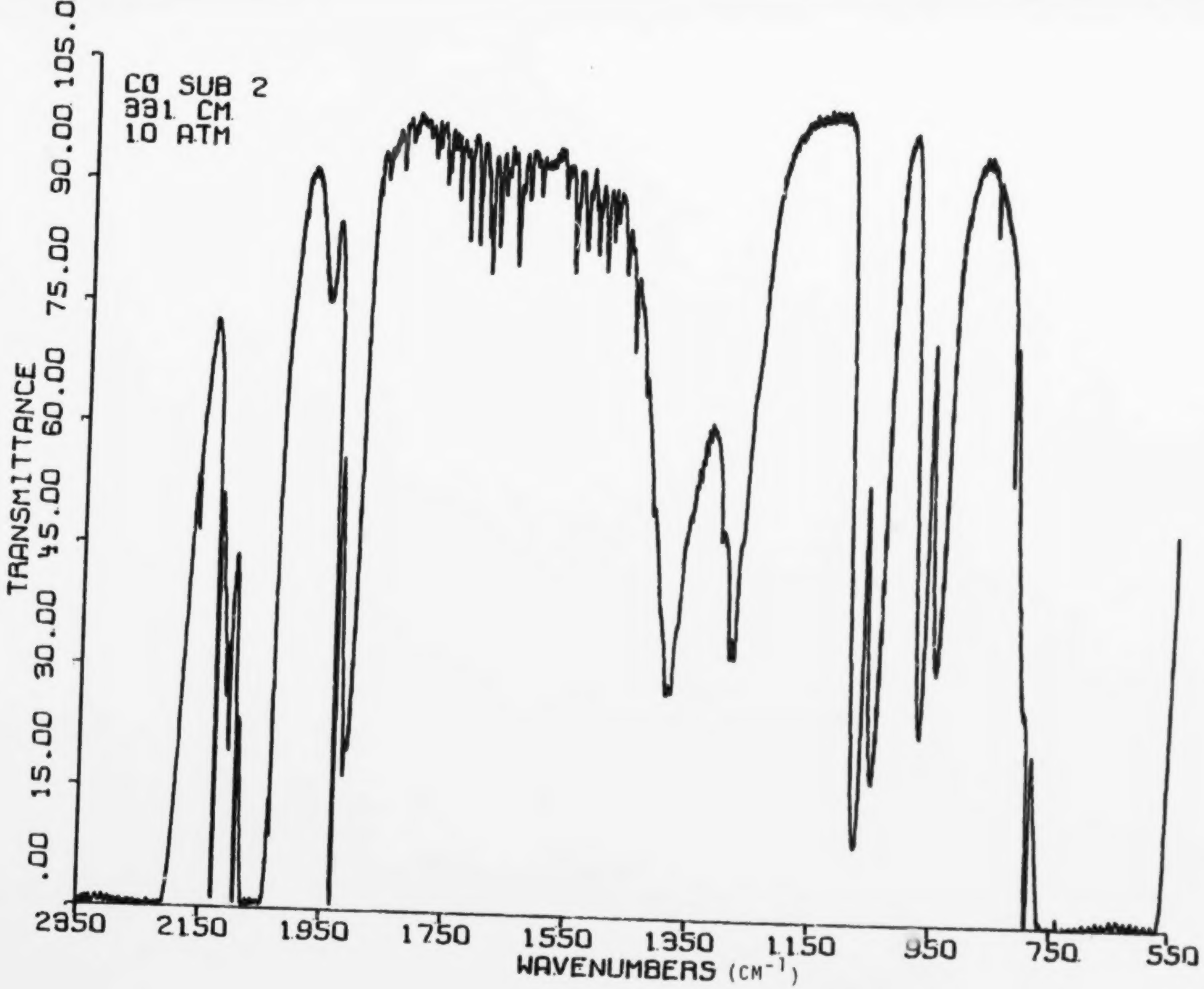

Figure 4. CO_2 spectrum.

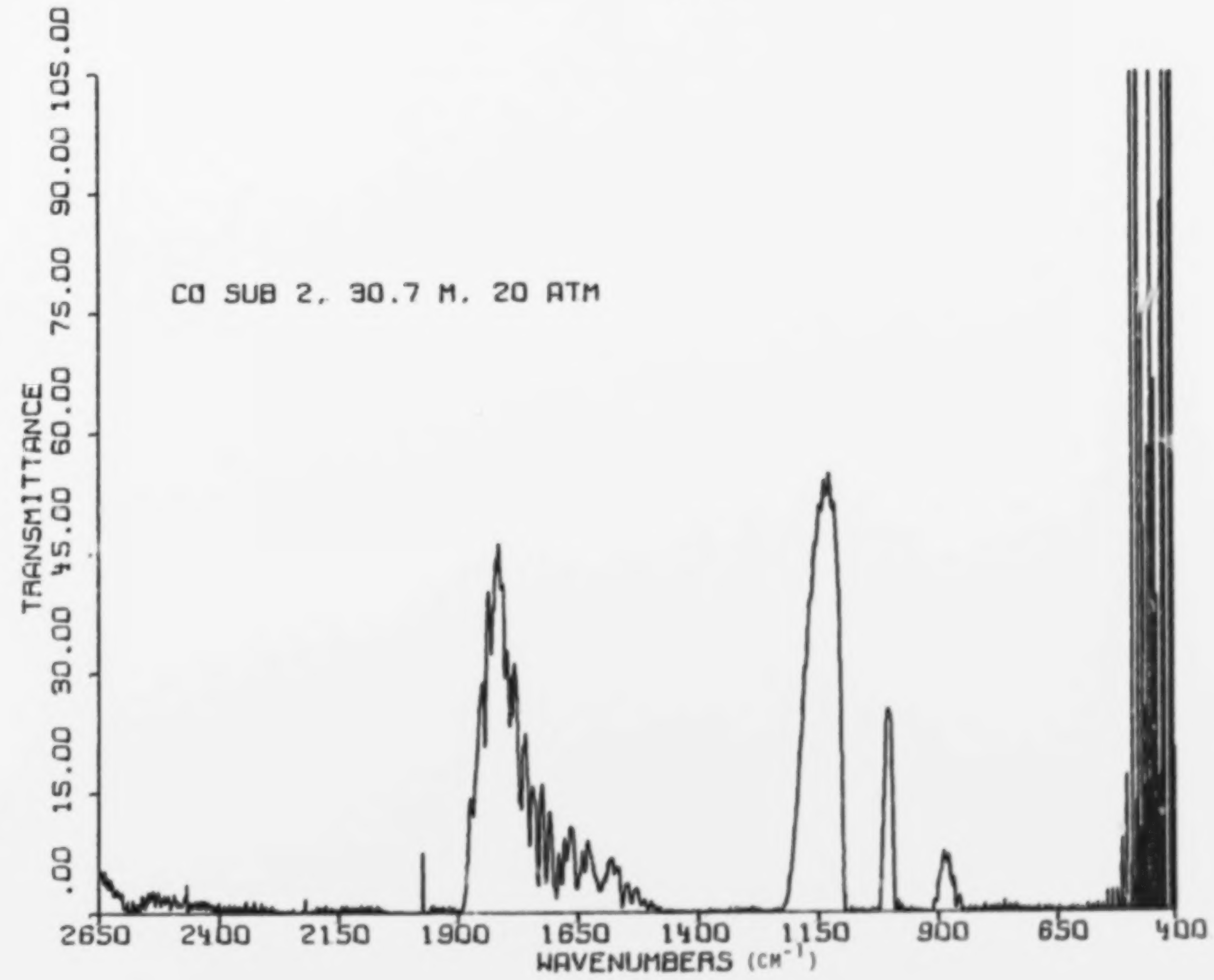

Figure 5. CO_2 spectrum.

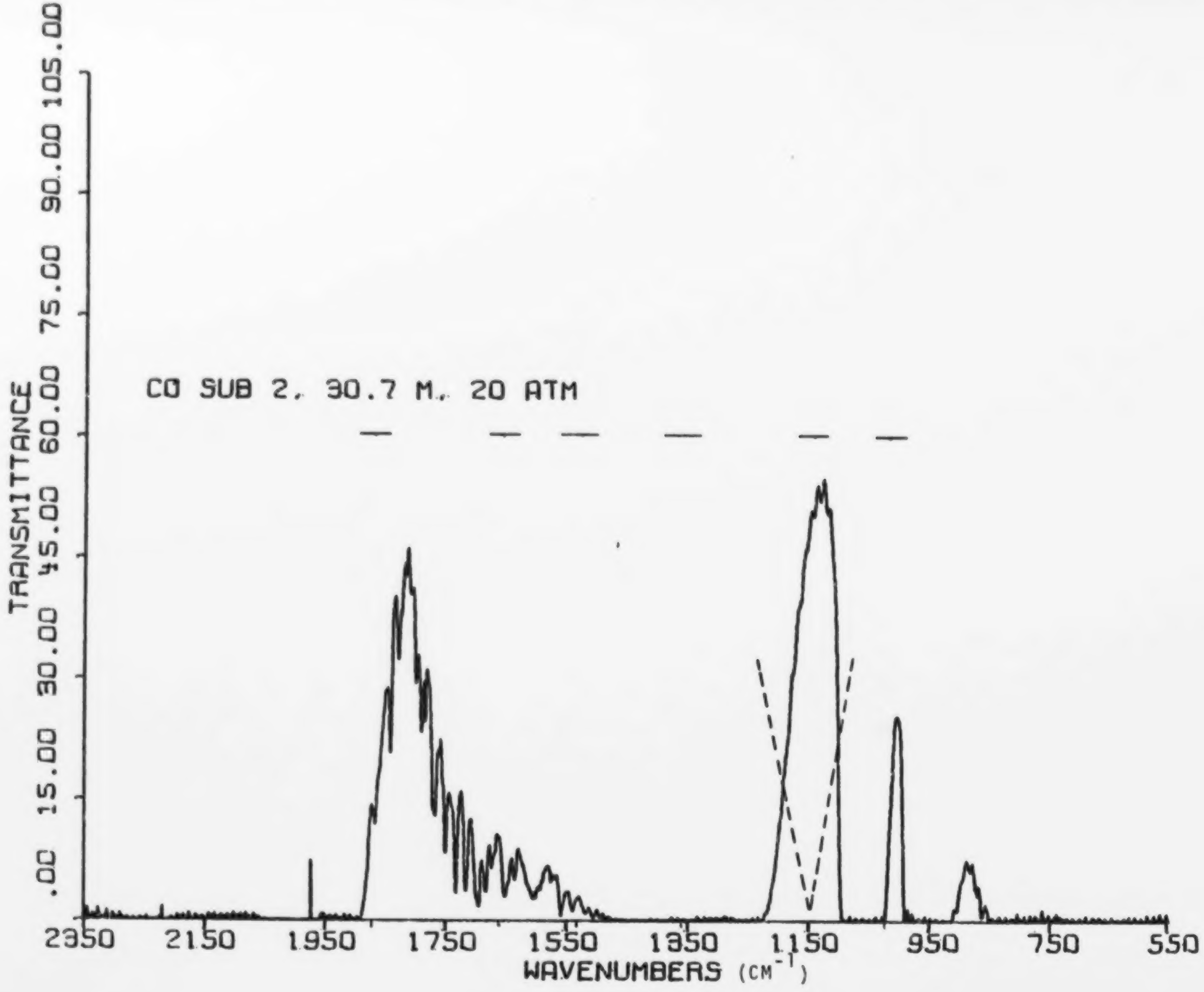

Figure 6. CO_2 spectrum, with SO_2.

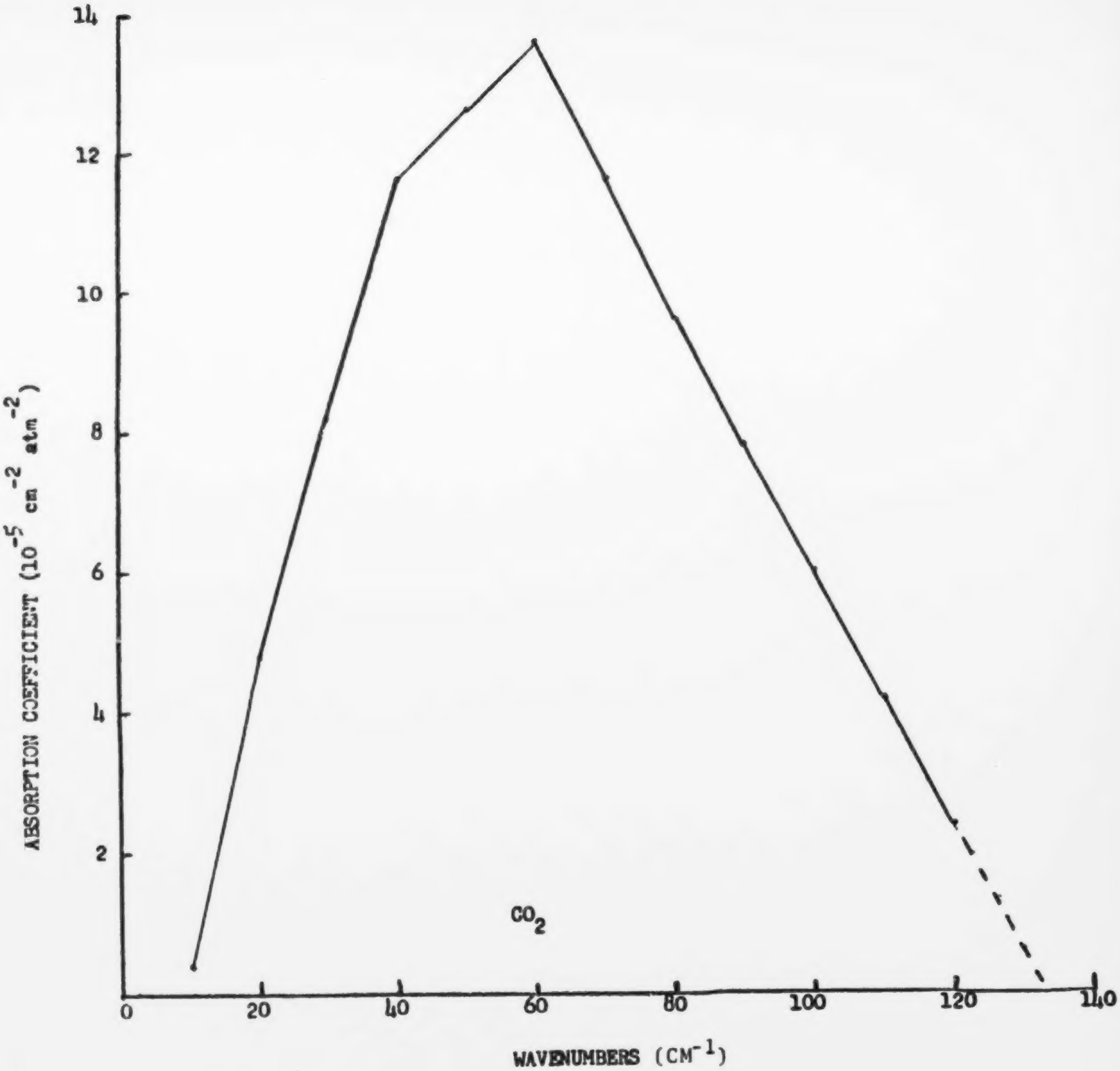

Figure 7. CO_2 spectrum.

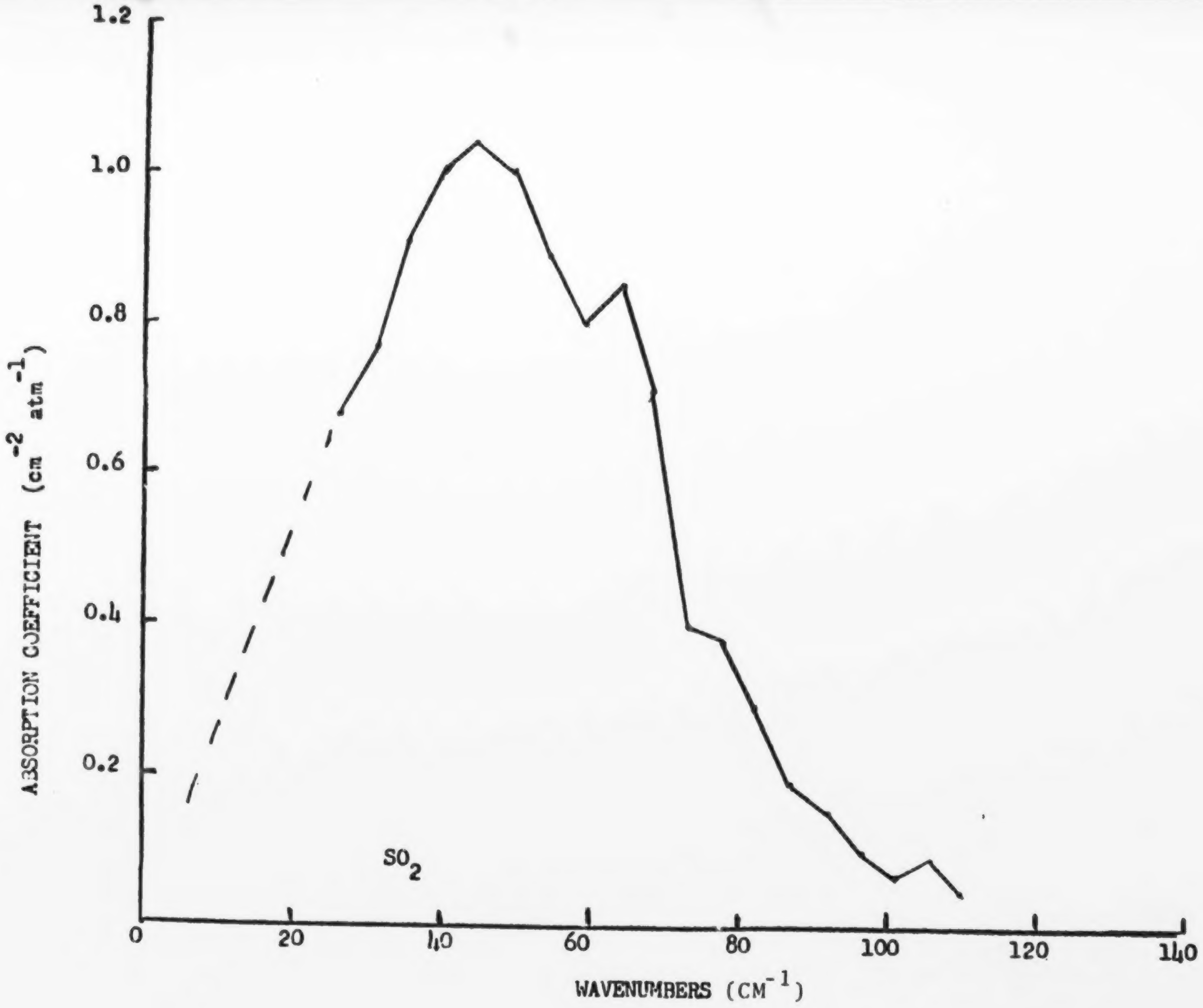

Figure 8. SO_2 spectrum.

Blank Page

THE SPECTROSCOPY OF VENUS

Reinhard Beer (JPL)

Venus has not been an especially active field for spectroscopy in the past ten years for two possible reasons: first, the almost total domination of the spectrum by CO_2 (including almost every conceivable isotopic combination) makes the search for other species very difficult, and the CO_2 bands themselves have been deeply analyzed by L. D. Gray Young and her colleagues; second, the knowledge that no wavelengths short of the microwave penetrate through the Venus cloud decks (or even very deeply into them) means that, at best, UV, visible and IR remote sensing can investigate only the middle and upper atmosphere, and even there quantitative analysis is vastly complicated by the intense multiple scattering.

Since G. P. Kuiper's pioneering efforts in the early post-war years, the infrared spectroscopy of Venus is largely the story of Pierre Connes and his associates. They transformed the field by their complete resolution of the hundreds of near-infrared CO and CO_2 bands and the dramatic discovery of $HC\ell$ and HF that lead to the proposal by G. T. Sill and A. T. Young that H_2SO_4 is a major cloud constituent on Venus. Since that time, new spectra by Connes have revealed oxygen airglow emissions from the Venus upper atmosphere, and just

---

* Actually, most of the orbiter experiments are still functioning properly.

prior to the Pioneer Venus encounter, E. C. Barker, using the powerful Reticon scanner at McDonald Observatory, discovered SO_2 from its UV bands on the extreme edge of the atmospheric window. A large number of problems were still unsolved: Where is the H_2O? the HBr? the 1-0 band of HCℓ (30 times stronger than the readily-detected 2-0 band)?

Following the Pioneer Venus mission* a vast amount of additional information has come to light, but primarily concerning the deep atmosphere. Although it now seems certain that concentrated (75-90%) H_2SO_4 is a major cloud constituent, it is equally certain that it is not the whole story: at least one component of the tri- (or even quadri-) modal clouds seems to be crystalline. The Pioneer Venus Orbiter Infrared Radiometer (OIR) has confirmed the existence of significant thermal anomalies near the terminators and a dramatic polar "collar" and dipole (the latter unfortunately invisible from Earth). The terminator anomalies are certainly amenable to ground-based investigation as is one of the major discoveries of the OIR: a strong 30-50 µm absorber locked to the sub-solar region of Venus. This broadband channel was installed as an H_2O detector, but it is not species-specific. Spectroscopy of Venus near the sub-solar point is very difficult, entailing observation when the planet is not only close to the Sun in the sky but also at its smallest apparent size. Nevertheless, the challenge exists: is the absorber the long-lost H_2O?

The spectrum of Venus is reasonably well-explored below 2.5 µm, which is not to say that further work is unwarranted: spectra of high spectral and spatial resolution coupled to extreme photometric precision might well be sought for evidence of isotopic fractionation in the CO and CO_2 bands as a measure of mixing efficiency following CO recombination. The region between 3 and 4 μm has not been attacked with high resolution, and the 5-10 μm region is virtually unexplored. It is probably in this latter window (on Venus, that is) that new discoveries remain to be made. It is here, for example, that the DCℓ fundamental lies. Since it has been hypothesized that Venus has suffered major hydrogen loss, the D/H ratio should be markedly enhanced over the canonical 5×10^{-5} solar system value. In addition, recent spectra obtained by Beer and Ridgeway using the Kitt Peak 4 m telescope show a substantial (and unidentified) absorber in the 5 μm region. Exploration at wavelengths between 5.5 and 8 μm will require extra-atmospheric bases such as Space Telescope*. Regrettably, none of the announced VOIR instruments will address any of these problems, so it seems that whatever progress is to be made within the foreseeable future will come from the concerted activities of ground-based observation and laboratory spectroscopy.

---

* Near Venus maximum elongation. Most current space platforms (such as SIRTF) may not point closer than 90° of the Sun, effectively eliminating the inner solar system from further study.

Discussion

Question (K. Fox): Can you see the 3-0 band of HCℓ?

Response: Not to my knowledge.

Question (U. Fink): Is the 1-0 band lost in the CO_2 absorption?

Response: No, its actually in the clear. It should be visible. There are lines that aren't in the clear, and we have looked very diligently for them and not seen a thing. I think that if you could get the resolution down to considerably better than 0.1 cm^{-1} it could be done.

Comment (A. Young): The problem is that this band lies in the region where sulphuric acid absorbs. The albedo is only a few percent there, and you don't have enough power to work with.

Response: Clearly, there are reasons why it hasn't been done. I'm just saying that here is a piece of spectroscopy waiting to be done. Another piece of spectroscopy, while we're on the subject of the hydrogen halides: A long long time ago Godfrey Sill said that there should be a measureable amount of HBr in the atmosphere, and it should be spectroscopically detectable. It has not been spectroscopically detected. It's a job for someone to do.

Comment (A. Young): One of the problems that arises, in connection with the observed hazes, is that observed differences in limb-darkening have to be attributed to opacity by sulphuric acid. However, you cannot have high speed winds at these altitudes, because the sulphuric acid takes something like a couple of months to fall or coagulate or otherwise get cleared out of a region where it exists. Also, there are apparent height differences of the order of several kilometers between the day side and the night side. Either you have to make these hazes entirely out of something other than sulphuric acid, that can be both formed and destroyed on a very short time scale (less than a day), and be absent during the night, or you have to do away with the 100 meters per second winds at these altitudes.

Response: I think 100 meter per second winds are reasonably well established. I don't think you can argue those away. There is now too much evidence for them. Since we're supposed to be talking about spectroscopic problems, let me just add one final comment. One of reasons why I think the spectroscopy of Venus went into the doldrums, was that we had all these wonderful spectra but could never interpret them. That's half the argument we've been hearing today - interpretations of the data - and one of the reasons was the lack of just the kind of information I'm showing you. We didn't know where to look on Venus to see what we wanted to see. Now we have more clues.

Comment (A. Young): Ed Barker has observed water at many different parts of the planet on the same day. His data don't show the kind of distribution of water that you attribute to your 50 micron absorber. He sees definite thatching in the water distribution, but it's a very irregular kind of thatching, not at all locked to the Sun. So I think that attributing the 50 micron absorption to water is inconsistent.

Response: That may well be, but then you have to find something else absorbing like hell at 50 microns. That might be an even worse problem.

Question: Wouldn't that have changed the altitude of the SO_2 *cloud also,* leaving some kind of .....(interrupted)

Response: Unfortunately, SO_2 has almost no opacity at 50 microns, certainly not for the abundances that have been reported.

Comment (M. Mumma): There is an important paper by Hanel and Kunde on observations in the 10 micron region taken with a resolution of .02 cm^{-1}. It very clearly shows sulphuric acid haze absorption, with many different bands of CO_2.....(interrupted)

Response: I don't think anyone disbelieves for one moment that there's sulphuric acid on Venus.

Comment (M. Mumma): I wasn't saying it for that reason. I don't disagree either. But the fact is that modelling such spectroscopic data, including the absorption due to haze, requires the complex index of refraction for sulphuric acid droplets. I think its very pertinent to the purposes of this Workshop to identify quantities like that which are needed for modelling.

Response: We have in fact tried to model the new 30-50 μm region with sulphuric acid. No plausible amount will work without having pools of sulphuric acid up there.

SPECTROSCOPIC MEASUREMENTS OF MARS AND VENUS WITH HETERODYNE TECHNIQUES

Albert Betz

Department of Physics
University of California
Berkeley, California 94720

Introduction

In the time provided, I'll try to illustrate the new types of planetary observations made possible with the high spectral resolution of heterodyne spectroscopy. The ability to observe individual line profiles with arbitrarily high resolution and yet essentially perfect frequency calibration opens up some new areas for spectroscopy in the study of planetary atmospheres, but it also stiffens the requirements for supporting laboratory measurements. Our applications of the heterodyne technique to planetary spectroscopy have included measurements of the exact shapes of CO_2 absorption lines in Mars and Venus to determine the vertical pressure-temperature structure, accurate measurements of absolute wind velocities in both the mesosphere and stratosphere of Venus from the Doppler shifts of narrow CO_2 lines, and, more recently, searches for minor molecular species of interest in modeling the stratospheric photochemistry of Mars and Venus.

This work supported in parts by NASA Grant NGR05-003-452.

Instrument

To begin, let's review the basic characteristics of the spectrometer. The schematic form illustrated in Figure 1 is identical to that of a microwave spectral line receiver of the type commonly used in radio astronomy. This spectrometer, designed for the 10 μm region, is operationally equivalent but is implemented with the technology appropriate to the infrared. The distinctive component difference is the use of a laser as the local oscillator (LO) in the infrared receiver. The laser beam, of course, does not actively probe a remote gas sample, as is normally the case in laboratory laser spectroscopy, but rather it acts to provide an extremely stable reference frequency against which the collected source radiation is mixed, or heterodyned, and then amplified. The local oscillator and signal beams are first combined by a NaCl beam combiner and then are focussed on an infrared diode photomixer. The mixing process between the monochromatic laser frequency and continuous band of signal frequencies produces a band of difference frequencies in the radio frequency region. The bandwidth of this difference frequency output, more commonly called the intermediate frequency (IF) output, is determined by the speed of response of the diode photomixer, and in our particular mixer is 1500 MHz (.05 cm^{-1}). Infrared frequencies within a band of 1500 MHz above or below the laser frequency are consequently down converted into the radio frequency region where they can be amplified, frequency converted a second time in a RF mixer, and finally filtered into a number of spectral channels before power detection. This "double-sideband" mixing of the infrared frequencies gives us a total spectral window of 0.1 cm^{-1} centered around the accurately known laser frequency. The laser used in our observations is a carbon dioxide gas laser capable of oscillating on any one of a

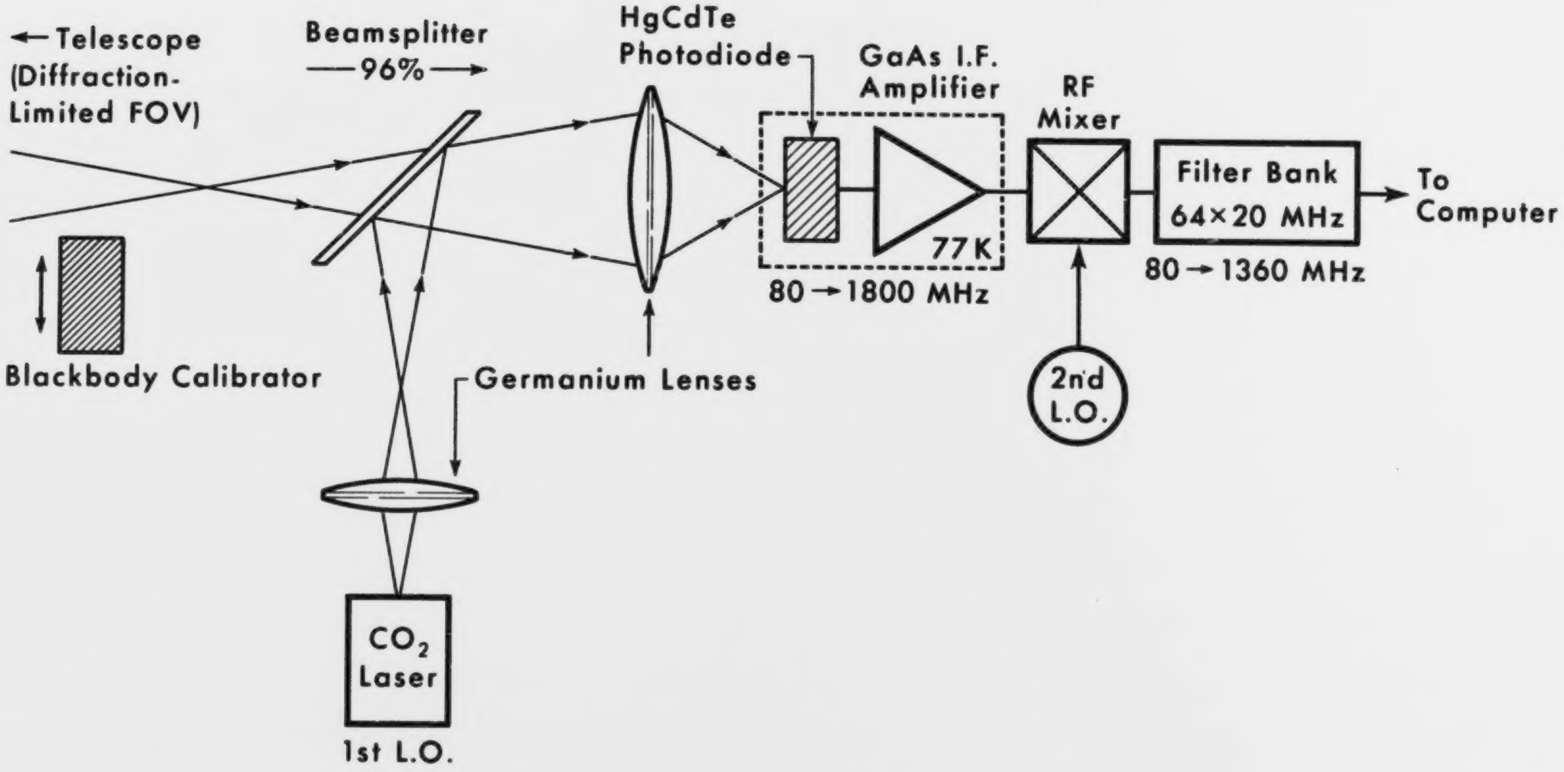
← Telescope
(Diffraction-
Limited FOV)
Beamsplitter
96%
Blackbody Calibrator
HgCdTe
Photodiode
GaAs I.F.
Amplifier
77 K
80 → 1800 MHz
RF
Mixer
Filter Bank
64×20 MHz
80 → 1360 MHz
To
Computer
2nd
L.O.
Germanium Lenses
CO_2
Laser
1st L.O.

Figure 1. Infrared heterodyne spectrometer.

hundred discrete rotational-vibrational transitions in the 10 μm region. Various isotopic variants of CO_2 may be used in the laser to further extend the number of LO frequencies to ∿1000. Since the lasing frequencies of CO_2 have been measured in various laboratories to better than 1 part in 10^8 absolute accuracy, and are resettable to better than 1 part in 10^{10}, the spectrometer has an essentially self-calibrated frequency scale. The burden of stability is placed on the laser for instrumental frequency accuracy; and since the laser frequency is in turn dependent on a resonant molecular process, extremely accurate frequency calibration is easily achieved. (The importance of such accuracy will become apparent from the observations mentioned later). Because of the large ratio between infrared and radio frequencies, and the inherent stability of the laser, the frequencies of the filter elements at the right of Figure 1 need only be measured to ∿1 part in 10^3 to get an overall spectrometer accuracy of 1 part in 10^8. By the way, we prefer to use 5 MHz channels (.00016 cm^{-1}) for planetary observations rather than the 20 MHz widths illustrated. The wider channels are more appropriate for spectral lines in circumstellar gas around late type stars. The 5 MHz channels are especially necessary for shape measurements of thermally-broadened emission line profiles from planetary mesospheres. Because of changes of the Doppler shift from the Earth's rotation (∿2 MHz/hr), a second tunable oscillator is provided to track out these predictable shifts and keep the line centered in the filter bank.

Sensitivity

The big question is whether a spectrometer with all this resolution can achieve an adequate signal to noise ratio on a planet in a reasonable length of time. What is the sensitivity? The signal level, of course, is proportional to the continuum temperature and has for the most part a blackbody distribution in frequency. The noise level is primarily determined by the shot noise of the laser power on the photomixer. However, the electric field strength of the laser power in effect amplifies those infrared signal frequencies which are down-converted into the radio region. For sufficiently strong laser powers (practically about 0.5 to 1.0 mW), the resulting signal-to-noise ratio per channel is independent of laser power and is proportional to $(Bt)^{\frac{1}{2}} (e^{h\nu/kT}-1)^{-1}$, where B is the channel width and t the integration time. Figure 2 illustrates the dependence of the S/N ratio on frequency for the continuum temperatures of various planets. For this calculation, a full bandwidth of 1500 MHz and an integration time of 1 second is assumed, as well as a 100% quantum efficiency for the photomixer. In practice, mixers with ~35% quantum efficiency are used and so the actual S/N ratios are several times worse than depicted. Also, the filter widths for spectroscopy are only 5 MHz wide, and so integration times of 300 seconds are needed to achieve the indicated S/N ratios. In any event, the curves show that the continuum radiation can easily be detected at 10 μm for planets with temperatures >200 K; consequently, from a detectability standpoint, Mars, Venus, and Mercury are suitable sources for absorption line spectroscopy. At longer wavelengths, the cooler outer planets become detectable. The 135 K continuum of Jupiter would easily be seen at 20 μm whereas it is just barely detectable at 10 μm, as our measurements have confirmed. Of course, any process

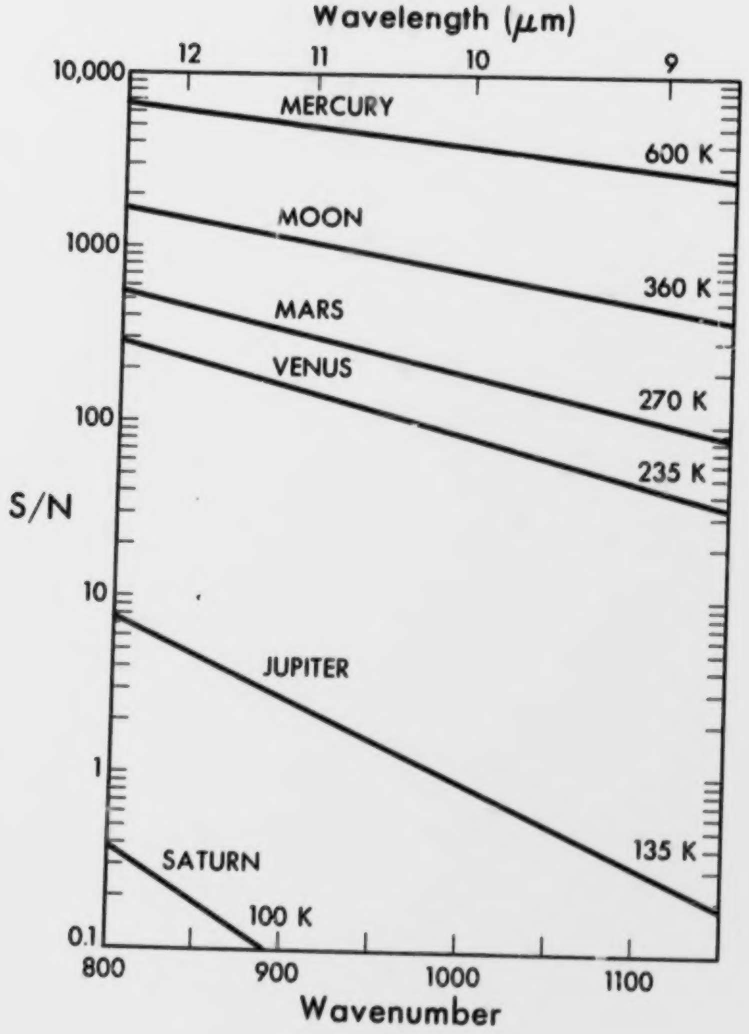

Figure 2. Dependence of signal-to-noise ratio on frequency, for continuum temperatures of various planets.

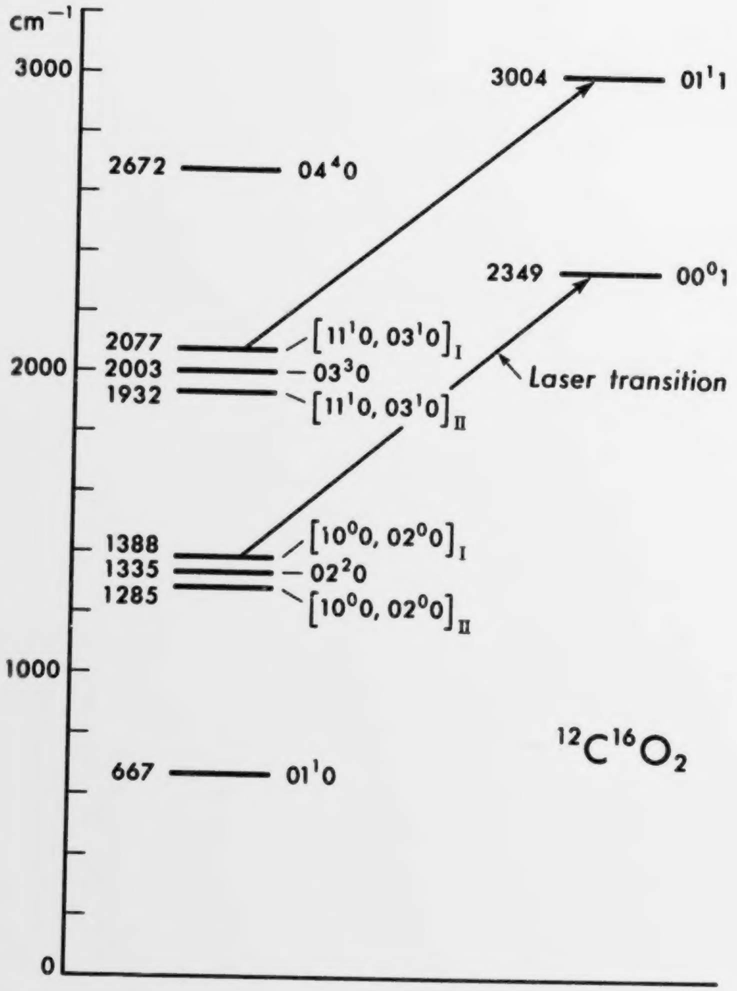
cm⁻¹
3000
2000
1000
0
3004
01^11
2672
04^40
2349
00^01
2077
$[11^10, 03^10]_I$
2003
03^30
1932
$[11^10, 03^10]_{II}$
Laser transition
1388
$[10^00, 02^00]_I$
1335
02^20
1285
$[10^00, 02^00]_{II}$
667
01^10
$^{12}C^{16}O_2$

Figure 3. Energy level diagram for $^{12}C^{16}O_2$, showing laser transitions.

BLANK
PAGE

which produces line emission stronger than these continuum temperatures would help in line observations of the cooler planets at the shorter wavelengths. For example, both ethane and acetylene have been seen with non-heterodyne techniques to be in strong constant emission in Jupiter.

Given that from a sensitivity viewpoint we are confined to Mars and Venus for 10 μm absorption line spectroscopy, it's time to decide on the particular molecular lines to observe. The discrete frequency nature of the CO_2 laser restricts our spectral coverage to $\sim 0.1\ cm^{-1}$ windows centered on the laser frequencies. For these two planets, however, the line choice is trivial, as CO_2 is in both cases the most abundant species. Furthermore, the terrestrial atmosphere is relatively transparent around the 10 μm CO_2 lines; and the frequency calibration necessary for Doppler-velocity measurements is guaranteed, since the planetary CO_2 lines involve exactly the same energy levels as those responsible for the laser emission (Fig. 3). Of course, other more excited bands of CO_2 in the 10 μm region and also transitions of molecules such as NH_3, C_2H_4, and OCS have frequency coincidences with laser lines and may also be of interest for planetary spectroscopy.

Applications

As an example of a well-resolved line profile, Figure 4 shows the P(20) absorption line of $^{13}C^{16}O_2$ in Mars. Each channel is 5 MHz and the effective integration time is 32 minutes. This line is part of data taken to model the vertical pressure-temperature structure of the atmosphere. A simple 4-parameter model was used to fit simultaneously a variety of $^{13}C^{16}O_2$ and $^{12}C^{16}O_2$ absorption line profiles [1]. The wing of the P(16) $^{12}C^{16}O_2$ line in Figure 5 shows the effect of varying the surface pressure parameter in this model. Each of the other three parameters: ground surface temperature, atmospheric surface temperature, and lapse rate, has its own effect on some part of the line profile. The integration time for Figure 5 was 40 minutes. Before attempting pressure estimates from line-shape modeling, it's of course necessary to have good lab data on the CO_2 self-broadening coefficient as a function of temperature. Fortunately the CO_2 laser bands are popular with laboratory spectroscopists, and such data is available. Figure 5 also shows two other interesting features. The absorption dip on the right is the P(23) transition of $^{12}C^{16}O^{18}O$ which occurs 1680 MHz lower than the $^{12}C^{16}O_2$ P(16) line. The P(23) line is in the opposite infrared sideband from the P(16), and shows the overlap blending problem which can sometimes occur with a double sideband heterodyne receiver. At the left of Figure 5, the central core of the P(16) line is seen to be in emission. The width of this Gaussian-shaped re-emission component is only 35 MHz and yet is easily resolved with the heterodyne spectrometer. The line width of the emission component implies a gas kinetic temperature of 170 K at the altitude of formation, and yet the emission intensity is much stronger than even that from a blackbody at this temperature and suggests a

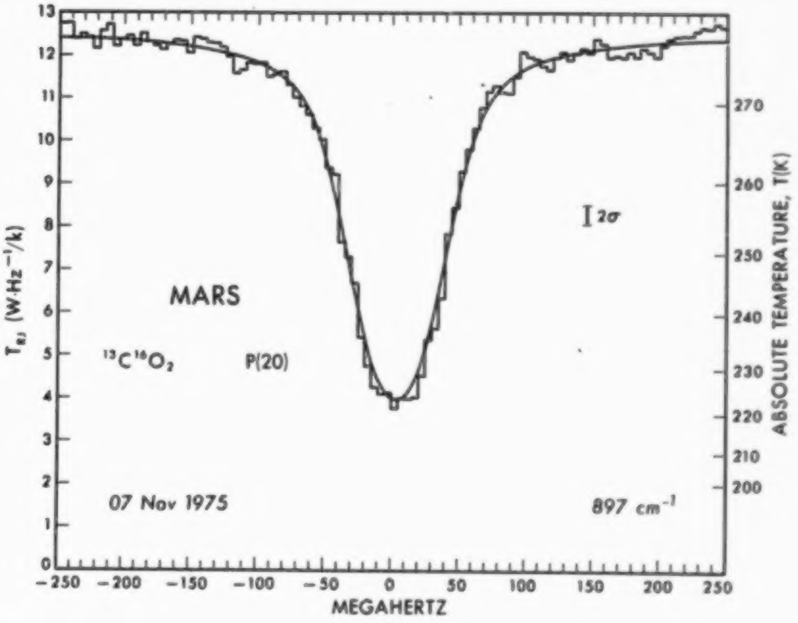

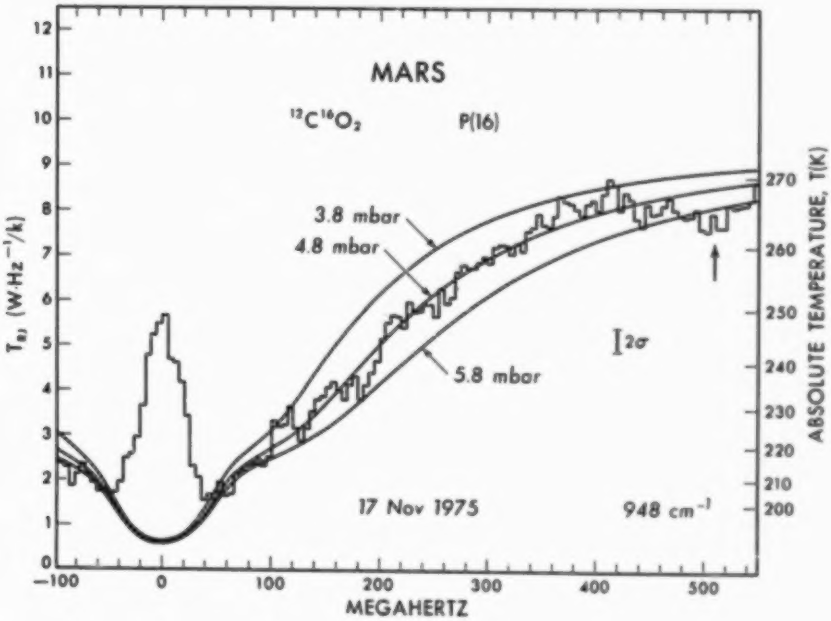

Figure 5. Wing of P(16) absorption line of $^{12}C^{16}O_2$ on Mars; also P(23) of $^{12}C^{16}O_2$ (arrow), and core of P(16) line in emission.

nonthermal excitation mechanism. The detection of similar and stronger re-emission cores in $^{12}C^{16}O_2$ absorption lines on Venus, as shown in Figure 6, strengthens the interpretation that the nonthermal excitation comes from direct solar pumping of the short wavelength CO_2 bands such as 3 ν_3 and 5 ν_3, with subsequent collisional equipartition of the ν_3 quanta [2] [3]. Direct radiative de-excitation via 4.3 μm photons to the ground state is trapped, leading to the observed 10 μm emission from the ν_3 level. The emitting CO_2 lies high in the mesospheres of the planets (75 km on Mars, 120 km on Venus), where CO_2 densities are $\sim 3 \times 10^{13}$ cm^{-3} and collisional effects cannot de-excite the ν_3 level and therefore quench the 10 μm "fluorescence." Figure 6 also shows the appearance of the P(16) re-emission core for three different positions on Venus at elongation. The top two lines required 16 minutes of integration time; the bottom one took 32 minutes. Sunlight illuminates the disc from the left in this diagram and is strongest at position 1, close to the subsolar point on the planet. The strength of emission is clearly seen to be proportional to the incident solar intensity. No emission is seen from the dark half of the planet at the right; only the relatively flat residual continuum level at the center of the very broad $^{12}C^{16}O_2$ absorption line is detected. On Venus, the column density of carbon dioxide is so high that absorption lines of $^{12}C^{16}O_2$ are "saturation broadened" to be much wider than our photomixer bandwidth. The linewidths of the Venus emission lines indicate that the kinetic temperature is close to 200 K at the 120 km altitude of line formation, thus giving us our first thermometer for this previously unsampled altitude. The complete profiles of weaker lines of $^{13}C^{16}O_2$ can readily be seen in absorption, however. For Venus, the Doppler-shifts of both the mesospheric $^{12}C^{16}O_2$ emission components (120 km) and $^{13}C^{16}O_2$ stratospheric

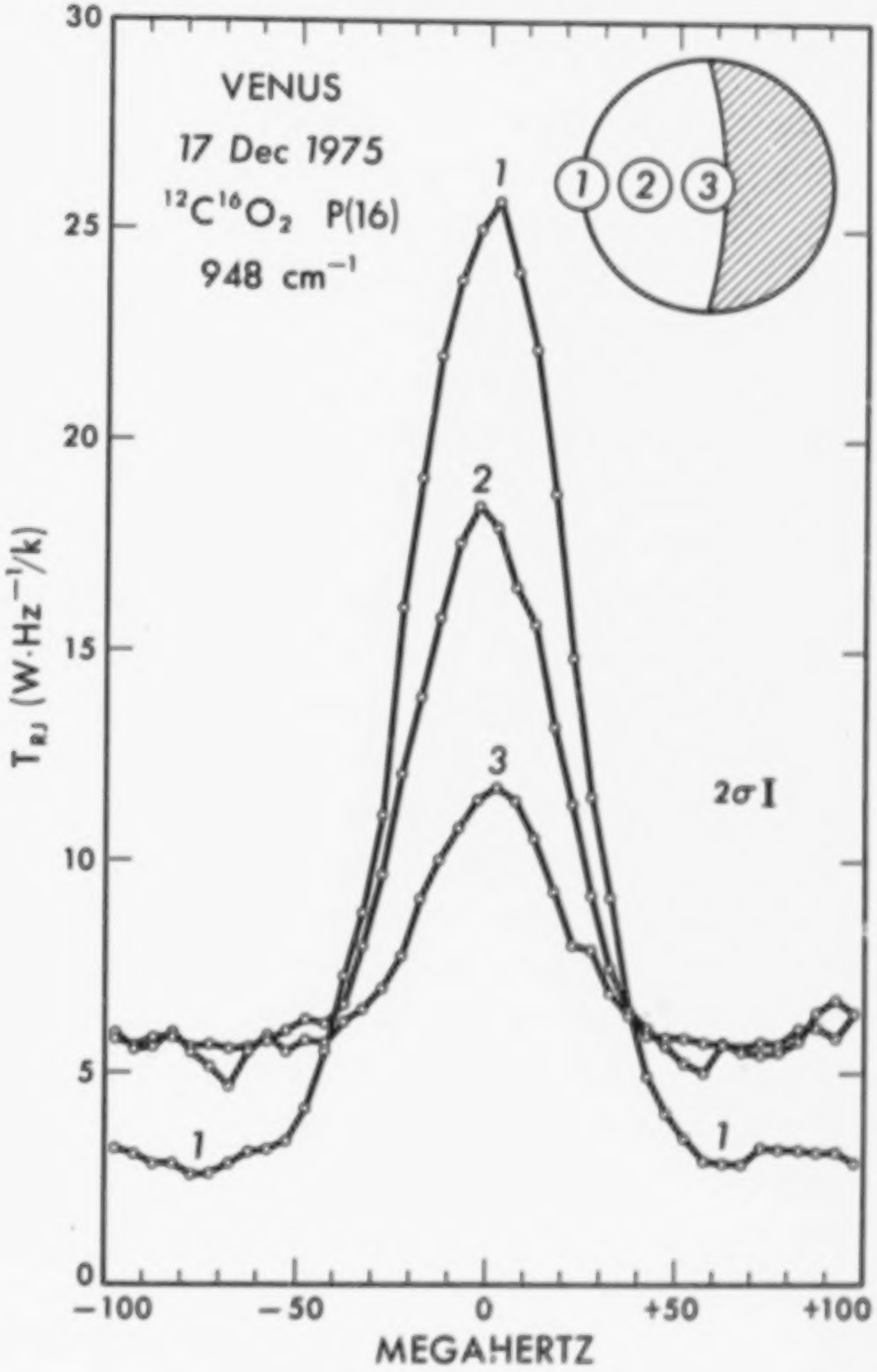

Figure 6. Re-emission cores for P(16) of $^{12}C^{16}O_2$, for three different positions on Venus at elongation.

absorption lines (80 km altitude) have been monitored for several years to get the average wind patterns at these altitudes [4]. The measurement accuracies are primarily limited by the signal-to-noise ratio on line detection; systematic errors associated with the spectrometer calibration are small. Doppler-velocity accuracies of 2 m/sec on $^{12}C^{16}O_2$ emission lines and about 15 m/sec on $^{13}C^{16}O_2$ absorption lines have been achieved. I should stress that the velocities actually measured are absolute line-of-sight wind velocities at specific positions on the planet and are not differential velocities such as from limb-to-limb or center-to-limb. The line-of-sight velocities from different locations on Venus are measured independently.

In the stratosphere the $^{13}C^{16}O_2$ absorption lines show us a retrograde zonal circulation with an average surface velocity of 90 m/sec, but with real variations up to ± 40 m/sec about this average. (The variations do not appear to fit any simple 4 or 5 day periodicity.) The western equatorial limb is seen to be approaching at 90 m/sec,on the average,while the eastern limb is receding at this value.

In the mesosphere $^{12}C^{16}O_2$ emission lines formed at altitudes around 120 km show us that the circulation there is essentially a symmetric subsolar to antisolar flow, with the velocity starting near zero at the subsolar region and accelerating to a velocity near 130 m/sec as the flow crosses the terminator. At times of elongation the subsolar region of Venus is at the limb and line-of-sight velocities near zero are observed, as reported in our initial publication on the emission lines [2]. However, at subsequent superior and inferior conjunctions, high velocities of recession and approach, respectively, are seen at the limbs close to the terminator. Especially in the weeks before and after inferior conjunction, when a small spot exactly on the limb can be monitored, the acceleration of the flow toward the terminator can be seen as the phase angle of the planet varies. Additional observations at latitudes up to ± 50° at the limb show that the flow is reasonably symmetric about the subsolar-antisolar axis. At the poles, however, deviations from a perfect symmetry are noted.

As illustrated in Figure 7, these results indicate that a fast retrograde rotation of the atmosphere extends at least as high as 85 km altitude, but that the circulation breaks down into a reasonably symmetric subsolar to antisolar flow before altitudes of 120 km are reached. In estimating the 85 km altitude of line formation for the $^{13}C^{16}O_2$ absorption lines, it is important that only the central core of 200 MHz be used for velocity measurements. The wings of the entire absorption profile are many times wider, and their inclusion would produce only a velocity average for a broad altitude range below 85 km. In addition it is important to confine the measurement to a narrow altitude range so that the necessary corrections for pressure shifts in line frequencies may be properly applied [4]. The magnitude of these pressure shifts in CO_2 can easily be measured with CO_2 laser techniques in the laboratory.

It would be desirable to probe an intermediate altitude between 85 and 120 km to get a better idea of where the circulation changes. To do this we may need to look at a high-J $^{12}C^{16}O_2$ line which does not have the nonthermal emission core. Because of the 89:1 ratio between ^{12}C and ^{13}C, absorption lines of $^{12}C^{16}O_2$ will become optically thick before those of $^{13}C^{16}O_2$ and thus will probe higher altitudes. Since CO_2 in the mesosphere is at ∿200 K, a high-J line will not show the nonthermal emission that would fill in the absorption at line center from $^{12}C^{16}O_2$ at ∿100 km

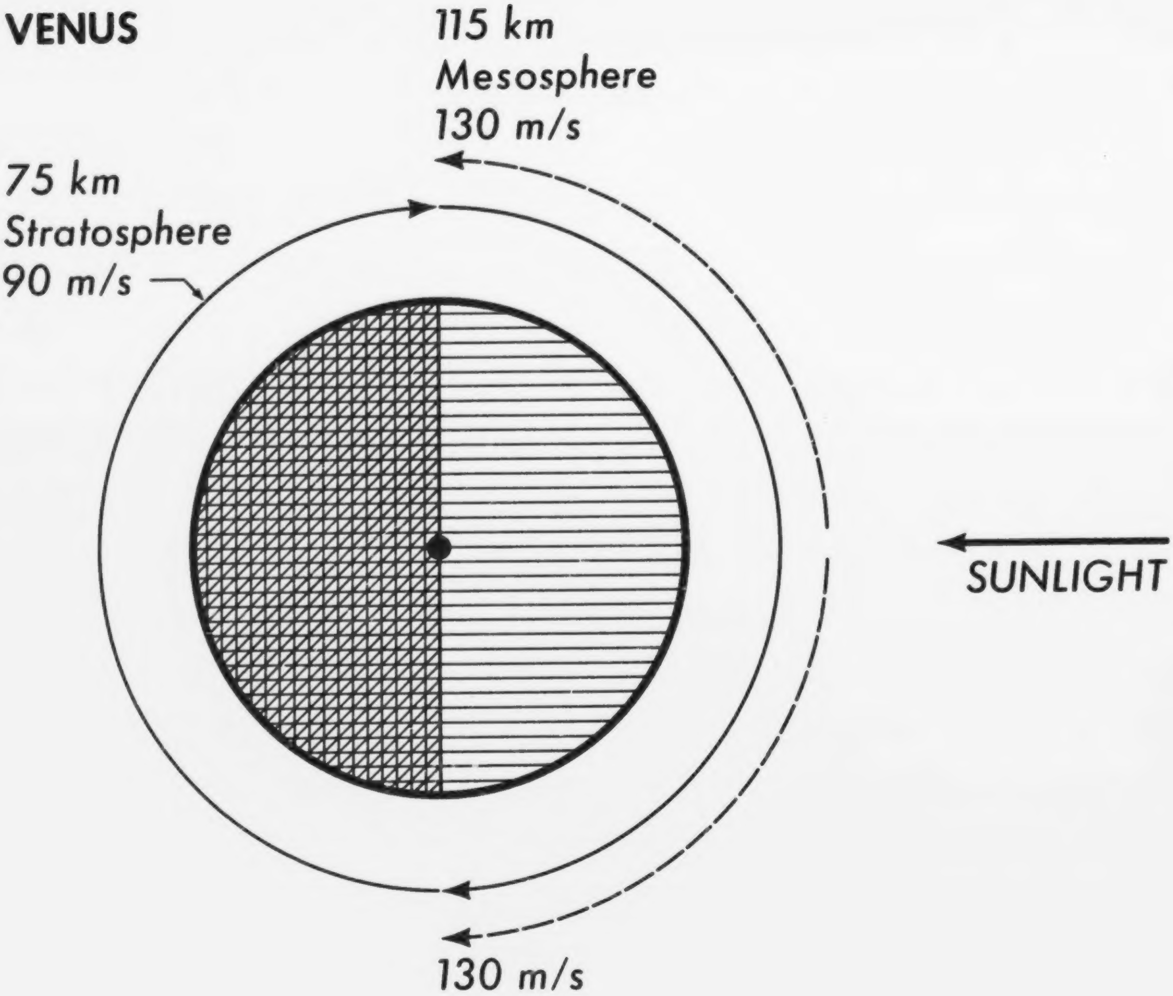
VENUS
115 km
Mesosphere
130 m/s
75 km
Stratosphere
90 m/s
SUNLIGHT
130 m/s

Figure 7. Atmospheric circulation as function of altitude on Venus determined by heterodyne spectroscopy of $^{12}C^{16}O_2$ and $^{13}C^{16}O_2$.

altitude. For wind measurements, it may also be possible to use another molecule such as OCS, which has strong fundamental absorption bands around 9.6 and 11.6 μm. Recent laboratory spectroscopy by an NBS group has determined OCS line frequencies to a few MHz absolute accuracy and indicated a number of frequency coincidences between OCS absorption and CO_2 laser lines. With our own spectrometer we have remeasured a few OCS - CO_2 frequency differences accurate to about 100 kHz, which translates to $\sim$1 m/sec Doppler-velocity uncertainty. There is, of course, no guarantee that OCS lines in Venus will be strong enough for Doppler-velocity measurements or even detectable at all. On the other hand, the observations are not difficult, and certainly an attempt should be made.

References

1. Betz, A.L.; McLaren, R.A.; Sutton, E.C.; and Johnson, M.A.: "Infrared Heterodyne Spectroscopy of CO_2 in the Atmosphere of Mars," Icarus, 30, pp. 650-662, 1977.

2. Betz, A.L.; Johnson, M.A.; McLaren, R.A.; and Sutton, E.C.: "Heterodyne Detection of CO_2 Emission Lines and Wind Velocities in the Atmosphere of Venus," Astrophys. J. Lett., 208, pp. 141-144, Sept. 15, 1976.

3. Johnson, M.A.; Betz, A.L.; McLaren, R.A.; Sutton, E.C.; and Townes, C.H.: "Nonthermal 10 μm CO_2 Emission Lines in the Atmospheres of Mars and Venus," Astrophys. J. Lett., 208, pp. 145-148, Sept. 15, 1976.

4. Betz, A.L.; Sutton, E.C.; McLaren, R.A.; and McAlary, C.W.: "Laser Heterodyne Spectroscopy," in Proc. Symposium on Planetary Atmospheres, pp. 29-33, Royal Society of Canada, Ottawa, Ontario, Aug. 16-19, 1977.

DISCUSSION

Question (A. Young): How large must the OCS mixing ratio be for you to detect it?

Response: The detection limit depends somewhat on where the line is formed relative to the 10 μm continuum. For gas in the stratosphere above 70 km, I would estimate a practical limit of 10^{-7}, if the OCS is uniformly mixed.

Question (A. Young): There is also a problem of the vertical distribution of the OCS, because it's destroyed very rapidly by solar UV light.

Response: Yes. Since we are most sensitive to narrow lines and hence those formed high up, dissociation may prevent the detection of OCS in the stratosphere. In that case we would try a high-J $^{12}C^{16}O_2$ line to probe the upper atmosphere around 100 km.

Blank Page

INFRARED ABSORPTION BY OH-CONTAINING COMPOUNDS

John J. Hillman (NASA/GSFC)

ABSTRACT

A review of the current state of spectroscopy of the relevant OH compounds as it applies to the inner planets is presented. Critical problems will be addressed and a projection of the future spectroscopic needs will be made.

INTRODUCTION

Carbon dioxide accounts for all but a few percent of the Martian and Cytherean atmospheres(1,2). Incident solar flux at wavelengths less than about 210 nm provides for photodissociation of CO_2 into CO + O. In these atmospheres, it is difficult to reconcile the relatively low values observed for the abundances of CO and O_2 (the direct recombination of CO and O into CO_2 is inefficient). This apparent contradiction is relaxed if HO_X catalytic cycles are active(1) in both atmospheres, in which case the resultant atmospheric stability is due to the catalytic effects of very dilute reactive species, in particular, HO_2 and H_2O_2(3). (See Table 1.) At the present time, we have no ground-truth observational data for HO_2 or H_2O predicted by the various photochemical models for the Venus and Mars atmospheres. We do have recent data(4, 5) for both of these species in the Earth's stratosphere.

In this talk I will discuss the current state of spectroscopy of the species H_2O, H_2O_2, and HO_2. The major thrust will be on their vibration-rotation transitions, although I will say a few words about the pure rotational transitions in the vibrational ground state of H_2O, since they contribute to opacity in the middle infrared region. I will address critical problem areas and summarize future directions suggested for experimental and theoretical efforts.

Table I

CO_2 STOICHIOMETRY

- $CO_2 + h\nu \rightarrow CO + O$; $R \equiv {}^{[CO]}/_{[O_2]} = 2$

MARS

- $R \sim 1/2$ — NEED EXTRA SOURCE OF O_2, PERHAPS

$$H_2O + h\nu \rightarrow OH + H$$
$$OH + HO_2 \rightarrow H_2O + O_2$$

VENUS

- $\gtrsim 50$ — WHERE IS O_2 ? TIED UP IN H_2O ?

VENUS AND MARS -- HO_x CHEMISTRY

- $CO_2 + h\nu \rightarrow CO + O$

- REFORM CO_2 FROM CO & O

  $CO + OH \rightarrow CO_2 + H$

  ($CO + O \rightarrow CO_2$, TOO SLOW)

- CATALYSIS COMPLETED (i.e., OH REFORMED)

  i) $H + O_2 + M \rightarrow HO_2 + M$

  $HO_2 + O \rightarrow \underline{OH} + O_2$

  ii) $H + O_2 + M \rightarrow HO_2 + M$

  $2HO_2 + O \rightarrow H_2O_2 + O_2$

  $H_2O_2 + h\nu \rightarrow \underline{2OH}$

- MARS MAIN SOURCE OF ODD HYDROGEN

  - PHOTOLYSIS OF $H_2O \rightarrow$
  - H_2, $H_2O + O(^1D) \rightarrow$

Table I (Continued)

VENUS MAIN SOURCE OF ODD HYDROGEN

- $HCl + h\nu \rightarrow H + Cl$

  net 2H

  $Cl + H_2 \rightarrow HCl + H$

BOTH SCHEMES REQUIRE LARGE SOURCES OF H_2

- $H + HO_2 \rightarrow H_2 + O_2$ (MAJOR H_2 SOURCE)
- VENUS - ADDITIONAL SOURCE MAY BE

  $CO + H_2O \rightarrow CO_2 + H_2$ (DEEP ATMOSPHERE)

- EFFICIENCY OF CATALYTIC SCHEMES DEPENDS ON ABUNDANCE OF RADICALS WHICH IN TURN DEPEND ON SOURCES AND ON RADICAL REMOVAL PROCESSES

- MAIN HO_x SCAVENGING REACTIONS
  - $OH + HO_2 \rightarrow H_2O + O_2$
  - $H + HO_2 \rightarrow H_2 + O_2$

    $\rightarrow H_2O + O$
  - $OH + H_2O_2 \rightarrow H_2O + HO_2$ (LESSER EXTENT)
  - ADDITIONALLY, FOR VENUS

    $OH + HCl \rightarrow H_2O + Cl$

    $Cl + HO_2 \rightarrow HCl + O_2$

SPECIES-SPECIFIC CONSIDERATIONS

Water is the most studied molecule in the HO_X family, and has three infrared-active fundamentals. Dr. Chackerian discussed the role of the ν_2 band (1595 cm^{-1}) as a potential major contributor to opacity in this spectral region and considered its efficiency as a thermal trap (Venusian Greenhouse effect). A summary of the state of spectral knowledge is given in Table II. Although line positions and absolute line strengths are in relatively good shape, our understanding of the line broadening process is weak.

Historically, the calculation of line widths of H_2O broadened by N_2 was carried out within the framework of a modified Anderson theory (6) in 1959. Subsequent to that work, a discrepancy was observed in 1972 revealing that the measured widths were much less than calculated (7). This discrepancy increased with the angular momentum quantum number, varying from 40 percent narrower to a factor of 4 narrower than predicated. In 1978, a quantum many-body theory (8) was applied to this problem. (This work will be included on the Rothman, AFGL tape(9).) In the low J region up to about J=7, both the Anderson(10)(ATC) model and the quantum Fourier transform(8) (QFT) model are in generally good agreement with experiment (where experiments exist). The ATC model is still able to use a minimum impact parameter of 3.22Å; the kinetic theory result(6). (This result is weighted to low J -- occupied states -- and therefore, provides little information on the appropriate impact parameter for high J transitions.) In the intermediate J region, $8 \leq J \leq 13$, both the ATC and QFT theories provide reasonable agreement with experiment, if the minimum impact parameter is reduced to ~ 1.5Å in the ATC theory. Above J=13 the ATC half-width saturates at about 0.01 cm^{-1} atm^{-1} independent of J, and the QFT results are also somewhat less than acceptable. It is now generally agreed that any calculation which treats the interaction as a sum of a short- (classical hard sphere) and a long-range potential will not provide an explanation of the narrow lines at high J for the $H_2O:N_2$ system. Table III summarizes our current understanding of this line broadening problem.

Often postulated but seldom observed, the hydroperoxyl radical, HO_2, is a molecule that has not been studied extensively by spectroscopists. Table IV summarizes the state of spectral knowledge. Of the three infrared-active

Table II

SPECIFIC SPECIES -- H_2O

- MOST STUDIED MOLECULE IN THE HO_x FAMILY

- ACTIVE IR FUNDAMENTALS (THREE)

BAND	POS (cm^{-1})	RES (10^{-3} cm^{-1})	BAND (cm^{-2} atm^{-1} @ 296K)
ν_1	3652	5	10.2
ν_2	1595	5	308.
ν_3	3756	5	172.

- ALL OF THE FUNDAMENTALS AND MANY OVERTONES AND COMBINATION BANDS HAVE BEEN STUDIED IN TERMS OF LINE POSITION, STRENGTHS, AND ASSIGNMENTS

- INDIVIDUAL LINE STRENGTHS HAVE BEEN MEASURED AND CALCULATED -- GENERALLY IN GOOD SHAPE ∽ 10% to 15% ABSOLUTE

- PURE ROTATIONAL SPECTRUM EXTENDS FROM MICROWAVE TO ABOVE 1000 cm^{-1} -- EXTENSIVELY STUDIED IN TERMS OF LINE POSITIONS, STRENGTHS, AND ASSIGNMENTS

- BROADENING -- GENERALLY IN POOR SHAPE BOTH EXPERIMENTALLY AND THEORETICALLY

Table III

LINE BROADENING IN H_2O -- STATUS

- H_2O-N_2 LINE WIDTHS CALCULATED WITHIN FRAMEWORK OF ATC THEORY -(1959)

- TDL SPECTROSCOPY REVEALS WIDTHS 2X TO 4X NARROWER THAN CALCULATED - (1972)

- QUANTUM MANY-BODY THEORY APPLIED - (1978)

- CURRENT STATUS:

  LOW J ($J + 7$) - ATC/QFT GENERALLY GOOD - QFT $\sim$ 5% SMALLER THAN ATC ($b_{min} = 3.2$A)

  INTERMEDIATE J ($8 \sim J \sim 13$) - GENERALLY GOOD IF $b_{min} = 1.5$A IN ATC

  HIGH J - ATC SATURATES AT ABOUT 0.010 cm^{-1}/atm ($b_{min} \sim 0$)

- CONSENSUS -- NO THEORY WHICH TREATS THE INTERACTION AS THE SUM OF A SHORT- AND LONG-RANGE PART CAN PROVIDE AN UNDERSTANDING FOR THE NARROW LINES AT HIGH J

- HIGH J LINES STILL IN NEED OF THEORETICAL UNDERSTANDING

Table IV

SPECIFIC SPECIES -- HO_2

- ACTIVE IR FUNDAMENTALS (THREE)

BAND	POS (cm^{-1})	RES (cm^{-1})	BAND STR (cm^{-2} atm^{-1} @ 296K)
ν_1	3410	8	274.
ν_2	1350	8	216.
ν_3	1097	LMR - DOPPLER LIMITED	188.

- BAND STRENGTHS ARE THEORETICAL - NO EXPERIMENTAL DETERMINATION HAS BEEN MADE
- ν_3 POSITIONS AND QUANTUM NUMBER ASSIGNMENTS IN GOOD SHAPE
- NO LINE STRENGTH DATA
- NO BROADENING DATA

fundamentals, only ν_3 (0-0 stretch) has been studied with Doppler-limited resolution(11). The other fundamentals have been observed either in matrix isolation(12) or by gas-phase molecular modulation(13) at relatively low resolution. The band strengths reported in Table IV were taken from the most recent calculations(14). These calculations were based on an assumed total dipole moment of 1.9 ± 0.1 Debye and with a specific orientation of the dipole moment relative to the O-H bond angle which has subsequently been experimentally determined to be in error by about a factor of 2(15). In general, the ν_3 line positions and quantum level assignments are held in high confidence. Since these lines were determined by laser magnetic resonance, it would be useful to make a zero-field confirmation of these absolute line positions. I am aware of no line strength nor broadening data.

Since hydrogen peroxide is the sink molecule for the HO_x family it is expected to be in relatively high concentration in the atmospheres of Venus and Mars. Theoretically, it is a very interesting species since it is the simplest molecule in which there is an active hindered internal rotation(16). A summary of our current spectroscopic knowledge is presented in Table V. There are six fundamentals; five vibrational and ν_4, the internal rotation. The band strength estimates (guesses) were obtained from band-contour integration of literature spectra. This technique, although not very accurate, leads to the conclusion that ν_6 is the strongest fundamental in the infrared. To my knowledge, there are no line strength or pressure broadening data available.

Table VI is a summary of species-specific recommendations based upon present data needs. It is by no means meant to be all-inclusive, and it is not the first time that you have seen these requests today. Specifically, for H_2O, measurements of intensities of high J transitions within ν_2 are needed. The line broadening in CO_2 and N_2, and temperature dependences must be determined. Pressure shift data are required, even at low J. There is a dramatic difference between the ATC and QFT predictions. Even the sign of the shift tends to differ, so these data are urgently needed. High J, N_2-broadening data will be used to check the range of validity of the models. Specific recommendations for H_2O_2 include an accurate quantum mechanical treatment of ν_6. We also need experimental data on line strengths. Band

Table V

SPECIFIC SPECIES -- H_2O_2

- o SIMPLEST MOLECULE WITH HINDERED INTERNAL ROTATION
- o ACTIVE IR FUNDAMENTALS (SIX)

BAND	POS (cm^{-1})	RES (cm^{-1})	BAND STR (cm^{-2} atm^{-1} @ 300K
ν_1	3607.8 3587.3	0.2	---
ν_2	1388	---	(Not observed experimentally)
ν_3	875	4	0.17 BCI
ν_4	317	0.3	---
ν_5	3610.7	0.2	20.8 BCI (ν_5 and ν_1)
ν_6	1266	0.02, TDL	37.7 BCI

- o ONLY THE FUNDAMENTALS ν_1, ν_4, ν_5, and ν_6 HAVE BEEN STUDIED IN ANY DETAIL. SOME COMBINATIONS HAVE BEEN STUDIED UNDER HIGH RESOLUTION.
- o NO LINE STRENGTH DATA
- o NO BROADENING DATA

Table VI

SPECIFIC RECOMMENDATIONS

H_2O

- MEASUREMENT OF INTENSITIES OF HIGH-J TRANSITIONS WITHIN ν_2 ARE NEEDED (LONG PATH LENGTHS)
- CO_2 - BROADENING AND TEMPERATURE DEPENDENCE MUST BE DETERMINED (H_2 AND He - JUPITER)
- PRESSURE-SHIFT DATA (EVEN AT LOW J)
- N_2 - BROADENING AT HIGH J

H_2O_2

- QUANTUM NUMBER ASSIGNMENT IN ν_6
- EXPERIMENTAL LINE STRENGTHS
- BAND STRENGTH DATA FROM EXPERIMENT AND AB-INITIO DIPOLE MOMENT
- CO_2 - BROADENING AND TEMPERATURE DEPENDENCE

HO_2

- BAND STRENGTHS EXPERIMENTALLY
- LINE STRENGTHS IN ν_2 -- FIRST STEP SHOULD BE RIGID ROTOR
- CO_2 - BROADENING AND TEMPERATURE DEPENDENCE

strength determinations from experiments and from ab initio dipole moment derivatives are required. Finally under H_2O_2, CO_2-pressure-broadening data and temperature dependence are needed. For HO_2, my list is not quite so large, but in light of the high reactivity of the species, it is a very ambitious undertaking. We need experimental band strength determinations, to check the most recent calculations in the literature$^{(14)}$. An attempt should be made to calculate line strengths in ν_2 using the available ab initio band strength. Perhaps, a rigid-rotor, simple harmonic oscillator calculation (F-factor set equal to one). The effects of spin-rotation must be taken into account in this calculation. Also, and finally, we need CO_2-broadening and temperature dependence data.

In conclusion, in this paper I have tried to review the current state of our spectroscopic knowledge of the relevant OH_x compounds (H_2O, HO_2, H_2O_2) with emphasis on the available high resolution data. In any review of the current literature, one is confronted with the reality that, at best, you are a year behind present day research. When possible, I have included tentative results based on unpublished, submitted, or work in progress. I have addressed some of the critical problem areas and summarized the future directions for experimental and theoretical efforts.

Acknowledgements

Much of the work reported here was supported by the NASA Planetary Atmospheres Program. The author expresses appreciation to M. J. Mumma for valuable suggestions and encouragement during this work.

Reference

1. T. Y. Kong and M.B. McElroy, "Photochemistry of the Martian Atmosphere," Icarus 3, 168 (1977).

2. N. D. Sze and M. B. McElroy, "Some Problems in Venus' Aeronomy," Planet. Space Sci. 23, 763 (1975).

3. See, for example, J. W. Chamberlain, Theory of Planetary Atmospheres: An Introduction to their Physics and Chemistry, (Academic Press, New York; 1978).

4. J. G. Anderson, H. J. Grassl, R. E. Shetter and J. J. Margitan, "In Situ Measurements of HO_2 in the Earth's Stratosphere", submitted to Geophy. Res. Lett.; Abstract and figures reproduced in Bull. Upper Atmos. Prog's. #79-5, Oct. 1979.

5. K. Chance, "Atmospheric Studies with a Fourier Transform Far Infrared Spectrometer", Poster paper at High Resolution Infrared Appl. & Develop., N.B.S. Gaithersburg, MD; June, 1980.

6. W. S. Benedict and L. D. Kaplan, "Calculation of Line Widths in H_2O-N_2 Collisions", Jour. Chem. Phys., 30, 388 (1959).

7. R. S. Eng, A. R. Calawa, T. C. Harman, P. L. Kelley and A. Javan, "Collisional Narrowing of Infrared Water-Vapor Transitions", Appl. Phys. Lett., 21, 303 (1972).

8. R. W. Davies and B. A. Oli, "Theoretical Calculations of H_2O Linewidths and Pressure Shifts: Comparison of the Anderson Theory with Quantum Many-Body Theory for N_2 and Air-Broadened Lines", J. Quant. Spectrosc. Radiat. Transfer, 20, 95 (1978).

9. L. S. Rothman, "Atmospheric Absorption Line Parameters Compilation", available in magnetic tape form from Natal Climatic Ctr. of NOAA; Asheville, NC.

10. C. I. Tsao and B. Curnutte, "Line-widths of Pressure-Broadened Spectral Lines", J. Quant. Spectrosc. Radiat. Transfer, 2, 41 (1962).

11. J. W. C. Johns, A. R. W. McKellar and M. Riggin, "Laser Magnetic Resonance Spectroscopy of the ν_3 Fundamental Band of HO_2 at 9.1μm, Jour. Chem. Phys., 668, 3957 (1978).

12. D. W. Smith and L. Andrews, "Argon Matrix Infrared Spectra and Vibrational Analysis of the Hydroperoxyl and Deuteroperoxyl Free Radicals", Jour. Chem. Phys., 60, 81 (1974).

13. T. T. Paukert and H. S. Johnston, "Spectra and Kinetics of the Hydroperoxyl Free Radical in the Gas Phase", Jour. Chem. Phys., 56, 2824 (1972).

14. A. Komornicki and R. L. Jaffe, "An ab-initio Investigation of the Structure, Vibrational Frequencies, and Intensities of HO_2 and HOCl", Jour. Chem. Phys., 71, 2150 (1979).

15. S. Saito and C. Matsumura, "Dipole Moment of the HO_2 Radical from its Microwave Spectrum", Jour. Mol. Spectrosc., 80, 34 (1980).

16. R. H. Hunt, R. A. Leacock, C. W. Peters and K. T. Hecht, "Internal-Rotation in Hydrogen Peroxide: The Far-Infrared Spectrum and the Determination of the Hindering Potential", Jour. Chem. Phys., 42, 1931 (1965).

Discussion

Comment (C. Chakerian): I would like to grant one of your wishes. the intensities of the ν_6 band of H_2O_2 at temperatures ranging from ambient down to 190K have been measured at NASA, Ames.

Response (J. Hillman): Have these data been published?

Comment (C. Chakerian): No, the data were obtained about one month ago.

Response (J. Hillman): I talked with Dr. Bonomo about 3 months ago and he told me of these plans, but they were having some equipment problems at the time.

Comment (M. Mumma): I'd like to make a comment directed to Prof. W. Person and any other band intensity theorists. The experimental groups have a very hard time measuring densities for radicals like HO_2, and so even a factor of 2 accuracy in an ab initio integrated band strength is extremely useful, because it's often better than the accuracy with which you can determine the radical density.

Response (W. Person): This is exactly our approach. We have to use ab initio HO_2 dipole moment derivatives right now. But that's a step in the right direction. It's absolutely necessary.

Question (W. B. Olson): In hydrogen peroxide, you showed numbers for the band centers of ν_1 through ν_6. What is your definition of those centers?

Answer (J. Hillman): These numbers were simply ball-park figures, telling one approximately where this species absorbs when activated in that particular fundamental mode. These numbers are only approximate. For example, for ν_6, one of the most studied bands, I listed 1266 cm^{-1} for that band, value dated from circa 1948.

Comment (J. Gelfand): The discussion about the comparison of the two theoretical approaches to the pressure broadening brings out something I said in my talk. I find in talking to people that they tend to discuss these things in terms of which theory is right, when in reality, in a particular case, they may just have a lousy potential. They piece together the potential functions from different measurements; the repulsive part of the potential is obtained from one measurement, the attractive part of the potential from another, and similarly for the intermediate region. It may well be that this is as important a contributor to the errors that you discussed as the theory itself.

Response (J. Hillman): Yes, this is exactly what I meant by one statement I made earlier. "No theory which treats the interaction potential as a sum of a short-range and long-range term (or any kind of potential characterization you want to make) will provide a basic theoretical understanding of the narrow lines at high-J." The characterization of the potential, not the collision model, may indeed be a major source of error.

Blank Page

Infrared Absorption of Sulfur-Bearing Compounds

Arthur Maki (NBS)

INTRODUCTION

The sulfur-bearing molecules of most interest in studies of planetary atmospheres are the simple, stable hydrides and oxides, H_2S, H_2SO_4, SO_2, and SO_3, and the carbon-containing species OCS and CS_2. This paper will deal primarily with those molecules.

A number of less stable molecules, such as CS, SO, HSO, H_2SO, etc., may well participate in the chemistry of planetary atmospheres, but their abundance is probably too low to be observed in the near future.

For interpreting spectroscopic observations, the properties that must be known are:

i) transition frequencies

ii) transition intensities

iii) transition assignments in terms of quantum number assignments and lower-state energy levels

iv) pressure broadening constants (including their temperature dependence)

These are rather general spectroscopic requirements which (if completely known for all molecules) would suffice for the interpretation of any spectroscopic observations, although specific observational data may require specific ensembles of these properties. For example, a heterodyne laser radiometer may require a single specific transition frequency, intensity, and lower-state energy (to calculate the intensity over a range of temperatures). It may also require the pressure broadening parameters for the specific transition over a broad range of temperature and broadening pressures for a specific mixture of broadening gases. On the other hand, a low-resolution Fourier Transform Spectrometer may require band shape and band intensity data for a specific temperature or range of temperatures. Such data can be calculated as a sum of transitions whose properties are known.

Of the four properties listed above, pressure broadening constants are the least understood and least well measured. The few molecules that do have pressure broadening data usually have data only for self-broadening and nitrogen broadening, and the data are usually taken only at room temperature.

For the remainder of this paper I shall consider each of the important molecules listed above and discuss briefly what spectroscopic data are available. Then I will summarize what I believe to be the most urgent future measurement needs for each molecular species. The end of the paper contains a bibliography of papers describing spectroscopic measurements on some sulfur-containing molecules. This bibliography is not complete, but may be a helpful starting place for anyone interested in the spectroscopy of these molecules.

PRESENT STATUS OF SPECTROSCOPIC DATA

OCS

Carbonyl Sulfide (OCS) is the spectroscopist's favorite molecule. I believe that more data are available on OCS than on any other sulfur containing molecule.

The frequencies of the strongest OCS lines are very well known. We have recently measured the ν, and $2\nu_2$ bands by laser heterodyne techniques[1] and Joe Sattler (Harry Diamond Laboratories, Washington, DC) has verified and extended the $2\nu_2$ measurements. Guelaschvili[2] has measured the ν_3 fundamental bands very precisely. In addition, Dr. Andre Fayt (University of Louvaen, Belgium) has calculated a great many OCS absorption lines from data in the literature, and we have our own compilation of over 3000 OCS absorption lines for the bands ν_1, $2\nu_2$, $\nu_1 + 2\nu_2$, $2\nu_1$, $4\nu_2$, and ν_3.

Our knowledge of the intensities for OCS is less satisfactory. Quite a bit of intensity information is available, but the data are probably not accurate to better than ± 20%, so there is room for improvement. Most of the intensity information is in the form of integrated band intensities, but OCS is well-behaved and line intensities can be calculated from band intensities without great errors, if high rotational quantum numbers are avoided.

A number of papers have reported pressure broadening measurements on OCS, mostly in the microwave region. Some are accurate to ±1%. Some data are available on the temperature dependence of pressure broadening. But there are very few really accurate data on infrared transitions over a range of rotational transitions and temperatures. There is also very little information on the pressure broadening of OCS by CO_2 or other broadening agents that are mainly of interest for applications involving planetary atmospheres.

SO_2

For both OCS and SO_2 many data are available from microwave measurements. This means that the pure rotational spectrum (far-infrared and microwave spectrum) is well characterized. All but the most recent microwave data are given in a monograph on microwave spectral tables compiled by Frank Lovas[3].

Although many infrared data on SO_2 are available, very few high resolution (i.e. Doppler-limited) measurements have been made on SO_2. Thus, there is a need for new measurements, particularly for Doppler-limited measurements of frequencies and intensities. Measured line intensities would be valuable for comparison with line intensities derived (with the help of theoretical models) from band intensities.

H_2S

Surprisingly few data are available on H_2S. The quite extensive work done many years ago has not been followed up by modern measurements taking advantage of newer, more powerful spectroscopic technologies. This is a serious deficiency since H_2S is one of the molecules for which line intensities cannot be readily deduced from band intensities.

As is well known, in H_2S there is a great disparity between the R-branch intensities and the P-branch intensities. H_2S is also notorious for the weakness of the infrared absorption in all its bands, which makes it difficult to observe in the infrared unless high concentrations are present. There are very few intensity measurements and I could not find any pressure broadening measurements in the literature. Much work needs to be done on this molecule.

H_2SO_4

So far, no one has been able to obtain a resolved infrared spectrum of sulfuric acid (H_2SO_4), even with the use of tunable diode lasers. This difficulty is not surprising. In order to get enough vapor pressure to observe H_2SO_4, it is necessary to heat it to about 200°C. At such high temperatures such a heavy molecule will have a very high density of absorption lines. Apparently the high density of overlapping lines has prevented resolving the individual transitions for H_2SO_4 even though Doppler-limited-resolution measurements have been made. For application to planetary atmospheres it may be necessary to simply measure the unresolved band shapes and intensities over the range of temperatures and pressures that are of interest.

Microwave and far-infrared measurements are in much better shape for H_2SO_4 since the Doppler widths are much smaller at lower frequencies. The microwave spectrum of H_2SO_4 has recently been measured by Kuczkowski *et al.*[4]

SO_3

Sulfur trioxide (SO_3) is a planar symmetric top molecule which has no intrinsic dipole moment. It has no microwave or far-infrared spectrum, apart from possible pressure-induced transitions. Very little high-resolution spectroscopy has been done on it. The only spectrum measured with sufficient resolution to allow a detailed analysis of the line structure was that made by Kaldor and Maki.[5] That work was done using a high resolution grating instrument. Considerable improvement could be obtained by taking advantage of the Doppler-limited resolution now available.

The intensity of the strongest band of SO_3 (at 1395 cm^{-1}) has been measured by Majkowski et al.[6], but no other intensity measurements seem to have been published.

No pressure broadening data are available for SO_3.

CS_2

Like SO_3, CS_2 has no dipole moment and consequently it has no microwave or far-infrared spectrum. In the infrared, the CS_2 spectrum has been extensively studied with the aim of understanding the energy levels and the frequencies of the infrared spectrum. The band intensities of the two infrared fundamentals have been measured, but very little else. No pressure broadening measurements have been made on CS_2.

Other Molecules

Of the other, less stable, molecules that might be of interest for planetary atmospheric studies, the most information is available for CS and SO. However, only absorption frequency and energy level information is available for these molecules. Microwave and far-infrared frequency and intensity data are available for CS, SO, and HSO, but no other intensity data are available. No pressure broadening measurements have been made.

Future Needs

OCS - The frequencies of the strongest and most important bands are adequately known, but more intensity measurements should be made, especially in the 2100 cm^{-1} region. Pressure-broadening measurements should also be made with O_2, N_2, and other atmospheric gases as the broadening agents.

SO_2 - The frequencies of the fundamental bands of SO_2 are fairly well known, so not much is needed in the way of new frequency measurements. More intensities are needed especially line intensities. A few more pressure broadening measurements would be desirable, particularly pressure broadening versus temperature. The weaker bands have not been very thoroughly studied, except $\nu_1+\nu_3$, so a lot more work is needed if the weaker bands are of interest.

H_2S - Much more needs to be done on H_2S. All the bands should be measured. For the fundamental bands, these re-measurements should be at Doppler-limited resolution. Since line intensities can't be deduced from band intensities for H_2S, individual line intensities should be measured. Pressure broadening measurements are also needed and the effects of collisional narrowing need to be taken into account, since such narrowing will be important for H_2S.

H_2SO_4 - Present indications are that resolved spectra are unattainable, although perhaps another attempt should be made. For applications to planetary atmospheric studies, it may be necessary to measure unresolved band profiles in the range of temperatures and pressure of interest.

$\underline{SO}_3$ - More band analyses are needed, including intensities and pressure broadening.

$\underline{CS}_2$ - The frequencies are well known, but intensities should be updated and improved, and pressure broadening should be measured.

REFERENCES

1. J. S. Wells, F. R. Petersen and A. G. Maki, Appl. Opt. 18, 3567-3573 (1979); J. S. Wells, F. R. Petersen, A. G. Maki and D. J. Sakle, Appl. Opt. 20, 1676-1684 (1981).

2. G. Guelaschvili, Opt. Comm. 30, 361-363 (1979).

3. F. J. Lovas, J. Phys. Chem. Ref. Data 7, 1445-1750 (1978).

4. R. L. Kuczkowski, R. D. Suenram and F. J. Lovas, J. Am. Chem. Soc. 103, 2561-2566 (1981).

5. A. Kaldor and A. G. Maki, J. Mol. Struct. 15, 123-130 (1973).

6. R. F. Majkowski, R. J. Blint and J. C. Hill, Appl. Opt. 17, 975-977 (1978).

SO_3 Bibliography

1. R. W. Lovejoy, J. H. Colwell, D. F. Eggers, Jr., and G. D. Halsey, Jr., J. Chem. Phys. 36, 612-617 (1962). Both gas phase and matrix isolated spectra of SO_3 and thermodynamic properties.

2. R. Bent and W. R. Ladner, Spectrochim. Acta 19, 931-935 (1963). Infrared spectrum of gaseous SO_3 and S_3O_9 (trimer).

3. B. Krakow and R. C. Lord, J. Chem. Phys. 44, 3640 (1966). Gas phase infrared spectrum of 1390 cm^{-1} fundamental for SO_3.

4. K. Stopperka, Z. Anorg. Allgem. Chem. 345, 277 (1966). Raman spectrum of SO_3.

5. J. B. Milne and A. Ruoff, J. Mol. Spectrosc 23, 408-415 (1967). Infrared spectrum of gaseous SO_3 - 1390 cm^{-1} and 529 cm^{-1} bands.

6. K. Stopperka and F. Kilz, Z. Anorg. Allg. Chemie 370, 49-58 (1969). Temperature dependence of H_2SO_4 system - infrared spectrum of H_2SO_4.

7. K. Stopperka and F. Kilz, A. Anorg. Allg. Chemie 370, 59-66 (1969). Gas-phase spectra of SO_3 and $(SO_3)_3$ above H_2SO_4.

8. R. K. Thomas and H. Thompson, Proc. Roy. Soc. A314, 329-339 (1970). Infrared gas phase spectrum of SO_3.

9. A. Kaldor and A. Maki, J. Mol. Struct. 15, 123-130 (1973). Infrared gas phase spectrum of band from 2740-2810 cm^{-1} - high resolution.

10. A. Kaldor, A. G. Maki, A. J. Dorney, and I. M. Mills, J. Mol. Spectrosc. 45, 249-252 (1973). Infrared and Raman spectrum of gas phase SO_3.

11. S.-Y. Tang and C. W. Brown, J. Raman Spect. 3, 337-390 (1975). Raman spectrum of gaseous and matrix-isolated SO_3.

12. N. J. Brassington, H. G. M. Edwards, D. W. Farwell, D. A. Long, and H. R. Mansour, J. Raman Spect. 7, 154-157 (1973). Pure rotational Raman spectrum of gas phase SO_3.

13. R. F. Majkowski, R. J. Blint, and J. C. Hill, Applied Optics 17, 975-977 (1978). Intensity measurements of 1390 cm^{-1} band of SO_3 and 1220 cm^{-1} band of H_2SO_4 - gas phase i.r. measurements.

14. A. J. Dorney, A. R. Hoy, and I. M. Mills, J. Mol. Spectrosc. 45, 253-260 (1981). An anharmonic force field calculation for SO_3.

H_2SO_4 Bibliography

1. P. A. Giguere and R. Savoie, Can. J. Chem. 38, 2467 (1960). Infrared spectrum of condensed H_2SO_4.
2. G. E. Walrafen and D. M. Dodd, Trans. Faraday Soc., 57, 1286 (1961).
3. P. A. Giguere and R. Savoie, J. Am. Chem. Soc. 85, 287-289 (1963). Gas and condensed phase infrared spectrum of H_2SO_4 and thermodynamic properties.
4. S. M. Chackalackal and F. E. Stafford, J. Am. Chem. Soc. 88, 723 (1966). Infrared spectrum of H_2SO_4 in gas phase.
5. K. Stopperka, Z. Anorg. Allg. Chem. 344, 263 (1966).
6. K. Stopperka and F. Kilz, Z. Anorg. Allg. Chem. 370, 49-58 (1969). Gas phase infrared spectrum in equilibrium with H_2O-H_2SO_4 liquid mixture.
7. K. Stopperka and F. Kilz, Z. Anorg. Allg. Chem. 370, 59-66 (1969). Gas phase infrared spectrum in equilibrium with SO_3 - H_2SO_4 liquid mixture.
8. R. S. Eng, G. Petagna and K. W. Nill, Appl. Opt. 17, 1723-1726 (1978). Diode laser spectrum of H_2SO_4.
9. R. Kuczkowski, R. D. Suenram, and F. J. Lovas, J. Am. Chem. Soc. 103, 2561 (1981). Present microwave spectrum and analysis - rotational constants and structure for H_2SO_4.

H_2S Bibliography

1. T. King McCubbin, Jr., J. Chem. Phys. 20, 668-671 (1952). Far infrared spectrum-comparison of calc. and observed intensities - 100 to 700 μm.
2. H. C. Allen, Jr. and E. K. Plyler, J. Res. NBS, 52 205-210 (1954). H_2S spectrum near 6300 cm^{-1}.
3. H. C. Allen, Jr. and E. K. Plyler, J. Chem. Phys. 22, 1104-1107 (1954). H_2S spectrum near 5100 cm^{-1}.
4. H. C. Allen, Jr. R. E. Naylor, and E. K. Plyler, J. Res. NBS, 53, 321-323 (1954). D_2S spectrum near 4600 cm^{-1}.
5. H. C. Allen, Jr. and E. K. Plyler, J. Chem. Phys. 25, 1132-1136 (1956) - H_2S spectrum near 1180 cm^{-1}.
6. H. C. Allen, L. R. Blaine, E. K. Plyler, and P. C. Cross, J. Chem. Phys. 24, 35 (1956). H_2S spectrum near 2350 and 2610 cm^{-1}.
7. Ordway, P. C. Cross, and E. Bair, J. Chem. Phys. 23, 541 (1955). H_2S spectrum between 7500-7800 cm^{-1}.
8. Innes, P. C. Cross, and E. Bair, J. Chem. Phys. 21, 545 (1953). H_2S spectrum near 8700 and 11000 cm^{-1}.
9. Grady, P. C. Cross, King, Phys. Rev. 75, 1450 (1949). H_2S spectrum near 10200 cm^{-1}.
10. P. C. Cross, Phys. Rev. 48, 7 (1935). H_2S spectrum near 9900 cm^{-1}.
11. H. C. Allen, Jr. E. K. Plyler, and L. R. Blaine, J. Res. NBS 59, 211-214 (1957). D_2S spectrum of 110-000 and 011-000 bands near 2750 cm^{-1} - also 1906 cm^{-1} band and 850 cm^{-1}.
12. J. B. Lohman, F. P. Redding, and D. F. Hornig, J. Chem. Phys. 19, 252 (1951). Low temp. crystal spectrum of H_2S and D_2S.
13. M. T. Emerson and D. F. Eggers, Jr., J. Chem. Phys. 37, 251-259

(1962). Intensity measurements for ν_1 and ν_2 bands of H_2S - consideration of P&R branch intensity anomaly.

14. R. E. Miller and D. F. Eggers, Jr. J. Chem. Phys. 45, 3028-3037 (1966). D_2S intensity and freq. analysis of ν_1 and ν_2 bands at 1896 and 855 cm^{-1}.
15. T. H. Edwards, N. K. Moncur, and L. E. Snyder, J. Chem. Phys. 46, 2139-2142 (1967). Improved measurement and reanalysis of two bands near 6300 cm^{-1} for H_2S - Equilibrium structure.
16. R. E. Miller, G. E. Leroi, and D. F. Eggers, Jr., J. Chem. Phys. 46, 2292-2297 (1967). D_2S spectrum of ν_2 band at 855 cm^{-1} - analysis with centrifugal distortion.
17. I. Gamo, J. Mol. Spectrosc. 23, 472-475 (1967). H_2S and D_2S force constants.
18. R. E. Cupp, R. A. Kempf, and J. J. Gallagher, Phys. Rev. 171, 60-69 (1968). Hyperfine structure of $1_{-1} - 1_1$ transition in H_2S at 169 GHz. Also observation of 4_0-4_2 line and others to 424 GHz.
19. T. Osaka and S. Takahashi, J. Phys. Soc. Japan 25, 1654-1663 (1968). Far infrared spectrum of H_2S and D_2S - 300-1500 µm.
20. L. E. Snyder and T. H. Edwards, J. Mol. Spectrosc. 31, 347-361 (1969). Measurement and analysis of two bands of H_2S near 3780 cm^{-1}.
21. R. E. Miller, G. E. Leroi, and T. M. Hard, J. Chem. Phys. 50, 677 (1969). Far infrared spectrum of H_2S and D_2S.
22. J. E. Lowder, L. A. Kennedy, K. G. P. Sulzmann, and S. S. Penner JQSRT 10, 17-23 (1970). Study of H-bonded dimer of H_2S via absorption feature near 2610 cm^{-1}.
23. C. Huiszoon, Rev. Sci. Instr. 42, 477 (1971). Millimeter-wave spectrum of $H_2{}^{34}S$ and $H_2{}^{32}S$.
24. F. C. Delucia, and J. W. Cederberg, J. Mol. Spectrosc. 40, 52

(1971). D_2S hyperfine splitting and molecular constants - millimeter wavelength spectrum.

25. P. Helminger, R. L. Cook, and F. C. DeLucia, J. Mol. Spectrosc. 40, 125 (1971). Millimeter and sub-millimeter spectrum and analysis of rotational constants for HDS.
26. R. L. Cook, F. C. DeLucia, and P. Helminger, J. Mol. Spectrosc. 41, 123 (1972). Millimeter and sub-millimeter spectrum of D_2S.
27. P. Helminger, R. L. Cook , and F. C. Delucia, J. Chem. Phys. 56, 4581 (1972). Microwave (mm and sub mm) spectrum of H_2S.
28. P. Helminger, F. C. Delucia, and W. H. Kirchoff, J. Phys. Chem. Ref. Data 2, 215-224 (1973). Summary of rotational spectrum and constants for H_2S.
29. S. Tang and C. W. Brown, J. Raman Spect. 2, 209-215 (1974). Raman spectrum of matrix isolated H_2S in H_2 and Ar.
30. R. L. Cook, F. C. DeLucia, and P. Helminger, J. Mol. Struct. 28, 237-246 (1975). Force field and structure of H_2S.
31. A. Anderson, O. S. Binbrek, and H. C. Tang, J. Raman Spect. 6, 213-220 (1977). Raman and infrared spectra of solid H_2S and D_2S.

SO_2 Bibliography

1. G. F. Crable and W. V. Smith, J. Chem. Phys. 19, 502 (1951).

2. R. D. Shelton, A. H. Nielsen, W. H. Fletcher, J. Chem. Phys. 21, 2178-2183 (1953). Infrared spectrum of SO_2 - 520 cm^{-1} to 5165 cm^{-1} (many band centers given).

3. D. F. Eggers, Jr., I. C. Hisatsune, and L. V. Allen, J. Phys. Chem. 59, 1124-1129 (1955). Infrared intensity measurements and bond moments for ν_1, ν_2, ν_3.

4. J. Morcillo and J. Herranz, An. Fis. Quim. 52A 207-216 (1956). Infrared intensity measurements for ν_1, ν_2, ν_3.

5. J. Morcillo and J. Herranz, An. Fis. Quim. 52A, 217-222 (1956). Calculation of bond moments from intensity measurements.

6. J. E. Mayhood, Can. J. Phys. 35, 954-960 (1957). Intensity measurements for ν_1, ν_2, ν_3.

7. A. Danti and R. C. Lord, J. Chem. Phys. 30, 1310-1313 (1959). Far infrared spectrum of SO_2 from 100-200 micrometers.

8. D. F. Eggers, Jr. and E. D. Schmid, J. Phys. Chem. 64, 279-280 (1960). Re-measured SO_2 intensity of ν_1, ν_2, ν_3.

9. C. O. Britt, C. W. Tolbert, and A. W. Straiton, J. Res. NBS 65D, 15-18 (1961). Frequency and width measurements for two lines that are not in Lovas' Tables (Author note: poor measurements of doubtful value.

10. M. deHemptinne, F. Greindl, and R. Van Riet, Bull. Cl. Sci. Acad. R. Belg. 48, 397 (1962). Microwave spectra of SO_2.

11. R. Van Riet, Bull. Cl. Sci., Acad. R. Belg. 43, 1291 (1962). Microwave spectra of SO_2.

12. A. Bauer, J. Bellet, P. Pouzet, and A. Remy, C. R. Acad. Sci. (Paris) 257, 3148 (1963). Microwave spectrum of SO_2.

13. Krishnaji and S. Chandra, J. Chem. Phys. 38, 232-236 (1963). SO_2 - N_2 pressure broadening of $8_{2,6} - 9_{1,9}$ transition.

14. Krishnaji and S. Chandra, J. Chem. Phys. 38, 1019 (1963). SO_2 - CO_2 pressure broadening of $8_{2,6} - 9_{1,9}$ transition.

15. Krishnaji and S. Chandra, J. Chem. Phys. 38, 2690-2692 (1963). SO_2 - CH_3Br collision broadening.

16. K. Takagi and S. Saito, J. Phys. Soc. Japan, 18, 1840 (1963). Microwave spectra of SO_2.

17. A. Bauer and J. Bellet, C. R. Acad. Sci. (Paris) 258, 873 (1964). Microwave spectra of SO_2.

18. R. Van Riet, Ann. Soc. Sci., Brux. 78, 237 (1964). Microwave spectra $S^{18}O_2$.

19. Y. Morino, Y. Kikuchi, S. Saito, and E. Hirota, J. Mol. Spectrosc. 13, 95 (1964). Microwave spectra of SO_2.

20. A. Bauer and J. Bellet, J. Phys. 25, 805 (1964). Microwave spectra of SO_2.

21. J. Bellet, Ann. Phys. 10, 827 (1965). Microwave spectra of SO_2.

22. P. A. Giguere and R. Savoie, can. J. Chem. 43, 2357-2362 (1965). Infrared spectrum from 400-3000 cm^{-1} at temperatures to 700°C.

23. H. A. Gebbie, N. W. B. Stone, G. Topping, E. K. Gora, S. A. Clough, and F. X. Kneizys, J. Mol. Spectrosc. 19, 7-24 (1966). Far Infrared spectrum of SO_2.

24. G. Steenbeckeliers, Ann. Soc. Sci Brux. 82, 331 (1968). Microwave spectrum of SO_2.

25. J. S. Murphy and J. E. Boggs, J. Chem. Phys. 51, 3891-3901 (1969). Pressure broadening and self-broadening of SO_2.

26. S. Saito, J. Mol. Spectrosc. 30, 1 (1969). Microwave spectrum of SO_2.

27. S. Chandra and R. A. Yadar, Indian Pure Appl. Phys. 7, 715 (1969).

Pressure broadening of microwave transitions.

28. Krishnaji and V. Prakash, J. Chem. Phys. 52, 2837-2840 (1970). SO_2-Ar pressure broadening.

29. Krishnaji and V. Prakash, J. Chem. Phys. 52, 4674-4677 (1970). SO_2 - N_2 broadening.

30. C. Secroun and P. Jouve, C. R. Acad. Sci., (Paris) 270B, 1610-1612 (1970). Intensity of ν_1, ν_2, ν_3, $2\nu_1$, $2\nu_3$, $\nu_1 + \nu_3$, $\nu_2 + \nu_3$.

31. Krishnaji and V. Prakash, J. Chem. Phys. 53, 1590-1593 (1970). SO_2 - OCS broadening.

32. S. H. Chan and C. L. Tien, J. Heat Transfer 93, 172 (1971). Infrared intensity measurements for ν_1, ν_3, $2\nu_1$, and $\nu_1 + \nu_3$ bands.

33. A. Barbe and P. Jouve, J. Mol. Spectrosc. 38, 273-280 (1971). Infrared spectrum of $S^{18}O_2$.

34. A. Barbe, C. Secroun, and P. Jouve, J. Phys. 33, 209-212 (1972). Potential constants for $S^{16}O_2$ and $S^{18}O_2$.

35. E. D. Hinkley, A. R. Calawa, P. L. Kelley, and S. A. Clough, J. Appl. Phys. 43, 3222-3224 (1972). Diode laser spectrum of ν_1.

36. G. D. T. Tejwani, J. Chem. Phys. 57, 4676-4681 (1972). Calculate pressure broadening of SO_2 by N_2 and O_2 - temperature dependence.

37. R. J. Corice, Jr., K. Fox, and G. D. T. Tejwani, J. Chem. Phys. 58, 265-270 (1973). Fit of low resolution spectra of ν_1, ν_2, ν_3.

38. G. D. T. Tejwani, K. Fox, and R. J. Corice, Jr., Chem. Phys. Lett. 18, 365-368 (1973). Measurement of $\nu_1 + \nu_2$ band intensities and calculation of dipole derivations of SO_2.

38a. W. H. Yang, J. A. Roberts, and G. D. T. Tejwani, J. Chem. Phys. 59, 4571 (1973). Microwave measurements of line broadening.

39. R. J. Corice, K. Fox, and G. D. T. Tejwani, J. Chem. Phys. 59, 672-675 (1973). Measurement of $\nu_1 + \nu_3$ band and intensity.

40. F. Allario, C. H. Bair, and J. F. Butler, IEEE J. Quant. QE-11,

205-209 (1975). Diode laser spectra of R-branch of ν_1 (no freq. given) - average self-broadening and N_2 broadening.

41. V. Dana and J. C. Fontanella, Mol. Phys. 30, 1473-1479 (1975). Spectra of ν_3 from 1333.6 - 1382 cm^{-1} (resolution 0.07 cm^{-1}; many lines still overlapped).

42. J. W. Fleming, Spectrochimica Acta 32A, 787-795 (1976). Far infrared spectrum(10-40 cm^{-1} with resolution of 0.05 cm^{-1}).

43. A. Barbe, C. Secroun, P. Jouve, B. Duterage, N. Monnanteuil and J. Bellet, Mol. Phys. 34, 127-130 (1977). I. R. spectrum of $\nu_1 + \nu_3$ of $^{34}S^{16}O_2$ - resolution 0.017 cm^{-1}.

44. M. Osumi and T. Kunitomo, JQSRT 21, 243-248 (1979). Gives calculated line widths and temp. dependence 300°K-1200°K - self and N_2 broadening - ν_1 and ν_3.

45. F. Herlemont, M. Lyszyk, and J. Lemaire, J. Mol. Spectrosc. 77, 69-75 (1979). Waveguide laser-stark measurements ν_1 band.

46. G. Bestmann, H. Dreizler, and H. Mäder, Z. Naturforsch. 34a, 1330-1333 (1979). Microwave measurement of pressure broadening - ν_2 and ground states for $^{34}SO_2$.

47. F. J. Lovas, J. Phys. Chem. Ref. Data 7, 1445-1750 (1978). Summary of microwave data for triatomics.

48. A. S. Pine and P. F. Moulton, J. Mol. Spectrosc. 64, 15-30 (1977). Doppler-limited measurements of $\nu_1 + \nu_3$ band of SO_2.

49. A. S. Pine, G. Dresselhaus, B. Palm, R. W. Davies, and S. A. Clough, J. Mol. Spectrosc. 67, 386-415 (1977). Complete listing of observed and calculated lines measured for $\nu_1 + \nu_3$ band.

50. A. Barbe, C. Secroun, P. Jouve, B. Duterage, N. Monnantenil, J. Bellet, and G. Steenbeckliers, J. Mol. Spectrosc. 55, 319 (1975). Grating spectra of $\nu_1 + \nu_3$ band of SO_2 - Analysis of main band and hot band - list of lines and relative intensities.

THE OUTER PLANETS – CURRENT KNOWLEDGE

Page

Thermal Structure of Jupiter and Saturn – Glen Orton 333

Composition of Jupiter – Ronald Prinn 363

Voyager IRIS Measurements of the Jovian
Atmosphere – Virgil G. Kunde 387

Jupiter and Saturn from 2 to 6 μm – Harold P. Larson 407

Blank Page

THERMAL STRUCTURE OF JUPITER AND SATURN

Glenn Orton (JPL)

I'll be using terms which may not be familiar to all of you; to save time I've listed them along with relevant explanations in the first figure.

Temperatures in the sensible regions of the atmospheres of the outer planets are quite cold. Figure 2 is a summary of temperature structures for Jupiter, Saturn, Uranus and Neptune, derived from the equilibrium models of Appleby and Hogan (1980, in preparation). In this figure, T_e is the assumed effective planetary temperature.

I will discuss the means by which we derive the vertical temperature profiles for Jupiter and Saturn, the molecular spectroscopic data which form the basis for this type of analysis, and the problems involved with these models for molecular absorption and with the recovery technique in general. I'll also give some results for Jupiter and Saturn from the Pioneer and Voyager infrared experiments and try to indicate how future experiments might improve on what we can do now, as well as what the present and future requirements are for molecular spectroscopic data. To save time, I will rely on Barney Conrath's exposition of the techniques of temperature sounding, without reviewing them again.

Why is temperature so important? Thermal structure is extremely basic, and needs to be known before any physics can be worked out for phenomena observed in the atmospheres, particularly for phenomena that are functions of altitude. Figure 3 serves as a brief summary of the imperative reasons for determining temperature as a function of height.

TERMS

- MIXING RATIO = $\frac{\text{NUMBER OF MOLECULES OF A GIVEN SPECIES}}{\text{TOTAL NUMBER OF MOLECULES}}$
- BRIGHTNESS TEMPERATURE = EQUIVALENT BLACKBODY TEMPERATURE CORRESPONDING TO AN OBSERVED BRIGHTNESS
- WAVENUMBER = CM^{-1}
- EMISSION ANGLE COSINE (μ) = ANGLE AT WHICH RADIATION IS EMITTED FROM A PLANETARY "SURFACE", MEASURED FROM THE LOCAL NORMAL

Figure 1.

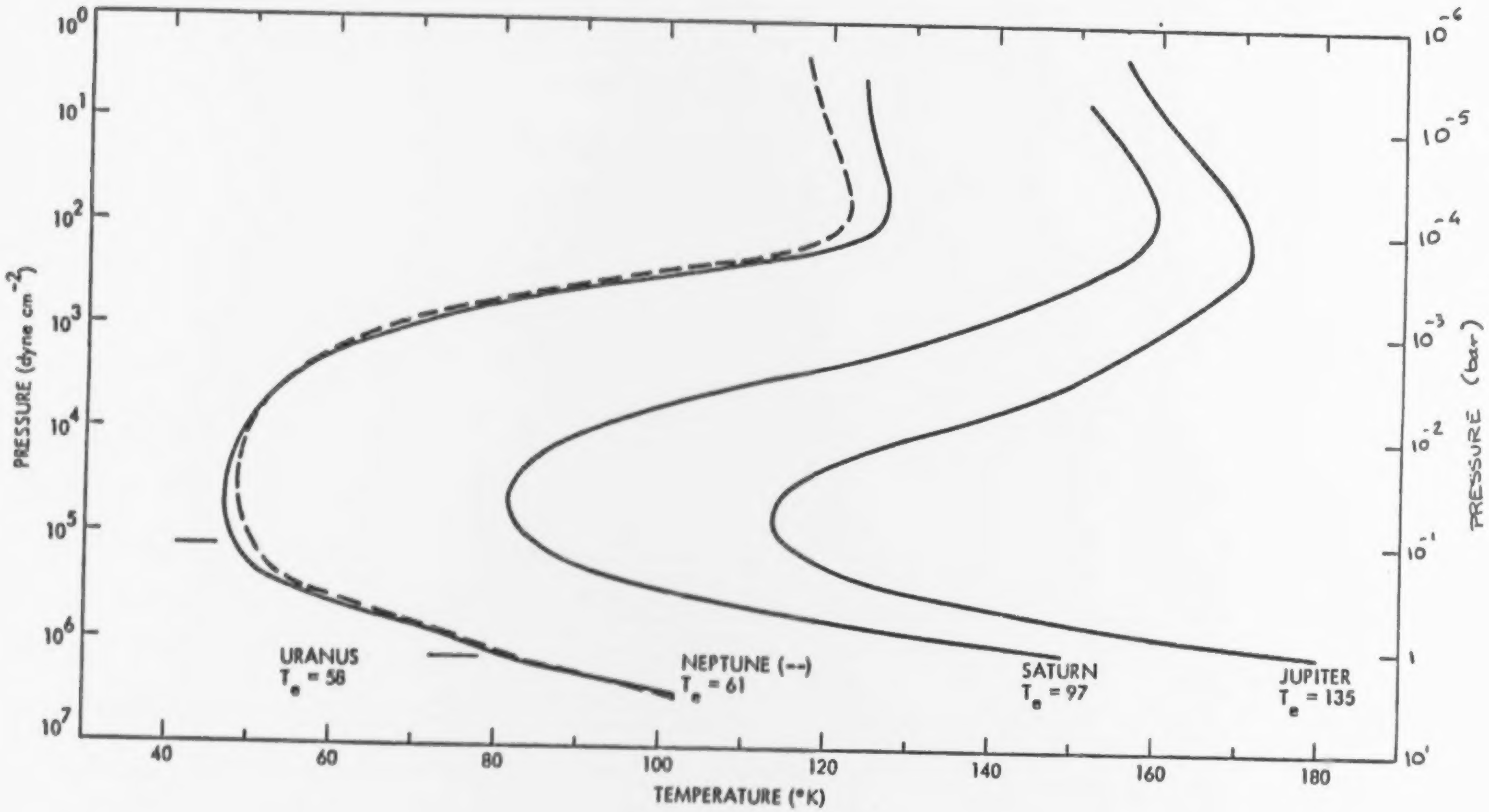

Figure 2. Derived pressure-temperature models for the outer planets (after Appleby and Hogan).

IMPORTANCE OF THERMAL STRUCTURE KNOWLEDGE

- KEY ELEMENT IN DEFINING BASIC CLIMATE AND WEATHER
- DEFINES FUNDAMENTAL ENERGETIC CONTROL
- DEFINES BOUNDARY CONDITION FOR INTERIOR MODELS
- NECESSARY FOR INTERPRETING ABSORPTION AND EMISSION OF THERMAL RADIATION BY GASES AND AEROSOLS
- PROVIDES CONTEXT FOR ASSOCIATION OF GAS AND AEROSOL VERTICAL PROFILES WITH COMPOSITION VIA EXPECTED PHASE CHANGES
- STRENGTH AND DIRECTION OF THERMAL WINDS IMPLIED BY TEMPERATURE VARIATIONS ALONG ISOBARS

Figure 3.

The hydrogen (H_2) collision-induced dipole is the most important opacity source in the thermal infrared for the outer planets. It dominates so much of the outgoing thermal emission, that it is not only useful for temperature sounding, but also controls much of the radiative equilibrium process. The plot in Figure 4 shows the location of unit optical depth (the peak of the weighting function is very close to this level) in the atmospheres of Jupiter through Neptune (assuming mixing ratios of 90% for H_2 and 10% for He). The graphs for Uranus and Neptune are virtually identical on the scale in this figure. It is easy to see a translational component at low frequencies, and the first two rotational lines. You can see that our vertical sounding capability covers the region from 1 bar to 0.1 bar. H_2 is a good opacity source because it is a pressure-squared absorber, so it has narrow weighting functions. The H_2 spectral features are quite broad, which means that you don't need to lose much vertical resolution when you increase the bandwidth to gather more signal. The hydrogen abundance is reasonably well known. (In the worst case, a guess of 50% mixing ratio would probably be correct to within a factor of two!)

This opacity source has been used by itself in broadband work done on early spacecraft experiments: the Infrared Radiometers on Pioneers 10 and 11. These instruments have two channels centered near 20 μm and 45 μm, with filter functions shown in Figure 5. A corresponding model spectrum is also shown in the figure. The 20 μm channel sees a region somewhat higher in the atmosphere (near 120 mb) than the 45 μm channel (near 500 mb).

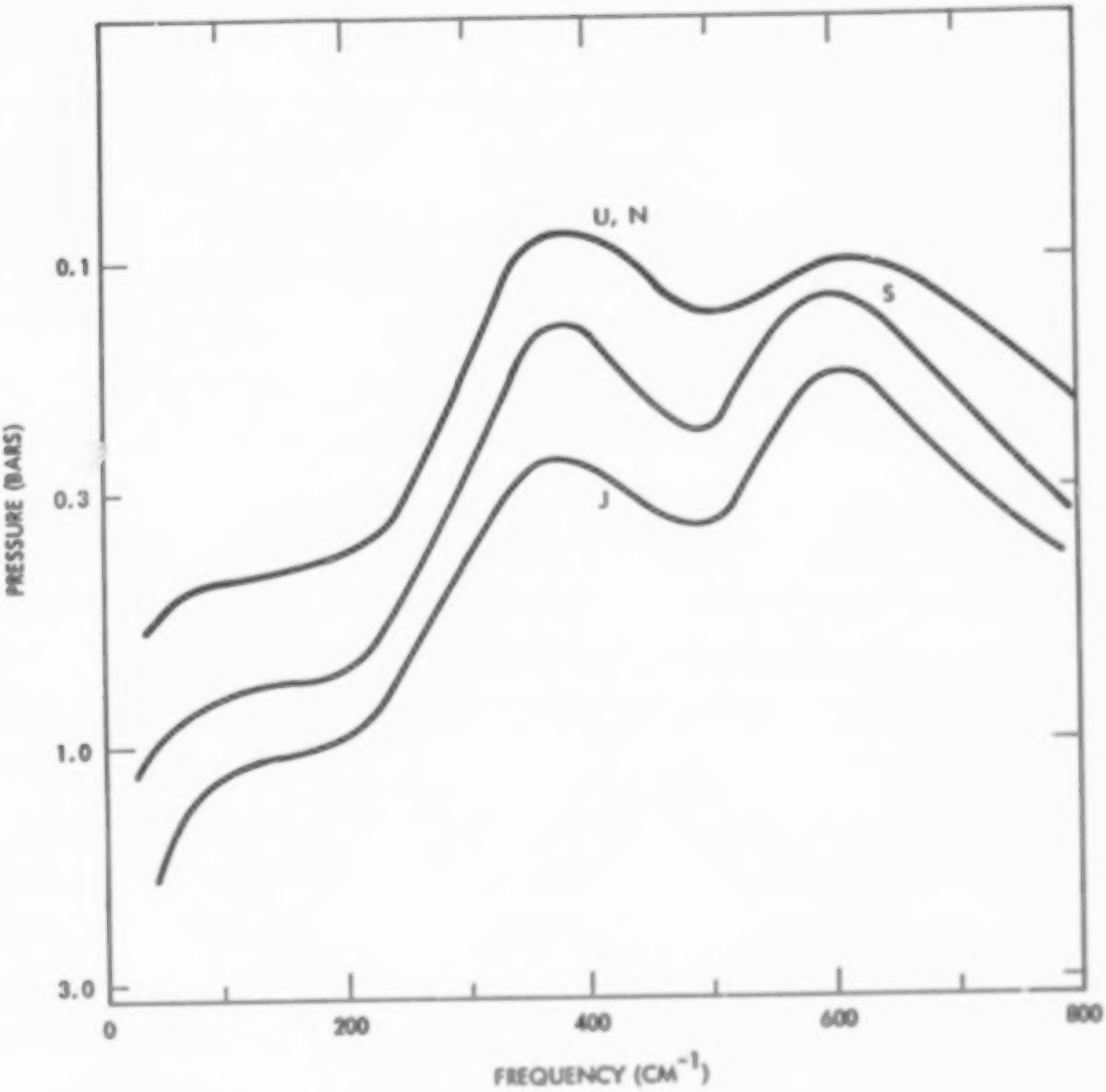

Figure 4. The pressure level for which optical depth unity is reached vs. frequency for the outer planets.

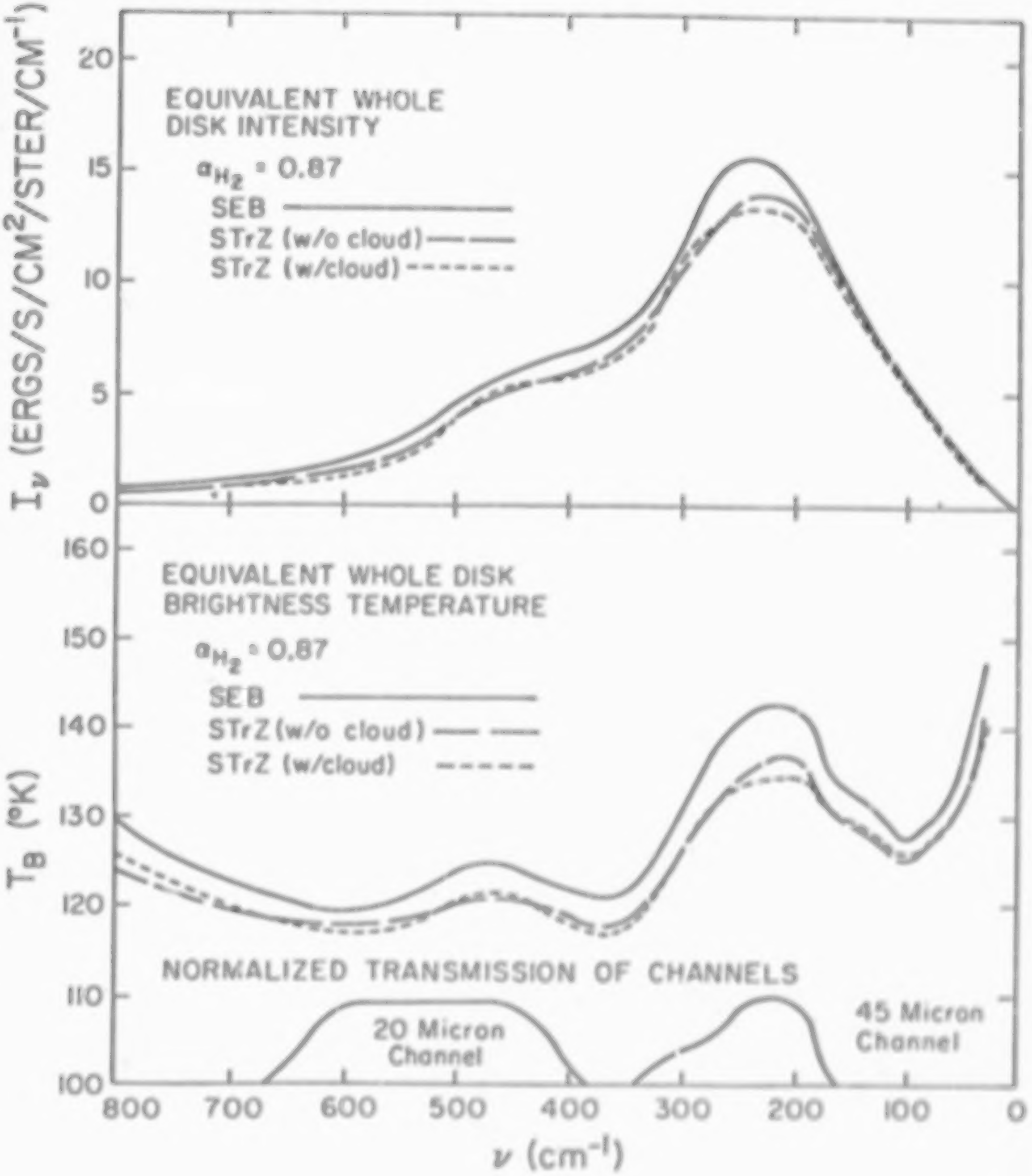

Figure 5. Jovian whole disk intensity and brightness temperature vs. frequency. The Pioneer Infrared Radiometer filter functions near 20μm and 45μm are also shown.

Since the Jovian work is somewhat passé, I'll show you very recent results for Saturn from Pioneer 11 (no doubt they will also be obsolete after Voyager's flyby in about six months). You can see the appropriate weighting functions in Figure 6. With the IRR instrument, we've had to use not only changes in spectral response, but changes in emission angle from a given point being sounded. That was impossible with Pioneers 10 and 11, because we never saw any single point on the planet more than once, because the instrument's cone angle was fixed with respect to the spacecraft. We therefore had to assume longitudinal homogeneity in the atmosphere. As a result, we are examining just the average structure of regions. For Jupiter, these regions are the rather obvious belts and zones, the prominent light and dark bands encircling the planet. On Saturn we are tempted to use a similar scheme (even though visual differences between various latitudes are not so prominent), for reasons which I'll get to in a moment. We cover Saturn's atmosphere vertically from about 400 mb to about 70 mb. Figure 7 shows the thermal structure derived from the data for two regions on the planet; results from one of the warmest regions is shown on the left, and results from one of the coolest is shown on the right. I refer to these as a "belt" and a "zone", respectively, because they follow the same correlation of infrared and visible radiation as for Jupiter. "Belts" are warm and dark, "zones" are cool and light.

Details of recovered structures are given in a report by Orton and Ingersoll (1980) now in press for the Journal of Geophysical Research. Regions around "zones" may not have lower kinetic temperatures, however:

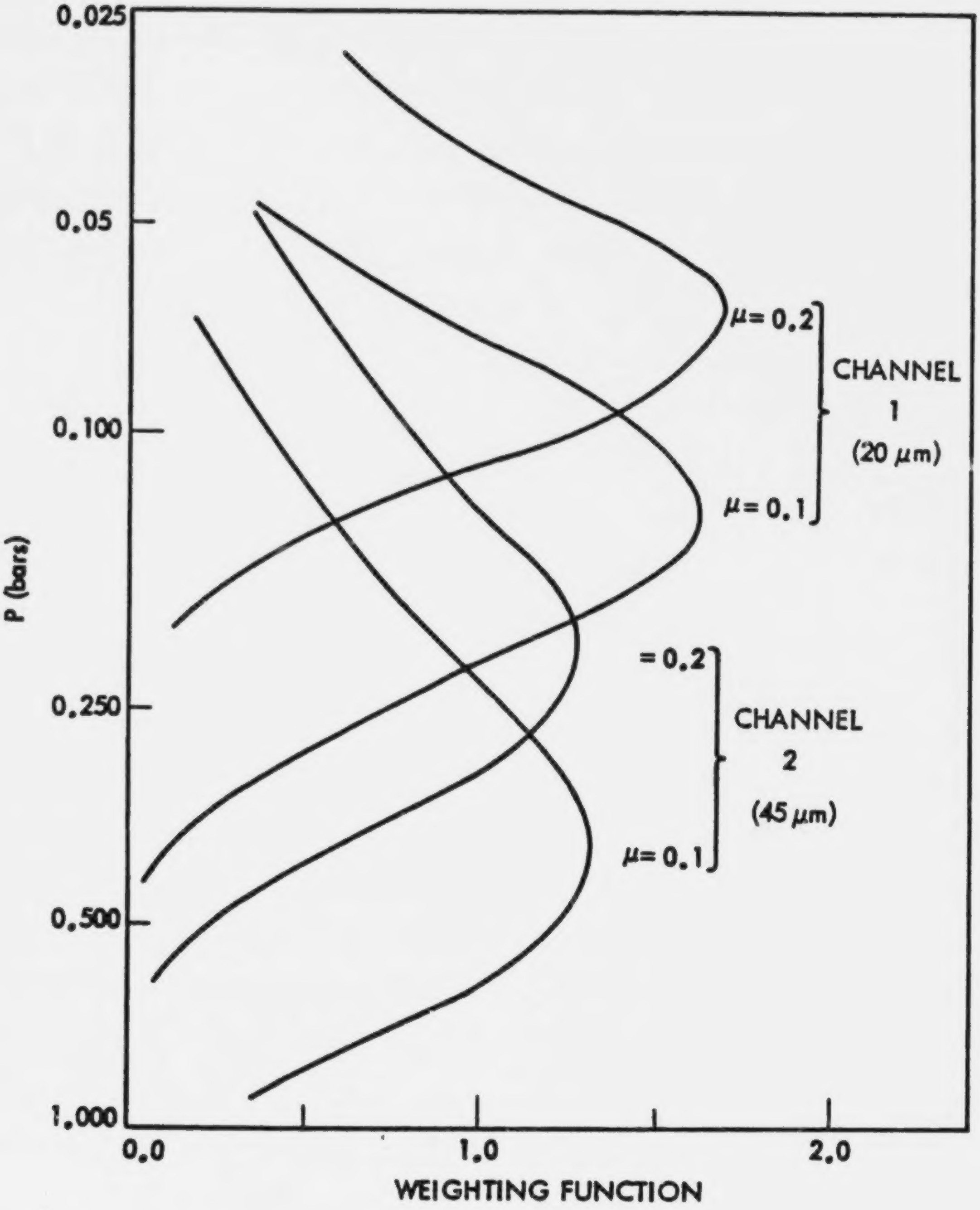

Figure 6. Weighting functions for the Pioneer II Infrared Radiometer observations of Saturn.

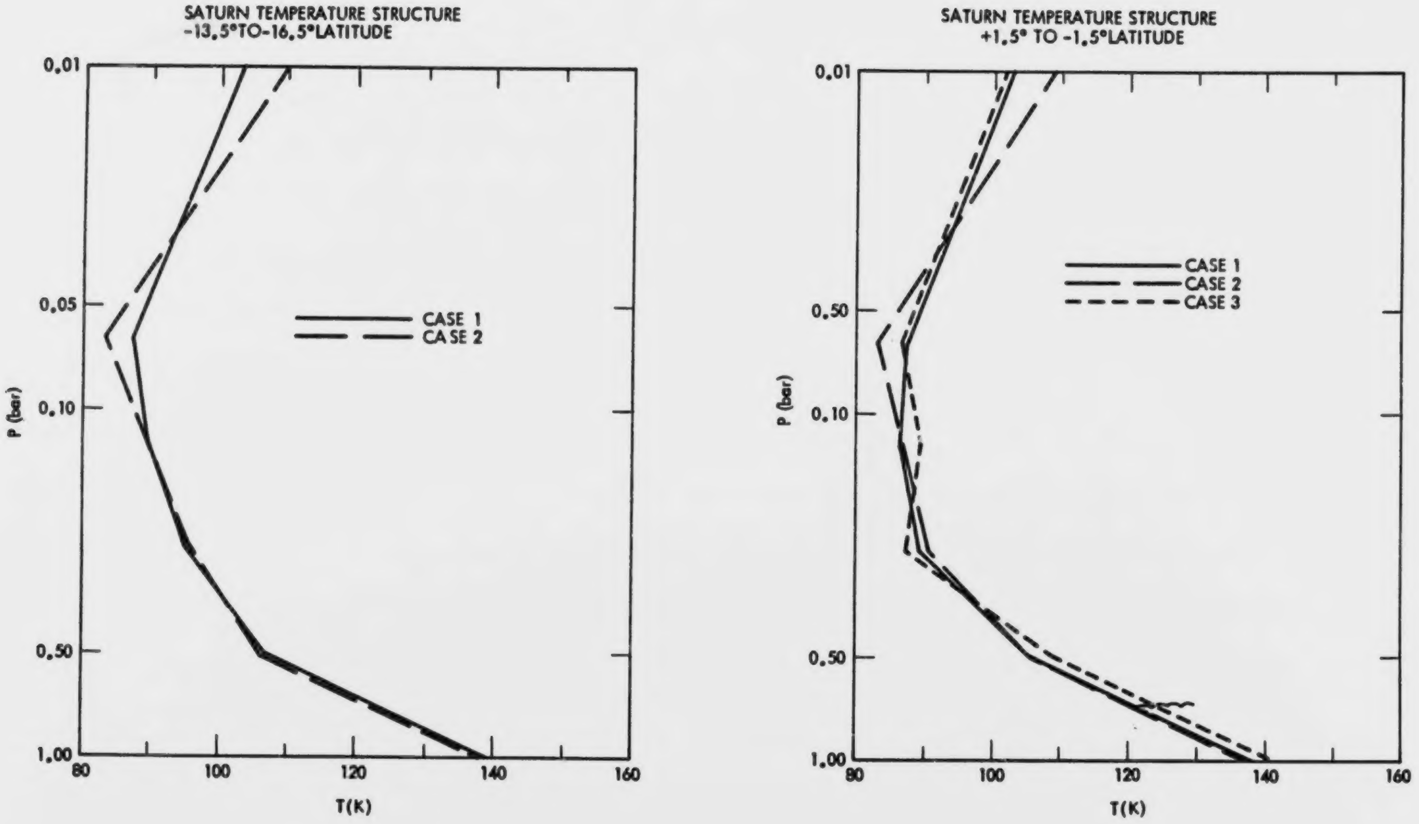

Figure 7. Thermal structure of Saturn derived from the Pioneer 11 Infrared Radiometer: Warm region (left) and cool region (right).

they may be covered by clouds around the 124 K level if kinetic temperatures in "belts" and "zones" are identical. Another point to note is that the thermal structure near the temperature minimum is very shallow, compared with the relatively sharp drop and subsequent steep rise with height in the Jovian atmosphere. Our use of different assumptions about the temperature structure overlying the 70 mb level is clearly marked in the figure and it has some effect on the recovered temperatures. We are also making what now appears to be an almost canonical assumption - that the temperature lapse rate is adiabatic in the deep atmosphere. Figure 8 shows a smoothed plot of temperature as a function of latitude for Saturn. The only thing I can point out is the very deep apparent drop in temperatures around the equator, roughly coincident with the bright equatorial band (possibly a "zone').

If we generate synthetic spectra from the estimated temperature profiles, integrate the total infrared output, and then plot the results of the various regions covered as a function of latitude, Figure 9 results. There is a dramatic drop in flux around the equator, again roughly coincident with the bright equatorial region.

Comment (L. Wallace): That's a minimum temperature?

Response: The minimum local effective temperature (near the equator) is around 95 K, the maximum is just under 97 K, and they are all substantially higher than the equilibrium temperature.

Question: What fraction of the disk did you integrate over?

Response: That's a good question. We only covered 10°N to 30°S latitude, and we have rings obscuring part of the northern latitudes.

(Talk resumes).

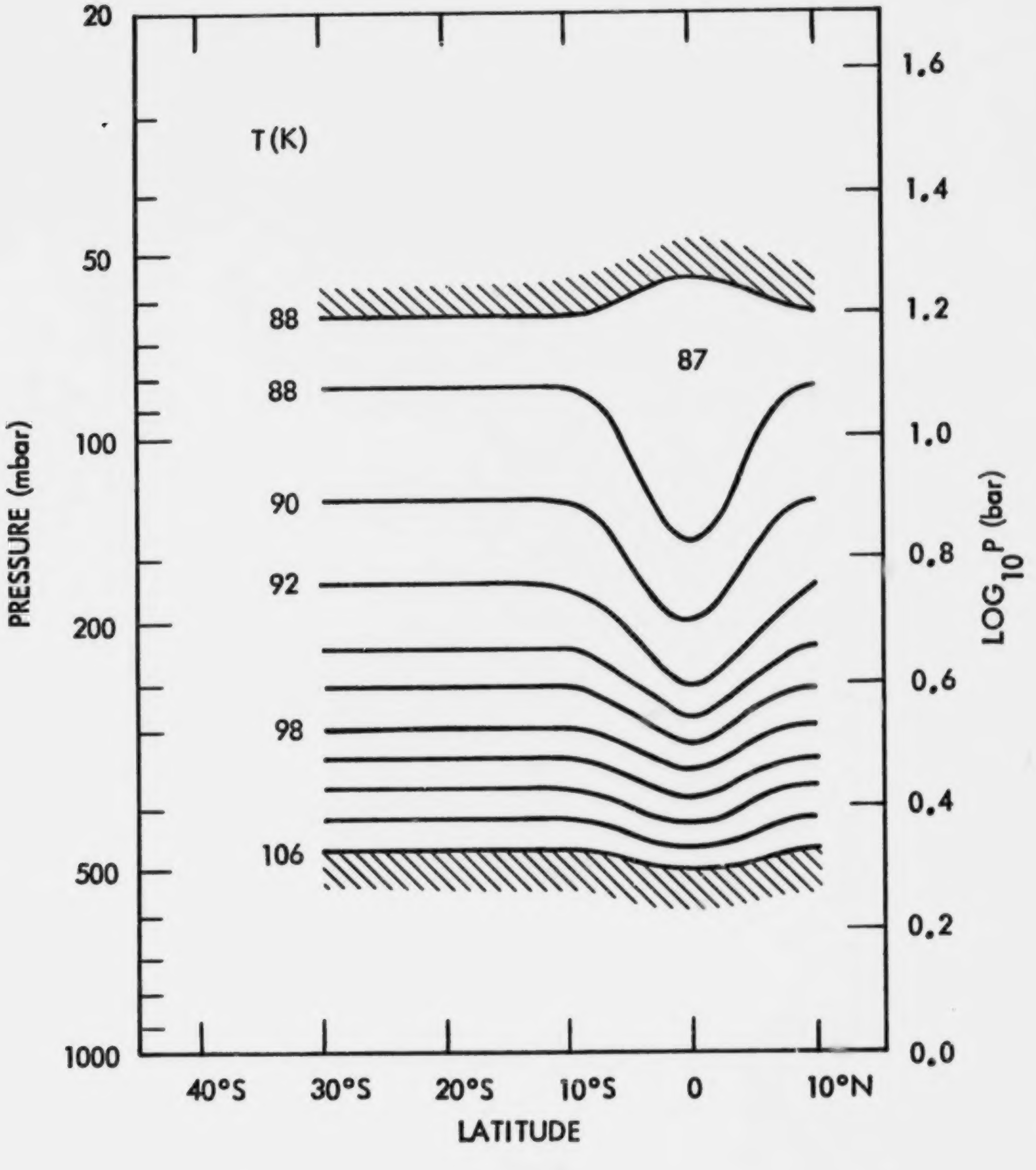

Figure 8. Temperature vs. pressure at various latitudes on Saturn from the Pioneer II Infrared Radiometer observations.

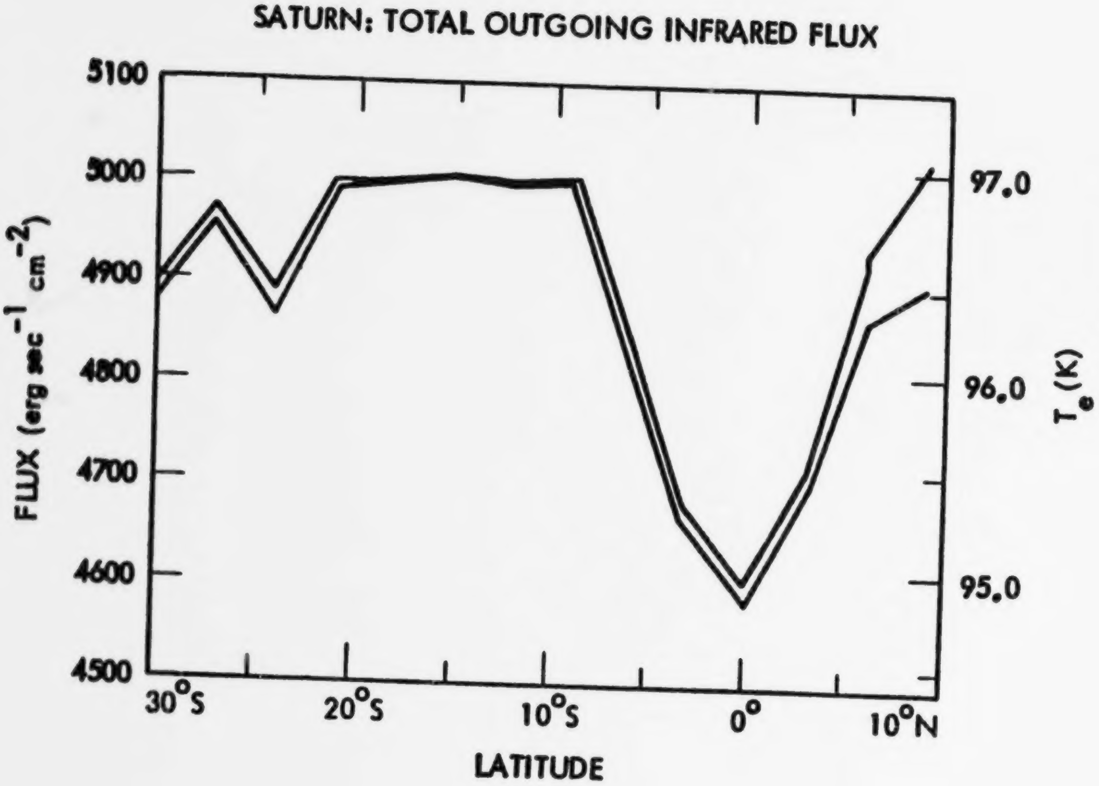

Figure 9. Effective brightness temperature and total outgoing flux vs. latitude for Saturn.

What are the problems with using hydrogen? We need to know the behavior of the collision-induced dipole over a broad range of frequencies and a wide range of temperatures. The temperature range includes a low point around 45 or 50 K for Uranus or Neptune, and temperatures intermediate to those where laboratory measurements have been made (roughly 77 K, 200 K and 300 K). We need to know the absorptions characterized by different ortho-H_2 vs. para-H_2 ratios. We have no substantial handle on what the ratio of these is in the atmospheres of the outer planets. Another source of worry is the appearance of other opacity sources with spectrally broad features, such as the distant wings of NH_3 rotational lines around 200 cm^{-1}, and the effect of aerosol absorbers such as NH_3 ice. Figure 10 shows the effect on the Jovian thermal spectrum of the addition of an NH_3 ice haze with a 1 km scale height, a base at 670 mb (147 K), and a narrow distribution of particle sizes centered near 3 μm. Unfortunately, the number density values got reversed when this figure was drawn up. The haze has a tremendous effect on the thermal spectrum and can't really be differentiated from the H_2 absorption by a clear spectral signature. Even at 50 μm wavelength the haze has a tremendous effect in reducing the total outgoing flux. I worry about this in trying to recover temperatures in the "deep" atmosphere, but so far it's something that no one, including me, has really paid sufficient quantitative attention to.

In order to extend our coverage up into the stratosphere, we use the opacity provided by the methane ν_4 band. You can see in Figure 11 the

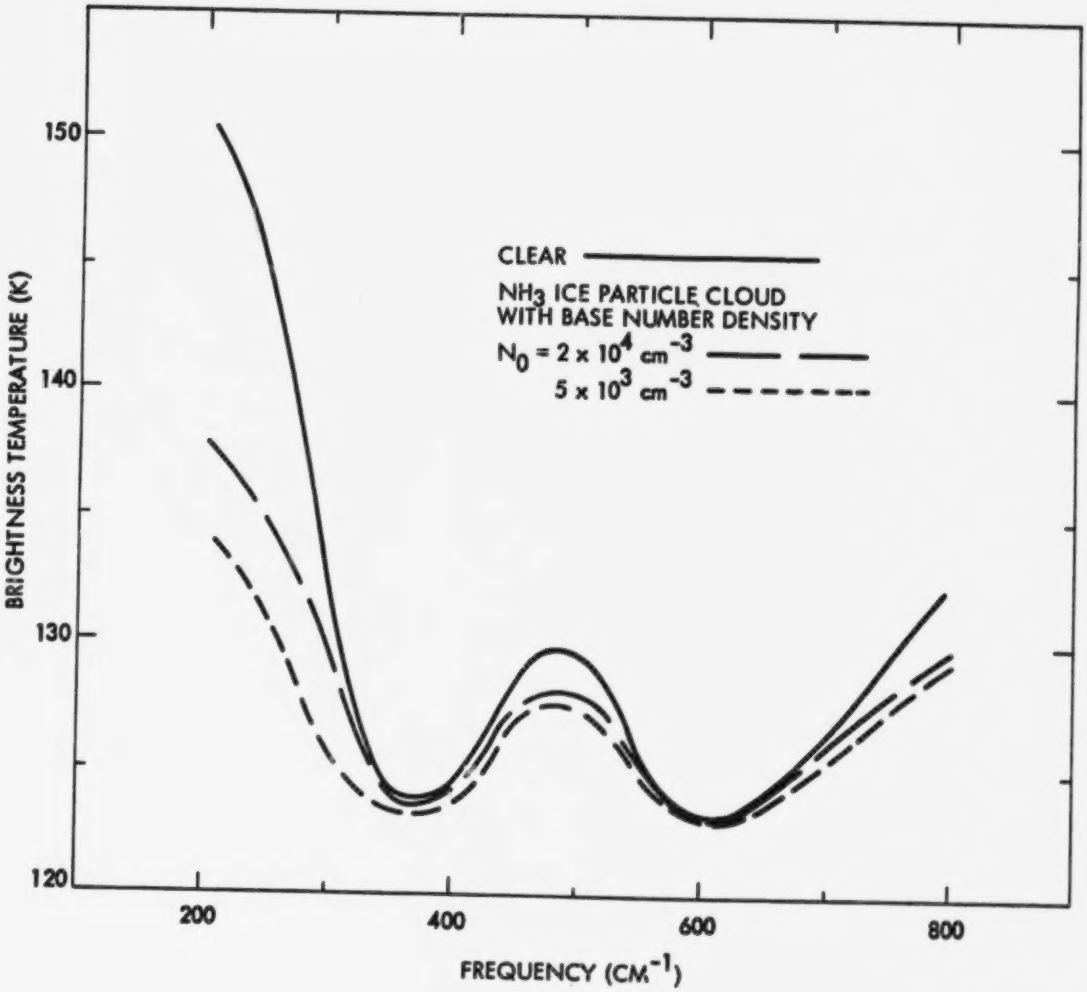

Figure 10. Model calculations of Jovian brightness temperature vs. frequency for clear-atmosphere and NH_3 ice haze models.

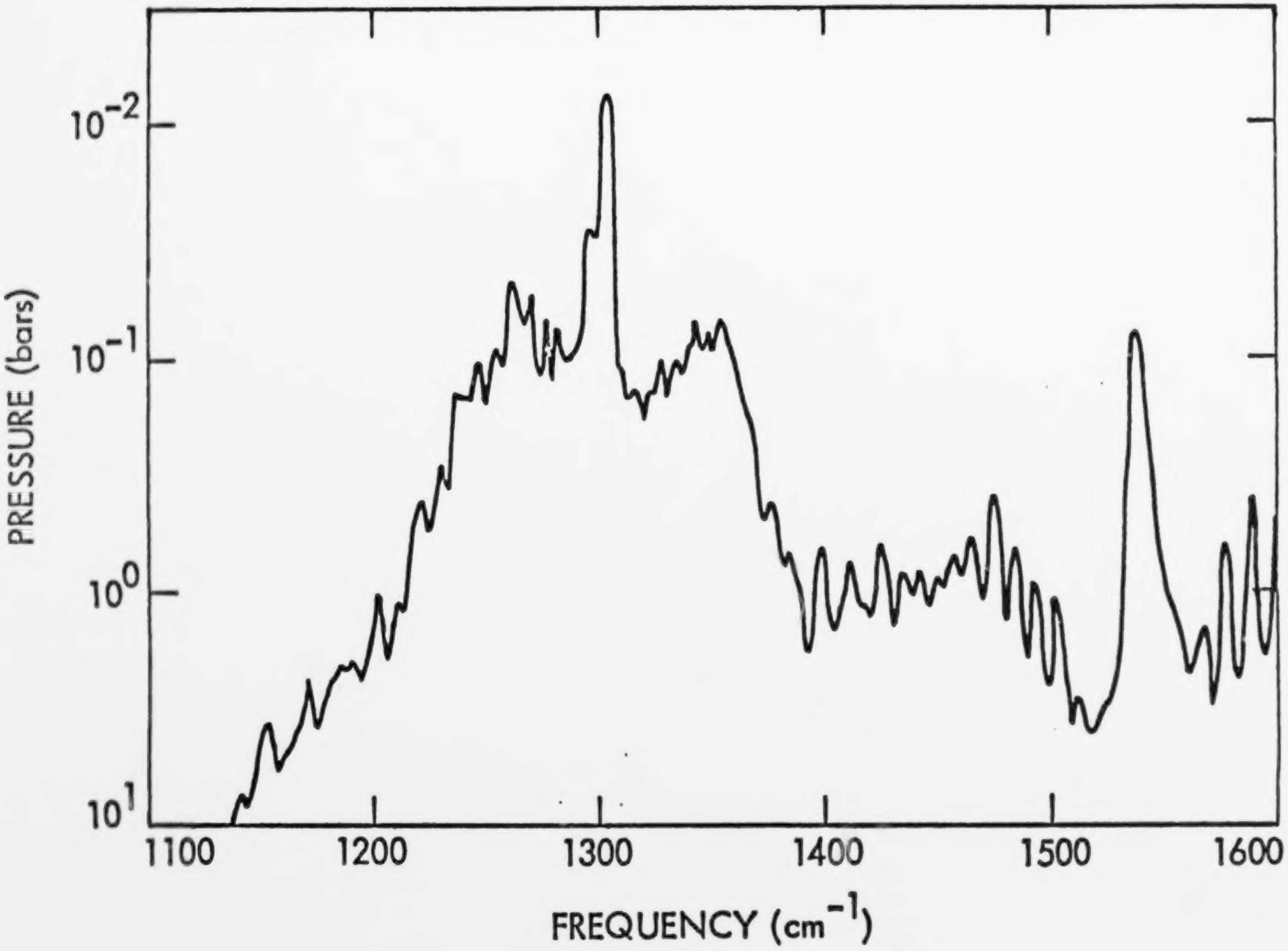

Figure 11. Altitude of the weighting-function peak vs. frequency in the CH_4 ν_4 band on Jupiter.

location of the weighting function peak vs. frequency for a Jovian atmospheric model (in which other opacity sources have been ignored). At the 4 cm^{-1} resolution element used in these calculations (close to the spectral resolution of the Voyager IRIS experiment), we can extend out coverage of the atmosphere from 100 mb to 10 mb. In fact, the higher the resolution, the higher we can sound in the atmosphere. IRIS results based on data from spectral regions dominated by H_2 and from those dominated by CH_4 are illustrated briefly in Figure 12, which is taken from Hanel _et_ _al_., (1979) _Science_ _204_, 972. These are spectacular results, showing detailed latitudinal features. There is a large area of depressed temperatures associated with the Great Red Spot, and the prospect of detailed analysis of these results is very exciting.

If we wish to, we can extend our coverage to higher in the stratosphere. Figure 13 is a plot of weighting functions based on infinite spectral resolution and centered around the R(0) line of ν_4 CH_4. It shows that we could go quite high in the atmosphere. We'd have no signal, but we could get that high in the atmosphere. Our problem would be that we would have to contend with a non-local thermodynamic equilibrium (non-LTE) source function in that area.

Question (M. Mumma): Why do you say you have no signal?

Response: The band pass in these calculations is infinitely narrow.

Comment: Yes, but your high weighting function and your low weighting function are separated by 0.006 cm^{-1}.

Response: That's right. So you have to have essentially infinite resolution; I'm separating out the very center of a line from a point

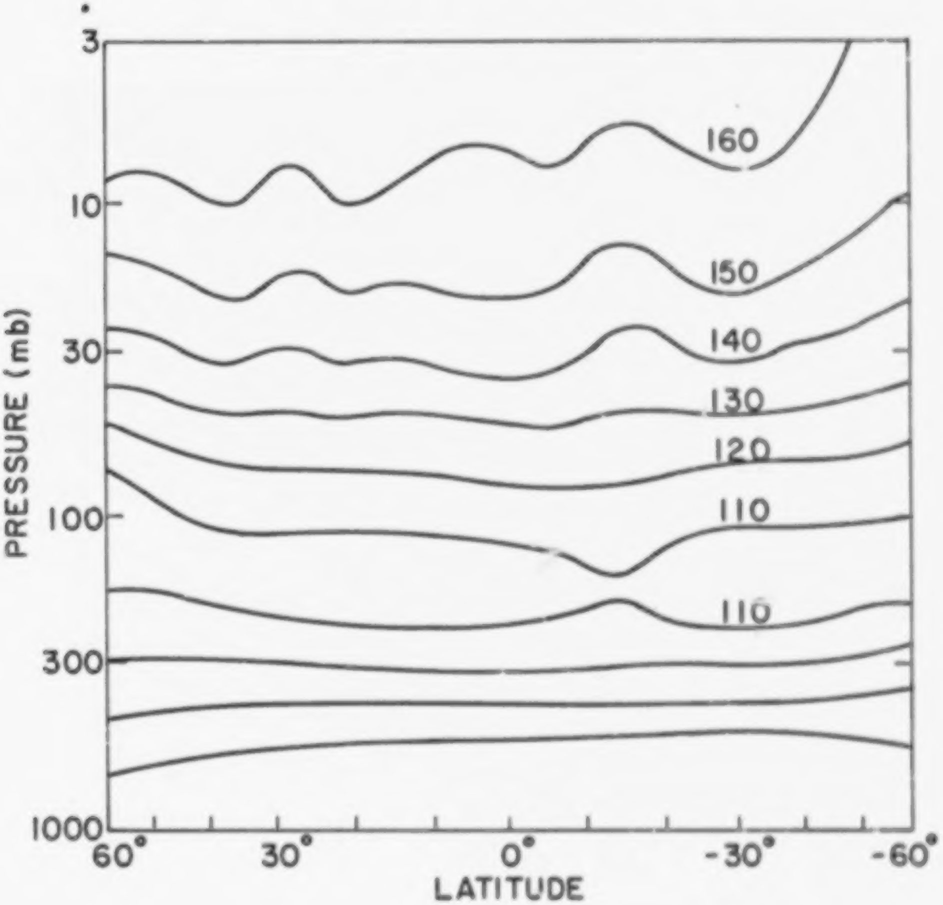

Figure 12. Voyager IRIS brightness temperatures vs. pressure at various latitudes on Jupiter (Hanel et al.).

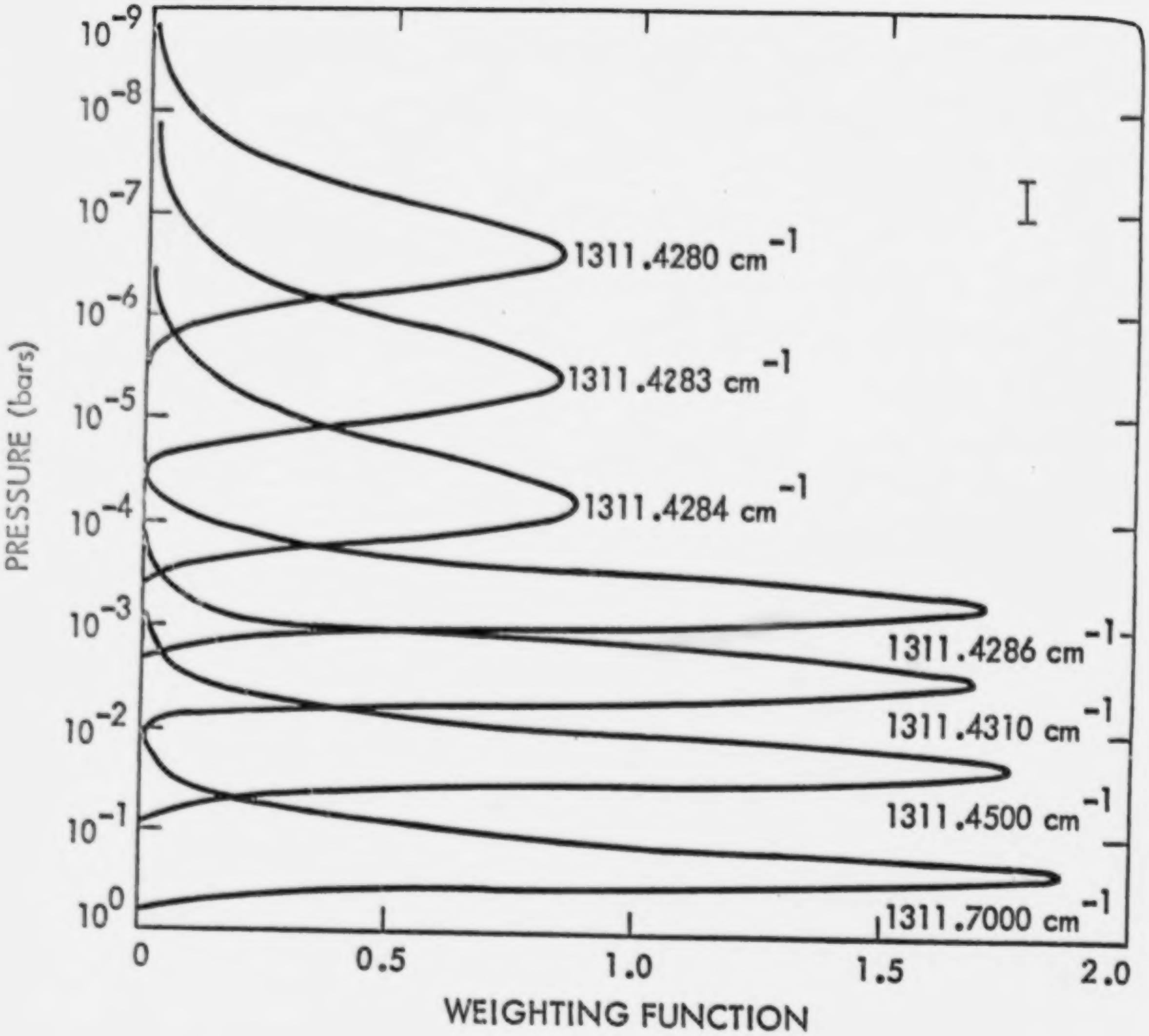

Figure 13. Monochromatic weighting functions near R(0) line of CH_4 ν_4 showing the extreme range of pressures sampled.

somewhere just off in the wing not really very far away. (Talk resumes).

Temperature sounding of the Jovian atmosphere with methane has its own share of difficulties, starting with the problem of determining a good value for the atmospheric mixing ratio. In the thermal infrared we could take advantage of a spectral region around 1100 - 1200 cm^{-1}, where CH_4 vertical coverage appears to overlap that provided by H_2 in the tropopause (refer to Figures 1 and 11). However, flux from this spectral region is probably highly influenced by NH_3 ice absorption. To carefully model NH_3 ice haze characteristics, we need to know the optical properties of NH_3 ice in this spectral region, and also the absorption provided by the far P-branch of the ν_4 CH_4 band and the far R-branch of the ν_2 NH_3 bands.

Another difficulty with CH_4 opacity has been demonstrated by Wallace and Smith (1976, Astrophys. J. 203, 760) and myself (Orton, 1977, Icarus 31, 41). The left panel of Figure 14 shows the CH_4 weighting functions associated with channels which are about 20 cm^{-1} wide (as well as two H_2 weighting functions). In the right panel I've plotted the contribution of each level to the outgoing intensity for the same frequencies. This is simply the weighting function times the Planck brightness function at each level. For the 1240 - 1280 cm^{-1} region, the temperature increase with height in the stratosphere produces an enormous change in brightness. As a result, the origin of the outgoing radiation at each frequency is not as well defined as the weighting functions themselves, and we are extremely dependent on whatever is assumed for temperatures in the overlying stratosphere. The temperature sounding problem is no longer well-

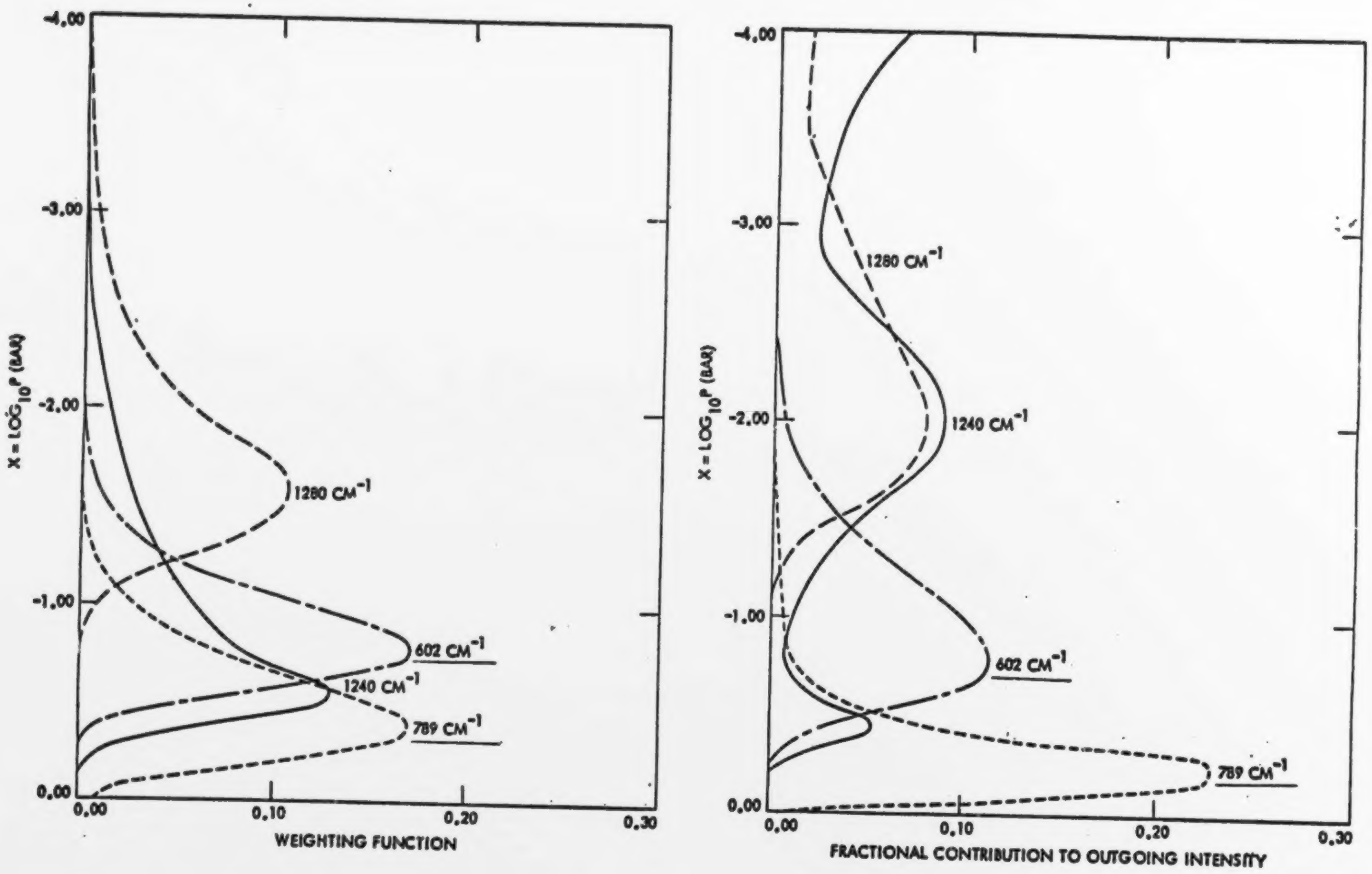

Figure 14. Weighting functions (left) and contributions to the emergent intensity at several frequencies on Jupiter.

posed, in that a small change in boundary conditions may produce a large change in the solution.

There are other problems with CH_4: there is at least a 20% uncertainty in the knowledge of the ν_4 line intensities; for Uranus and maybe Neptune, CH_4 condenses out of the vapor phase; and there may also be confusion with weak bands of C_2H_2 (the $\nu_4+\nu_5$ band) and C_2H_6 (the ν_6 or ν_8 bands).

We can also extend our coverage deeper into the atmosphere. For Jupiter this can be done via the 5 μm region, which Virgil Kunde will address. It can also be done for all the outer planets using radiation at microwave frequencies. I won't elaborate on this, but Figure 15 shows a composite of the microwave spectra of the outer planets. In the case of Uranus and Neptune, we have some indication that the H_2 collision-induced dipole is still dominating the atmospheric opacity out to 2 or 3 mm wavelength.

Question (G. Birnbaum): At what pressure are you seeing hydrogen in the microwave spectrum?

Response: For Uranus and Neptune, somewhere around 3 to 5 bars. Let me point out that in the case of Jupiter and Saturn, I suspect that we're seeing rotation and inversion lines of NH_3 predominantly, rather than H_2. For Uranus and Neptune, NH_3 condenses sufficiently deep in the atmosphere so that outgoing radiation isn't influenced by it. (Talk resumes).

Now I'd like to make one illustrative comparison of infrared results to results obtained by other means. I apologize for the busy nature of Figure 16, but it compares Voyager 1 IRIS results for 3 regions with 3 Voyager radio occultation results and with 2 of the equilibrium models of Appleby and Hogan. The bump in lower stratospheric temperatures

MICROWAVE SPECTRA OF THE OUTER PLANETS

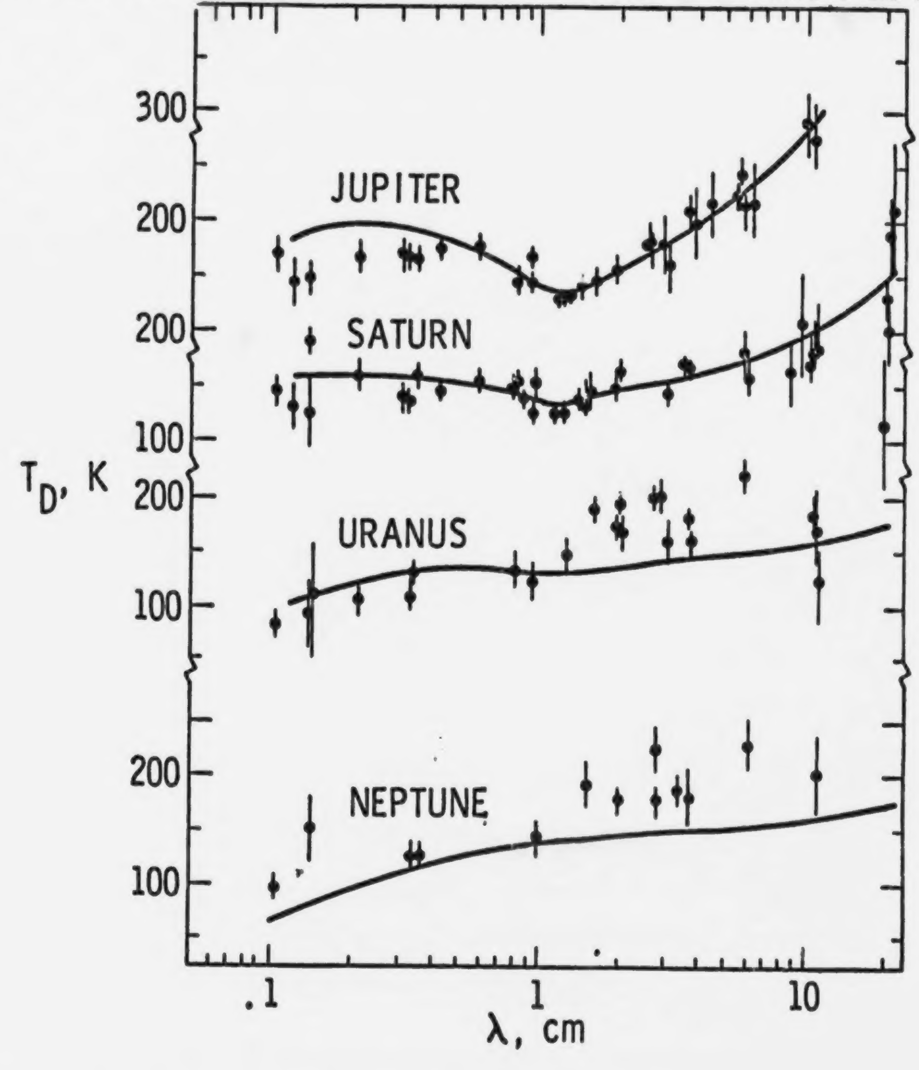

Figure 15. Brightness temperatures of the outer planets from microwave measurements.

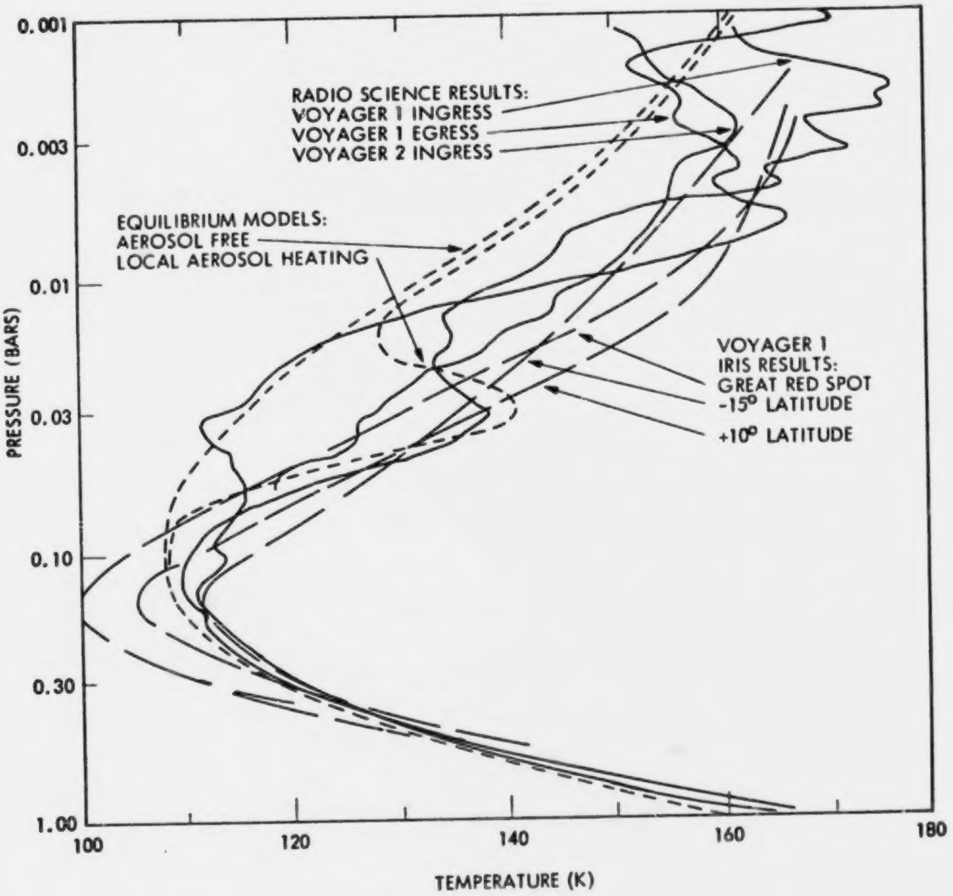

Figure 16. Experimental results and equilibrium models for the temperature-pressure profiles on Jupiter.

observed by the radio occultation experiment (for the Voyager 1 ingress signal) would not be resolved in the infrared temperature retrieval process, for reasons Barney Conrath alluded to earlier. The equilibrium model can approximate the bump by distributing "dust" (or some sort of insolation absorber) in a layer at this point in the atmosphere so that it absorbs about 4% of the incident sunlight at this level. In other respects, the thermal structures are very close to one another, particularly below the tropopause.

In conclusion, I've summarized several of the requirements of present and future attempts to sound the atmospheres of the outer planets, and I've listed them in Figure 17.

Question (P. Varanasi): What do you mean by overall strength?

Response: I'm distinguishing that from individual line strengths; that is, I don't believe any of the line strengths for the ν_4 CH_4 band are known with an absolute uncertainty better than 20%. (Talk resumes).

Let me make a couple of explanatory comments about Figure 17. An accurate model for H_2 opacity in the microwave region will allow us to do temperature sounding in the deep atmospheres of Uranus and Nepturn. Again, I'm emphasizing the P-branch of ν_4 CH_4 because that is the region where CH_4, NH_3 vapor and NH_3 ice may all be important contributors to the total atmospheric opacity. The CH_4 ν_4 relaxation time constant is an important but poorly known quantity in the determination of the CH_4 non-LTE source function. The low frequency boundary window for Jupiter is provided by the NH_3 ν_4 band, but its line parameters have never been published in any extensive form; line strengths in particular are difficult to predict

SUMMARY OF PROBLEMS NEEDING RESOLUTION INVOLVING MOLECULAR PROPERTIES

H_2:

- Accurate model for temperature dependence
  - between 77, 195, 297K
  - below 77K
- Differentiation between para-H_2 and ortho-H_2 properties
- Accurate model at very low frequencies

CH_4:

- Accurate overall line strength for ν_4
- Accurate parameters for weak ν_4 P-branch lines ($\nu \gtrsim 1200$ cm^{-1})
- Relaxation time constant for H_2 collisions (and He collisions)
- Parameters for lines, especially temperature dependence, (br gross temperature dependent properties) in 1100-17000 cm^{-1} region

General:

- Parameters for NH_3, including shape, for rotational lines and for ν_4 and $2\nu_2$ lines
- Parameters for PH_3 for infrared and sub-mm. lines
- Parameters for "weak" lines in 1800-2300 cm^{-1} region
- Parameters for C_2H_2 and C_2H_6 lines
- Optical properties (N_i, N_R) or ices: NH_3, CH_4, NH_4SH

Figure 17.

theoretically in a simple way because of the strong interactions taking place between the ν_4 and the $2\nu_2$ bands. PH_3 has bands in the 1100 cm^{-1} and the 2300 cm^{-1} regions and contributes substantial to the opacity in these regions, in the Jovian atmosphere. Some very recent data is available from Sill, Fink and Ferraro on NH_3 ice properties, but work should continue for other candidate ices: NH_4SH deeper in the Jovian atmosphere and CH_4 in Uranus and Neptune.

Author's note: A complete description of techniques and results of temperature sounding in outer planet atmospheres can be found in the following reference, which was completed a few months after the above discussion took place:

G. S. Orton, "Atmospheric Structure of the Outer Planets from Thermal Emission Data", In International Astronomical Union Symposium 96: Infrared Astronomy, D. Reidel Publishing Co., Dordrecht. 1981.

DISCUSSION

Question (K. Fox): Regarding the intensity in the 7 μm band of methane, what are your requirements for the present and foreseeable future (say, five to ten years) for line strength accuracies?

Response: I'd be happier at the moment with anything better than 20%. Five percent would be fine for most studies. Ultimately, I'd like to see 1%, unless that's ridiculous for any except the strongest lines.

Comment (K. Fox): I'm going to show some data this afternoon that I think will demonstrate that the intensities are known to possibly better than 20%, but not as well as 5%.

Response: It may be useful to compare more recent results, such as yours, with comparable lines in the work that Robiette and I did. We took a total band strength from the grand canonical average that Chedin *et al*., (1978, *J*. *Molec*. *Spectrosc*. *71*, 343) used. I'd like to see individual line strengths covered by other techniques.

Comment (M. Mumma): I'd like to address the question of relaxation coefficients for a minute. I think that's an extremely important parameter that's been grossly neglected in laboratory spectroscopy.

Question: Are there any measurements?

Comment: No, but there have been a number of elegent calculations on cross sections for that system, for individual rotational as well as vibrational transitions (I assume the latter are not part of the processes). They should be good calculations, and I think that perhaps there is some shock-tube data.

Response: There are measurements for hydrogen-methane and methane-methane combinations in the laboratory, but somehow people do not like shocking hydrogen-methane combinations in the laboratory!

Comment (M. Mumma): My comment is really directed at the general problem of relaxing vibrational states in polyatomics. That's a terribly neglected problem.

Comment (J. Caldwell): Let me ask you to comment on the Saturn profile that you showed; your result and also Arv Kliore's radio occultation method. It shows the temperatures at the 10 mb level or higher to be much less than other models. There is a very good ground-based observation by Gillett at 8 microns; it gives a brightness temperature around 135 K. The models that you're showing there can't reproduce that, because you are some 10 - 15 K cooler, at least.

Response: You can do something if you vary the upper temperature any amount. I mean, as I've alluded to in the Jupiter problem, you may have really difficult problems in separating out the contributions to the outgoing intensity from regions in the upper and in the lower stratosphere. Probably all bets are off once you allow the temperature to do anything in the upper atmosphere.

Comment (L. Wallace): You still have a good point. The real temperature has to go to 135 K somewhere.

Response: Sure. I'm saying it can certainly do that above the highest region where temperatures were determined (to a level of acceptable uncertainty) by the radio occultation results. But you're basically right; otherwise, it is very difficult to get a given temperature, even when you vary the CH_4 to H_2 mixing ratio to help yourself out.

Comment (P. Varanasi): I have just one general comment. You mentioned the need for methane and amonia data and so on. If I can elaborate on it, the type of data that we need from lasers and high resolution measurements has not been determined yet. In many "high resolution" measurements, you can't determine line widths at all from the spectra, so that the line intensity could be dependent on the line widths that are used, introducing systematic uncertainties along with the data. Some of the discrepancies that you mentioned in the line strengths, that were discussed earlier, might be resolved once and for all. You didn't explicitly mention line width measurements in your list.

Response: I said "line parameters".

Comment (P. Varanasi): Line widths should be included. If you look at the available data on methane and amonia, whether the data come from my laboratory or another laboratory, there are still significant differences in the line widths.

The other point is about line intensities in CH_4 ν_4. You said you would be very happy if the line intensities were known to better than 20%. I don't think you would be happy with that at all, particularly if it were measured by one person.

Comment (M. Mumma): An interesting point. It is not sufficient to have just one measurement of a line strength to one percent. You have to have agreement between several laboratories, using a variety of techniques.

COMPOSITION OF JUPITER

Ronald Prinn (MIT)

I will very briefly review our understanding of the chemistry of Jupiter's atmosphere. At the same time, I will indicate which remote observations of the planet are most likely to yield new knowledge, in other words, which types of observations would be most useful, according to these models.

Figure 1 simply summarizes the various molecules that have been discovered on Jupiter. As far as chemistry is concerned we are interested in all of these compounds: methane, ammonia, water, ethane, acetylene, carbon monoxide, phosphine, and germane. I talked to Hal Larson and he still believes that he has definitive evidence for germane. Germane is not unexpected in the atmosphere if there is very rapid convection, as I'll discuss shortly.

Those were the compounds that have been discovered, but of course we naively believe that the elemental composition of Jupiter is roughly solar, perhaps enhanced somewhat in some of the elements heavier than hydrogen and helium. Recall that our list of observed gases took us through the elements (Figure 2) down to germanium (if indeed you believe that germane is present in the atmosphere). So it is interesting to look further up in Figure 2 and see what we haven't observed. Since for germanium we have detected abundances as low as a few parts in 10^{10}, what interesting gaps among the lighter elements might we hope to fill?

One of them is selenium. You can expect reasonable amounts of hydrogen selenide in the deep atmosphere, perhaps a few parts per billion. I don't know anything about the spectroscopy of hydrogen selenide; maybe nobody does. Fluorine is a little higher up on the list of elements, and we would also expect observable amounts of hydrogen fluoride, at about 100 parts per billion; i.e., 0.1 parts per million. We would expect to observe hydrogen selenide and hydrogen fluoride only if we can look down through the water clouds, i.e., in regions where temperatures are greater than 300°K.

Question: Are their vapor pressures very high?

Response: Not in the upper atmosphere. As I just mentioned they can be seen in the vapor phase only if you look down below the water clouds at say temperatures (depending on the species) of about 300 to 500°K. You'd see essentially the solar ratio for something like hydrogen selenide at 500°K and the same for hydrogen fluoride at 300°K. The problem with hydrogen fluoride is that it has a condensation reaction that involves precipitation of ammonium fluoride, and you've got to get below that condensation level. That again is around 300°K so you want to look down into hot spots to see these more exotic species. But they are well worth searching for, because they are further tests of the solar-composition hypothesis. (Talk resumes)

Figure 3 shows some other species, and our present idea of what the clouds are composed of. This is a highly idealized model, that involves assuming thermo-chemical equilibrium at every layer in the atmosphere. As I'll show shortly this is not always a very good assumption, but nevertheless it gives you some idea of the compounds to expect. Ammonia solution is a possible cloud condensate beginning at temperatures around 280° K or somewhat less. Water ice, ammonium hydrosulfide and ammonia are toward the top of the Figure 3. None of these compounds are colored, of course. The figure shows the concentrations of methane, ammonia, hydrogen sulfide and water vapor. Water vapor hydrogen sulfide and ammonia precipitate out in the ammonia solution and ice clouds, ammonium hydrosulfide clouds, and ammonia crystal clouds respectively. Thus their mixing ratios decrease very, very rapidly with altitude.

Figure 4 shows why the assumption of thermo-chemical equilibrium is no good. UV light is penetrating into the atmosphere, and dissociating essentially all the species of interest that were in the previous graph: methane, phosphine, ammonia and even hydrogen sulfide are all photo-dissociating.

To me, the most interesting observation that could come in next couple of years would be some stringent upper limit on the abundance of hydrogen sulfide, or even better, the discovery of the gas on the planet. We expect it to be there. At its expected abundance, it should be easily observable if we can look down in the hot spots where presumably we are seeing below the water cloud base.

I'm going to go briefly through our ideas of the chemistry of methane, ammonia, hydrogen sulphide, and phosphine, pointing out along the way that although the models look very elegant, in fact they are based upon incredibly little observational evidence.

Methane

We know that methane is present, and we can deduce the way in which it would photodissociate. Then, based on models, we can predict abundances for various compounds: methane, ethane, ethylene and acetylene, as shown in Figure 5. Acetylene and ethane have been observed. The abundances are not known very well, to say the least, particularly for acetylene, but they are in the right ballpark according to the models. Ethylene has not been observed, and it would be nice to observe it: with a model as simple as this (this is a relatively simple chemical model), simply having these two compounds (acetylene and ethane) observed with abundances within factors of 3 or 4 of what you'd predict is really unsatisfactory for testing the model. So we need better abundances, much better abundance estimates for acetylene, and it would be really nice to observe ethylene, to get some further idea as to how well we understand the photochemistry of methane on Jupiter.

The other things that are missing from this diagram are the higher hydrocarbons. Any search for higher hydrocarbons is worthwhile, to the extent that it will tell us whether this simple picture is all there is to the chemistry of carbon in the upper atmosphere. Based on what we know at the moment, I don't think that you could rule out somewhat more complex hydrocarbons (they would be aliphatic most probably) than those indicated on the graph.

Ammonia

The ammonia system is shown in the Figure 6. It appears to have relatively simpler chemistry, although you have probably noted from Figure 4 that there is some overlap between the ammonia and methane photodissociation regions. Of course we often naively ignore any potential cross-products, although there have been some rough estimates of these particular cross-products; in actual fact I don't think that the problem of the crossing of the ammonia, phosphine, and methane photodissociation regions has been fully developed. So there are good reasons for looking spectroscopically for species like methylamine, for example, as probable cross-products of the ammonia and methane photodissociation schemes that we've been discussing.

Nobody has observed hydrazine in the atmosphere. Yet the models do predict amounts of hydrazine which, if it remains in the gas phase, would be easily observable. It would be nice to get some evidence pro or con for the presence of gaseous hydrazine or droplets of hydrazine.

I presume that the Galileo entry probe is going to find the molecular nitrogen in the cycle shown in this figure.

Hydrogen Sulphide

Hydrogen sulphide(Figure 7) has never been observed, so any observations will help us. We think hydrogen sulfide is there, simply because sulfur is very, very abundant in a solar composition model. A chemical reason for hoping for hydrogen sulfide is that it photodissociates with reasonably rapid rates, and gives rise to elemental sulphur, and hydrogen and ammonium polysulfides, and these species are all colored. They range from dark brown to very light yellow. Of course, we know that there are dark browns to light yellows on the planet. So this is one of the leading candidates for explaining some of the colorations on the planet. It would be very nice to get definitive evidence from remote spectroscopy of at least the presence of hydrogen sulfide. Again, this is an example of where, to see measurable amounts, one would have to look down into the warmer regions of the planet, not just up at the ammonia cloud tops, because hydrogen sulfide precipitates as ammonium hydrosulfide. Figure 8 is a Voyager photograph of one of the structures that the meteorologists now call a "raft"; there are a number of them. All the evidence about these rafts indicates that they are regions of sinking air, and are relatively clear of the upper white clouds. In other words, when you are looking at these rafts you are seeing deeper into the planet than you are in the regions surrounding them. The rafts are the deep brown color that one expects from the photodissociation of hydrogen sulfide and of ammonium hydrosulfide in the particulates one would produce. It would be very interesting to get the sort of spatial resolution that enables you to look at a feature like that (there are many other rafts in the same class), and ask, "Is hydrogen sulfide present?"

Phosphine

Phosphine shown in Figure 9 was discovered several years ago on the planet. The interesting thing about the photochemistry of phosphine is that it can also lead to colored particulates, and in particular to red phosphorus. There are some intermediates that are all relatively short lived. There was an identification of P_2 on the planet about a year or two ago but unfortunately it had to be withdrawn, so the only evidence we have for the validity of all the chemistry shown in the figure is: (1) we have observed phosphine; (2) phosphine mixing ratios decrease with altitude; (3) there are red colors, in particular in the Great Red Spot. You expect this scheme to apply when you have rapid upward mixing, as indeed we now suspect occurs in the Great Red Spot. The most intense cycling through this scheme occurs in regions where there's very rapid mixing of the atmosphere from the deep levels, around 800° Kelvin, all the way up to the visible levels; under those conditions, you would expect the highest rates of production of red phosphorus.

Figure 10 shows the Great Red Spot. It is my understanding from the meteorology, that these white spots adjacent to the Red Spot are similar to it in the sense that there is upwelling in these regions. We then have to ask why they are bright white while the Great Red Spot is red, right in the same region. The answer is presumably in the rates of convection; you are able to most rapidly bring up the precursors of the colored species from very deep in the Great Red Spot. Again this points out the need for spatial resolution in looking at Jupiter.

Minor Species

We now look in Figure 11 at the carbon system very, very deep in the planet. I'm going to temperatures that will range up to 1500° K or so, and you suddenly see in thermochemical equilibrium the appearance of carbon monoxide here, deeper in the atmosphere. It is interesting to ask if we can mix the carbon monoxide up to the cool parts of the upper atmosphere more rapidly than carbon monoxide can be converted to methane; if so, then we will mix a species that is stable only in the deep atmosphere right up into the visible atmosphere. We have in fact studied the chemistry for converting carbon monoxide to methane. You can work out the rate at which it occurs, compare that to a transport time, and determine whether you expect to see carbon monoxide in the atmosphere. The result is shown in Figure 12, which gives you as a function of the rate of vertical diffusion the carbon monoxide mixing ratio which one would see. If for the vertical diffusion rates you take typical values that people believe from free convection from the internal heat source of Jupiter, you see an expected abundance of carbon monoxide of parts in 10^9.

Question (M. Mumma): Where is that? At what altitude?

Response: That would be at all altitudes. It would be mixed up from the 1100° K level all the way through the atmosphere, except at the very top where there is going to be a little photochemistry going on.

Question (M. Mumma): Beyond the tropopause?

Response: The tropopause is where the photochemistry will begin, so yes, up to the tropopause. (talk resumes)

You can do the same for nitrogen, with the ammonia-nitrogen system (Figure 13). Nitrogen gets more and more stable very deep in the planet and since in fact it approaches mixing ratios exceeding a part per million in the very deep atmosphere you can ask the same question: Is the conversion of nitrogen to ammonia slow relative to the rate at which you mix a parcel of gas from the deep part of the atmosphere to the upper atmosphere? If it is indeed slow, then the mixing ratio you see for nitrogen deep in the atmosphere applies throughout the troposphere. I've gone through some calculations of this (and they are more complicated to do, because this reaction is catalyzed on iron particles), and it appears from this scheme that you might expect a part per million of nitrogen in the atmosphere.

There is another source of minor species: extra-Jovian inputs to the planet. One such source (Figure 14) is meteorites. If the meteorites are carbonaceous chondrite material, this input could provide plenty of oxygen in the upper atmosphere in the form of H_2O if you believe the meteorite fluxes that some people predict. So there is a source of oxidizing material pouring into the top of the atmosphere; that is another very plausible explanation for the observed carbon monoxide. There are other species that come along with this theory. Silicon monoxide is also produced if you are ablating meteorites; its detection would be a crucial test of the theory that meteoritic material is coming into the upper atmosphere, providing an oxidizing agent, which is producing unexpected oxidized species in Jupiter's atmosphere. There is also another idea put forward by Strobel and Yung (both present here) who suggested that inputs from the Jovian satellites could also provide oxidizing material. Again, these theories provide numerous compounds that are worth looking for. We've already seen carbon monoxide in the atmosphere. I hope the search for oxidized species will not stop at carbon monoxide. We should look for several other interesting oxides in the atmosphere, perhaps even nitrogen oxides, to explore this chemistry further.

The last figure (Figure 15) summarizes my suggestions for future directions and the potential payoffs.

(1) First, better spatial resolution would let us study the horizontal variability of phosphine, acetylene, carbon monoxide and water vapor absorptions, between the belts and zones, or between the red and white spots, and so on, and would be very, very helpful. Of course, we have already observed all these species, but if we can get the spatial resolution necessary to look at small parts of the planet, it would be very, very helpful in understanding the chemistry going on in the visible regions. At the same time, better spatial resolution might help us in the search for species we haven't observed: hydrogen sulfide, hydrogen selenide, hydrogen chloride, hydrogen fluoride, silane, H_3BO_3 (surprisingly,

1. BETTER SPATIAL RESOLUTION
    - (a) horizontal variability of PH_3, C_2H_2, CO, H_2O, etc. between belts, zones, red and white spots, etc.
    - (b) search for H_2S, H_2Se, HCl, HBr, HF, SiH_4, H_3BO_3, AsH_3, AsF_3, GeS, CH_3SH, CH_3NH_2, etc. in dark-brown "hot spots" (e.g., in "rafts")
2. BETTER SPECTRA (e.g., improved spectral resolution and observing platforms in space).
    - (a) search for C_2H_4, P_2, N_2H_4, CH_3NH_2, CH_3PH_2, SiO, HCN, etc. in addition to species tabulated in 1(b) above
    - (b) rotational temperatures to help determine vertical distributions (e.g., for CO, H_2O)
    - (c) confirmation and/or improved abundance estimates for GeH_4, C_2H_2, etc. and for $NH_3:H_2$ and $CH_4:H_2$ ratios
3. BETTER INTERPRETATION
    - (a) laboratory spectra for line positions, strengths, half-widths, etc.
    - (b) multiple scattering models including horizontal as well as vertical variability for abundance estimates (e.g., are the C:H and N:H ratios 2 and 1.5 times solar, and are the NH_4HS clouds thin or absent as recently suggested?)

Figure 15. Remote spectroscopy of Jupiter: Future directions and potential payoffs.

if you could look down below the clouds you might expect it at about 10 parts per billion; I bet nobody knows its spectroscopy), arsine, germanium sulfide, methyl mercaptan, methyl amine. These are the sorts of species that we would potentially be able to see if we looked down into these hotter spots, and were able to resolve them and run the spectrometer long enough.

(2) Better spectra: Simply improved spectral resolution and observing platforms in space. I think the most useful thing is to search for ethylene, for the P_2 species in the upper atmosphere, for hydrazine, for methyl amine, for cross-products between the phosphine and methane chemistry (for example, this particular organic phosphorus compound, methyl phosphine $CH_3 PH_2$, and also a great number of other ones that you can suggest), and finally for SiO (gas phase) in the very high atmosphere. HCN can be expected in rather small amounts, but perhaps our ideas about its abundance are wrong, and perhaps it is present in observable amounts. It would be well worth searching for HCN. The rotational temperatures are very, very helpful to understanding the chemistry, because they give us some idea of the altitude distributions. We would like to know with better accuracy the rotational temperature for carbon monoxide and water vapor (in fact for all of the species, but those are the two that are in my mind right now). It would be very, very useful to know their

rotational temperatures with better accuracy than what we have at the moment. The confirmation and/or improved abundance estimates for germane (improved spectroscopy of germane: at the moment we have only Larson's data, one Q-branch line only), acetylene and the ratios $NH_3:H_2$ and $CH_4:H_2$.

(3) Finally, better interpretation. The most important thing besides improved laboratory spectra is improved interpretation. There is in fact only one comprehensive interpretation of Jovian data I've seen, that really tries to take everything into account: a recent paper by Sato and Hansen, in the Journal of Atmospheric Science, I think is a first step in this direction. There's not much use in going and learning all the laboratory parameters for these spectra, if at the same time you don't develop the sophisticated models that you require to interpret the absorptions on the planet itself.

Figures

Fig. 1	See Table II of Ridgway *et al*., in *Jupiter* (ed. T. Gehrels, Univ. of Arizona Press, 1976) p. 384.
Fig. 2	See Table I of Prinn and Owen, in *Jupiter*, *ibid*., p. 319.
Fig. 3	See Figure 3 of Weidenschilling and Lewis, *Icarus*, *20*, 465, 1.
Fig. 4	See Figure 2 of Lewis, in *Chemical Evolution of the Giant Planets* (ed. C. Ponnamperuma, Academic Press, 1976) p. 13.
Figs. 5-7	See Figures 5, 6, and 8 of Prinn and Owen, *ibid*.
Fig. 8	Voyager 1 photograph, March 2, 1978, 13-18°N.
Fig. 9	See Figure 9 of Prinn and Owen, *ibid*.
Fig 10	Voyager 1 photograph, March 1, 1978, GRS region.
Figs. 11-12	See Figures 1 and 2 of Prinn and Barshay, *Science*, *198*, 1031, 1977.
Fig. 13	See Figure 3 of Barshay and Lewis, *Icarus*, *33*, 593, 1978.
Fig. 14	See Figure 2 of Prather et al., *Astrophys. J.*, *233* 1072, 1978.

Editor's note: Facsimile reproductions of Figure 1-14 were not made available to us. References to the Figures are given above. We apologize for the inconvenience to the reader.

DISCUSSION

Comment (A. Young): Concerning sulfur compounds; These are only colored appreciably at room temperature and temperatures near room temperature, so for the most part as soon as you get them down another 50° or so they become colorless. Also the polysulfides are pretty unstable to photodecomposition, and if you got them high enough to be irradiated by sunlight, I would expect them to be converted to sulfur pretty quickly, and again, at low temperature sulphur is essentially white, not yellow or brown. So I think it is not a terribly good idea to try to attribute these colors on Jupiter to sulphur compounds.

Response: I can only say that I disagree 100 percent with what you said. First of all, the colors that I am talking about are indeed being formed at reasonably high temperatures, perhaps even around 250 or 270° Kelvin. Secondly, ultra-violet irradiation of ammonium hydrosulfide produces visible and near-ultra-violet absorptions even at much cooler temperatures.

Comment (A. Young): At those temperatures these things are white.

Response: They are not white at 270° Kelvin. Ammonium polysulfide and hyrogen polysulfide are colored at this temperature.

Comment (A. Young): At 250°, they're white.

Response: You are looking at different temperatures than I am. Incidentally, why would they turn white by decreasing the temperature?

Comment (A. Young): What you are looking at is the wing of a Gaussian band which is centered at about 2800 Angstroms. If the temperature goes down, that band contracts very rapidly, and that's the reason why these things turn white.

Response: The polysulfides absorb right into the visible, they have visible absorptions.

Comment (A. Young): There are no bands in the visible. You are just seeing the wing of a band in the ultraviolet. That's the reason for the color in these things.

Response: I disagree. There has been a lot of spectroscopy done on the sulfur and polysulfide species by Meyer, Lebofsky, and others. The polysulfides have visible and near ultra-violet bands when produced by ultra-violet irradiation of solid ammonium or hydrogen sulfide.

Comment (A. Tokunaga): There is another possible way to be sure photochemistry is going on, using ammonia and phosphine. There is no evidence of emission from these gases at 10 microns. That suggests to me that they're being destroyed in the stratosphere, and we can put a very stringent limit on how much ammonia and phosphine there is, based on our data at high spectral resolution. So there is another possible way to be sure that there is photochemistry.

Response: Yes. There is already something along that line of evidence from the UV, of course: the fact that one doesn't see the UV absorptions.

Comment (L. Wallace): And besides, you have UV sunlight hitting the planet!

Response: Yes!

Comment (J. Caldwell): Let me comment on your call for confirmation of the acetylene abundance. There is a paper which I think appeared in the February 15 APJ, although I haven't actually seen it on the newstands yet. The IUE spectra of Jupiter, published by Toby Owen and a cast of thousands do in fact show evidence for acetylene on Jupiter. Jack Margolis has convinced me that the absorption coefficients used there are not in bad shape after all, and the mixing ratios derived are in rather good agreement with the infrared analysis by Glenn Orton and his colleagues. So the techniques are sufficiently different, and I think the numbers are in agreement to within a factor of 2. The numbers are so good and the agreement is so good that I think it will be a long time before you get better than that.

Response: I wasn't aware of that work. It would certainly suggest that further confirmation is not required.

Comment (V. Kunde): Additional evidence confirming the acetylene abundance comes from the Voyager IRIS spectra. A strong Q-branch is evident at 729 cm^{-1}, and this spectral feature is being used to derive the latitudinal distribution of acetylene on Jupiter.

Question: You mentioned several things you might see in the hot spots. To the best of my knowledge, the highest temperature after Westphal's initial observation is 260° K, and this implies maybe 290° K. How many of these compounds can be seen at those temperatures?

Response: It depends on the water vapor abundance. The condensation of water can remove a lot of these species. If the water vapor abundance that Larson and company observed, which is only a part per million,is in fact present in these relatively clear spots, then I think there's a chance of seeing these species even at temperatures below 273° K. Hydrogen fluoride can be removed by ammonium fluoride condensation. So if ammonia is dried out in these so-called hot spots, then perhaps you might see hydrogen fluoride. I would be very doubtful myself of hydrogen fluoride. For H_3BO_3, for example, which dissolves in water, the hope would be that the water vapor abundance is depleted in these hot spots so that perhaps one can see it. Admittedly, this is grasping for straws, but I hope that we will look into some of these hot spots. I see higher spatial resolution and looking at details on the planet as the areas where really good advances can be made in our understanding of atmospheric chemistry.

Comment (V. Kunde): We see the highest 5-micron temperature in the Voyager IRIS spectra when we are at the best spatial resolution (about 1 degree in latitude). In this case we see about 262° K, which represents a vertically averaged temperature. The region of formation for this 5-micron radiance is roughly from 2 to 6 bars, corresponding to atmospheric temperatures in the range from 210 to 300° K. Either the water cloud or continuum opacity sources seem to preclude our seeing substantially deeper in the atmosphere.

Question (R. Prinn to H. Larson): What was your estimate of the water vapor rotational temperatures? Do you have any estimate at all?

Comment (H. Larson): I think they were about room temperature, 300° K, with error bars.

Comment: In connection with Virgil Kunde's last comment, I'm not sure that we can see that high a temperature. At the hot spot, I believe the continuum is determined by the pressure-induced vibration-rotation spectrum of hydrogen.

So that opacity limits your optical depth to a temperature that is around 270° or so; just what you observed. Higher resolution won't let you deeper into the atmosphere because you really have a continuum of pressure-induced vibration-rotation absorption in hydrogen, and you've got a continuum on a lot of things.

Comment (V. Kunde): We'll come back to that after my talk.

Question (Y. Yung): I want to ask the time constant for converting phosphine into red phosphorus, that is, into P_4. I checked your paper, and your time constant is more than 6 months. In that time the red compounds will all get diffused, so how can you concentrate them in localized areas?

Response: I don't think it was 6 months; I thought it was only about 12 days or something like that.

Comment (Y. Yung): Yes, 12 days for the dissociation of phosphine itself, but you have to use a four-center reaction, PH + PH making P_2 and that reaction takes much longer than 12 days.

Response: Well, because we don't know the PH abundances, I am not prepared to estimate whether P_2 formation takes longer or shorter than 12 days.

Question (D. Strobel): With regard to the shopping list of sulphur compounds, I recall that in a model that Yuk Yung and I put together we also predicted significant quantities of CS and CS_2.

Response: I will add them to the shopping list.

Blank Page

Blank Page

Voyager IRIS Measurements of the Jovian Atmosphere

Virgil G. Kunde (GSFC)

Abstract

The scientific interpretation of the Voyager IRIS data is limited in many instances by a lack of knowledge in the basic molecular data. The most significant of these is the far wing collisional line shape of CH_4 and NH_3 as it effects interpretation of all Jovian "window" regions. It is recommended that a focused theoretical and laboratory effort, similar to that for H_2 in the 0-2000 cm^{-1} region, be carried out for these two gases to quantify their far wing line shape.

Introduction

In this report, I will review some of the Jovian atmospheric observations from the Voyager infrared investigation (IRIS). At the same time I would like to emphasize several spectroscopic problem areas presently limiting scientific interpretation of the data.

For perspective, the Jovian structure for the North Equatorial Belt (NEB) is summarized in Fig. 1. The temperature profile in the .015-.8 bar range has been obtained by inversion of the radiative transfer equation, using IRIS measurements of the NEB (see Figs. 2, 4, 6) at selected wave numbers in the 1304 cm^{-1} CH_4 band, and in the S(0) and S(1) hydrogen lines. The dashed portion of the curve represents an extrapolation of the IRIS temperature profile to deeper atmospheric levels along a 2.1 K/km adiabat. Also shown in Fig. 1 are the base levels of the three principal cloud layers predicted by an adiabatic, solar composition, thermochemical equilibrium model (Lewis, 1969): an ammonia cloud at the 148K level, an NH_4SH cloud at the 210K level, and a H_2O cloud at the 273K level. Observations seem to be in agreement with the upper white cloud deck being NH_3 condensate. No conclusive observational evidence exists for the two lower cloud decks.

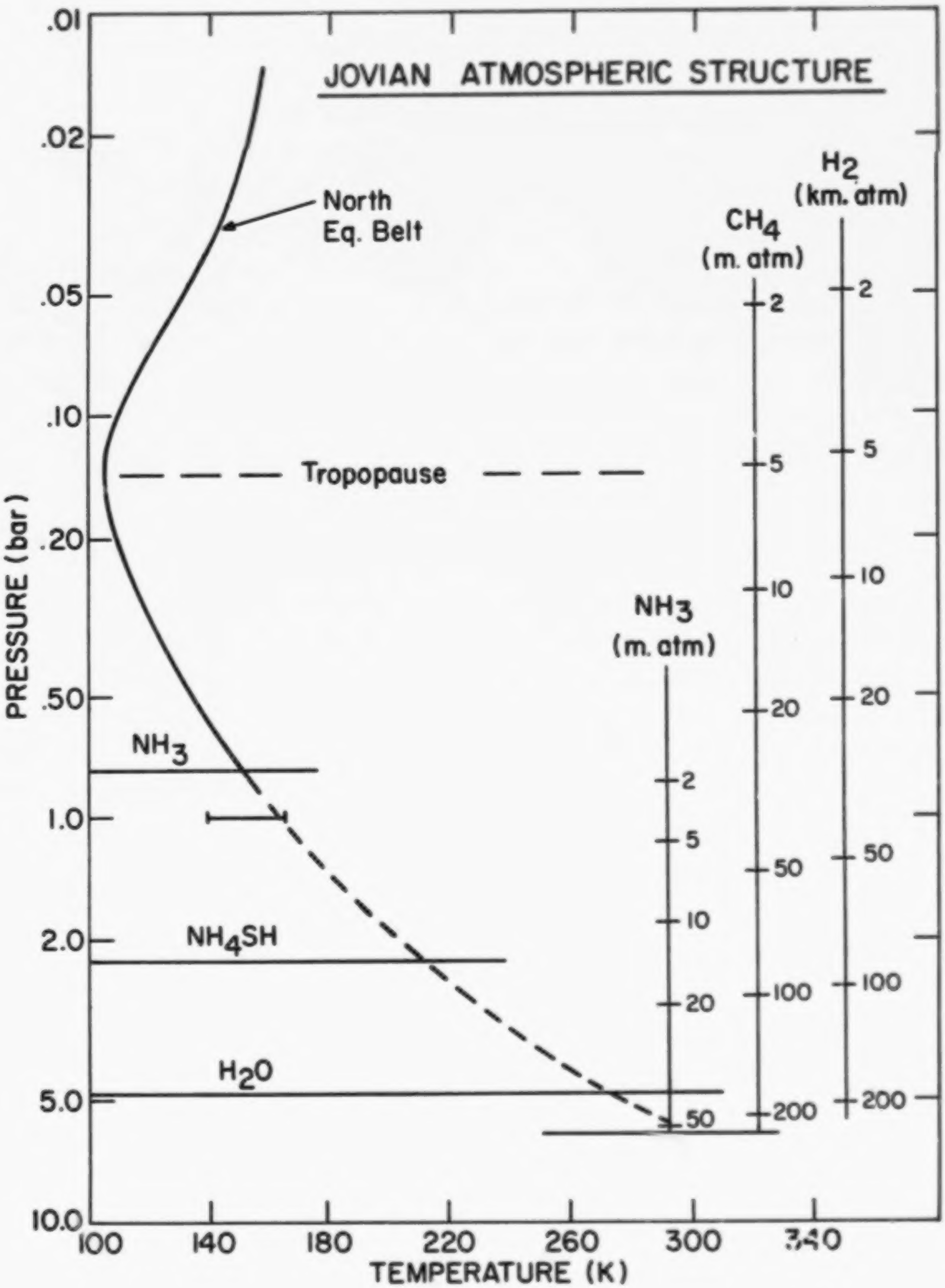

Figure 1. Jovian atmospheric structure.

The columnar amount of gas for the three most abundant infrared active molecules is shown on the right hand side of Fig. 1. For a belt region, we "see" into the atmosphere to approximately the 5 bar level which corresponds to ~200 km atm for H_2, 200 m atm for CH_4, and 50 m atm for NH_3. To infer physical parameters from infrared remote sensing measurements, such as Voyager IRIS, we must understand the molecular opacities for H_2, CH_4, and NH_3 for the temperature and path length conditions represented in Fig. 1.

Observations

The Voyager IRIS experiment uses a Michelson interferometer to measure the thermal emission spectrum of the Jovian atmosphere from 180-2500 cm^{-1} (55-4μm) with an apodized spectral resolution of 4.3 cm^{-1}. More than 50,000 spectra were acquired by Voyager 1 and Voyager 2. The narrow $.25^{\circ}$ field of view permitted recording full-disk spectra 3 - 4 weeks before closest approach with spatial resolution increasing to a maximum of almost 1/100 of the apparent disk at closest approach. Included in the IRIS data are measurements of the thermal emission for varying conditions of latitude, longitude, local time, phase, and emission angles. Additionally, measurements exist for a number of specific observational links which were designed to take advantage of the unique advantages of the fly-by mission and to maximize the returned composition information. Included in these links are the systematic mapping of belts and zones at normal and high angle viewing, and high spatial resolution mini-mosaics of selected hot spot regions.

The gross characteristics of the IRIS spectra are illustrated in Fig. 2 for a belt-like and a zone-like spectrum. The belt-like spectrum is an average of 51 individual spectra from the North Equatorial Belt (NEB), selected with an average brightness temperature in the 1950-2150 cm^{-1} region greater than 250K. The average emission angle is 15.8°, corresponding to an air mass of 1.04. The zone-like spectrum is an average of 343 individual spectra from the entire disk of Jupiter with the 1950-2150 cm^{-1} average temperature in the 180-210K range. The average emission angle is 19.7°, corresponding to an air mass of 1.06. The spectra clearly show evidence for H_2, CH_4, C_2H_2, NH_3, PH_3, H_2O, GeH_4, and CH_3D. Emission by C_2H_6 is evident in high air mass spectra. Preliminary results concerning composition from these

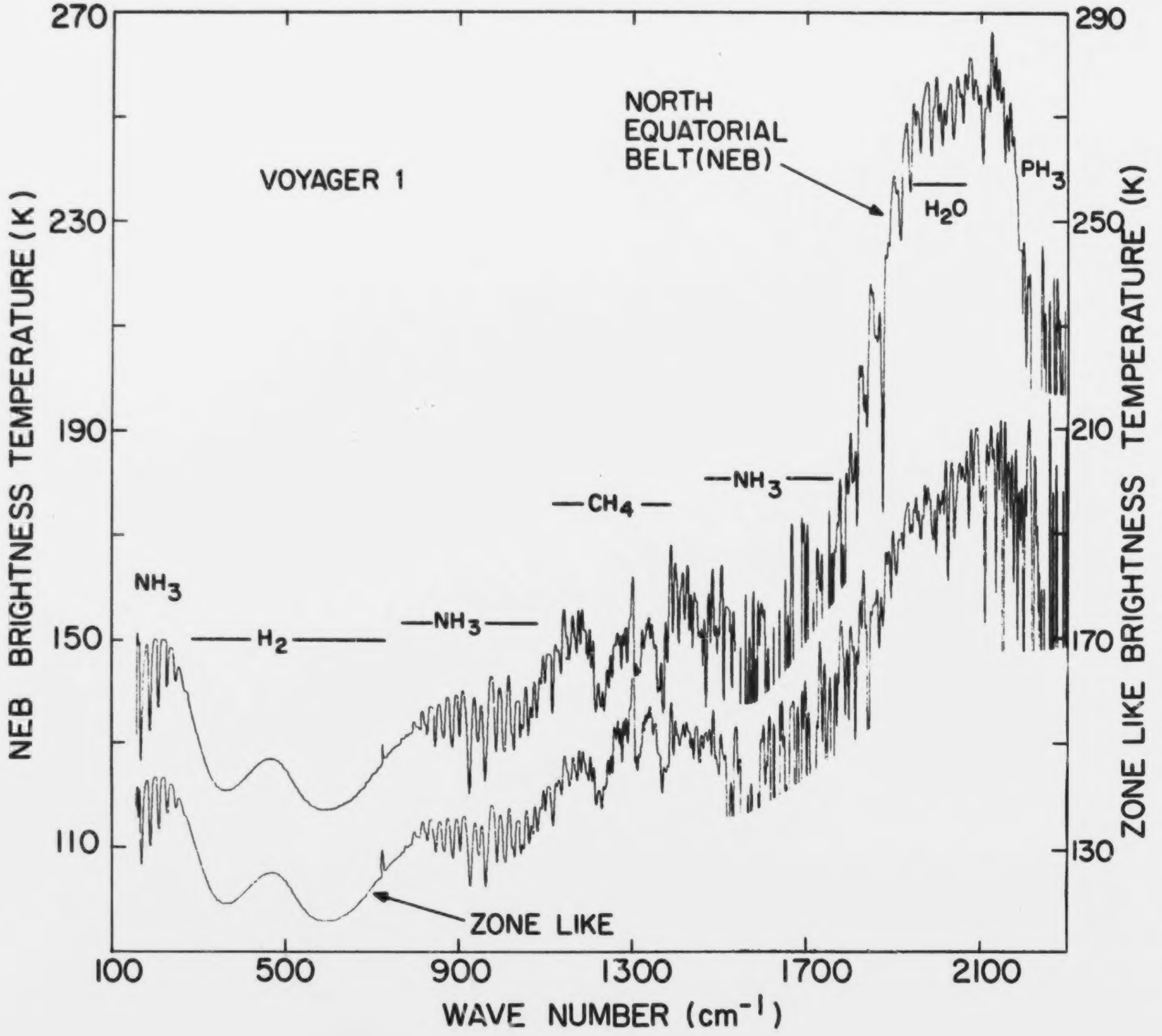

Figure 2. Observed Voyager IRIS spectra of Jupiter for the North Equatorial Belt (NEB) and for a zone-like region.

spectra may be found in Hanel, et al. (1979a), Hanel, et al. (1979b), Gautier, et al. (1981), and Kunde, et al. (1981).

The 5μm Jovian window is transparent to the dominant Jovian gaseous absorbers, H_2, CH_4, NH_3, and in the absence of dense clouds or hazes allows infrared radiation from the deep atmosphere to emerge (Terrile and Westphal (1977), Terrile, et al. (1979)). Only the clouds and/or aerosols provide sufficient absorption to supply the varying opacity for the observed contrasts in the 5μm region. The temperature contrast between the NEB and the zone-like spectra of Fig. 1 is ~ 50K. The 5μm temperature contrast observed by Voyager IRIS is further shown in Fig. 3 for three large scale morphological regions ranging from a clear belt-like area to a zone-like area.

The NEB spectrum is shown on an expanded scale in Figs. 4 and 6. The NEB spectrum divides naturally into two regimes: the 180-1400 cm^{-1} region (Fig. 4) which corresponds to thermal emission from above the visible cloud deck, and the window region from 1700-2300 cm^{-1} (Fig. 6) corresponding to emission from below the visible cloud deck. The altitude region from which the emission originates for each spectral region is illustrated in Figs. 5 and 7, which show the atmospheric level corresponding to unit optical depth. As the maximum contribution to the emergent emission originates near that level, the figures indicate the approximate level of the atmosphere sampled in each spectral interval. The 1/e levels have been computed from a Jovian model atmosphere.

Radiative Transfer Aspects

The monochromatic radiance for vertical viewing for a planetary atmosphere in local thermodynamic equilibrium is

$$I(\nu) = \int B(\nu,T)\, d\tau(\nu,P) \qquad (1)$$

where the integration is through the planetary atmosphere from the top of the atmosphere to the lower boundary, ν is frequency in wave numbers, P is pressure, T is temperature, and B is the Planck function at temperature T. The monochromatic slant path transmittance through an inhomogeneous medium is

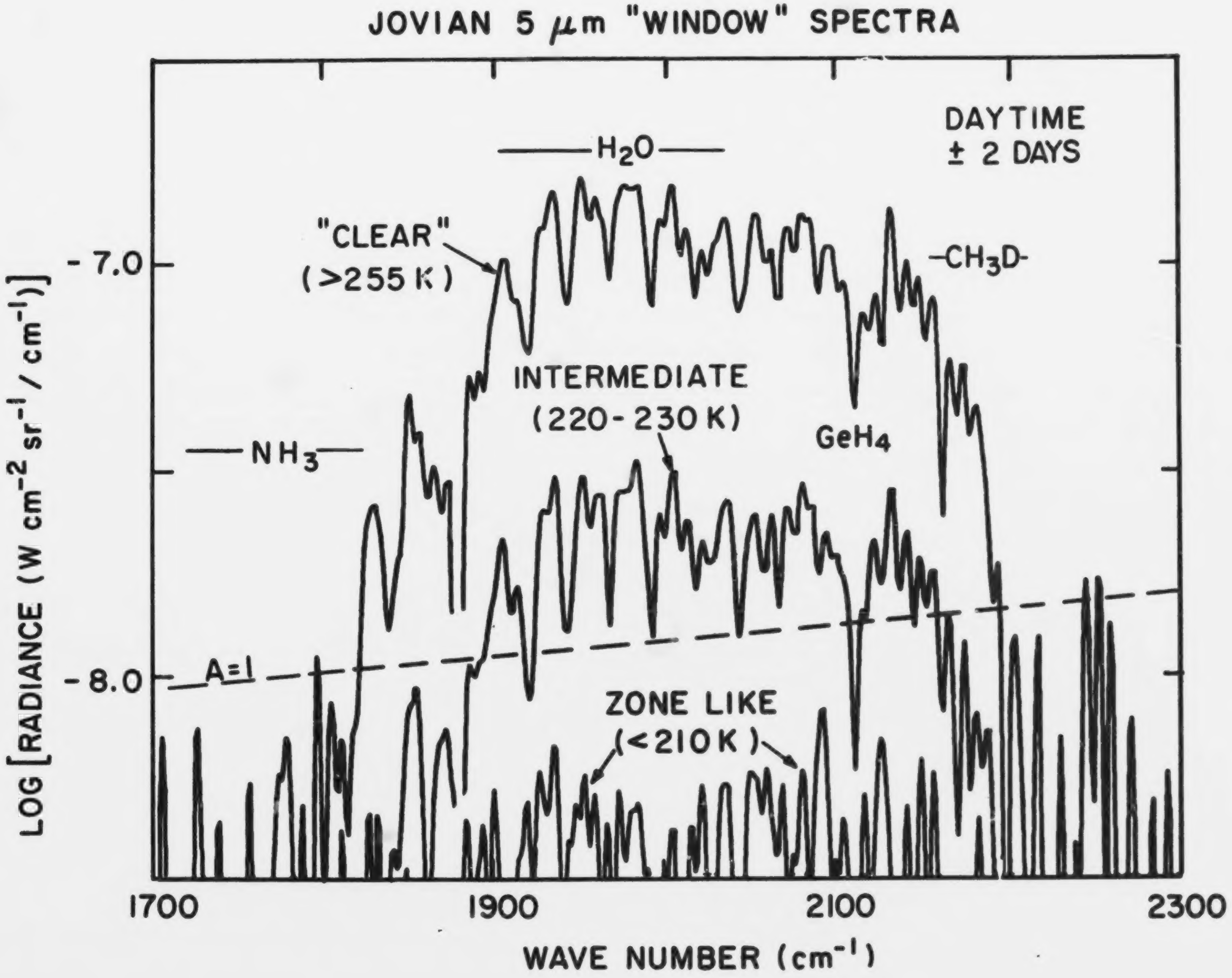

Figure 3. Spatial variation in the 5μm "window" radiation.

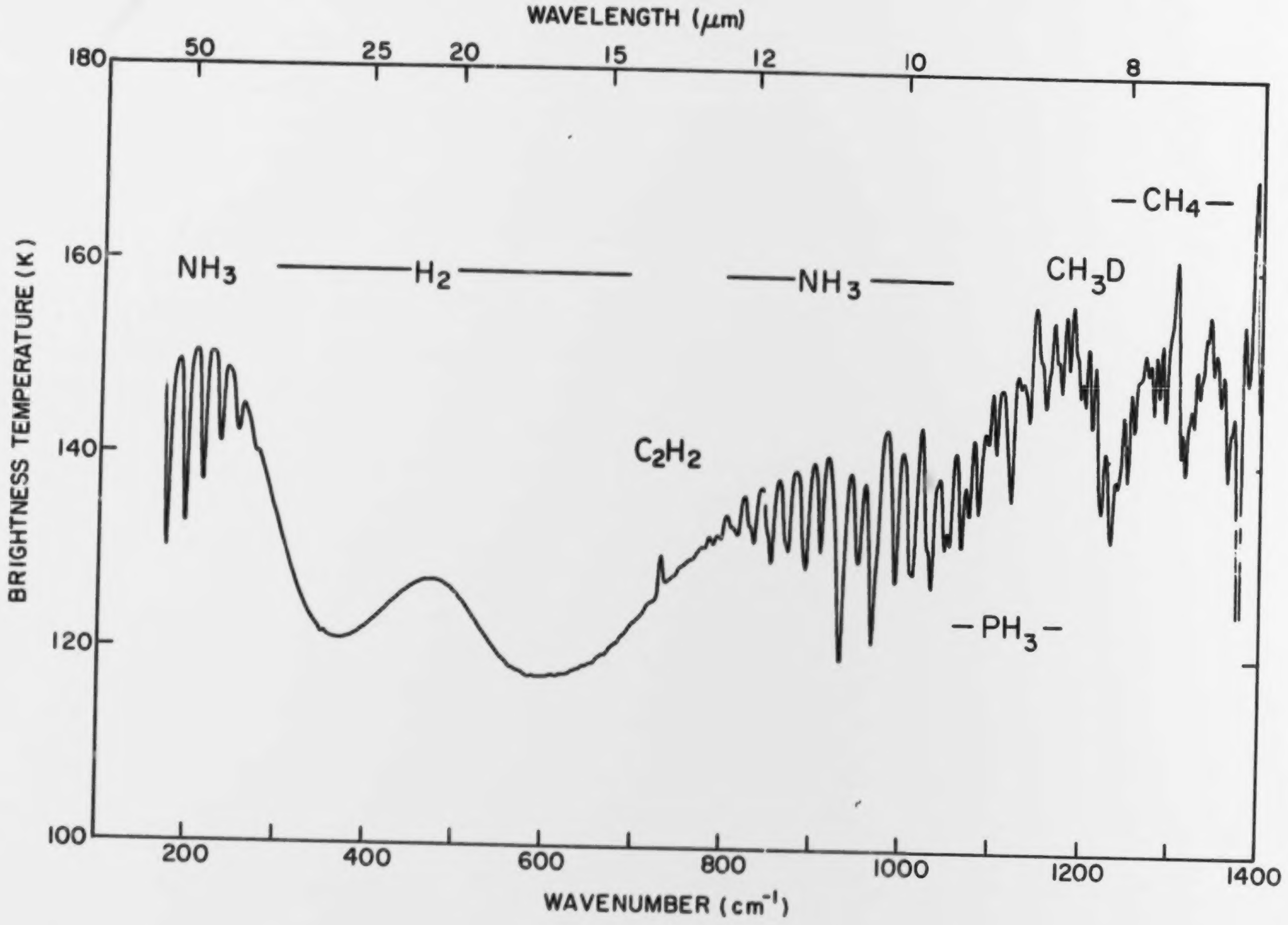

Figure 4. Observed Voyager IRIS spectrum of Jupiter for NEB.

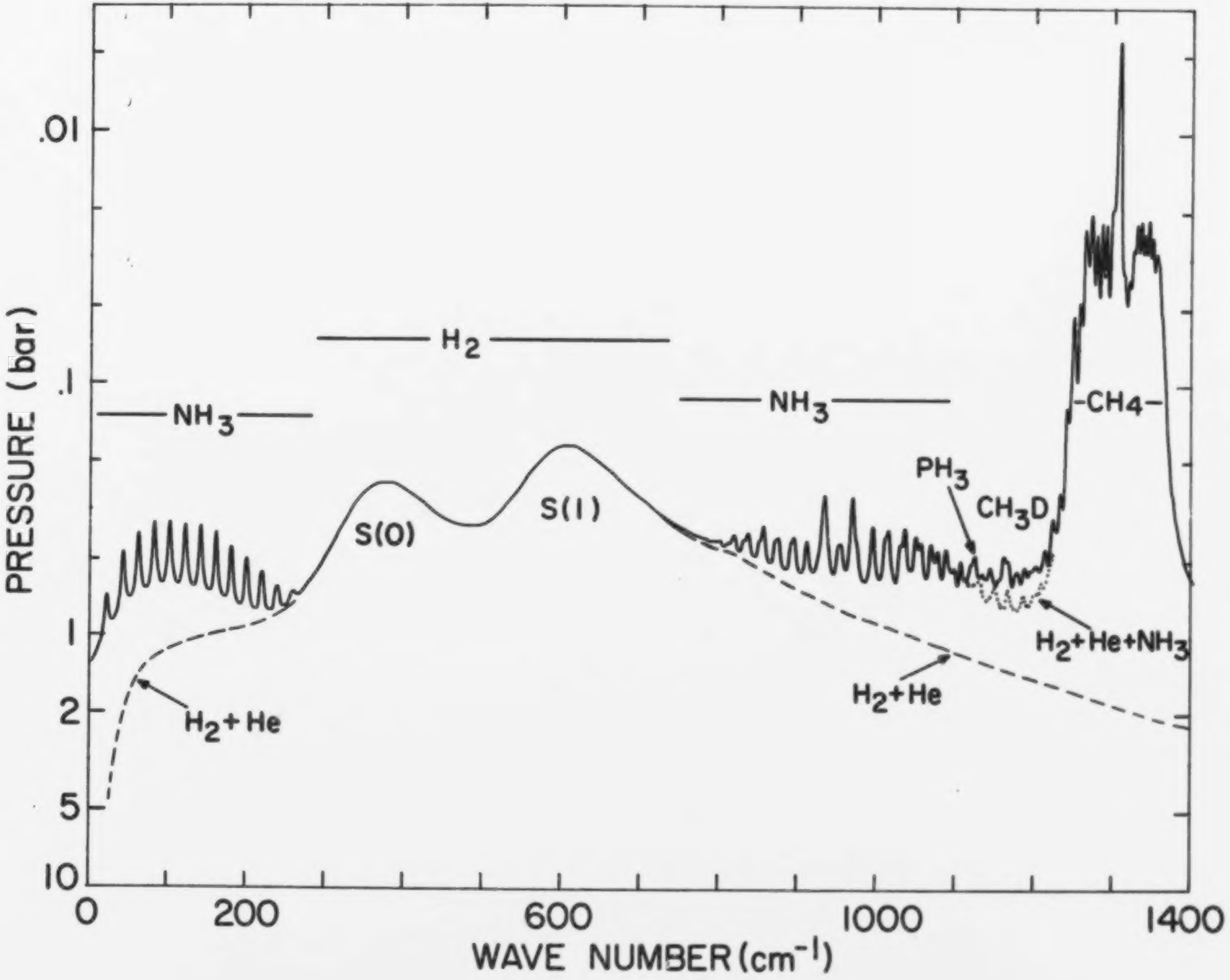

Figure 5. Pressure level for which the optical depth equals unity for the NEB.

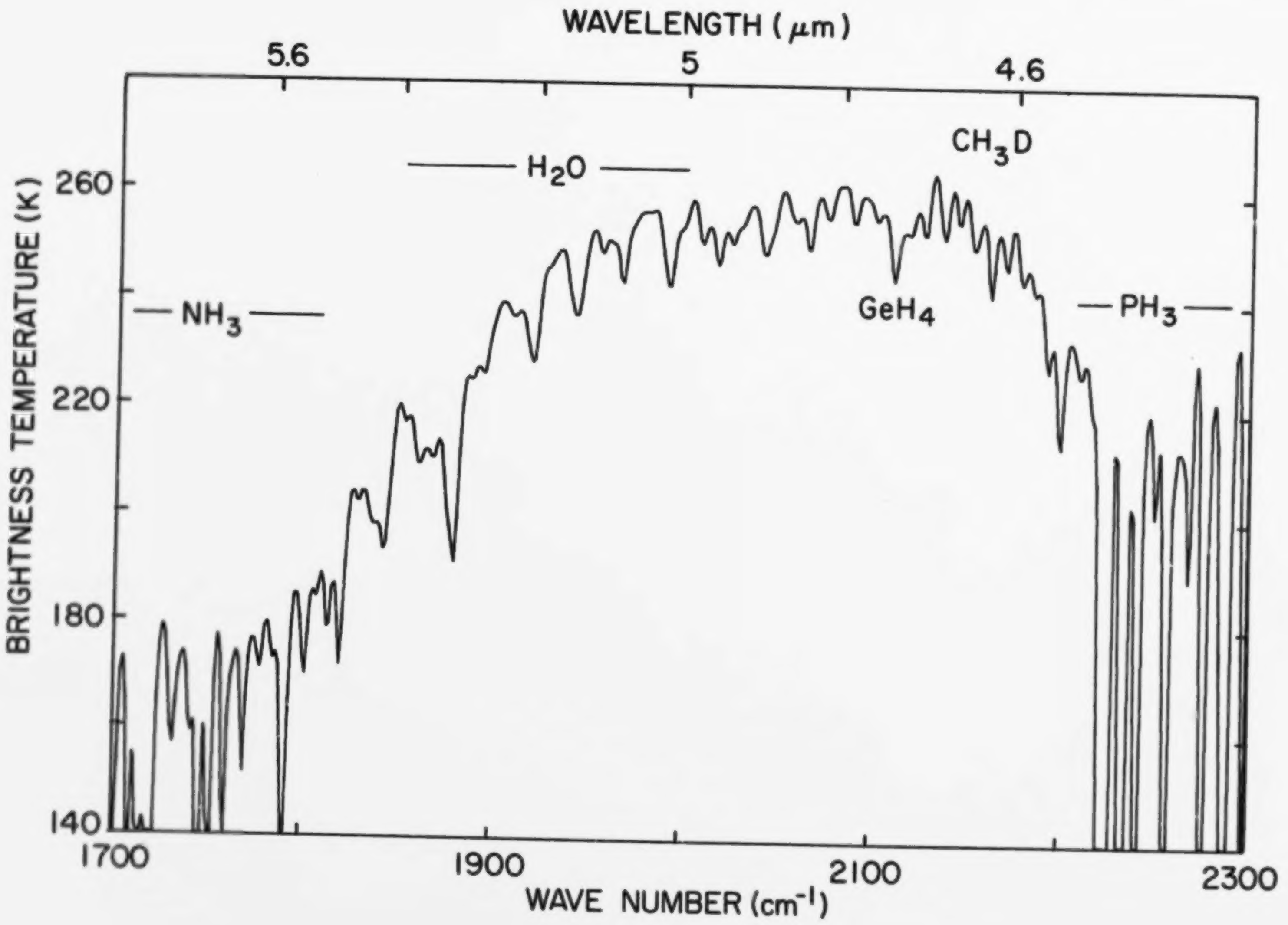

Figure 6. Observed Voyager IRIS spectrum of Jupiter for the NEB.

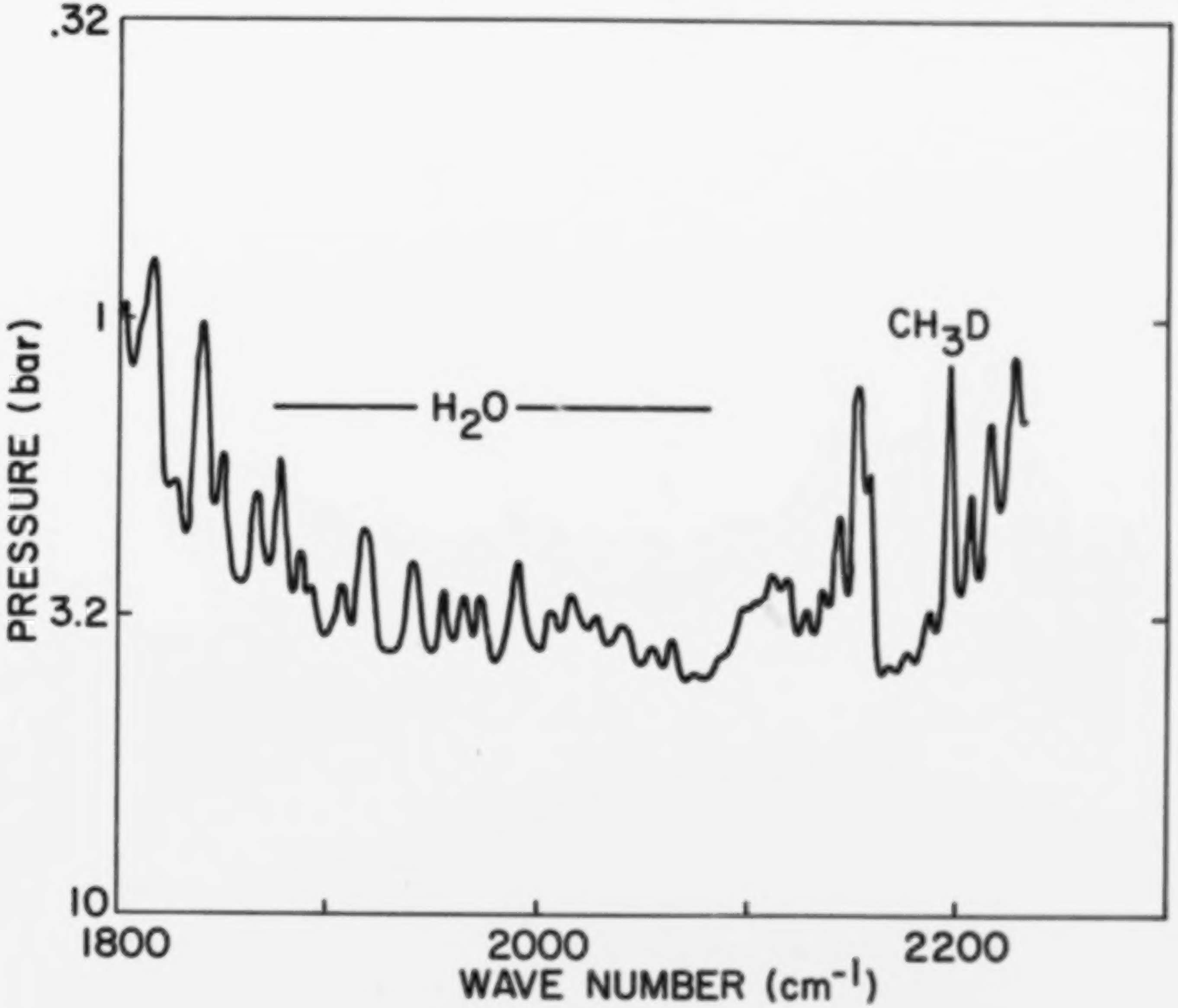

Figure 7. Pressure level for which the optical depth equals unity for the NEB.

$$\tau(\nu,P) = \exp\left[-\sum_i \int k_\nu^i(P,T)du_i\right] \qquad (2)$$

where the total molecular absorption coefficient and optical path length for the i-th gas are k_ν^i and u_i, respectively. The total molecular absorption coefficient at a specific wave number is the summation of the contribution from each of the individual molecular absorption lines, ℓ_ν,

$$k_\nu^i(P,T) = \sum_m \ell_{\nu_m}^i(P,T) \qquad (3)$$

where m is the summation index over the total number of lines for the i-th gas.

An individual molecular absorption line can be described by four parameters: line position (ν_o), integrated line intensity (S), relative line shape (b), and line half-width (α). In terms of these parameters the absorption coefficient for a single line is

$$\ell_\nu(P,T) = S(T)b(\nu - \nu_o, \alpha), \qquad (4)$$

where the relative line shape $b(\nu - \nu_o, \alpha)$ depends on the type of line-broadening mechanism considered. The mixed Doppler-Lorentz line shape is used for $b(\nu - \nu_o, \alpha)$ if the total pressure is less than 100 mb and the distance from the line center, $\Delta\nu = \nu - \nu_o$, is less than 0.2 cm^{-1}. For higher pressures and for $\Delta\nu \geq 0.2$ cm^{-1} the relative line shape is evaluated from the classical Lorentz expression

$$b(\Delta\nu, \alpha) = \frac{\alpha_L}{\pi[\Delta\nu^2 + \alpha_L^2]} . \qquad (5)$$

where α_L is the line half-width due to collisional broadening. The collisional line half-width is

$$\alpha_L(P,T) = \alpha_L(P_o, T_o) \frac{P}{P_o} \left(\frac{T_o}{T}\right)^n \qquad (6)$$

where n is the coefficient relating to the temperature dependence of α. Kinetic theory predicts $n = 0.5$.

Computed monochromatic radiances are convolved with the IRIS instrument function to obtain spectra with a resolution compatible with the measured spectra. The numerical calculation employs a multi-layer atmosphere using direct integration for the molecular absorption of H_2, CH_4, NH_3, PH_3, H_2O, GeH_4, and CH_3D.

Spectroscopic Problems in IRIS Data Interpretation

Shortcomings and uncertainties in our knowledge of line positions, intensities, collisional half-widths, and collisional line shapes limit the scientific interpretation of the IRIS spectra in a number of specific instances. Some specific spectroscopic shortcomings are:

CH_4:

1) theoretical-analytical far wing collisional line shape ($\Delta\nu > 25$ cm^{-1}) for various broadening gases (H_2, He, CH_4, NH_3).

2) laboratory measurement of temperature coefficient n.

NH_3:

1) theoretical line parameters for bands in 1500-2500 cm^{-1} region.

2) theoretical near wing collisional line shape ($\Delta\nu < 25$ cm^{-1}).

3) theoretical-analytical far wing collisional line shape for various broadening gases.

4) laboratory measurement of n.

PH_3: 1) molecular analysis of bands in 1800-2200 cm^{-1} range.

2) laboratory measurement of α_L and η for various broadening gases.

H_2O: 1) laboratory measurement of α_L for H_2O lines in 1800-2100 cm^{-1} range.

Spectroscopic Continuum Problems in Jovian "Windows"

In this section I would like to illustrate only one of the above problem areas, the serious and continuing spectroscopic problem in specifying the proper collisional line shape for the far wings ($\Delta\nu > 25$ cm^{-1}) of pressure-broadened molecular lines. The absorption due mainly to the overlapping of the far wings of lines in strong vibration-rotation bands determines the molecular continuum in four specific regions of the IRIS spectrum. These four atmospheric "windows", evident in the NEB spectrum of Figs. 2, 4 and 6 are at:

1) 1900-2200 cm^{-1} - This "window" is defined on the low wave number side by the far wings of the ν_4 NH_3 band (1500-1700 cm^{-1}), the ν_4 and ν_2 CH_4 bands (1200-1600 cm^{-1}) and the pure rotational lines of H_2 (354, 587 cm^{-1}). The high wave number side is formed by the far wings of the ν_1 and ν_3 PH_3 fundamentals (2200-2400 cm^{-1}), the ν_3 CH_4 fundamental (2900-3100 cm^{-1}), and the fundamental band of H_2 (3800-4800 cm^{-1}),

2) 1375-1425 cm^{-1} - The low wave number contour of this window is due to the ν_4 fundamental of CH_4 (1200-1375 cm^{-1}), and the high wave number side to the ν_2 CH_4 fundamental (1500-1600 cm^{-1}), and the ν_4 NH_3 fundamental (1500-1700 cm^{-1}),

3) 1125-1200 cm^{-1} - The low wave number profile is caused by the strong lines of the ν_2 fundamentals of NH_3 (875-1075 cm^{-1}) and high wave number side by the ν_4 CH_4 fundamental (1200-1375 cm^{-1}), and,

4) 180-250 cm^{-1} - The pure rotational lines of NH_3 (50-150 cm^{-1}) create the low wave number side of this "window", and the rotational-translational lines (354, 587 cm^{-1}) the high wave number side.

In general, the molecular continuum in the above four "window" regions are determined by the far wings of H_2, CH_4, and NH_3.

Although the Lorentz line shape is widely used for atmospheric transmission computations in the far wings of lines, a large body of experimental data now exists indicating substantial deviations from the Lorentz shape for many gases (Winters, et al. (1964); Burch et al. (1970). The line shape problem has been discussed by Birnbaum (1979). For the most abundant Jovian gases, the far wings of H_2 are now known relatively well due to the experimental and theoretical studies of Cohen and Birnbaum (1981); Birnbaum (1978); Birnbaum and Cohen (1976). However, there is no available information on the far wing shape for CH_4-H_2 collisions for the IRIS "window" regions. For NH_3, the only far wing information available is for the 2000-2200 cm^{-1} region, the experimental work of Varanasi and Pugh (1973) indicating a sub-Lorentzian behavior. However, the far wing line shape could not be quantitatively analyzed due to local line absorption by the uncharacterized $2\nu_2^S$ and $2\nu_2^A$ bands of NH_3 at 1882 and 1936 cm^{-1}, respectively. Thus for modeling and spectral analysis studies of Jupiter, the far wing line shape of CH_4 and NH_3 must be assumed. For the IRIS investigations the Lorentz profile was computed out to $\Delta\nu = 100$ cm^{-1}. For larger distances from the line center, the line profile was terminated. This simplistic treatment yields sub-Lorentzian behavior which hopefully represents the actual line shape. Thus the far wing shape of CH_4 and NH_3 is not known to a sufficient accuracy to quantitatively establish the individual contribution of these gases in the above "window" regions. This also means that we cannot absolutely establish the pressure levels in the atmosphere which are being sensed.

The effect of the line cut-off on the emergent spectrum is illustrated in Fig. 8 for the 5μm "window". Increasing $\Delta\nu$ from 200 to 500 cm^{-1} decreases the brightness temperature by ~10K. Another example is given in Fig. 9 for the 8.5μm "window" for $\Delta\nu$ = 100 and 200 cm^{-1}. The resultant difference in the

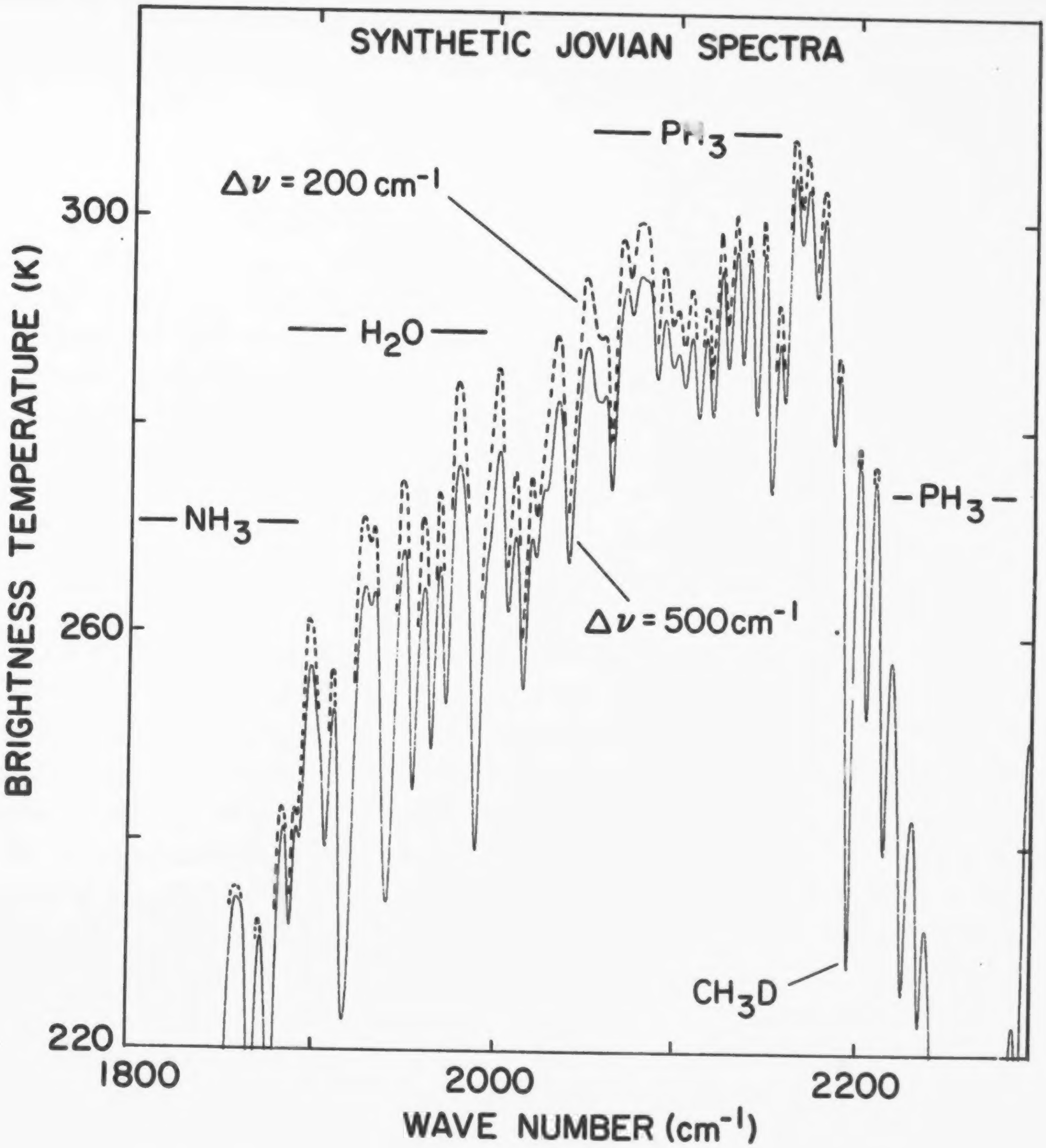

Figure 8. Effect of molecular line cut-off on the 5μm "window" spectrum.

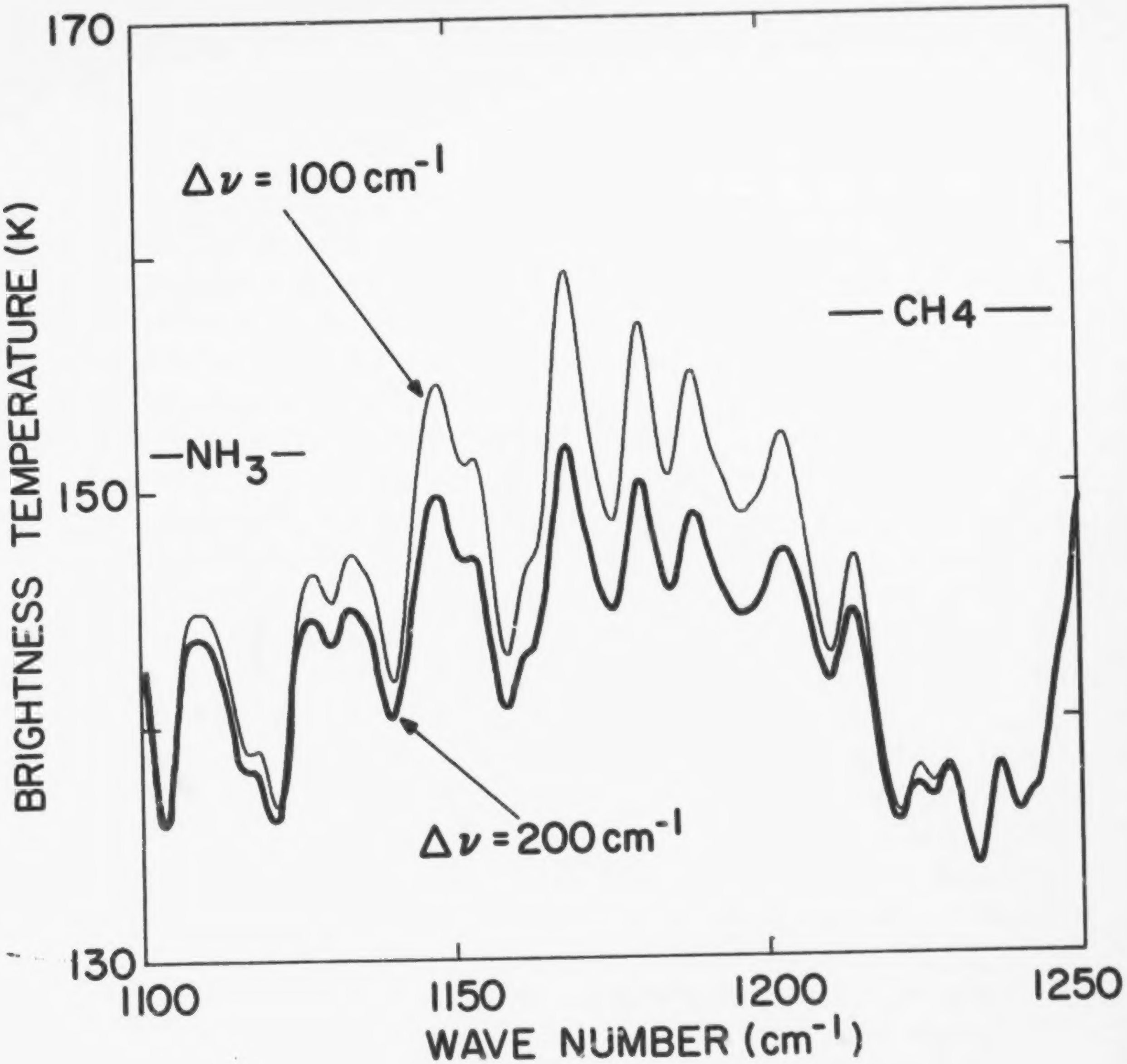

Figure 9. Effect of molecular line cut-off on the 8.5μm "window" spectrum.

continuum of the emergent spectrum at 1148 cm^{-1} is 8K. A systematic error of 8K leads to uncertainty of a factor of two in the derived NH_3 mole fraction from this spectral region. Thus the uncertainty in the far wing line shape is the dominant error in the retrieval of NH_3 distributions at the .9 bar level.

Summary

The scientific interpretation of the Voyager IRIS data is limited in many instances by a lack of knowledge in the basic molecular data. The most significant of these is the far wing collisional line shape of CH_4 and NH_3 as it affects interpretation of all Jovian "window" regions. It is recommended that a focused theoretical and laboratory effort, similar to that already accomplished for H_2, be carried out for these two gases to quantify their far wing line shape.

References

Birnbaum, G., J. Quant. Spectrosc. Radiat. Transfer, 21, 597, 1979.

Birnbaum, G., J. Quant. Spectrosc. Radiat. Transfer, 19, 51, 1978.

Birnbaum, G., and E. R. Cohen, Can. J. Phys., 54, 593, 1976.

Burch, D. E., Philco-Ford Corporation Aeronautic Division publication U-4784, January 31, 1970.

Cohen, E. R., and G. Birnbaum, National Bureau of Standards Report NBSIR 80-2175(R), April, 1981.

Gautier, D., et al., J. Geophys. Res., submitted for publication, 1981.

Hanel, R. A., et al., Science, 204, 972, 1979a.

Hanel, R. A., et al., Science, 206, 952, 1979b.

Kunde, V., et al., J. Geophys. Res., submitted for publication, 1981.

Lewis, J. S., Icarus, 10, 393, 1969.

Terrile, R. J., and J. A. Westphal, Icarus, 30, 274, 1977.

Terrile, R. J., et al., Science, 204, 67, 1979.

Varanasi, P., and L. A. Pugh, J. Quant. Spectrosc. Radiat. Transfer, 13, 1225, 1973.

Winters, B. H., Silverman, S., and W. S. Benedict, J. Quant. Spectrosc. Radiat. Transfer, 4, 527, 1964.

Comment (Birnbaum): The importance of the far-wing line-shape problem for pressure broadened lines deserves additional comment. (1) In order to calculate the absorption coefficient in the trough between neighboring lines, it is necessary to use the theory for overlapping lines; it is not correct just to sum the wing contribution from neighboring lines. The theory gives an additional contribution which takes into account the effect of cross-relaxation. (2) In the far wings, at frequencies removed from most of the strong transitions, one must also deal with the effect of overlapping lines. However, the Lorentz shape, which is adequate for frequencies not too far removed from the resonance frequency, is incorrect in the far wings. Indeed, it can be argued on general grounds that the absorption there must decrease faster than predicted by the Lorentz function. (3) Apart from the problem of pressure-broadened line shape in the far wings and the effect of overlapping lines, one should consider the possibility of collision-induced absorption. Although this absorption is generally very weak compared with that produced by allowed transitions, the latter becomes very weak in the far wings.

Blank Page

Jupiter and Saturn from 2 to 6 μm

Harold P. Larson (Univ. of Arizona)

I. Introduction

This paper summarizes some recent earth-based spectroscopic observations that support current compositional and structural analyses of planetary atmospheres. The lack of appropriate laboratory measurements frequently prevents complete use of these astronomical data, however. I will therefore identify some major interpretive opportunities where laboratory spectroscopists can become productively involved with planetary astronomers.

II. Overview of the IR Spectra of Jupiter and Saturn

The overview of Jupiter's IR spectrum in Figure 1 illustrates a fundamental constraint to observations of the outer planets: atmospheric studies are restricted to narrow, isolated windows defined by the planetary absorbers H_2, CH_4, NH_3, and PH_3. Some of these planetary windows, such as at 1.6 μm, are accessible in ground-based observations, but others, such as at 1.9 and 2.7 μm, are totally obscured by terrestrial H_2O. For this reason, high altitude sites, such as aircraft, balloons, and spacecraft, have become essential for IR spectral studies of the outer planets.

Saturn's composite IR spectrum would be similar to that of Jupiter in Figure 1. One important difference is Saturn's lack of NH_3 absorption, which leads, for example, to a wider 3 μm atmospheric transmission window on Saturn. Another difference is that Saturn's 5 μm thermal emission spectrum is scaled to a lower temperature (T ~ 190 K) than for Jupiter (T ~ 300 K).

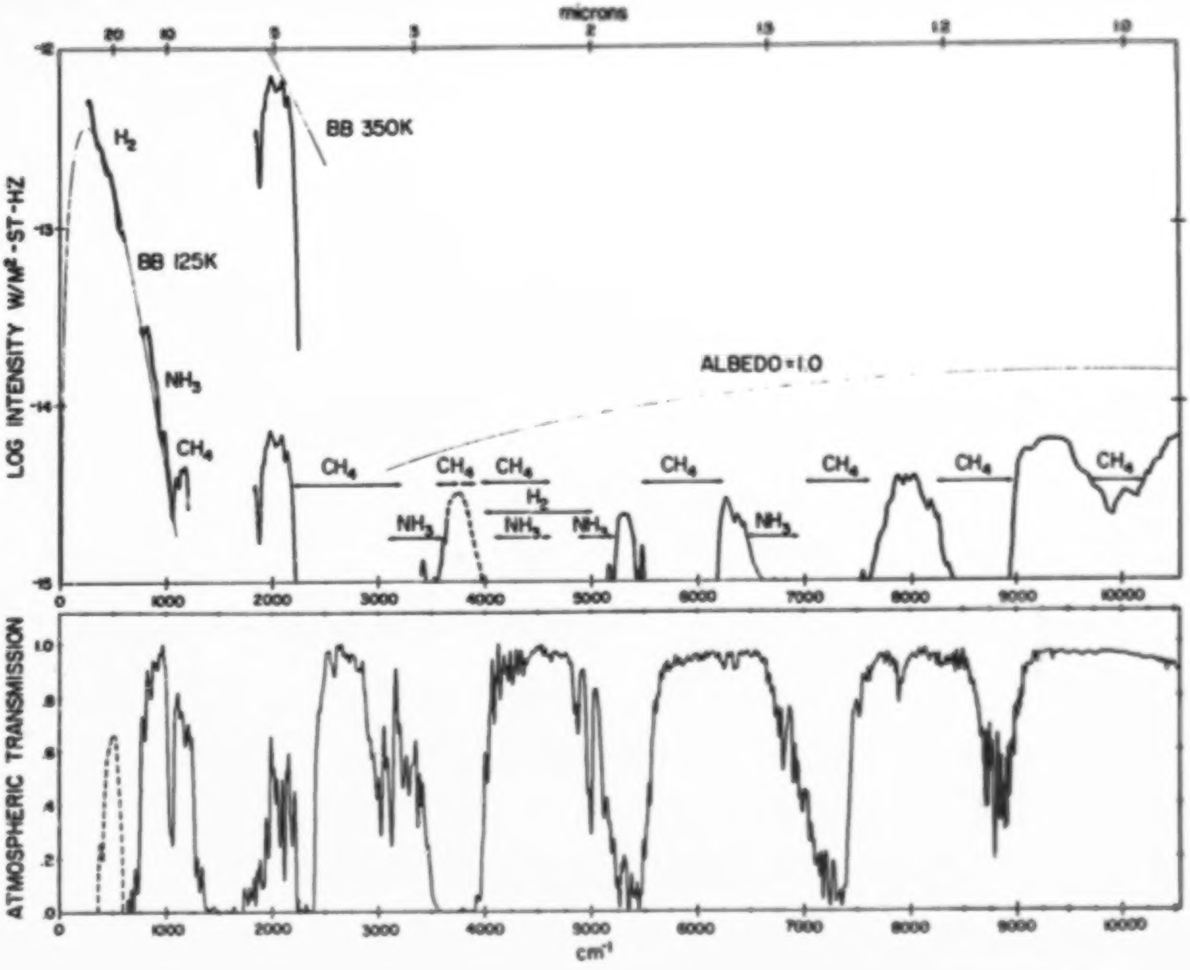

Figure 1. Top spectrum: Composite IR spectrum of Jupiter assembled from many sources. Bottom spectrum: The transmission of the earth's atmosphere under typical mountain-top conditions. Figure reproduced from Ridgway et al. (1976).

For the purposes of this paper it is convenient to identify three groups of spectral features in the planetary data:

Group A: Continuum features assigned to the atmosphere's major spectroscopically active species. These molecules (H_2, CH_4, NH_3) have been known for decades, but their spectral features are still being interpreted in terms of abundance, pressure, temperature, mixing ratios and elemental ratios. The distinguishing requirement of this group, as far as laboratory measurements are concerned, is that the detailed spectral behavior of each of these molecules must be understood for conditions appropriate to real planetary atmospheres (reduced T, scattering, high abundance).

Group B: Obvious, non-saturated bands (Q-branches, rotational lines) produced by trace constituents with mixing ratios with respect to H_2 between 10^{-5} and 10^{-9}. Their identifications are firm because of positional information, but the molecules may not be sufficiently analyzed to permit precise quantitative measurements of other atmospheric parameters (T, P, abundance). Most recent detections fall into this group. For example, several obvious PH_3 bands exist in Saturn's airborne 3 µm spectrum (Larson et al. 1980),but their assignment to specific overtone or combination modes is uncertain.

Group C: Vague features (shoulders, bumps, isolated linds, etc.) that do not provide enough positional information to support assignment to any molecule. This group is most likely to provide exciting, future discoveries as better observational data are produced and laboratory comparisons are extended to more exotic species.

The following sections of this paper review the major regions of transparency in the atmospheres of Jupiter and Saturn in terms of these three groups of spectral signatures.

III. Near IR Region ($\lambda < 2\mu m$)

There is no lack of observational data in this wavelength region because the planetary atmospheric transmission windows coincide with those in the earth's atmosphere (see Figure 1). Although high spectral resolution is required for most analyses, the composite of spectra in Figure 2 demonstrates the value of broad spectral bandwidth, low resolving power observations for comparing the hydrogen-rich atmospheres of the outer planets. Analyses of these data represent the use of Group A spectral behavior in interpreting planetary observations. Some general conclusions are:

1. Methane is the major, spectroscopically active constituent in the atmospheres of all of the outer planets. Each planetary spectrum mimics the characteristics (isolated transmission windows) of a long path laboratory CH_4 spectrum (bottom trace in Figure 2).

2. Molecular hydrogen also produces continuum features in the near-IR, especially between 2-3 μm. For example, the absence of a 2 μm CH_4 window on Uranus is because of the high H_2 abundance in this atmosphere.

3. Each spectrum is unique, although each is produced by the same known constituents (H_2, CH_4, and, on Jupiter, NH_3). The obvious differences in their continuum features are due to the different abundances, scattering mechanisms, and vertical structures characterizing each atmosphere.

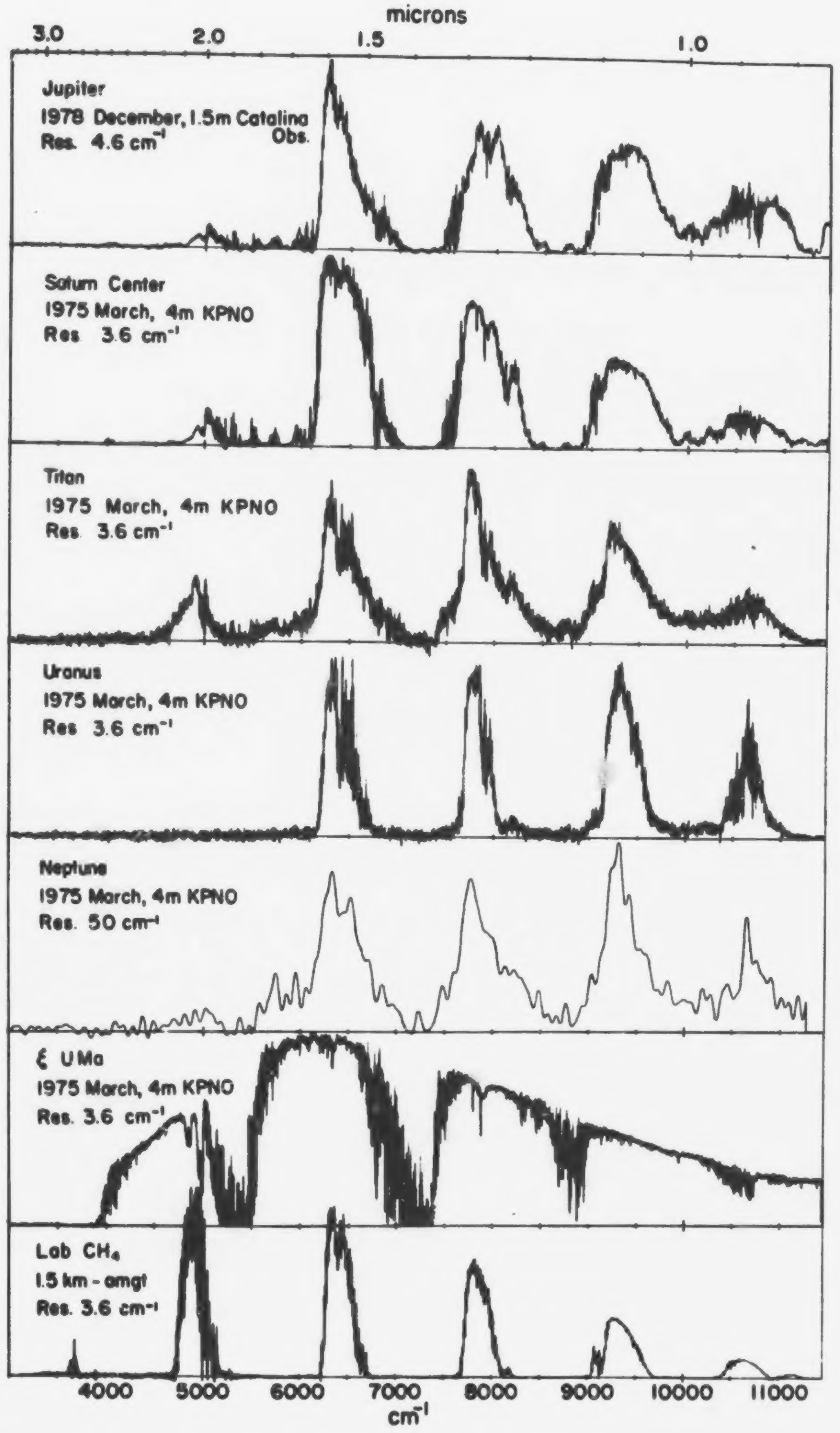

Figure 2. Comparison of the near-IR spectra of the outer planets and Titan. All spectra were produced by a Fourier spectrometer. (reproduced from Fink and Larson (1979).

Additional details on the interpretation of these data, and the corresponding limitations of available laboratory measurements, are discussed by Fink and Larson (1979).

At higher spectral resolution, attention turns to Group B spectral features and the study of trace atmospheric constituents. Historically, however, the near-IR spectral region has been unproductive in terms of new detections on the outer planets. Requirements include very high spectral resolution ($R \leq 0.1\ cm^{-1}$), complete knowledge of the CH_4 and NH_3 spectra, and accurate line measurements of candidate species. In practice, ever higher resolution just reveals more CH_4 lines. This spectrum must first be better understood (interlopers, pressure broadening effects, temperature-induced intensity anomalies, etc.) before the observational data can be used for more complex modeling tasks (scattering mechanisms, cloud structure, etc.). The $3\nu_3$ CH_4 band near 1.2 μm has been exhaustively studied, for example, but even modest agreement on the CH_4 abundance has not yet been achieved (see discussion in Ridgway, Larson and Fink 1976).

Figure 3 summarizes the trace constituent detection possibilities available in the 1.6 μm planetary window. At this moderate spectral resolution ($3.6\ cm^{-1}$), only upper limits to numerous species have been determined. In Figure 4, however, new observations of Saturn at $0.09\ cm^{-1}$ (Davis et al. 1980) provide unprecedented sensitivity for searching for trace constituents.

IV. 2-3 μm Region

Very little is known about the spectra of the outer planets in this wavelength region. As the data in Figure 1 demonstrate, the two regions

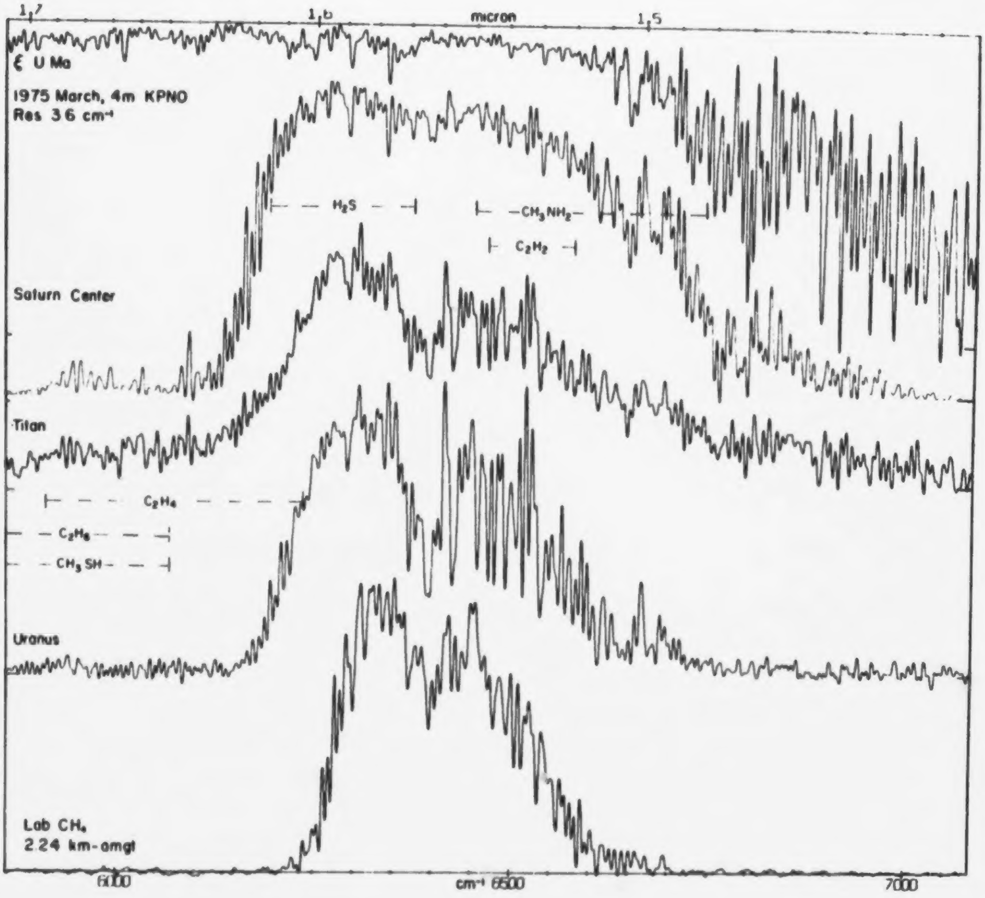

Figure 3. Illustration of the high resolution spectral detail in the 1.6 μm CH_4 window in the atmospheres of the outer planets. Telluric absorptions are identified with the help of the solar-type comparison star. All planetary absorptions seem due to CH_4. The locations of numerous potential trace constituents are marked, but none of them has yet been detected in this region. Figure reproduced from Fink and Larson (1979).

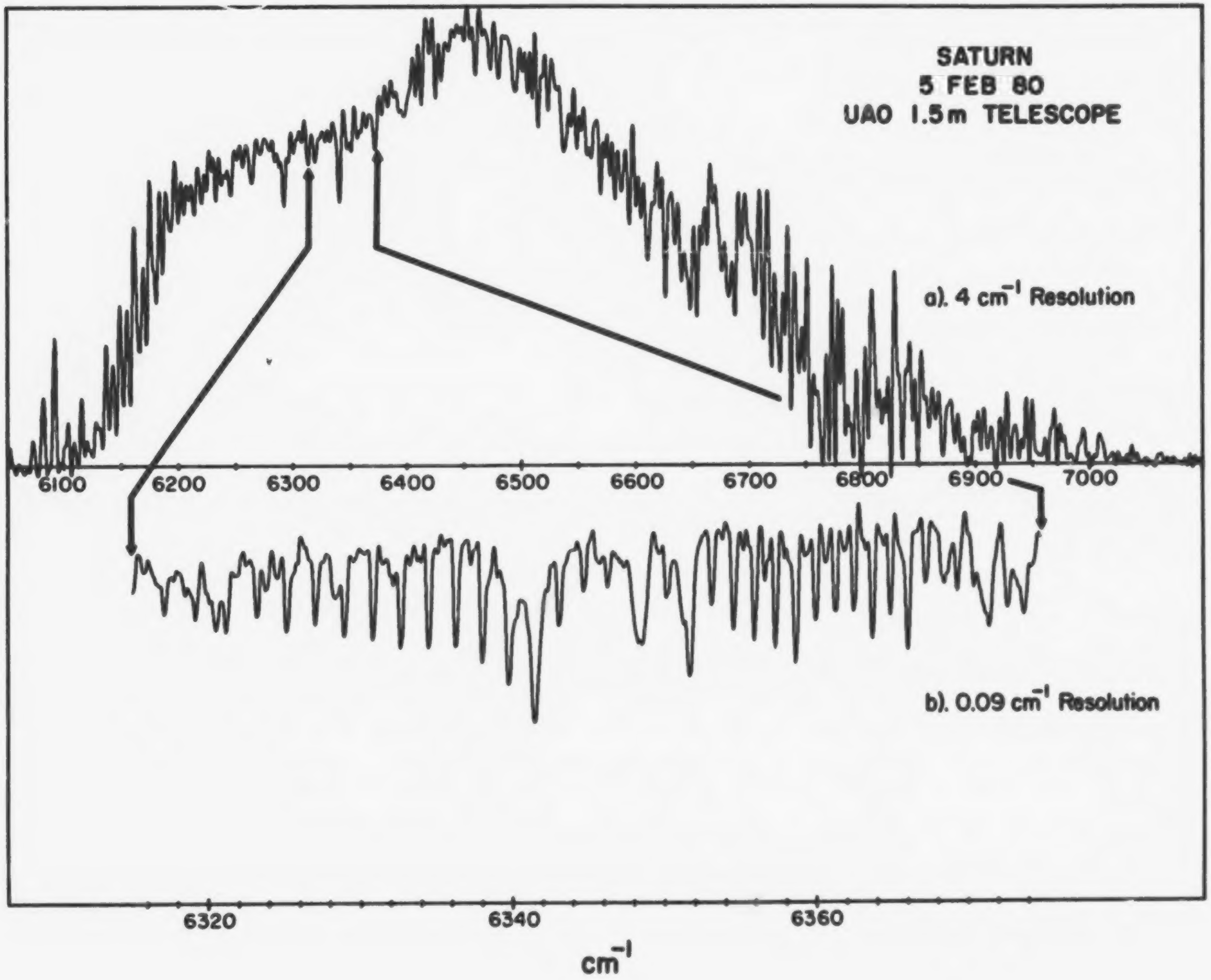

Figure 4. Recent high resolution observations of Saturn using a new Cassegrain Fourier spectrometer. The improved combination of spectral resolution and signal-to-noise in these data, compared to previous observations, means that searches for trace constituents (see possibilities in Figure 3) can be pushed to lower abundances. Figure reproduced from Davis et al. (1980).

of transmission near 2.0 and 3.0 μm on Jupiter are completely masked by terrestrial H_2O. Other objects in the outer solar system with H_2/CH_4 atmospheres would be similarly obscured. The existence of Jupiter's 2 and 3 μm windows was first demonstrated by Danielson (1966) using a balloon-borne spectrometer. His spectrum (Figure 5) emphasized the importance of the 1-0 pressure-induced spectrum of H_2 in interpreting Jupiter's continuum spectrum. Molecular hydrogen is totally absorbing between 2.1 and 2.5 μm, and the wings of this band are potentially significant diagnostic tools for establishing such atmospheric parameters as T, He/H, H_2 abundance, etc. Even today, however, these interpretive possibilities have not been fully exploited. Continuous spectral coverage of the 2-3 μm region at high spectral resolution has only recently been achieved, and, again, the incomplete knowledge of the spectrum of CH_4 is delaying interpretation of the H_2 spectrum.

Figures 6 and 7 contain high altitude spectra of Jupiter and Saturn in the 2-3 μm region. The spectral resolution of these data, compared to that in Figure 5, represents a tremendous increase in information content. All three groups of spectral features are present in these planetary spectra. Molecular hydrogen (Group A) contributes continuum features that help form the planetary windows, but broad, saturated CH_4 bands must also be included in the analysis of the wings of the H_2 lines. The detections of PH_3 (Larson _et al_. 1980) and C_2H_6 (Bjoraker _et al_. 1980) on Saturn at 3 μm are very obvious examples of Group B features. Strong, unassigned lines in Saturn's spectrum near the CH_4 ν_3 band at 3.3 μm illustrate the nature of Group C features. Other molecules important to the detailed chemical structure of a planetary atmosphere, such as NH_3, H_2S, HF, and HCN, have bands coincident with these planetary windows.

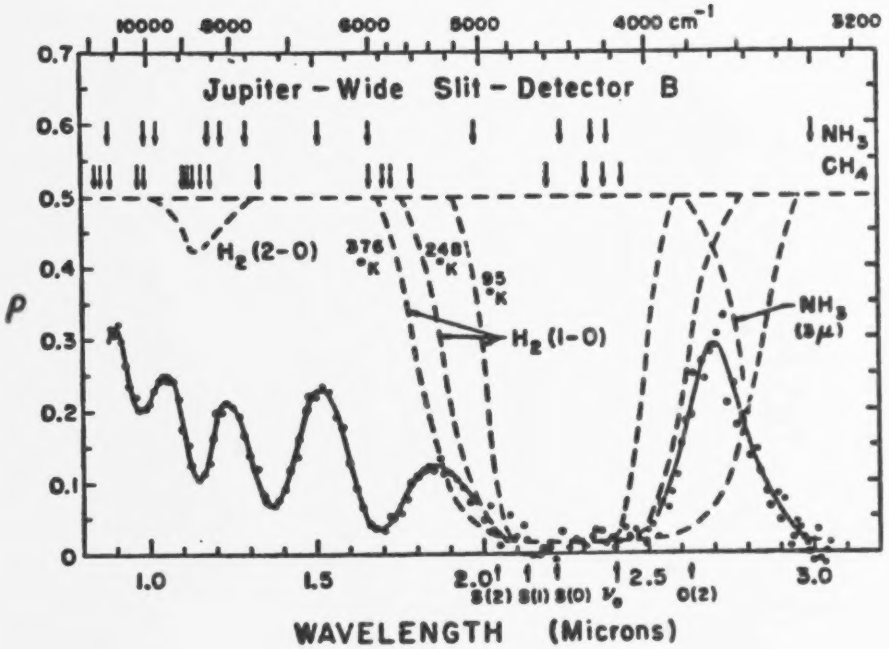

Figure 5. The IR spectrum of Jupiter recorded from the Stratosphere II balloon (reproduced from Danielson (1966)).

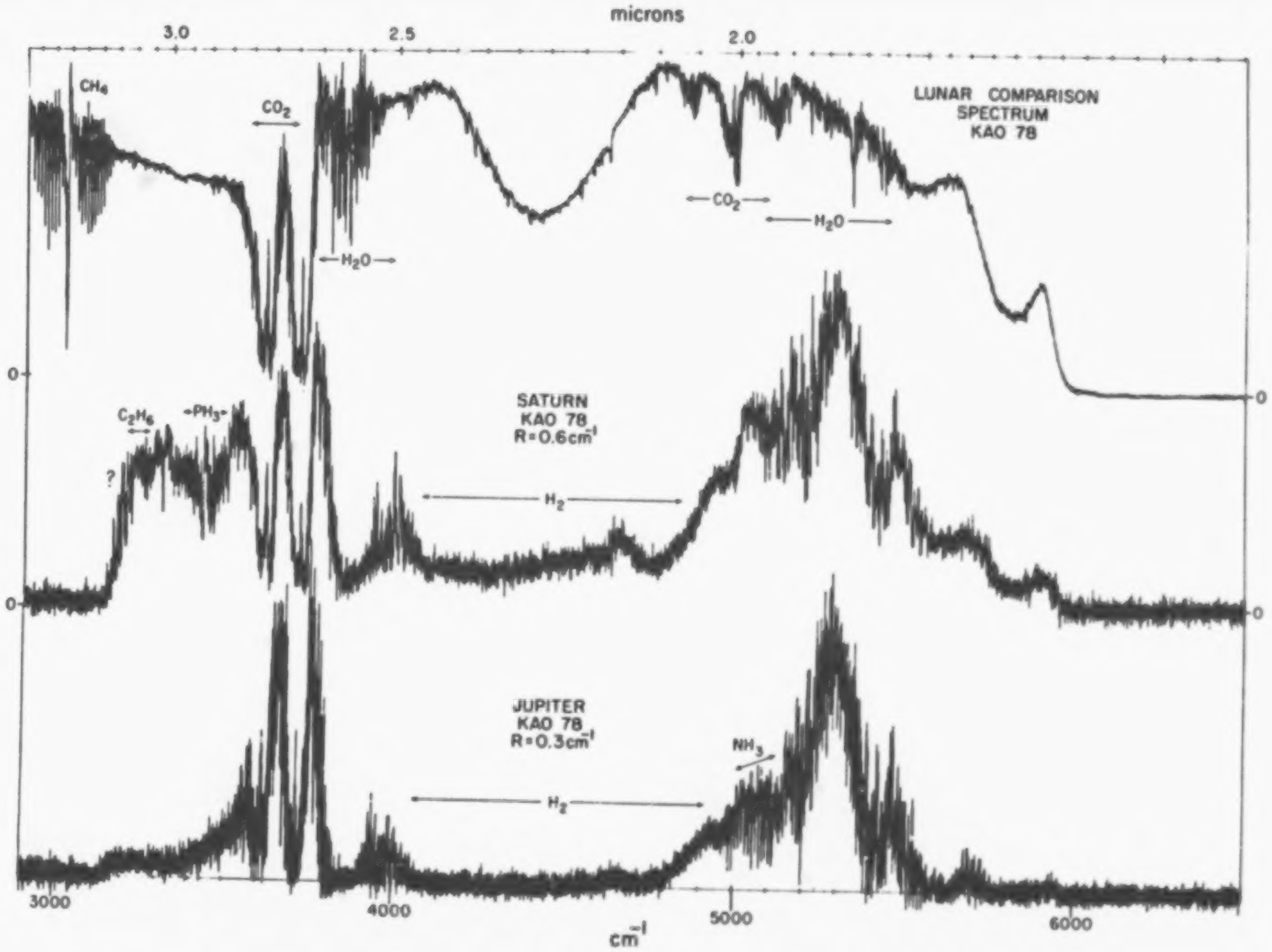

Figure 6. Comparison of the spectra of Jupiter and Saturn in the 2–3 μm region. A Fourier spectrometer was used on the Kuiper Airborne Observatory to record these data. The lunar comparison spectrum indicates instrumental response and telluric absorptions for the planetary observations. These are the only high resolution observations of either planet that provide continuous spectral coverage in this wavelength region.

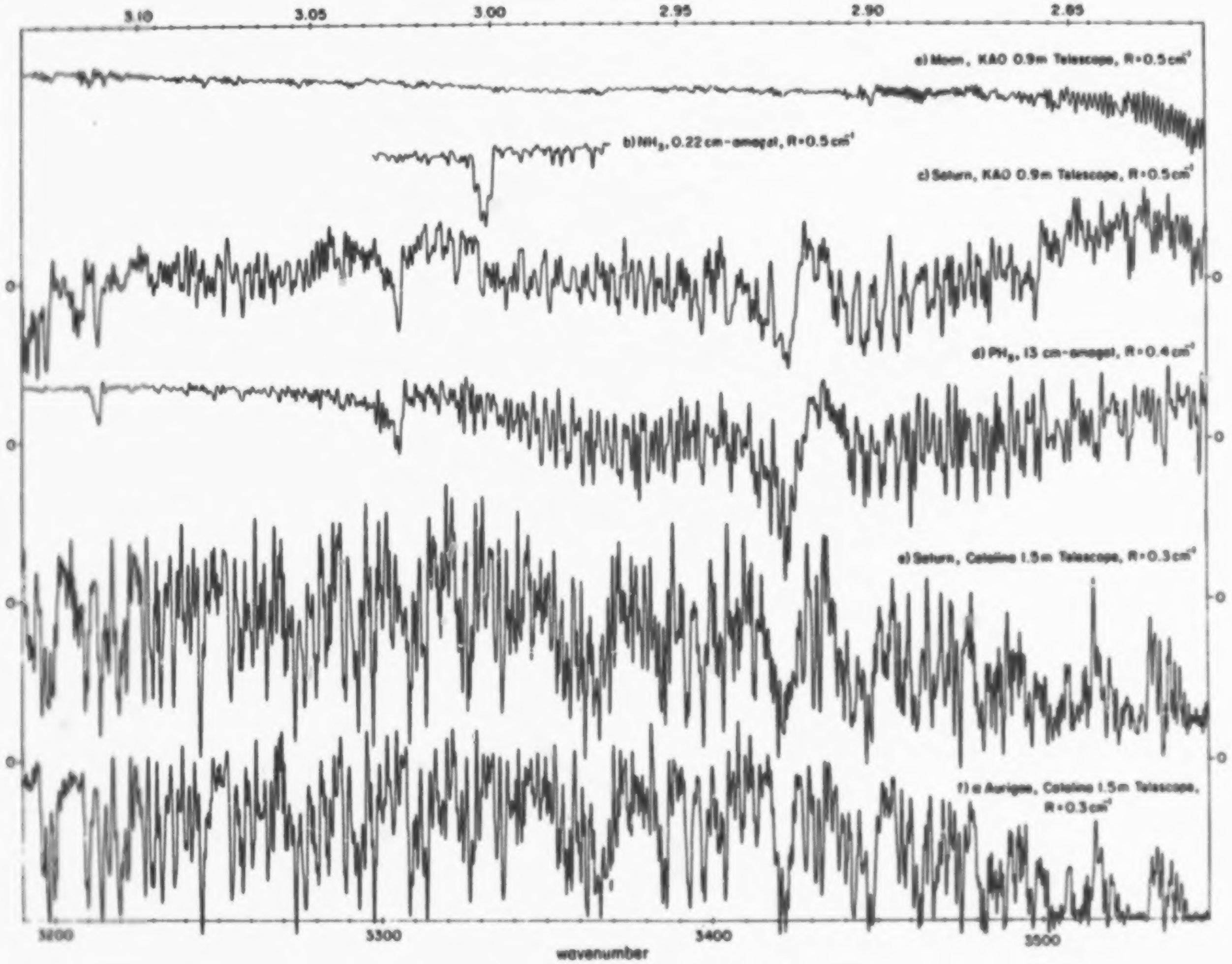

Figure 7. Comparison of high resolution observations of Saturn in the 3 μm region from a conventional telescope and from the Kuiper Airborne Observatory. These spectra are excerpts from the data in Figure 10. The high altitude observations permit analyses of the presence and distribution of several key molecules in Saturn's atmosphere, including NH_3, PH_3 and C_2H_6. Figure reproduced from Larson et al. (1980).

Clearly, the availability of high resolution spectroscopic observations from the Kuiper Airborne Observatory has added an important, new dimension to planetary astronomy.

Figures 8 and 9 illustrate some laboratory comparison measurements that were used in analyses of the planetary spectra in the previous two figures. The C_2H_6 data, in particular, emphasize the frequently encountered situation where only weaker, more obscure molecular bands are coincident with planetary windows. A more favorable situation exists for searching for HCN on Saturn. Its ν_3 fundamental mode coincides with Saturn's 3 μm window, thereby permitting a very sensitive upper limit determination (0.1 cm-amagat, Larson et al. 1980). By contrast, NH_3 obscures the 3 μm region of Jupiter's spectrum (see Figure 6), and the test for HCN in its atmosphere was 100x less sensitive (Treffers et al. 1978), since a much weaker HCN band near 5 μm had to be used instead.

V. 3-6 μm Region

THe spectral composite in Figure 10 compares ground-based and airborne observations of Jupiter and Saturn in the 3-6 μm region. A portion of the 5 μm planetary transmission windows is accessible from conventional telescopes, but complete coverage of the spectra of these planets requires the Kuiper Airborne Observatory and the high resolution spectrometers that it accommodates.

Studies of Jupiter at 5 μm have been especially exciting since its thermal flux emanates from holes in its cloud cover, thereby revealing a chemical regime that would otherwise remain hidden from remote spectral observations. Many of the recent detections and stringent upper limits to

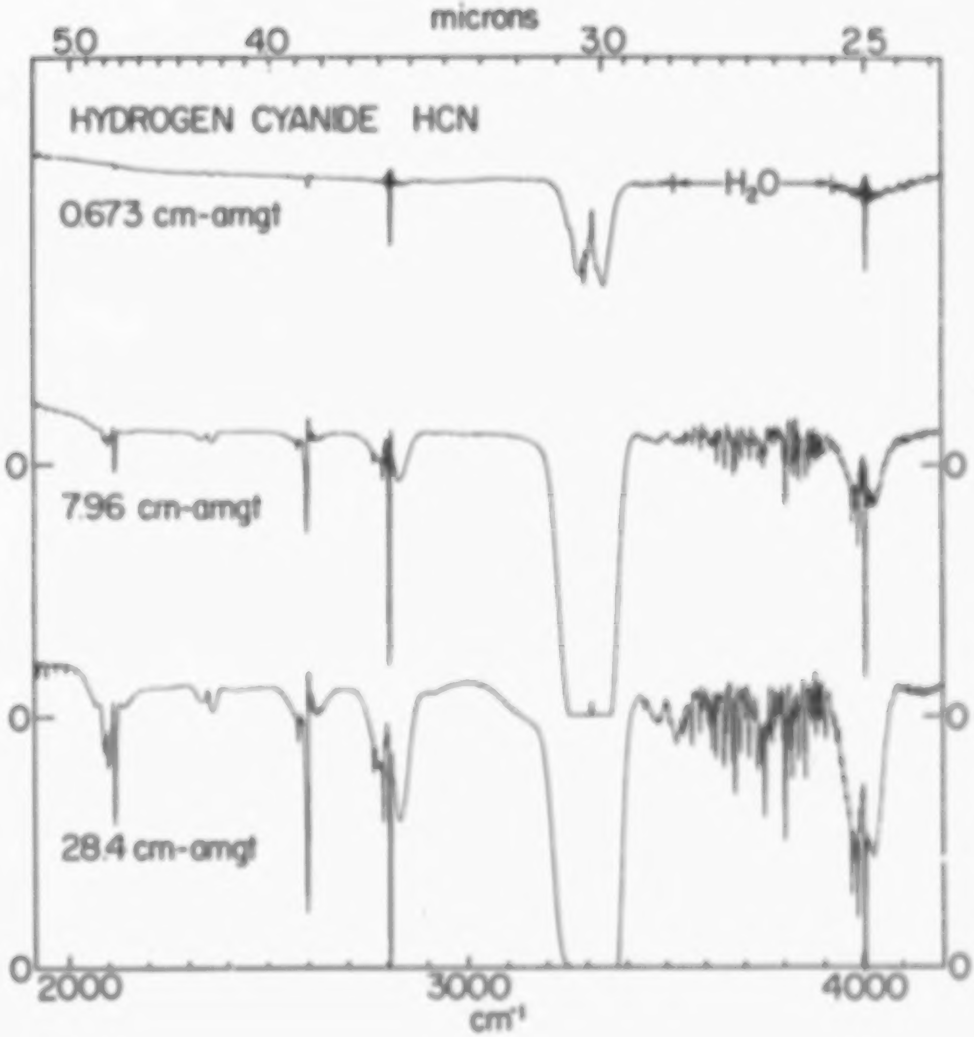

Figure 8. Laboratory spectra used to establish upper limits to HCN on Jupiter and Saturn.

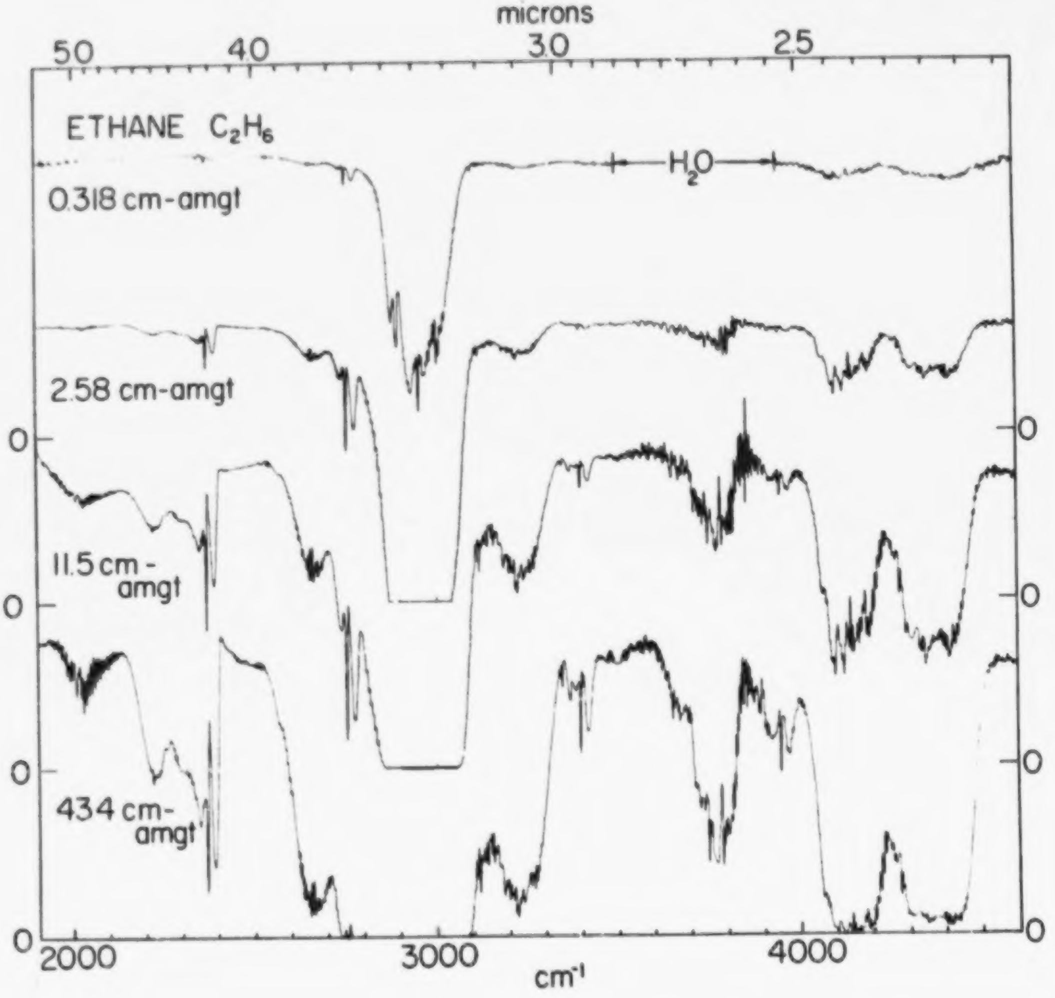

Figure 9. Laboratory spectra used to study C_2H_6 on Jupiter and Saturn.

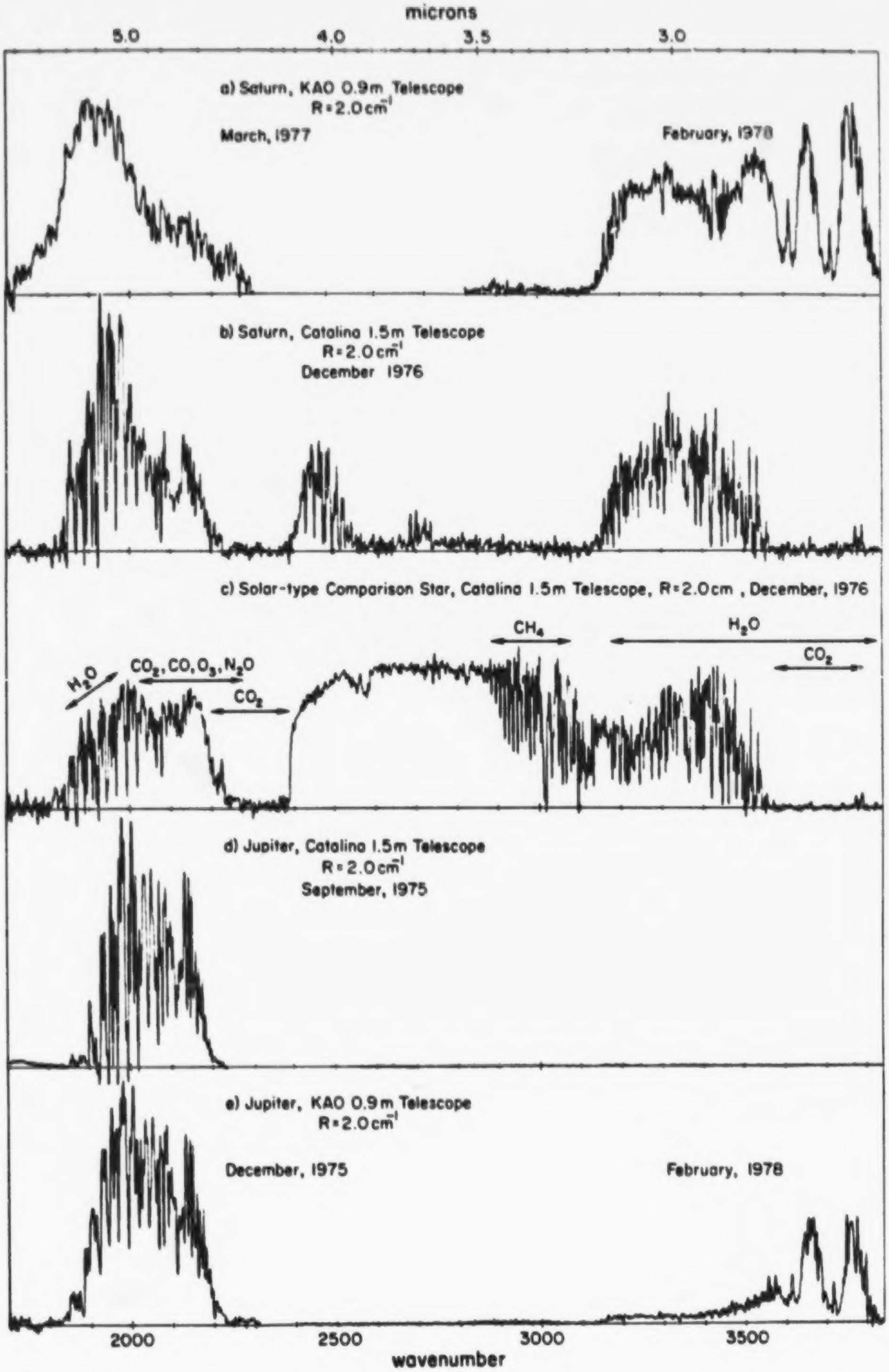

Figure 10. Comparison of the middle-IR spectra of Jupiter and Saturn from conventional and airborne telescopes. In this region the planetary windows are defined by CH_4, PH_3 and, on Jupiter, NH_3 absorptions. Only airborne observations permit complete spectroscopic coverage of these planetary windows. Figure reproduced from Larson et al. (1980).

Jovian trace atmospheric constituents are products of these observations in the thermal IR (see reviews by Ridgway, Larson and Fink 1976, and Larson 1980). The combination of high spectral resolution and high altitude has been particularly rewarding as regards Group B spectral features. Figure 11 compares two airborne spectra of Jupiter at 5 μm at spectral resolutions of 2.5 and 0.5 cm^{-1}, respectively. The spectroscopic detection and analyses of such molecules as H_2O, PH_3 and GeH_4 would not have been possible without NASA's support of high resolution planetary spectroscopy from aircraft.

The observations of Saturn at 5 μm in Figure 10 are very recent results. Figure 12 exhibits these data on an expanded wavelength scale. This figure also includes supporting laboratory measurements used in the detections of CH_3D (Fink and Larson 1978) and PH_3 (Larson _et al_. 1980) on Saturn. Improved instrumentation and continued applications on the Kuiper Airborne Observatory should produce even higher quality data in the 1980's. This means that even more opportunities will become available for spectral analyses, with new demands upon laboratory measurements oriented to conditions in planetary atmospheres.

VI. Major Requirements Upon Laboratory Data

The following molecules deserve special attention by laboratory spectroscopists interested in planetary applications.

1. CH_4: This molecule needs to be studied at all wavelengths, particularly in the 2-3 μm region where planetary observations are just becoming available.

2. H_2: The use of the 1-0 pressure-induced dipole spectrum of H_2 to generate atmospheric sturcture parameters is now feasible, given attention to the CH_4 analysis above.

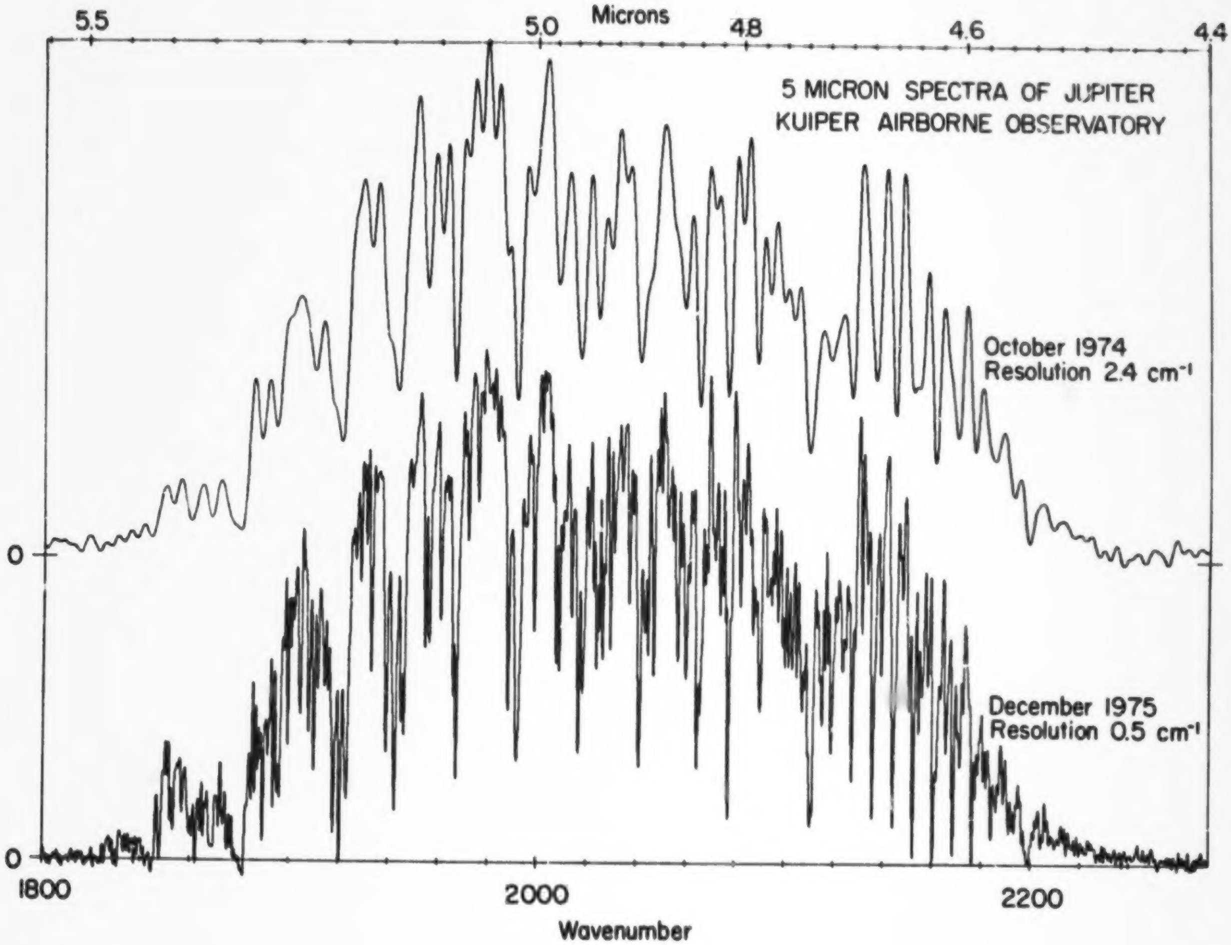

Figure 11. Comparison of two 5 μm airborne spectra of Jupiter illustrating the rapid increase in information content that accompanies higher spectral resolution.

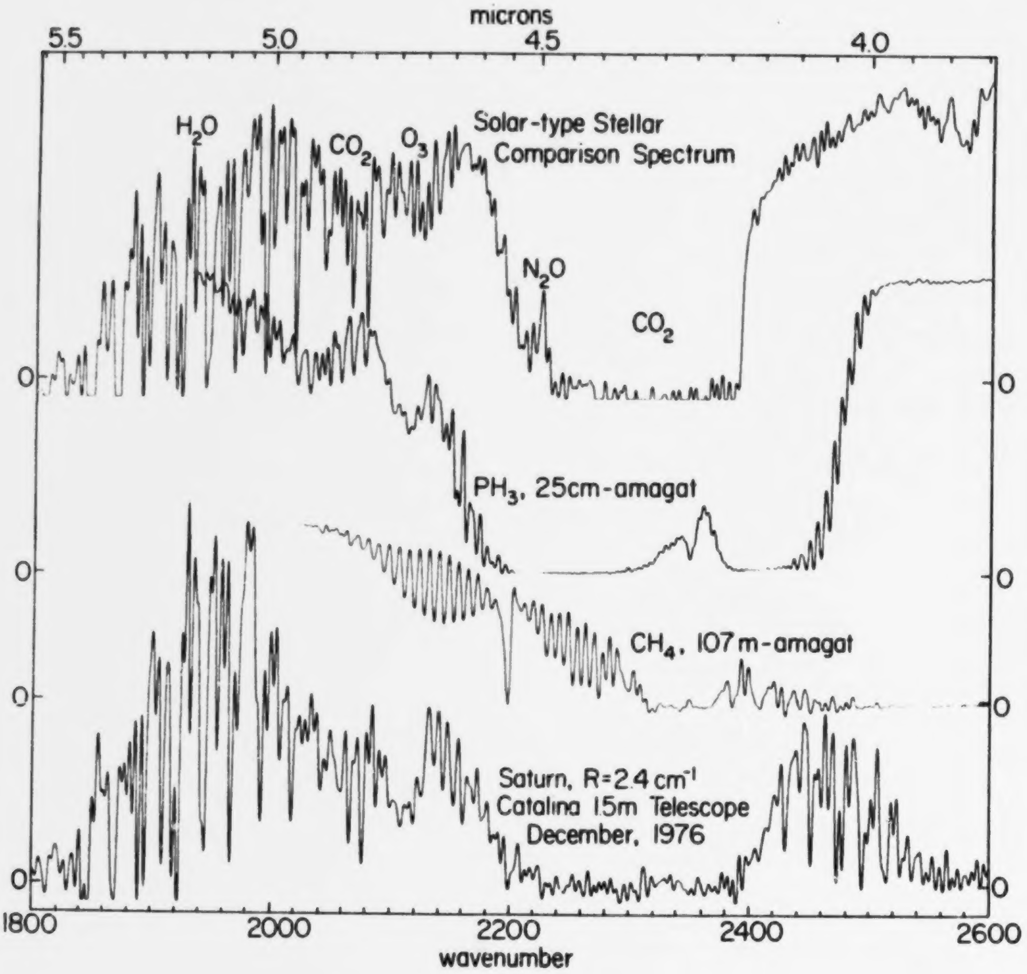

Figure 12. Ground-based observations of Saturn at 5 μm. Phosphine and CH_3D laboratory data illustrate the role of these two molecules in forming part of Saturn's 5 μm window. The region of transmission in Saturn's spectrum at 4 μm is very shallow since much lower CH_4 and PH_3 abundances, compared to these at 5μ, are required to model it. Figure reproduced from Larson et al. (1980).

3. NH_3: Interpretation of the various observations of, or upper limits to, gaseous and solid NH_3 on Saturn is a particularly challenging task facing planetary scientists.

4. PH_3: This molecule has been detected with P/H values in excess of the solar ratio in three of Saturn's atmospheric windows (3, 5, 10 μm). It is the only uniformly mixed constituent detected so far at 3 μm, and its spectrum could serve as a spectroscopic probe of Saturn's atmosphere if the observed bands were analyzed.

5. Trace constituents: Laboratory comparison data are needed for any molecule reasonably compatible with a reducing atmosphere with bands fortuitously placed within the planetary windows.

This paper was presented with support from NASA Grant NGR 03-002-332.

References

Bjoraker, G. L., Larson, H. P., Fink, U., and Smith, H. A., 1980, Astrophys. J., submitted.

Danielson, R. E., 1966, Astrophys. J. 143, 949.

Davis, D. S., Larson, H. P., Williams, M., Michel, G., and Connes, P., 1980, Appl. Optics, submitted.

Fink, U., and Larson, H. P., 1978, Science 201, 343.

Fink, U., and Larson, H. P., 1979, Astrophys. J. 233, 1021

Larson, H. P., Fink, U., Smith, H. A., and Davis, D. S., 1980, Astrophys. J., in press.

Larson, H. P., 1980, Ann. Rev. Astron. Astrophys., in press.

Ridgway, S. T., Larson, H. P., and Fink, U., 1976, in Jupiter, ed. T. Gehrels, University of Arizona Press (Tucson), p. 384.

Treffers, R. R., Larson, H. P., Fink, U., and Gautier, T. N., 1978, Icarus 34, 331.

1. Report No.
CP-2223

2. Government Accession No.

3. Recipient's Catalog No.

4. Title and Subtitle
Vibrational-Rotational Spectroscopy for
Planetary Atmospheres - Volume I

5. Report Date
April 1982

6. Performing Organization Code
693

7. Author(s)
Michael Mumma, Kenneth Fox, and John Hornstein

8. Performing Organization Report No.
82B0303

9. Performing Organization Name and Address
Goddard Space Flight Center
Greenbelt, Maryland 20771

10. Work Unit No.

11. Contract or Grant No.

13. Type of Report and Period Covered
Conference Publication

12. Sponsoring Agency Name and Address
National Aeronautics and Space Administration
Washington, D.C. 20546

14. Sponsoring Agency Code

15. Supplementary Notes

16. Abstract

Volumes 1 and 2 contain the proceedings of a Workshop on Vibrational-Rotational Spectroscopy relevant to the study of planetary atmospheres. The Workshop was organized by co-chairmen, Michael Mumma, NASA, Goddard Space Flight Center, and Lloyd Wallace, Kitt Peak National Observatory, and by Kenneth Fox, University of Tennessee, and Virgil Kunde, Goddard Space Flight Center, with the sponsorship of NASA Headquarters. The Workshop was held in Annapolis, Maryland, March 17-19, 1980. The Workshop participants included experts in the areas of planetary atmospheres, radiative transfer, molecular structure, photo-chemical modeling, laboratory spectroscopy, and remote sounding.

These volumes contain the scientific papers presented by the 39 invited speakers, the edited discussions which followed each paper, the transcriptions of a panel discussion on planetary observations from space in the next decade, an executive summary of recommendations for needed support, and a detailed summary of the working session.

17. Key Words (Selected by Author(s))
Planetary Atmospheres
Vibrational Spectroscopy
Molecular Spectra
Infrared Spectroscopy

18. Distribution Statement
Unclassified-Unlimited

Subject Category 91

19. Security Classif. (of this report)	20. Security Classif. (of this page)	21. No. of Pages	22. Price*
Unclassified	Unclassified	436	A19

*For sale by the National Technical Information Service, Springfield, Virginia 22151.

NASA-Langley, 1982